UNIVERSITY OF ICELAND

Bayesian flood analysis with added uncertainty in extreme discharge measurements

Fjalarr Pall Manason

BAYESIAN FLOOD ANALYSIS WITH ADDED UNCERTAINTY IN EXTREME DISCHARGE MEASUREMENTS

Fjalarr Pall Manason

60 ECTS thesis submitted in partial fulfillment of a
Magister Scientiarum degree in Financial Engineering

Advisors
Birgir Hrafnkelsson
Sigurdur M. Gardarsson
Olafur P. Palsson

Faculty Representative
Daniel F. Gudbjartsson

Faculty of Industrial Engineering, Mechanical Engineering and Computer
Science
School of Engineering and Natural Sciences
University of Iceland
Reykjavik, Febuary 2012

Bayesian flood analysis with added uncertainty in extreme discharge measurements
60 ECTS thesis submitted in partial fulfillment of a M.Sc. degree in Financial Engineering

Ágrip

Tilgangur þessa verkefnis er að útbúa líkan sem getur framkvæmt flóðagreiningu. Hönnun líkansins er höguð þannig að gefin rétt gögn mun það geta framkvæmt slíka greiningu fyrir allar ár. Fjórar ár á Íslandi eru til skoðunar í þessu verkefni.

Tvenns konar líkön eru útbúin fyrir árnar til skoðunar. Annars vegar, svokallað block maxima líkan (BM), sem notast við árleg hágildi vatnsrennslis, og hins vegar, svokallað þröskuldslíkan (TM), sem notast við vatnsrennslisgildi sem fara yfir ákveðinn þröskuld. Mismunandi aðferðir við val á þröskuldi eru vandlega skoðaðar. Almenna hágildisdreifingin er notuð í block maxima líkaninu og almenna Pareto dreifingin er notuð í þröskuldslíkaninu.

Almenna hágildisdreifingin hefur þrjá stika, þ.e. staðsetningarstika, skölunarstika og lögunarstika. Almenna Pareto dreifingin hefur tvo stika, þ.e. skölunarstika og lögunarstika. Lögunarstikar þessara dreifinga segja til um hverning halar dreifinganna haga sér og eru því sérstaklega til skoðunar í þessu verkefni.

Bayesískar tölfræðiaðferðir og Monte Carlo hermun eru notaðar við líkanagerðina. Athugað er sérstaklega hvernig þrenns konar mismunandi val á fyrirframdreifingum lögunarstikanna hefur áhrif á flóðagreiningunna.

Einnig er óvissan í úteiknuðum vatnsrennslisgildum sérstaklega skoðuð. Vatnsrennslisgildin eru reiknuð út frá vatnshæðum með svokölluðum rennslislyklum. Rennslislyklar lýsa vörpun vatnshæðar yfir í vatnsrennsli og þessari vörpun fylgir óvissa. Líkanið tekur tillit til þessarar óvissu í flóðagreiningunni. Niðurstöður sýna að þessi viðbætta óvissa rennslisyklanna hefur þau áhrif að heildaróvssa 100 ára atburða eykst um allt að 15%.

Abstract

The purpose of this project is to build a model which can conduct flood analysis on any river, given the proper data. This is done using extreme value theory with Bayesian statistics and a Markov chain Monte Carlo (MCMC) simulations for posterior inference. Two types of extreme value models are constructed, namely a block maxima model and a threshold model. The block maxima model uses annual maximum values of discharge for flood analysis while a threshold model uses discharge values exceeding a certain threshold. Methods for choosing an appropriate threshold value for the threshold model are investigated. The data used in the block maxima

model are fitted to the generalized extreme value (GEV) distribution and the data used in the threshold model are fitted to the generalized Pareto (GP) distribution. The three parameter GEV distribution and the two parameter GP distribution both have a shape parameter ξ, controlling the shape of the tail of the distributions. A negative shape parameter leads to a bounded upper tail leading to an upper limit on extremes. For a non-negative shape parameter the tails of the distributions becomes unbounded and they grow thicker as ξ increases leading to a higher probability of large values. Using the Bayesian methodology it is explored whether constraining the shape parameter, using prior knowledge, is beneficiary and if it is statistically acceptable.

The goal is to try and understand the behavior of a river and predict the magnitude of water discharge likely to arise for a particular time span. This magnitude of discharge is visually described in return level plots. The uncertainty in the return level plots is often quite large. The uncertainty in an extreme value analysis is of major importance. One source of uncertainty is due to sampling. There is another source of uncertainty taken into account in the thesis. Namely, the uncertainties in the discharge values. The discharge is found by transformation from water level using a discharge rating curve. Whether the discharge rating curve uncertainty has a significant effect on the over all uncertainty in return level plots or not, is studied.

The parameters of the GEV and GP distributions are evaluated through the Bayesian approach. Posterior densities are compared for the two different types of models (GEV and GP) using three different cases of prior distributions with and without a discharge rating curve uncertainty. This comparison is done for four rivers in Iceland. The research showed that the added discharge rating curve uncertainty has the effect of increasing the over all uncertainty in a 100-year event for up to 15%.

Acknowledgements

Contents

Contents

List of Figures

List of Tables

1. Introduction

1.1. Motivation

Extreme events such as floods are, as the name implies, extreme; departures from a norm or something unexpected. Extreme value theory is intriguing for many reasons, if not only to shed light on these unexpected events. It is the purpose most extreme value analysis to try to predict these departures from the norm, i.e. to try to predict them so precautions can be made. When using these theories to predict future events, the result of an analysis has often a high level of associated uncertainty. Its understandable as the time length of predictions is often greater than the time length of the data used for the analysis. The analysis uses discharge time series to predict future floods. However, due to high cost of discharge measurements, the discharge values are rarely measured but usually transformed from measured water levels using so called discharge rating curves (DRC). A DRC is a curve expressing discharge as a function of water level. There is a degree of uncertainty associated with the transformation from water level to discharge which effects the overall flood analysis uncertainty. In this thesis the influence of the DRC uncertainty on the over all uncertainty in the analysis is investigated. The discharge rating curve uncertainty is merged with the sampling uncertainty using a Bayesian Markov chain Monte Carlo simulation. Furthermore, by using the framework of Bayesian statistics, it will be investigated what effect a priori knowledge will have on the results of the flood analysis by restraining the parameters in the proposed distributions used in the analysis.

Quantifying uncertainty in extreme analysis is of great importance. Underestimation can have catastrophic consequences since structures such as bridges and roads are designed to withstand floods of magnitudes estimated by extreme analysis.

1.2. Literature review

In this thesis a model that performs flood analysis was constructed using Bayesian statistics and extreme value theory. The most popular models used for extreme

value analysis is the block maxima model and the threshold model. This thesis studies both of these models using the generalized extreme value distribution (GEV) in the block maxima model and the generalized Pareto (GP) distribution in the threshold model. The Bayesian framework is especially useful when implementing prior knowledge in statistical analysis and, three different cases of prior knowledge were examined in each of the models.

The data used for the analysis was daily discharge values. The discharge is calculated from measured values of water levels, using discharge rating curves. The discharge rating curves express discharge as a function of water level and in this thesis, the uncertainty in this water level to discharge transformation is especially examined and merged with the over-all uncertainty from the flood analysis.

Many academics have studied extreme value theory and used it in for real life predictions of all sorts of phenomena. In the last couple of decades the use of Bayesian modeling has grown in popularity. One of the main advantages in Bayesian modeling is using prior knowledge which can be especially useful when working with extremes.

Smith (1985) studied the generalized exrteme value distribution using maximum likelihood methods. The tail behavior of the GEV distribution was investigated closely and effects the shape parameter ξ has on it. He concluded that when the shape parameter is below -1, the the maximum likelihood estimators are unlikely to be obtainable.

Makkonen (2006) studied plotting positions of extreme values on return level plots. He concluded that the best formula to use, was the Weibull formula.

Reis Jr. and Stedinger (2005) explored Bayesian Markov Chain Monte Carlo methods for evaluating posterior distributions of flood quantiles, flood risk, and parameters of both the log-normal and the Log-Pearson Type 3 distributions.

Karim and Chowdhury (1995) compared four distributions used in flood frequency analysis in Bangladesh. The distributions being compared were: the GEV distribution, the log-normal distribution, Gumbel distribution and log-Pearson type 3 distribution. They came to the conclusion that the GEV distribution was more suitable for flood frequency analysis than any of the other three distributions.

Øverleir and Reitan (2009) examined the joint impact of sample variability and rating curve imprecision, using likelihood-based methods.They assumed that the discharge rating curve followed the standard power-law model and the annual maximum discharges values followed the generalized extreme value distribution.

Davison and Smith (1990) used the generalized Pareto distribution (GP) to model

2

river flow peaks over threshold (POT). They studied methods for selecting an appropriate threshold value to use with the GP distribution and also methods for de-clustering the POTs in order to eliminate the correlation between peaks.

Van Montfort and Witter (1986) used the generalized Pareto distribution to model extremes in stream flows and rainfall series.

Coles and Tawn (1996) used Bayesian methods for modeling extreme rainfall series. They illustrated how expert knowledge regarding the data being analyzed can enhance the estimates of extremal behavior. They used Markov chain Monte Carlo methods to model 100-year return levels for daily rainfall, relying on the knowledge of an expert hydrologist, for choosing prior distributions for the GEV parameters. They concluded that, if reliable information concerning the extremes of a process is available, then the arguments in favour of Bayesinan analysis are compelling.

Smith and Naylor (1987) did a study comparing maximum likelihood and Bayesian estimators, for the three parameter Weibull distribution. The study was an extreme analysis on fiber strength, and they came to the conclusions that there are practical advantages to the Bayesian approach.

Parent and Bernier (2003) used Bayesian methods to model peaks over threshold (POT), using semi-conjugate informative priors, for flood analysis. They showed that prior expertise can significantly reduce uncertainty in flood analysis.

Coles and Pericchi (2003) used Bayesian methods and MCMC algorithm to model extreme rainfall in Venezuela.

Hrafnkelsson et al. (2012) used Bayesian methods to improve the estimates of discharge rating curves by extending the standard power-law with B-spline functions.

1.3. Introduction

Human kind has always been trying to understand the random behavior of nature and prepare for its destructive aspects. Now a days there are several ways of predicting the behavior of the elements. The use of extreme value theory to predict extreme events is fairly new. It was in the 1950's when engineers first started to use this methodology for the modeling of physical phenomenon to determine design criteria. Since then its role has grown enormously in the process of risk analysis, from determining physical risk of natural events to determining the intangible risk of stock market crash (Reiss and Thomas (2007)).

1. Introduction

Extreme value analysis is an increasingly popular way of determining the premise of which a structure should be designed. Floods in rivers can be highly destructive, damaging infrastructure which can lead to economical and human loss. Therefor, the ability to be able to predict the behavior of a river can be of substantial value. Knowing the frequency a flood of a particular size will occur is a major factor when designing a bridge or a road. A design will have to account for the possible extreme events it is subjected to, but within a certain economical frame established through cost-benefit analysis.

This work examines daily discharge values of four rivers in Iceland. The length of the data sets for the rivers ranges from 37 to 57 years. It also uses paired sets of water level and discharge to construct discharge rating curves which describe the discharge as a function of water level. The rating curves are different for each river and possess some uncertainty within them. All the daily discharge values used in the analysis come from a rating curve transformation of water level. To be able to assess the uncertainty in the discharge time series for a particular river, the discharge rating curve is constructed and analyzed. Within the Bayesian framework, the objective is to perform flood analysis taking into account both the uncertainty of the rating curves and the uncertainty due to sampling variability.

Traditionally the rating curve uncertainty is not taken into account when a flood analysis is performed. However, Øverleir and Reitan (2009) did so using likelihood-based methods. The uncertainty of rating curves usually gets greater, the higher the water level. One of the objectives of this study is to investigate whether rating curve uncertainty has considerable effect on the overall uncertainty of the flood analysis.

Two types of models were constructed for the flood analysis for each river. First, the annual maximum values were investigated and the generalized extreme value (GEV) distribution fitted to those values. Second, the values exceeding a certain threshold were fitted to the generalized Pareto (GP) distribution. In both cases, the parameters in the distributions were examined and it was investigated how the posterior distributions are affected by different types of prior distributions selected for those parameters. A Markov Chain Monte Carlo (MCMC) simulation was used to produce samples from the posterior distributions for the parameters, both in the GEV and the GP distribution.

The generalized extreme value distribution combines the work of three pioneers in extreme value analysis, Waloddi Weibull, Maurice Frechet, and Emil Gumbel. Each of them published articles describing models for extreme behavior. Frechet, in 1927, devised a limiting distribution for a sequence of maxima. The Weibull distribution, published in 1951, was originally developed to address problems for minima arising in material sciences but due to its flexibility it is widely used in many other areas. The Gumbel distribution, first published in 1958, has been widely used in extreme analysis. Gumbel applied it in various problems such as annual floods.

4

The Generalized Extreme Value (GEV) distribution is a family of limit distributions combining the Gumbel, Weibull, and Frechet distributions. The GEV distribution was independently proposed by Jenkinson (1955) and von Mises (1954).

The types of tail behaviors that arise from these distribution are different from each other. Understanding of the tail behavior of distributions is very important in extreme value analysis. The three distributions do all have different types of tail behavior. In the case of maxima both tails of the Gumbel distribution are unbounded, while the Weibull distribution has an upper bound and the Frechet distribution has a lower bound. The GEV distribution has three parameters; a location parameter denoted by μ, a scale parameter denoted by σ, and a shape parameter denoted by ξ, which controls the tail behavior of the distribution. The value of the shape parameter in the GEV distribution determines which of the underlying three distributions it follows. Namely, $\xi = 0$ corresponds to the unbounded Gumbel distribution, $\xi > 0$ corresponds to the lower bounded Frechet distribution, and $\xi < 0$ corresponds to the upper bounded Weibull distribution. By combining the Gumbel, Weibull, and Frechet distributions in the GEV distribution, all possible tail behaviors of the underlying distributions are possible, making the GEV distribution much more flexibility than any one of its individual parts.

The method of modeling peaks over threshold (POT) has been used as an alternative to modeling annual maxima in flood frequency analysis. The peaks over threshold are modeled using the generalized Pareto (GP) distribution. It was Pickands, in 1975, that first introduced the idea of using the generalized Pareto distribution to model POTs and it has since been used in a variety of extreme value applications. Davison and Smith, in 1990, used the GP distribution to model river-flow POTs. Van Montfort and Witter (1985) also applied the GP distribution to model POTs of stream flows and rainfall series.

Bayesian extreme value analysis has been used in the past to predict natural phenomena, with good results. Coles & Tawn (1996) used a MCMC method to perform an extreme analysis on rainfall data. They used prior information concerning the extremes for choosing prior distributions for the GEV parameters. They concluded that, if reliable information is available, then using historical data and expert knowledge for choosing prior distributions can enhance the estimates of extremal behavior. Smith & Naylor (1987) compared maximum likelihood estimators to Bayesian estimators for the three parameter Weibull distribution and concluded that there are practical advantages to using the Bayesian approach.

The main purpose of this thesis is to extend Bayesian methods for flood analysis. The main novelty involves taking uncertainty in flood values rising from uncertainty in discharge rating curves into account. This is done for both annual flood analysis and peak over threshold analysis. The effect of three different prior distributions for the shape parameter is also investigated. Two of these prior distributions only

allow negative values of the shape parameter. These various model choices are compared through an application to data from four rivers in Iceland. The objective is to construct a model which is capable of analyzing the extremes in any river. The extremes will be modeled with the GEV and GP distributions and it will be investigated whether it is feasible to constrain the parameters of the distributions using prior distributions.

2. Methods

2.1. Extreme value analysis

The purpose of extreme value analysis is to determine the statistical behavior of extreme values. For a sequence of independent random values $X_1, ..., X_n$ having a common distribution function, F, the focus is on the statistical behavior of M_n, where

$$M_n = \max\{X_1, ..., X_n\}$$

.

The X_i can represent, e.g., hourly measured wind speed or daily mean values of rain fall, but in this study the X_i represents average daily values of water discharge in rivers.

In Coles (2001) the theories and methods used in extreme value analysis are well documented. In theory the distribution of M_n can be derived exactly for all values of n,

$$
\begin{aligned}
Pr\{M_n \leq z\} &= \Pr\{X_1 \leq z, ..., X_n \leq z\} \\
&= \Pr\{X_1 \leq z\} \times \cdots \times Pr\{X_n \leq z\} \\
&= (\Pr\{X_1 \leq z\})^n \\
&= F^n(z)
\end{aligned}
$$

However, this approach is inadequate in practice since the distribution, F, is unknown and even if one were to use some techniques to estimate F from observed data the smallest discrepancies in the estimate of F would lead to substantial discrepancies for F^n.

An alternative approach is to accept the fact that F is unknown and model F^n directly. Proceeding by examining the behavior of F^n as $n \to \infty$ is not enough in

itself as for all $z < z_+$, where z_+ is the upper limit of F, $F^n(z) \to 0$ as $n \to \infty$, so that the distribution of M_n degenerates to a point mass on z_+. To find a limit distribution for maxima, the maximum variable, M_n, needs to be transformed such that the limit distribution of the new variable is a non-degenerate one. Because of this problem it is necessary to perform the following linear re-normalization of the variable M_n,

$$M_n^* = \frac{M_n - b_n}{a_n}$$

for sequences of constants $\{a_n > 0\}$ and $\{b_n\}$.

It is therefore necessary to find a limit distributions for M_n^*, with appropriate choices of $\{a_n\}$ and $\{b_n\}$, rather than M_n. This re-normalization of the maximum values was introduced by Fisher and Tippett (1928). Following up on their work, Gnedenko (1943), obtained three types of non-degenerated distributions for the re-normalized maximum, M_n^*: The Frechet, Weibull and Gumbel distributions.

Jenkinson (1955) and von Mises (1954) independently proposed the generalized extreme value distribution (GEV), which includes the three limit distributions distinguished by Gnedenko.

Theorem 3.1.1 in Stuart Coles' book *An Introduction to Statisctial Modeling of Extreme Values* (2001) states the following,

Theorem 2.1.1 *If there exist sequences of constants $\{a_n > 0\}$ and $\{b_n\}$ such that*

$$Pr\{(M_n - b_n)/a_n \le z\} \to G(z) \quad \text{as} \quad n \to \infty$$

for a non-degenerate distribution function G, then G is a member of the Generalized extreme value, GEV, *family*

$$G(z) = \exp\left\{ -\left[1 + \xi\left(\frac{z - \mu}{\sigma}\right)\right]^{-1/\xi} \right\} \tag{2.1}$$

defined on $\{z : 1 + \xi(z - \mu)/\sigma > 0\}$, where $-\infty < \mu < \infty$, $\sigma > 0$ and $-\infty < \xi < \infty$
□

The theorem suggests using the GEV family when modeling maxima of long sequences. The apparent problem of finding the normalizing constants is easily solved through the following reasoning,

$$Pr\{(M_n - b_n)/a_n \leq z\} \approx G(z),$$

for large enough n is equivalent to

$$Pr\{M_n \leq z\} \approx G\{(z - b_n)/a_n\}$$
$$= G^*(z),$$

where G^* is another member of the GEV family. Therefore, if the theorem enables approximation of the distribution of M_n^* by a member of the GEV family for large n, the distribution of M_n itself can also be approximated by a different member of the same family. Since the parameters of the distribution have to be estimated regardless, it is irrelevant in practice that the parameters of the distribution of G are different from those of G^*.

2.2. Block maxima model: The generalized extreme value distribution

A block maxima model is constructed in the following way; data series are gathered and the series are viewed as a combination of many blocks. For each of these blocks a maximum or minimum value is obtained, depending on whether the objective is to look at high or low extremes. These values are then fitted to the GEV distribution. The block period is selected for each particular project. There is a clear trade-off between bias and variance when considering the block size used in the model. For a block size too small it is likely that the approximation by the limit model in Theorem 2.1.1 is not suitable. On the other hand, a block size too big is likely to result in insufficient amount data for the model, resulting in a large estimation variance. A popular pragmatic way of selecting the size of the blocks is to use annual extremes. That approach has been selected for the scope of this study, i.e. the annual maximum value is used for the purpose of flood frequency analysis.

It is unrealistic to assume that all the daily discharge values have a common distribution function. For example, the water discharge levels are likely to change with seasons. That, strictly speaking, is not in accordance with the assumption that the

values share a common distribution function as stated in Section 2.1. However, it would not be beneficiary to try to take this into account in the modeling by having smaller block sizes, to account for different seasons. That would result in maximum values from one season being significantly different from another leading to results that would likely be inaccurate. By having a block size of one year it is very plausible that individual block maxima have a shared common distribution even though the daily discharge values do not.

For a particular river, water discharge time series span m years, and are denoted as $\{Q\}$. The GEV distribution is fitted to $\{Q^M\}$, the corresponding annual maximum water discharge levels, using Bayesian statistics.

The GEV distribution is composed of three parameters; a location parameter, μ, a scale parameter, σ, and shape parameter, ξ. The shape parameter is of great interest when it comes to flood analysis as it relates to the thickness of the tail in the distribution. If the shape parameter is negative the tail will be bounded and therefore also the extreme values. If the shape parameter is greater than or equal to zero the tail will be unbounded. With an unbounded tail a random variable can take on any possible extreme value. With larger positive shape parameter, the upper tail of the probability density function (pdf) becomes thicker, and so the possibility of a large extreme event becomes greater. This is demonstrated in Figure 2.1. The top figures show the pdf of the GEV distribution and the bottom figures display the return level plots calculated from those distributions. A return level plot shows the return period against the return level. The return level is the discharge level that is expected to be exceeded, on average, once every T years. The return period is the amount of time, T, expected to wait for the exceedance of a particular return level. Figure 2.1 shows that when the shape parameter is negative (left panel), the pdf has an upper limit and hence the return period plot converges to an asymptote as return time increases. When the shape parameter is equal to zero (middle panel) the pdf is no longer limited and the return period plot is linearly increasing for an increasing logarithmic return time. With positive shape parameter (right panel) the tail of the pdf is thicker resulting in exponential increase in the return levels with increasing return time.

Smith (1985) studied the behavior of the GEV distribution in detail with regards to the shape parameter and obtained that when $\xi > -0.5$ the maximum likelihood estimators have asymptotic properties while loosing those properties when $\xi < -0.5$. In extreme value modeling, the interval that the shape parameter takes place on is, almost without exception between, -0.5 and 1. The case where $\xi \leq -0.5$ corresponds to a distribution with a very short bounded upper tail and it rarely happens in extreme value modeling.
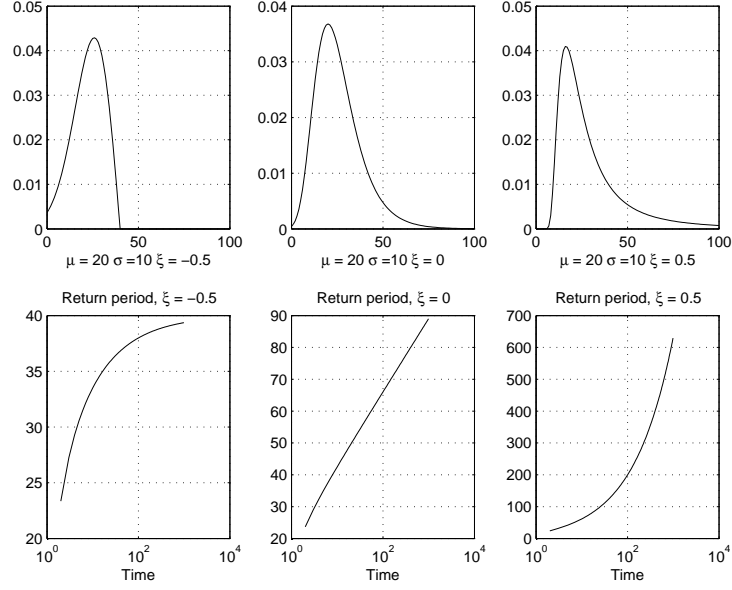
Figure 2.1: Probability density function and Return plots for different values of the shape parameter

2.2.1. Return level plots for the block maxima model

According to Coles (2001), estimates of extreme quantiles of the GEV distribution are obtained by inverting Equation (2.1),

$$z_p = \begin{cases} \mu - \frac{\sigma}{\xi}[1 - \{-\log(1-p)\}^{-\xi}] & \text{for } \xi \neq 0, \\ \mu - \sigma \log\{-\log(1-p)\} & \text{for } \xi = 0, \end{cases} \qquad (2.2)$$

where z_p is the $(1-p)$ quantile, i.e., $G(z_p) = 1 - p$. This means that the value z_p is exceeded by the annual maximum in any particular year with probability p. Therefore, z_p is the return level associated with the return period $1/p$ since the level z_p is expected to be exceeded on average once every $1/p$ years.

When looking at long return periods, plotting them on logarithmic scale becomes useful. By defining $y_p = -\log(1-p) = -\log(1-1/T)$ it becomes possible to write Equation (2.2) in the form:

$$z_p = \begin{cases} \mu - \frac{\sigma}{\xi}[1 - y_p^{-\xi}] & \text{for } \xi \neq 0, \\ \mu - \sigma \log y_p & \text{for } \xi = 0, \end{cases} \qquad (2.3)$$

If z_p is plotted against y_p on logarithmic scale the plot is linear in the case when

11

$\xi = 0$. If $\xi < 0$, the plot is convex with asymptotic limit as $p \to 0$ at $\mu - \sigma/\xi$. If $\xi > 0$, the plot is concave and has no finite bound. This behavior of the return level plot on logarithmic scale with regards to different values of the shape parameter (ξ) is shown in Figure 2.1

Return level plots are convenient for both model presentation and validation. In this case, they show the expected size of floods for a particular time period. Thus, the value of return level corresponding to particular return period expresses the expected size of a maximum flood that would happen once on average, during that period.

2.2.2. Model validation

Plotting position for the empirical data

Based on Makkonen (2006), the Weibull plotting position formula was chosen to fit the empirical data to the return level plots. The annual maximum discharge levels, $\{Q^M\}$, are ranked in increasing order of magnitude, $\{Q^{M,S}\}$, from the smallest $Q^{M,S}_{(i=1)}$ to the largest $Q^{M,S}_{(i=m)}$. The Weibull formula states the following,

$$P_{(i)} = 1 - 1/T_{(i)} = \frac{i}{m+1},$$

where $P_{(i)}$ is the estimated probability of Q^M being less than $Q^{M,S}_{(i)}$ and $T_{(i)}$ is the estimated return period. Rearranging gives the return period for each of the annual maximum values

$$T_{(i)} = \frac{1}{1 - P_{(i)}} = \frac{1}{1 - \frac{i}{m+1}}.$$

Plotting the sorted annual maximum values $Q^{M,S}_{(i)}$ as a function of return time $T_{(i)}$ on the return period plot, makes it possible to visually observe the validity of the proposed model. The *annual maximum - return time* pairs that are plotted on the return period plot are

$$\left(T_{(i)}, Q^{M,S}_{(i)} \right), \quad i=1,...,\text{m}.$$

Probability plot

The probability plot consists of the empirical distribution function of the annual maximum values versus the distribution function of the estimated model. The annual maximum discharge levels are ranked in increasing order of magnitude from the smallest $Q_{(i=1)}^{M,S}$ to the largest $Q_{(i=m)}^{M,S}$. The method, for constructing a probability plot, is discussed in detail in Coles (2001).

The empirical distribution function evaluated at $Q_{(i)}^{M,S}$ is,

$$\tilde{G}(Q_{(i)}^{M,S}) = \frac{i}{m+1}.$$

The empirical distribution function is compared to the GEV distribution function with the model based estimates for the GEV parameters. The GEV distribution function from Equation (2.1) with the parameter estimates from the block maxima model is,

$$\hat{G}(Q_{(i)}^{M,S}) = \exp\left\{ -\left[1 + \hat{\xi}\left(\frac{Q_{(i)}^{M,S} - \hat{\mu}}{\hat{\sigma}}\right)\right]^{-1/\hat{\xi}}\right\}.$$

If the GEV model provides a good fit to the data, the empirical distribution function and the GEV distribution functions should be similar, that is, for each $i = 1, ..., m$,

$$\tilde{G}(Q_{(i)}^{M,S}) \approx \hat{G}(Q_{(i)}^{M,S}).$$

The probability plot consists of the points

$$\left(\tilde{G}(Q_{(i)}^{M,S}), \hat{G}(Q_{(i)}^{M,S})\right), \quad i\text{=1,...,m.}$$

If the model provides a good fit to the data, the points should lie close to the unit diagonal. A substantial departure from the unit diagonal suggests that the GEV model is inadequate for the data.

Quantile plot

The focus of extreme value analysis is the investigation of extremes. The probability plot's main weakness is that both the $\tilde{G}(Q_{(i)}^{M,S})$ and $\hat{G}(Q_{(i)}^{M,S})$ are bound to approach 1 as $Q_{(i)}$ increases. Therefore it is a major weakness of the probability plot that it does provide the least information in the region of most interest, i.e. the region of the largest values. A quantile plot is another way of visually showing the accuracy of the proposed model, avoiding the problem of crowding the largest values close to 1. The method, for constructing a quantile plot, is discussed in detail in Coles (2001). The quantile plot consists of the points

$$\left(\hat{G}^{-1}(i/(m+1)), Q_{(i)}^{M,S} \right), \quad i\text{=1,...,m.}$$

where

$$\hat{G}^{-1}\left(\frac{i}{m+1} \right) = \hat{\mu} - \frac{\hat{\sigma}}{\hat{\xi}} \left[1 - \left\{ -\log\left(\frac{i}{m+1} \right) \right\}^{-\hat{\xi}} \right], \quad \text{if } \hat{\xi} \neq 0$$

and

$$\hat{G}^{-1}\left(\frac{i}{m+1} \right) = \hat{\mu} - \hat{\sigma} \log\left\{ -\log\left(\frac{i}{m+1} \right) \right\}, \quad \text{if } \hat{\xi} = 0.$$

The quantile plot should be close to linear for a suitable model. Departures from linearity indicates that the model does not adequately fit the data.

Bayesian p-value - Anderson-Darling test

Using the Anderson-Darling test to find a Bayesian p-value for the use of model checking, is discussed in Gelman et al. (2003). The Anderson-Darling test statistics is given by

$$A^2 = -n - S$$

where

$$S = \sum_{i=1}^{m} \frac{2i-1}{m} \left[\log F(Q_{(i)}^{M,S}) + \log(1 - F(Q_{(m+1-i)}^{M,S})) \right]$$

and $Q^{M,S}$ is again a vector containing the annual maximum values ranked in order of magnitude. F is the cumulative density function for the GEV distribution, with parameters $\theta^l = (\mu^l, \sigma^l, \xi^l)$, where $l = 1, 2, 3, .., L$. At this point, $L = 40{,}000$ sets of samples of GEV parameters have been simulated. For the l-th set of simulated GEV parameters the value of A^2 is calculated and denoted by A_l^2.

This process is repeated, but instead of using the annual maximum values, Q^M, a random sample of extremes from the GEV distribution, is generated, for each set of GEV parameters. The number of random values generated from each set of parameters is the same as the number of annual maximum values, m, and will, just as the annual maximum values, be ranked in order of magnitude. These replicated annual maximum values, denoted as y_l^{rep}, are used to calculate a value for $A_{l,rep}^2$ which is then compared to the value of A_l^2.

A vector I, having the length L is constructed. The vector is filled with either the values 0 or 1, depending on the A_l^2 vs. $A_{l,rep}^2$ comparison. The values of I are determined with the following formula

$$I_l = I_{A^2(y_l^{rep}, \theta^l) \geq A^2(Q^M, \theta^l)}$$

i.e. if the simulated value $A_{l,rep}^2$ is larger or equal to the observed value A_l^2, then the corresponding value of I becomes equal to 1, but 0 otherwise.

The Bayesian p-value is then found with the following equation

$$\hat{p}_B = \frac{1}{L} \sum_{l=1}^{L} I_l.$$

If the Bayesian p-value is very high or very low, i.e., smaller than 0.01 or larger than 0.99, it is a clear indication that the model does not fit the data accurately. If the Bayesian p-value lies between 0.05 and 0.95 it indicates that the model fits the data reasonably well.

2.3. Threshold Model: The generalized Pareto distribution

The obvious disadvantage of using the annual block maxima model is the obligation of using one extreme value from each year. That can have the effect of missing out on extreme data to use in the model if there are more than one extremes for any of the inspected years. It can also have the undesirable effect of using data that are not to be thought of as extremes. Within the inspected years there might have been some years with no suitable extreme events but the block maxima model would use data from those years regardless. For these reasons another well known approach to model the extremes was tried; threshold models.

Threshold models differ from block maxima models. Instead of specifying periods and analyzing maximum values within them, the threshold models are based on values which exceed a particular threshold. Thus, there may be many extreme values used from a single year and none from other years.

By looking only at the values that exceed the threshold and subtracting the threshold value, the transformed data set consists of positive extreme values. An appropriate model for data of this type is the generalized Pareto (GP) distribution, which is closely related to the GEV distribution. It has two parameters instead of three but the two distributions share the same shape parameter.

2.3.1. Theory

The alternative to the generalized extreme value distribution, where excesses over high threshold can be modeled by the generalized Pareto distribution, was introduced by Pickands in 1975 .

Theorem 4.1 in Stuart Coles' book *An Introduction to Statisctial Modeling of Extreme Values* states the following.

Theorem 2.3.1 *Let $X_1, X_2, ...$ be a sequence of independent random variables with common distribution function F, and let*

$$M_n = \max\{X_1, ..., X_n\}.$$

Denote an arbitrary term in the X_i sequence by X, and suppose that F satisfies Theorem (2.1.1), so that for large n,

$$\Pr\{M_n \leq z\} \approx G(z),$$

where

$$G(z) = \exp\left\{-\left[1 + \xi\left(\frac{z-\mu}{\sigma}\right)\right]^{-1/\xi}\right\}$$

for some $\mu, \sigma > 0$ and ξ. Then, for large enough u, the distribution function of $Y = (X - u)$, conditional on $X > u$, is approximately

$$H(y) = 1 - \left(1 + \frac{\xi y}{\tilde{\sigma}}\right)^{-1/\xi} \tag{2.4}$$

defined on $\{y : y > 0 \text{ and } (1 + \xi y/\tilde{\sigma}) > 0\}$, where

$$\tilde{\sigma} = \sigma + \xi(u - \mu). \tag{2.5}$$

$\square$

The family of distributions defined by Equation (2.4) is called the *generalized Pareto distribution (GP)*, with parameters $\tilde{\sigma}$ and ξ. Theorem (2.3.1) implies that, if block maxima extracted from a particular data set follow the GEV distribution then threshold excesses extracted from that same data set would follow the GP distribution. The two distributions would have the same shape parameter, ξ and the relationship between the threshold, u, the scale parameter of the GP distribution, $\tilde{\sigma}$, and the parameters of the GEV distribution, μ, σ, and ξ would be in accordance to Equation (2.5).

Justification of the generalized Pareto model

Let X have a distribution function F. By the assumption of Theorem (2.1.1) for large enough n,

$$F^n(z) \approx \exp\left\{-\left[1 + \xi\left(\frac{z-\mu}{\sigma}\right)\right]^{-1/\xi}\right\}$$

for some parameters $\mu, \sigma > 0$ and ξ. Hence,

$$n \log F(z) \approx -\left[1 + \xi\left(\frac{z-\mu}{\sigma}\right)\right]^{-1/\xi}.$$

But for large values of z, a Taylor expansion implies that

$$\log F(z) \approx -\{1 - F(z)\}.$$

Combining two previous equations and rearranging, gives

$$1 - F(u) \approx \frac{1}{n} \left[1 + \xi \left(\frac{u - \mu}{\sigma} \right) \right]^{-1/\xi}$$

for large u. Similarly, for $y > 0$,

$$1 - F(u + y) \approx \frac{1}{n} \left[1 + \xi \left(\frac{u + y - \mu}{\sigma} \right) \right]^{-1/\xi}.$$

Hence,

$$
\begin{aligned}
\Pr\{X > u + y | X > u\} &\approx \frac{n^{-1}[1 + \xi(u + y - \mu)/\sigma]^{-1/\xi}}{n^{-1}[1 + \xi(u - \mu)/\sigma]^{-1/\xi}} \\
&= \left[\frac{1 + \xi(u + y - \mu)/\sigma}{1 + \xi(u - \mu)/\sigma} \right]^{-1/\xi} \\
&= \left[1 + \frac{\xi y}{\tilde{\sigma}} \right]^{-1/\xi},
\end{aligned}
\tag{2.6}
$$

where
$$\tilde{\sigma} = \sigma + \xi(u - \mu),$$

as required.

2.3.2. Return level plots for the threshold model

The return level plot shows the return period against the return level. The return level is the discharge level that is expected to be exceeded, on average, once every T years. The return period is the amount of time, T, expected to wait for the exceedance of a particular return level. Construction of return level plots for threshold models is explained in Coles (2001).

From Equation (2.4) it can be derived that the following holds for an extreme variable X and a threshold u,

$$\Pr\{X > x | X > u\} = \left[1 + \xi \left(\frac{x - u}{\tilde{\sigma}} \right) \right]^{-1/\xi}.$$

It follows that

$$\Pr\{X > x\} = \zeta_u \left[1 + \xi \left(\frac{x - u}{\tilde{\sigma}} \right) \right]^{-1/\xi},$$

where $\zeta_u = \Pr\{X > u\}$ is the *crossing rate*, i.e., the probability of an individual observation exceeding the threshold u. Hence, the level x_m that is exceeded on average once every m observations is the solution to

$$\zeta_u \left[1 + \xi \left(\frac{x_m - u}{\tilde{\sigma}} \right) \right]^{-1/\xi} = \frac{1}{m}.$$

By using the equation above it is easy to derive the *m-observation return level*. However, determining the *N-year return level* is of more interest. For n_y observations per year, $m = N \times n_y$, and the *N*-year return level, z_N, is determined with,

$$z_N = \begin{cases} u + \frac{\tilde{\sigma}}{\xi}[(Nn_y\zeta_u)^{\xi} - 1] & \text{for } \xi \neq 0, \\ u + \tilde{\sigma}\log(Nn_y\zeta_u) & \text{for } \xi = 0. \end{cases} \tag{2.7}$$

The crossing rate, ζ_u is equal to the sample proportion of points exceeding u, i.e.,

$$\zeta_u = \frac{k}{n}$$

where k is the number of values exceeding u and n is the total number of observations.

2.3.3. Model validation

Plotting position for the empirical data

The Weibull plotting position formula is used to fit the empirical data to the return level plots. The *peaks over threshold* (POTs), denoted by Q^P, are ranked in increasing order of magnitude in a vector denoted as $Q^{P,S}$. The values of $Q^{P,S}$ are ranked from the smallest $Q^{P,S}_{(i=1)}$ to the largest $Q^{P,S}_{(i=n)}$, where n is the total number of POTs. Unlike the block maxima model, the number of POTs are not necessarily the same as the number of years inspected. It is therefore necessary to account for that in the plotting position formula by using the crossing rate, ζ_u. Using the Weibull plotting position formula it is possible to include the crossing rate in the calculation

2. Methods

$$P_{(i)} = 1 - \frac{1}{T_{(i)} \times \zeta_u} = \frac{i}{n+1}$$

where $P_{(i)}$ is the estimated probability of Q^P being less than $Q^{P,S}_{(i)}$ and $T_{(i)}$ is the estimated return period. Rearranging gives the return period for each of the POTs

$$T_{(i)} = \frac{1}{(1 - P_{(i)})\zeta_u} = \frac{n+1}{(1 + n - i)\zeta_u}.$$

Plot of the empirical data versus the return period using the plotting position described above is very useful in visually evaluating the fit of the proposed model to the data.

Probability plot

As in the case of the block maxima model, the probability plot for the threshold model compares the empirical distribution function to the distribution function of the estimated model. The method, for constructing a probability plot, is discussed in detail in Coles (2001). The peaks over threshold are ranked in increasing order of magnitude from the smallest $Q^{P,S}_{(i=1)}$ to the largest $Q^{P,S}_{(i=N)}$.

The empirical distribution function evaluated at $Q^{P,S}_{(i)}$ is,

$$\tilde{G}(Q^{P,S}_{(i)}) = \frac{i}{n+1}$$

for $i = 1, 2, 3, .., n$.

The empirical distribution function is compared to the GP distribution function with the model based estimates for the GP parameters. The GP distribution function from Equation (2.4) with the parameter estimates from the threshold model is,

$$\hat{G}(Q^{P,S}_{(i)}) = 1 - \left(1 + \frac{\hat{\xi}Q^{P,S}_{(i)}}{\hat{\sigma}}\right)^{-1/\hat{\xi}}.$$

If the GP model gives a good fit to the data then the empirical and the GP distri-

bution functions should be similar, that is, for each i,

$$\tilde{G}(Q^{P,S}_{(i)}) \approx \hat{G}(Q^{P,S}_{(i)})$$

The probability plot consists of the points

$$\left(\tilde{G}(Q^{P,S}_{(i)}), \hat{G}(Q^{P,S}_{(i)}) \right), \qquad i=1,...,\text{n}.$$

If the model provides a good fit to the data, the points should lie close to the unit diagonal. A substantial departure from the unit diagonal suggests that the GP model is inadequate for the data.

Quantile plot

The method, for constructing a quantile plot, is discussed in detail in Coles (2001). By rearranging Equation (2.7) and acknowledging that $Nn_y\zeta_u = 1/p$, a quantile function of the GP distribution is constructed. As before, the POTs are ranked in increasing order of magnitude from the smallest $Q^{P,S}_{(i=1)}$ to the largest $Q^{P,S}_{(i=n)}$. The empirical data are compared to the quantile function of the estimated model which is based on the model based estimates of the GP parameters. The quantile function of the GP distribution is given by

$$\hat{H}^{-1}(p) = \begin{cases} u + \frac{\hat{\sigma}}{\hat{\xi}}[p^{-\hat{\xi}} - 1] & \text{for } \xi \neq 0, \\ u + \sigma \log(p^{-1}) & \text{for } \xi = 0. \end{cases} \tag{2.8}$$

The empirical cumulative density function is as before

$$P_{(i)} = \frac{i}{n+1}$$

So the quantile plot consists of the pairs

$$\left(\hat{H}^{-1}(i/(n+1)), Q^{P,S}_{(i)} \right), \quad , i=1,...,\text{n}.$$

The quantile plot should be close to linear for a suitable model. Departures from linearity indicates that the model does not adequately fit the data.

3. Model

3.1. Data

The data used in this thesis come from the Icelandic Meteorological Office (IMO). The IMO runs a water level measuring system which collects water level data continuously from rivers in Iceland. These water level measurements are converted to discharge by the use of discharge rating curves (DRC). The DRC express the discharge as a function of water level. However, the uncertainty in the DRC has not been taken into consideration in the water level to discharge conversion, therefore the data are daily point estimates of water discharge levels.

Discharge rating curves are constructed by fitting a curve through points of measured water levels against measured discharge at a location where downstream hydraulic control assures a stable, sensitive, and monotonic relationship between water level and discharge (Mosley and McKerchar, 1993; ISO, 1983). The DRC are used to estimate discharge due to high cost of discharge measurements. Water level measurements are, however, relatively inexpensive and and well suited for automation.

The data sets are from four rivers in Iceland, namely, Sanda in Thistilfjordur, Olfusa by Selfoss, Hvita by Kljafoss and Svarta in Skagafjordur. For the purpose of this analysis, pairs of water level and discharge data were used to construct a discharge rating curve. The discharge rating curves were used to estimate the uncertainty in the discharge time series. The water discharge time series and the water level and discharge pairs for the four rivers can be seen in Figure 3.1.

For Sanda in Thistilfjordur, a total of 11 water level and discharge pairs were available, spanning a water level range from 1.2 m to 2.3 m. The discharge time series span a time period of 43 years, from 1965 to 2008.

For Olfusa by Selfoss, a total of 43 water level and discharge pairs were available, spanning a water level range from 1.7 m to 5.3 m. The discharge time series span a time period of 57 years, from 1950 to 2007.

For Hvita by Kljafoss, a total of 38 water level and discharge pairs were available,
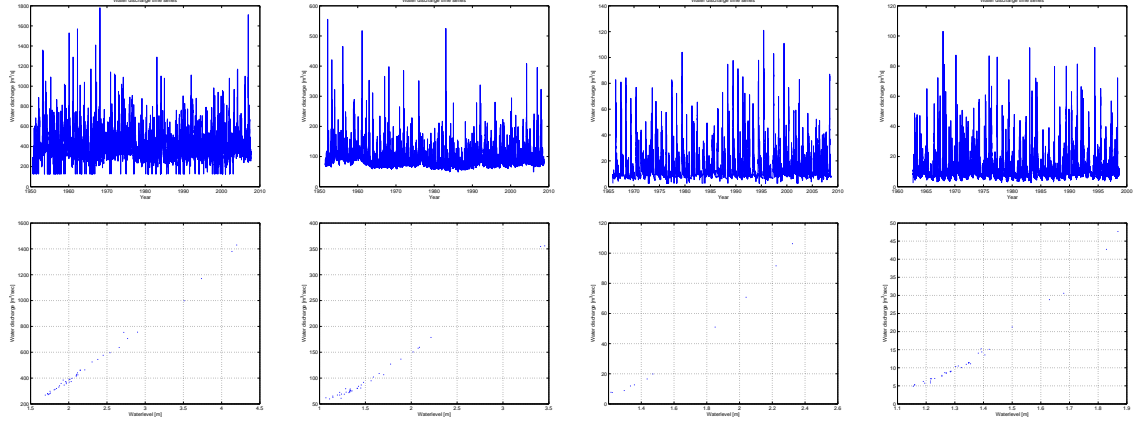
Figure 3.1: Top row: Water discharge time series. Bottom row: Water level and discharge pairs. First panels from the left: Olfusa. Second panels from the left: Hvita. Third panels from the left: Sanda. Fourth panels from the left: Svarta

spanning a water level range from 1.1 m to 3.5 m. The discharge time series span a time period of 57 years, from 1951 to 2008.

For Svarta in Skagafjordur, a total of 36 water level and discharge pairs were available, spanning a water level range from 1.2 m to 1.9 m. The discharge time series span a time period of 36 years, from 1962 to 1998.

The paired water level and discharge data are used to construct a B-spline discharge rating curve which will be used to estimate the uncertainty in the discharge time series used for the flood analysis.

The data sets used in the flood analysis are daily series of water discharge from four rivers in Iceland. The model is set up to analyze extremes in any river given this type of data. Flood analysis based on the model does not only provide point estimates of various quantities but it also takes into account the uncertainty in the underlying discharges and the uncertainty in the extreme analysis. This is accomplished by using Bayesian approach and Markov chain Monte Carlo (MCMC) algorithms. In particular, Gibbs samplers were used to construct the Markov chains in this study. The methods for constructing a Gibbs sampler are explained in detail in Gelman et al. (2003).

In this section, Bayesian inference for discharge rating curves and extreme value distributions is viewed. Then a new method for flood analysis is introduced. This method takes into account uncertainty in the extreme discharge values and the uncertainty in the parameters of the extreme value distributions. The uncertainty in the extreme discharge values is evaluated through the uncertainty in the corresponding discharge rating curves which can be accessed with the Bayesian approach. The

uncertainty in the parameters of the extreme value distributions stems from the uncertainty in the extreme discharge values and the usual uncertainty due to sampling, and is also accessed with the Bayesian approach.

3.2. B-spline discharge rating curves

The standard power-law methodology is traditionally used to model discharge rating curves. In, Hrafnkelsson et al. (2012), by using the Bayesian approach, the estimates of the rating curves were successfully improved with the use of B-spline extension to the standard power-law. The method, proposed by Hrafnkelsson, for constructing discharge rating curves with added B-splines, are used in this study. The first part of the method involves estimating the uncertainty in the water discharge data. This uncertainty comes from the fact that the water discharge levels are not measured but transformed from measured water levels. It is assumed that the water level is measured without uncertainty. The water level at each river is measured using devices that keep track of the water level at a fine time scale. These water levels are then transformed to water discharge by using discharge rating curves. The uncertainty in this transformation, and its effect on the flood analysis, is kept track of.

The most commonly used discharge rating curve is the standard power-law (Lambie (1978); Mosley and McKerchar (1993)). The standard power law relates the water level to the water discharge with the following equation

$$q = a(w - c)^b$$

where q is the water discharge, w is the water level, a is a positive scaling parameter, b is a positive shape parameter, and c is the water level when the discharge is zero. These parameters are estimated using pairs of water level and water discharge measurements. Since the pairs are expensive to collect, they are observed as often as resources allow and the timing of the measurements is chosen in order to get the widest range of both water level and water discharge.

For some rivers the standard power-law does not sufficiently represent the effect that a change in water level has on water discharge. Hrafnkelsson et al. (2012) showed how B-splines can be used to extend the standard power-law. The following is a model transforming water level to water discharge using the sum of the standard power law and a B-splines function,

$$q_i = a(w_i - c)^b + \sum_{l=1}^{L_k} \lambda_l B_{li} + \epsilon_i$$

where ϵ_i is a mean zero measurement error and

$$B_{li} = B_l((w_i - w_{low})/r), \quad l = 1, ..., L_k, \quad i = 1, ..., n$$

where n is the number of observations for a given site, and (w_i, q_i) denotes the i-th pair of observation. The terms $B_l(z)$ are cubic B-splines kernels which have support on the interval $[0, 1]$. Also, $r = w_{upp} - w_{low}$, where w_{upp} and w_{low} are the upper and lower points of the interval influenced by the B-spline. The B-spline parameters in $\lambda = (\lambda_1, ..., \lambda_L)$ are unknown and L_k is the number of B-spline kernels. The number of B-spline kernels was chosen to be 9. See further details on the construction of the B-spline rating curves in Hrafnkelsson et al. (2012).

MCMC algorithm is used to construct the B-spline rating curves. There are 4 chains, each having 10,000 iterations after the burn-in period. Thus, matrices of the size of $4 \times 10,000$, for the parameters a, b, and c, emerge for a set of water level/discharge pairs. And matrices of the size $4 \times 10,000$ for the B-spline parameters, representing $4 \times 10,000$ iterations for each of the B-spline parameters. Therefor, there are a total number of 40,000 different B-spline rating curves for each set of water-level/discharge pairs which represent the imprecision in the water-level to water-discharge transformation.

3.3. The block maxima model

The objective is to perform flood analysis using the data available while taking into account the uncertainty in the estimated discharge rating curves. This is accomplished using the Bayesian approach. The first task is to evaluate the uncertainty in the water discharge time series. These discharge levels are calculated with the use of discharge rating curves. The original water levels, that the discharge is calculated from, were not available but the discharge rating curves used for the transformation were. The water discharge time series are only point estimates and those estimates are the median value of a transformation from water levels using discharge rating curves with a range of uncertainty that should, at the correct stage, be taken into account.

The annual maximum levels of water discharge were collected. Figure 3.2 shows a

water discharge time series with the annual maximum values marked specifically.
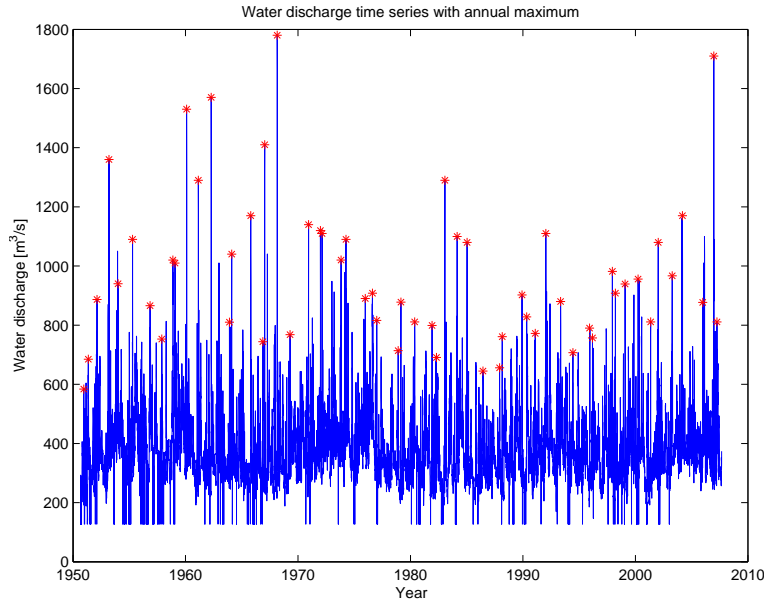
Figure 3.2: Water discharge time series with annual maximum values

The next goal was to estimate the uncertainty in the annual maximum water discharge levels. This was done through the B-spline discharge rating curves. At this point a MCMC analysis had already been performed on the B-spline rating curve based on the water-level/water-discharge pairs. A total of 40,000 different rating curves were sampled, all describing the relationship between water level and water discharge. A B-spline discharge rating curve is shown in Figure 3.3. The central curve is the median posterior of the discharge rating curve. The other two curves give a marginal 95% posterior interval and represent the uncertainty in the discharge rating curve.

After collecting the annual maximum point estimates for the water discharge it is possible to fit each and every one of them to the median value of a discharge rating curve, and the corresponding water levels associated with the water discharge levels are found. The water levels found by using the water discharge point estimates and the median of a rating curve, are then converted to water discharge again. This time, a set of $L = 40,000$ discharge levels are sampled for each of the water levels using a Gibbs sampler. The L discharge values, corresponding to each water level, represent the uncertainty in the point estimates originally used in the model, with the original values being the median values of each set. Figure 3.4 show the same B-spline rating curve as in Figure 3.3 but with the 2.5%, 50% and 97.5% percentiles of the calculated annual maximum water discharge levels. Figure 3.5 shows the water discharge time series with the same calculated percentiles for the annual maximum values.
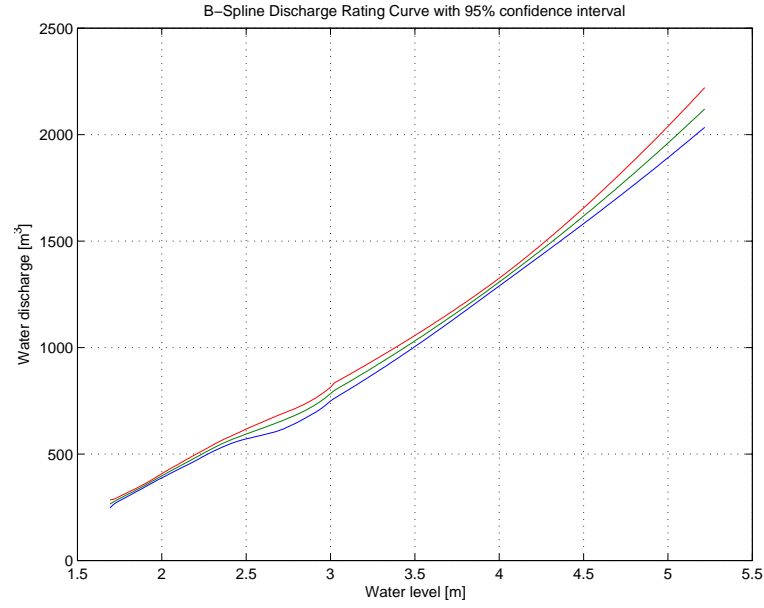
Figure 3.3: B-spline Discharge Rating curve with 95% confidence interval
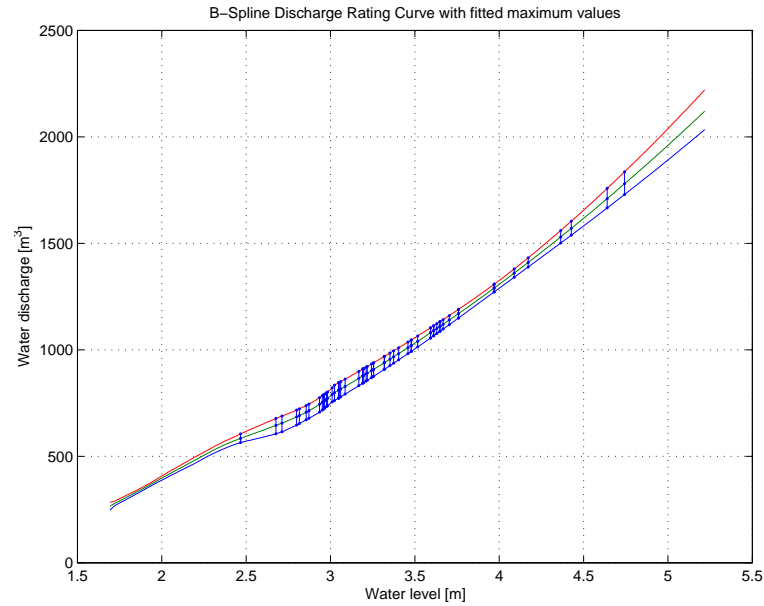
Figure 3.4: Discharge rating curve with fitted annual maximum values and their 95% confidence interval

For a given river, each annual maximum value is represented once in each vector of maximum values which corresponds to one sample of the discharge rating curve. Also, a single maximum value in one vector is related to a another maximum value in the same vector by the fact that they are all created by the same discharge rating curve. Therefore, there are 40,000 vectors of annual maximum values which will be fitted with the Generalized Extreme Value distribution in a Bayesian computing
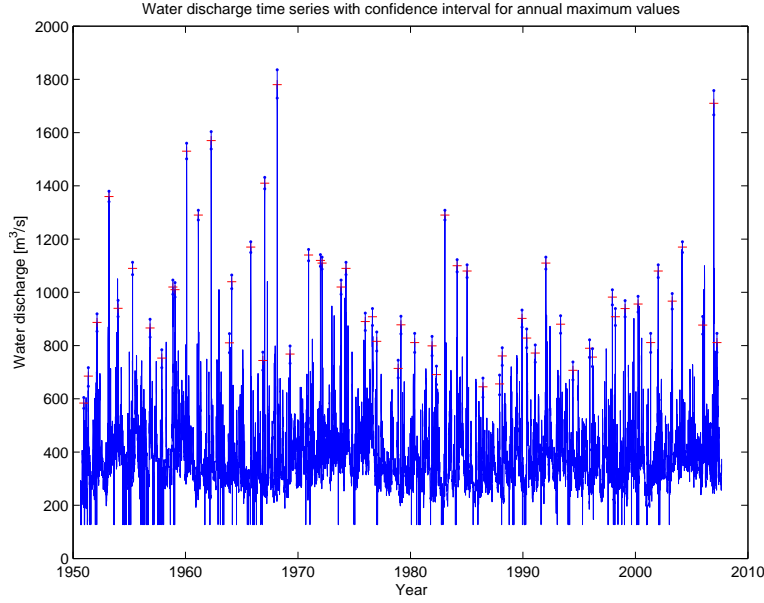
Figure 3.5: Water discharge time series with 95% confidence interval for extreme values

scheme.

3.3.1. Sampling distribution

The following sampling distribution is assumed for the annual maximum values, namely the Generalized Extreme Value distribution, which is given by

$$p(y_i|\mu,\sigma,\xi) = \frac{1}{\sigma}\Big[1+\xi\Big(\frac{y_i-\mu}{\sigma}\Big)\Big]^{-(\frac{1}{\xi})-1} \times \exp\Big\{-\Big[1+\xi\Big(\frac{y_i-\mu}{\sigma}\Big)\Big]^{-\frac{1}{\xi}}\Big\} \qquad (3.1)$$
$$= \text{GEV}(y_i|\mu,\sigma,\xi)$$

Where y_i is a set of extreme values generated with the B-spline rating curve, μ is a location parameter, σ is a scale parameter, and ξ is a shape parameter.

3.3.2. Prior distribution of μ, σ and ξ

Prior distributions provide the region of values for the parameters and corresponding prior probabilities. The prior distributions can have a substantial effect on the posterior distributions, both the region of values and the probabilities. For example,

29

the region of values of the posterior distribution cannot be outside the region of values of the prior distribution. If a noninformative prior distribution is chosen for the parameters, the posterior density will converge toward the maximum likelihood function of those parameters. But an informative prior distributions can have a great effect on how the posterior distribution of those parameters will look like. By choosing informative prior for one or more of the parameters, certain limits can be set the posterior density. For example, a prior distribution containing negative values only, will force the corresponding posterior samples to be negative. Thus the task of choosing an informative prior has to be done with great care, as it can influence the result of the statistical model.

For the scale parameter, σ, a noninformative prior is chosen, allowing the posterior to take any desired value and to be mainly determined by the data.

The prior distribution for the location parameter, μ, is a noninformative prior. It is a normal distribution which centers around zero and has a very large variance. Because of its large variance, will not constrain the posterior in any way and is therefore very non-informative.

For the shape parameter, ξ, three different cases are examined, and the effect of these different prior distributions is compared. In the first case, the prior distribution is non-informative. It is a normal distribution which centers around zero and has a large variance, making it highly non-informative. The second and third case constrain the shape parameter to negative values. That results in the tail of the GEV distribution to be bounded, i.e., it has an upper limit and so do the extreme values. The reasoning for allowing this constraint is that, it is reasonable to assume that water discharge can not be infinitely great.

The prior distributions chosen for the μ and σ parameters are as follows:

$$p(\mu) = \text{N}(\mu | \eta_\mu = 0, \tau_\mu^2 = 1000000) \tag{3.2}$$

$$p(\sigma) = \text{Inv} - \chi^2(\nu_0 = 10^{-12}, s_0^2 = 1) \tag{3.3}$$

The three different prior distribution for the ξ parameter are given below.

The normal prior density is given by

$$p(\xi) = \text{N}(\xi | \mu_\xi = 0, \sigma_\xi^2 = 1000) \tag{3.4}$$

This normal distribution is an noninformative prior. It has a large variance and does not restrict the ξ parameter.
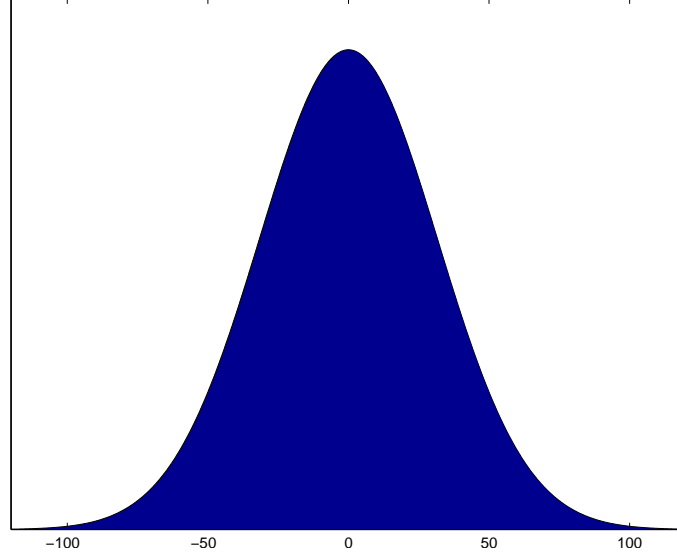
Figure 3.6: Normal prior density for ξ with $\mu = 0$ and $\sigma^2 = 1000$

The negative gamma prior density is given by

$$p(\xi) = \text{Neg-Gamma}(\xi|\alpha, \beta) \tag{3.5}$$

$$= \frac{\beta^\alpha}{\Gamma(\alpha)}\xi^{\alpha-1}e^{\beta\xi}, \qquad \xi < 0 \tag{3.6}$$

where $\alpha > 0$ and $\beta > 0$.

With $p(\xi) = \text{Neg-Gamma}(\xi|1, 5)$ as a prior distribution, the ξ parameter is constrained to negative values only. That has the effect that the upper tail of the posterior distribution will be bounded and thus there will be an upper limit on the size of floods.

Majority of the mass of the distribution is close to the y-axis as is shown in Figure 3.7. The purpose of that, is to investigate wether the restriction would lead to better results for data sets that were prone to positive values of the shape parameter, than to use a negative uniform prior distribution, as is done in Case 3.

The negative beta prior density is given by

$$p(\xi) = \text{Neg-Beta}(\xi|a, b) \tag{3.7}$$

$$= \frac{\Gamma(a + b)}{\Gamma(a)\Gamma(b)}(-\xi)^{a-1}(1 + \xi)^{b-1}, \qquad -1 \leq \xi \leq 0 \tag{3.8}$$

where $a > 0$ and $b > 0$

Negative Gamma Distribution with $\alpha = 1$ and $\beta = 5$
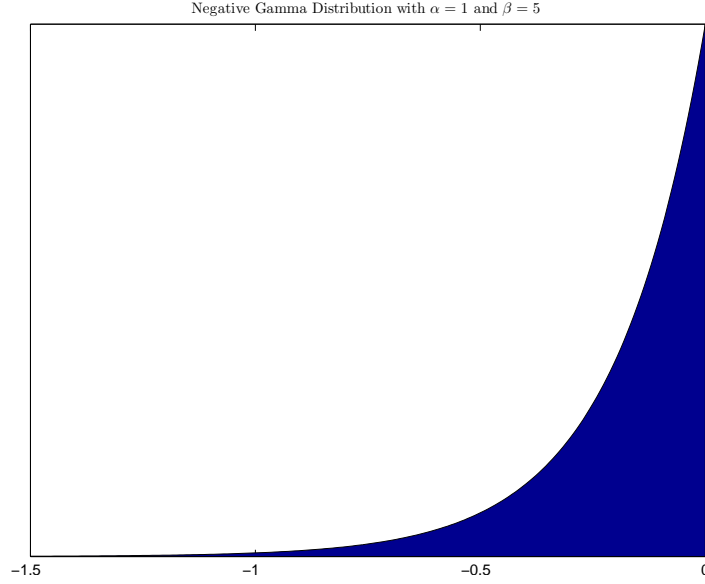
Figure 3.7: Negative gamma prior density with $\alpha = 1$ and $\beta = 5$

With $p(\xi) = \text{Neg-Beta}(\xi|1,1)$ as a prior distribution, the ξ parameter is constricted to negative values only. The prior is a uniform distribution evenly distributed along the interval $[-1, 0]$. As is discussed in Section 2.2, the interval of possible values that the shape parameter can take is approximately $[-0.5, 1]$. Values below -0.5 rarely occur in extreme value analysis and hence the negative beta prior distribution eliminates all positive values of the posterior distribution, resulting in a bounded upper tail distribution, without further effects on the shape of the posterior distribution within the negative region. The prior distribution is shown in Figure 3.8.

3.3.3. Posterior distribution of μ, σ and ξ

The posterior distribution of $\theta = (\mu, \sigma, \xi)$ is not based on a single vector of n independent observations of extreme discharge but on L vectors of length n sampled through the uncertainty in the discharge rating curve, which reflect the uncertainty in the observed discharge. Denote the k-th vector by y_k and $y_k = (y_{1k}, y_{2k}, ..., y_{nk})$. Since each of the L vectors is equally likely to be drawn, they should have an equal influence on the posterior density of θ. Thus the posterior density of θ is a mixture of the posterior densities corresponding the each of the vectors of length n, each with weight L^{-1}.

The form of the posterior density of θ is given by

Negative Beta Distribution with $\alpha = 1$ and $\beta = 1$
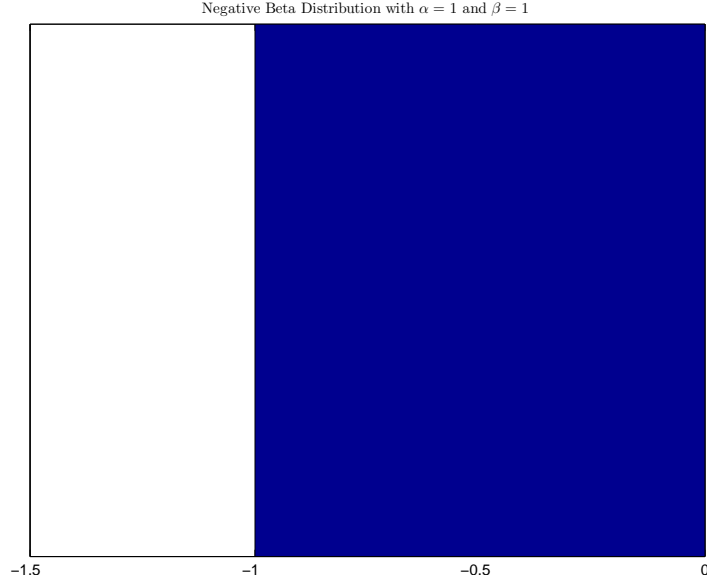
Figure 3.8: Negative beta prior density with $a = 1$ and $b = 1$

$$p(\theta|y) = \sum_{k=1}^{L} p(\theta|k, y_k)p(k) \cdot L^{-1} \tag{3.9}$$

$$= \sum_{k=1}^{L} p(\theta|y_k) \cdot L^{-1} \tag{3.10}$$

$$= \sum_{k=1}^{L} \frac{p(\theta)p(y_k|\theta)}{p(y_k)} \cdot L^{-1} \tag{3.11}$$

$$= L^{-1}p(\theta) \sum_{k=1}^{L} \frac{p(y_k|\theta)}{p(y_k)} \tag{3.12}$$

where y is the collection of all the y_k vectors and each vector y_k has a number of n elements.

More specifically, using μ, σ, and ξ instead of θ, the posterior density of μ, σ, and ξ is given by

$$p(\mu, \sigma, \xi|y) \propto p(\mu)p(\sigma)p(\xi) \left\{ \sum_{k=1}^{L} \frac{p(y_k|\mu, \sigma, \xi)}{p(y_k)} \right\}$$

$$\propto p(\mu)p(\sigma)p(\xi) \left\{ \sum_{k=1}^{L} \prod_{i=1}^{n_k} \left[\frac{\text{GEV}(y_{ik}|\mu, \sigma, \xi)}{\int\int\int \text{GP}(y_{ik}|\mu, \sigma, \xi)d\mu d\sigma d\xi} \right] \right\}$$

A general sampling scheme based on the Gibbs sampler should be as follows. Sample k from 1,2,...,L with equal probability L^{-1} and obtain corresponding y_k. Given k, sample $\theta = (\sigma, \xi)$ from

$$p(\mu, \sigma, \xi|y_k) = \frac{p(\mu, \sigma, \xi)p(y_k|\mu, \sigma, \xi)}{p(y_k)} \propto p(\mu, \sigma, \xi)p(y_k|\mu, \sigma, \xi)$$

The Gibbs sampler is applied for this simulation, i.e., samples are drawn from the following conditional distributions,

$$p(\mu|\sigma, \xi, y_k) \propto p(\mu) \times \prod_{i=1}^{n} \text{GEV}(y_{ik}|\mu, \sigma, \xi)$$

$$p(\sigma|\mu, \xi, y_k) \propto p(\sigma) \times \prod_{i=1}^{n} \text{GEV}(y_{ik}|\mu, \sigma, \xi)$$

$$p(\xi|\mu, \sigma, y_k) \propto p(\xi) \times \prod_{i=1}^{n} \text{GEV}(y_{ik}|\mu, \sigma, \xi)$$

However, since L is large and the weight of each $p(\mu, \sigma, \xi|y_k)$ is the same in $p(\theta|y)$, then μ, σ and ξ are only sampled once for each y_k. The construction of a Gibbs sampler is explained in details in Gelman et al. (2003).

The Gibbs sampler uses Metropolis and Metropolis Hastings algorithms to sample from the posterior distributions of the GEV parameters. These algorithms are adaptations of a random walk that uses an acceptance/rejection rule to converge to the specified target distributions (Gelman et al. (2003)). A Metropolis step is used to sample from the posterior distribution for μ. A Metropolis Hastings step with a gamma proposal density is used to sample from the posterior distribution of σ. The simulation for the posterior distribution of the ξ parameter depends on what type of prior distribution was used for the parameter. For a normal prior distribution, a Metropolis step is used to sample from the posterior distribution. A Metropolis Hastings step with gamma and beta proposal densities are used when sampling from

the posterior distribution in the cases when the prior distribution is the negative gamma distribution and the negative beta distribution, respectively. The parameters of the proposal distributions are fine tuned in order to get the acceptance rate of the simulations approximately equal to 44%, form optimal convergence (Gelman et al. (2003)).

Since there are 40,000 sets of annual maximum values, 40,000 samples from the posterior distributions are generated.

3.4. The threshold model

It is more complicated to gather data to use in the threshold model than it is for the block maxima model when the uncertainty in the discharge rating curve is taken into account. The objective is to find all data above a certain threshold, u. The values that exceeded the threshold, u, were found and the threshold value subtracted from the them. These threshold excesses are called peaks over threshold (POT). The POTs were fitted to a GP distribution using the Bayesian approach for inference for the parameters. The original point estimates of water discharge were examined to find this data. Just as in the block maxima model, the uncertainty of the discharge estimates is taken into consideration. The vectors of uncertainty for the discharge come as a result of the uncertainty in the discharge rating curves (DRC), projecting water levels to water discharge.

Figure 3.9 shows the water discharge time series along with the threshold value displaying the point estimates that will be used as extreme values in the model. The figure also displays the calculated uncertainty interval. Note that there are point estimates being used as extremes that are below the threshold value. These values are marked as red in Figure 3.9. This is due to the uncertainty in the discharge values. 40,000 sets of parameters have been sampled for the DRC which are used to estimate the uncertainty in the discharge values. A number of them will overlap the threshold value, i.e., for point estimates of discharge close to the threshold value, the vector representing the discharge will consist of values both over and under the chosen threshold. In those instances only the values that exceed the threshold, u, were used. For that reason the *effective number of POTs* is introduced. It is the true value of the number of POTs used in the model. Thus, for example, if the median of a extreme value is exactly the same as the threshold value, then 50% of the values in the discharge vector will be below the threshold and 50% will be above it. Only the values that exceed the threshold are used in the model. This particular POT would therefore only be used in 50% of the iterations in the Gibbs sampler and would count as a half effective POT.

Water discharge time series
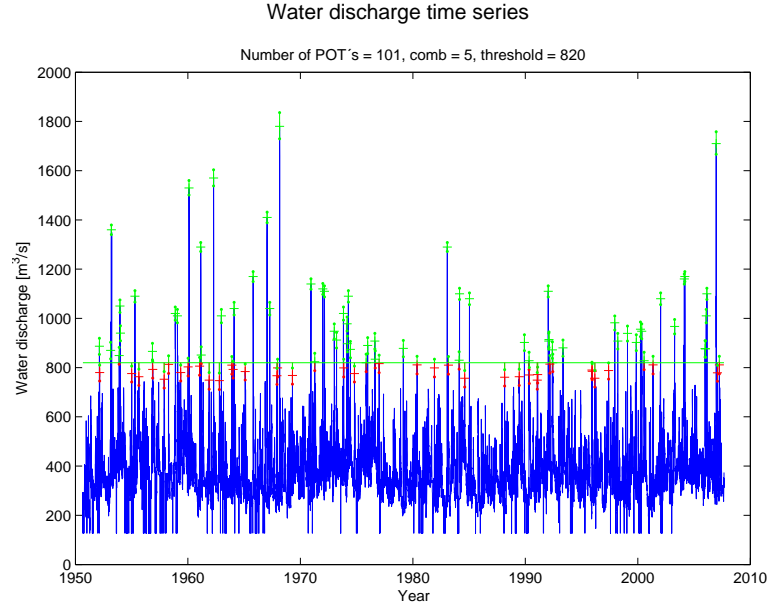
Figure 3.9: Time series of water discharge with threshold and a comb

In Figure 3.10 the peaks over threshold and the uncertainty in each peak are plotted as a function of water level. There are 40,000 values representing each POT but only the values exceeding the threshold will be used in the threshold model in the corresponding iterations in MCMC scheme. Therefore, in the MCMC algorithm that follows, the number of peaks over threshold will vary in each iteration depending on the set of parameters used for the DRC in that iteration.
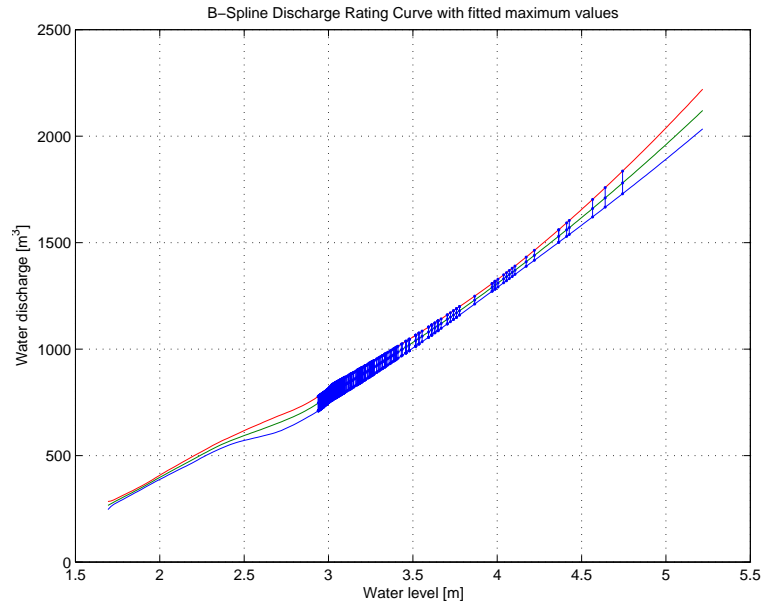
Figure 3.10: Discharge rating curve with fitted POT values

3.4.1. De-clustering the POTs

One of the problems with the threshold model is identifying extreme events. It is realistic to think of the water discharge time series as being auto-correlated, hence an extreme event is likely followed by another big event. This is the case for most natural phenomena, as is evident in day-to-day life, e.g., an extremely hot day is likely to be followed by another. Similarly, big floods are not necessarily limited to one day but are more likely to last for some period of time. Therefore, it is not sufficient to take all values above a threshold as some of the values are likely to belong to the same event. Therefore the peaks over threshold were de-clustered (Davison and Smith (1990)). With the purpose of removing undesired correlation between peaks, water discharge levels are grouped into clusters where each cluster is regarded as a single event. The largest value in each cluster is then used in the model.

A variable, referred to as *the comb*, is used to describe the methodology when de-clustering the data. If, for example, the value of the *comb* was set equal to 1, then for a new extreme event to take place there would have to be at least 1 discharge value in between peaks where the discharge was less than the threshold value. For a *comb* = 0 there is no de-clustering. In broader terms: for a comb value equal to C, two clusters/events will have to be separated with at least C consecutive days between peaks where the discharge is less than the threshold value. After the peaks were sorted to clusters, only the largest discharge value per cluster was used in the threshold model. Figure 3.11 illustrates the de-clustering of POTs with 4 different comb values.

Figure 3.12 shows how the number of POTs changes with respect to threshold value, for different comb values.

3.4.2. Choosing a threshold

Choosing an appropriate threshold value is very important in extreme analysis. The objective is to gather appropriate data to model the tail behavior of the underlying distribution, i.e. explore the extremes. Too small threshold value would result in too many POTs which should not be regarded as extremes, skewing the result of the flood analysis. A too high of a threshold value would leave to many extreme values
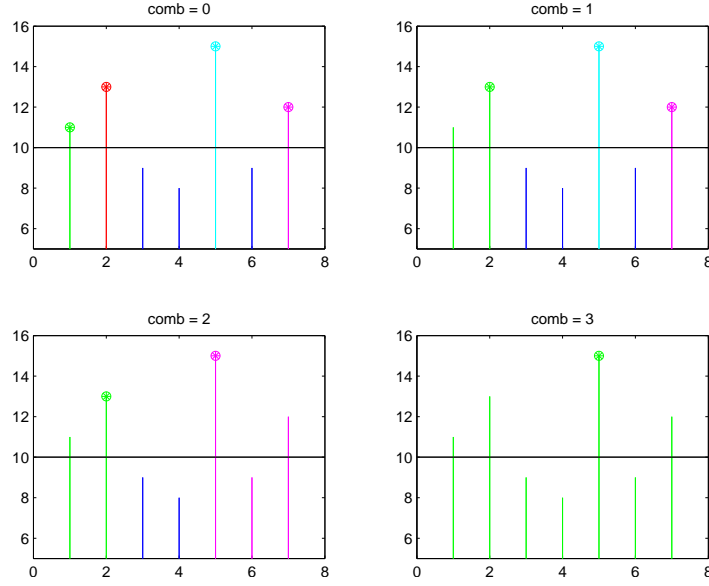
Figure 3.11: De-clustering data for 4 different values of the comb. Each cluster is displayed as a certain color and the maximum value of each cluster marked with a circle.
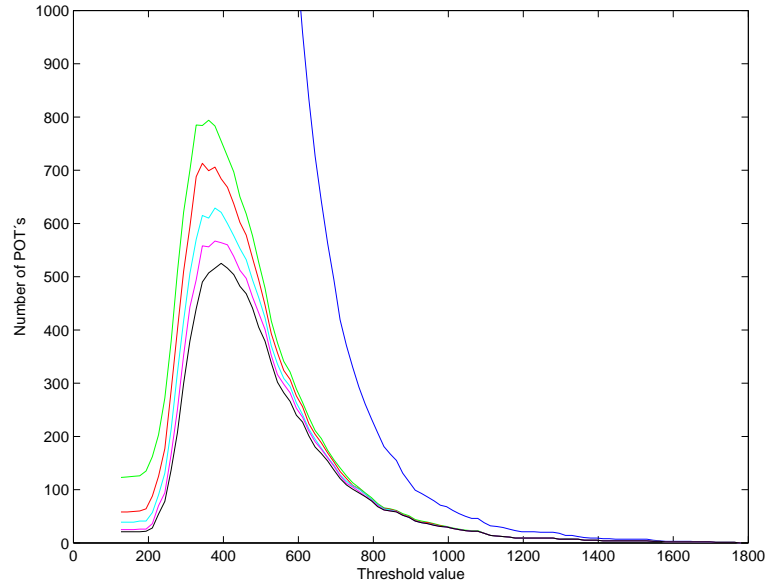
Figure 3.12: The effect of the comb on the number of POTs for the river Olfusa. Displaying curves showing the number of POTs w.r.t. threshold for comb values: 0, 1, 2, 3, 4 and 5 with appropriate curves being blue, green, red, cyan, magenta and black, respectively.

out of the analysis, increasing the sampling uncertainty. Extreme values that could have helped in understanding the tail behavior would be left out and therefore the results will not be as accurate as they could have been. In the quest of finding the best threshold value a few guidelines, discussed below, were adopted.

Mean residual life plot (MRLP)

The mean residual life plot for threshold selection was examined in details by Davison and Smith (1990). Since then, it has been a popular method for selecting a threshold. According to the extreme analysis theory: If Y has a GP distribution, the following holds

$$E(Y) = \frac{\sigma_t}{1 - \xi}$$

where σ_t and ξ are the parameters of the GP distribution with threshold t. Therefore, if X is a time series and u_0 is a threshold value,

$$E(X - u_0 | X > u_0) = \frac{\sigma_{u_0}}{1 - \xi}$$

where σ_{u_0} is the scale parameter of the GP distribution corresponding to the threshold value u_0. Since $(X - u_0)$ conditional on $X > u_0$ follows the GP distribution every threshold value larger than u_0 has to have the same affect, i.e., the conditional excess over threshold value follows the GP distribution. Therefore if $u > u_0$:

$$E(X - u | X > u) = \frac{\sigma_u}{1 - \xi}$$

However, there is a clear relationship between scale parameters with different threshold values,

$$E(X - u | X > u) = \frac{\sigma_{u_0} + \xi(u - u_0)}{1 - \xi} \tag{3.13}$$

that is, the mean of the residual life with respect to the threshold, u. So if u_0 is the smallest possible threshold value that leads to a GP distribution for the peaks over threshold (POT), then the expected value of the POT is linear with respect to u, for all u larger than u_0. That is shown in Equation (3.13) since the shape parameter (ξ) is, in theory, constant for all $u > u_0$

Based on the theory explained above, a *mean residual life plot (MRLP)* was developed. A *MRLP* is constructed in the following way: let u be any threshold value less than x_{max}, where x_{max} is the largest observation. Let $x_{(i)}$ denote the i-th largest

value out of n_u largest values, where n_u is the number of peaks over threshold for a given u.

$$\left\{ \left(u, \frac{1}{n_u} \sum_{i=1}^{n_u} \left(y_{(i)} - u \right) \right) : u < y_{max} \right\} \tag{3.14}$$

A threshold value is determined by looking at the *MRLP* and finding the smallest value where the plot becomes linear with respect to u.

An example of MRLP is shown in Figure 3.13.
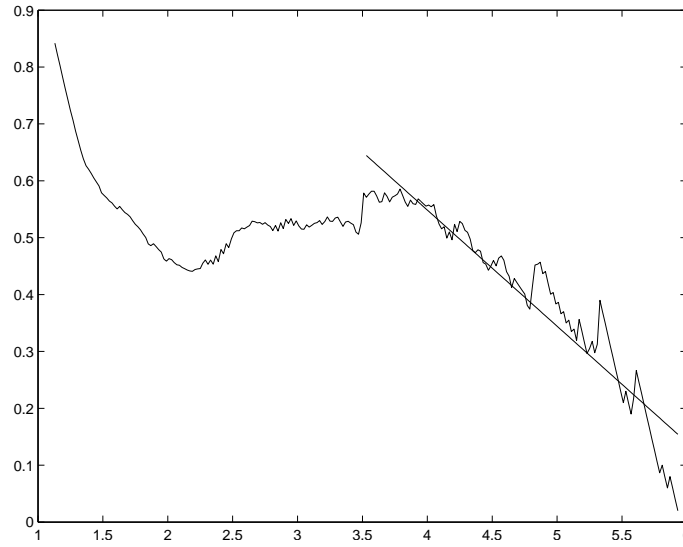
Figure 3.13: Mean Residual Life plot (MRLP) along with a line illustrating the linear relationship between mean residual life and u. An appropriate threshold value according to this MRLP could be $u \approx 3.5$

Parameter estimates

Another way of determining an appropriate threshold value is observing the behavior of the scale- and shape parameters of the GP distribution with increasing threshold value. This approach was also discussed in detail by Davison and Smith (1990). The theory states that for all threshold values larger than the smallest possible threshold value, u_0, there is a strong relationship between the GP parameters. i.e. for all $u > u_0$ the shape parameter (ξ) remains the same and the relationship between the scale parameters, σ_u and σ_{u_0} are as follows:

$$\sigma_u = \sigma_{u_0} + \xi(u - u_0)$$

Define σ^* as

$$\sigma^* \equiv \sigma_{u_0} - \xi u_0 = \sigma_u - \xi u.$$

The new scale parameter, σ^*, is a function of σ_{u_0}, ξ and u_0 and should thus be constant for all threshold values, u, that are larger than the smallest possible threshold value, u_0.

Using this information it is possible to observe whether the parameters, σ^* and ξ change with increasing threshold value, u. When the *smallest desired threshold value*, has been reached, u_0, these two parameters should be constant for all larger values of the threshold. In theory, the ideal threshold value is u_0. All values below would skew the result of the flood analysis, because too many values are being used in the analysis. A too high of a threshold value would leave to many extreme values out of the analysis, increasing the sampling uncertainty. This method of choosing a threshold is shown in Figure 3.14.
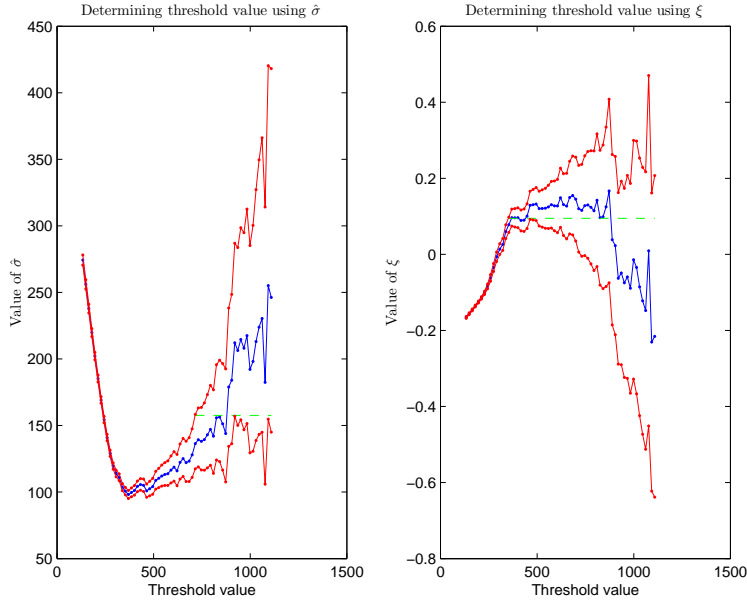
Figure 3.14: σ^* and ξ along with their 95% confidence interval as a function of threshold value

Figure 3.14 shows both the σ^* parameter and the ξ parameter as a function of threshold value along with 95% confidence interval of the parameter estimates. From

Figure 3.14, using the left panel, relying on σ^*, it would be concluded that a reasonable value for *the smallest desired threshold* is approximately $u_0 = 750$. From the right panel of the figure, relying on ξ, it would be concluded that the smallest desired threshold is approximately $u_0 = 500$. These values are approximately the lowest threshold value where a single value for the parameters fits inside the 95% confidence interval for all $u > u_0$. In theory these two threshold values should be the same. From this it would be concluded that the threshold value should not be chosen below $u_0 = 750$, which is the lowest threshold value to be applicable in both methods.

General methods

Along with the methods described above in finding an appropriate threshold value, a couple of "rules of thumb" were used.

Firstly, a threshold was chosen so that the number of *peaks over threshold* will be in the range of $1 - 2.5$ times the number of years of data available. The *Generalized extreme value distribution* is the foundation of the *Generalized Pareto distribution* and the GEV distribution is based on sorting the data into blocks, which could be regarded as independent, and picking the maximum value of that block. A time span of one year is an obvious block size when looking at data which depend on an annual cycle. Thus, it seems a reasonable constraint to limit the number of POTs w.r.t. number of years of data as described above. If the number of POTs is greater than 2.5 times the number of years it is likely that some of the them should not be regarded as extremes.

Secondly, a special consideration is given to the threshold value that produce a number of POTs that is exactly the same as the number of years inspected. This method has been used at the *Icelandic Meteorological Office* as a rule of thumb. It has proved a successful and simple way of determining a threshold value. This method of determining the threshold will be referred to as the *fixed frequency method* (FFM).

With the fixed frequency method a threshold is chosen so the number of point estimates of discharge that are above the threshold, after de-clustering, are equal to the number of years of data used in the analysis. However, some of the simulated discharge values (corresponding to a given day) will have a point estimate of discharge below the threshold and only some of the simulated values will be above the threshold. Similarly, some of the discharge values used in the model will be such that the point estimate is just barely above the threshold and thus the portion of their uncertainty vector that falls below the threshold will not be used in the model. This has the effect that, on average, the effective number of POTs used for a par-

ticular river will be the same as the number of discharge point estimates above the threshold.

The method of choosing a threshold by using the mean residual life plot, the parameter estimates, and having the number of POTs in the range of $1 - 2.5$ times the number of years, is from now on referred to as the *diagnostic based method* (DBM).

3.4.3. Sampling distribution

When modeling POTs, water discharge series over a fairly long period is needed. A suitable threshold is determined, denoted u, and all the values of the series which exceed u are found. Then the threshold value, u, is subtracted from these discharge value. Next the POTs are de-clustered using a comb value equal to 5 and the new de-clustered series fitted with the generalized Pareto distribution. This new series will be denoted by y_i, $i = 1, 2, ..., n_u$. The cumulative density function (cdf) for the GP distribution is

$$H(y) = 1 - \left(1 + \frac{\xi y}{\tilde{\sigma}}\right)^{-\frac{1}{\xi}} \tag{3.15}$$

defined on $y : y > 0$ and $(1 + \xi y / \tilde{\sigma}) > 0$, where

$$\tilde{\sigma} = \sigma + \xi(u - \mu)$$

Therefore the sampling distribution of y_i is

$$p(y_i | \tilde{\sigma}, \xi) = \frac{\xi}{\tilde{\sigma}} \left[1 + \frac{\xi y_i}{\tilde{\sigma}}\right]^{-\left(1 + \frac{1}{\xi}\right)} \tag{3.16}$$

for $i = 1, 2, ..., n_u$, where $y = x_i - u$ and $y > 0$, where x_i is the corresponding discharge value.

3.4.4. Prior distribution

The same reasoning as in the block maxima model is applied when choosing prior distributions for the parameters of the GP distribution. There are only two parame-

ters to emulate in the GP distribution as apposed to three in the GEV distribution, but the two are closely related to the comparable ones in the GEV distribution.

For the scale parameter, $\tilde{\sigma}$, a non-informative prior distribution was chosen, allowing the posterior to take any desired value. The prior distribution for the scale parameter is:

$$p(\tilde{\sigma}) = \text{Inv-}\chi^2(\nu_0 = 10^{-12}, s_0^2 = 1) \tag{3.17}$$

For the shape parameter, ξ, as in the case of the block maxima model, three different prior distribution were examined. The first one is non-informative, a normal distribution with the mean equal to zero and a large variance, allowing the parameter to take all possible values. In the second and third cases the prior distribution is constrained to negative values only.

The three different cases for the prior distribution for the ξ parameter are given below.

The Case 1 normal prior density is given by

$$p(\xi) = \text{N}(\xi|\mu_\xi = 0, \sigma_\xi^2 = 1000000) \tag{3.18}$$

The Case 2 negative gamma prior density is given by

$$p(\xi) = \text{Neg-Gamma}(\xi|\alpha_\xi = 1, \beta_\xi = 5) \tag{3.19}$$

with $p(\xi) = \text{Neg-Gamma}(\xi|1, 5)$ as a prior distribution, the ξ parameter is con-stricted to negative values only. Majority of the mass of the distribution is close to the y-axis as is shown in Figure 3.7

The Case 3 negative beta prior density is given by

$$p(\xi) = \text{Neg-Beta}(\xi|\alpha_\xi = 1, \beta_\xi = 1) \tag{3.20}$$

With $p(\xi) = \text{Neg-Beta}(\xi|1, 1)$ as a prior distribution, the ξ parameter is constricted to negative values only. The prior is a uniform distribution evenly distributed on the interval $[-1, 0]$. The prior distribution is shown in Figure 3.8

3.4.5. Posterior distribution of σ and ξ from the generalized Pareto distribution

The posterior distribution of $\theta = (\hat{\sigma}, \xi)$ is not based on a single vector of n independent observations of extreme discharge but on L vectors of length n_k, where $k = 1, ..., L$. The vectors are sampled through the uncertainty in the discharge rating curve, which reflect the uncertainty in the observed discharge. Denote the k-th vector by y_k and $y_k = (y_{1k}, y_{2k}, ..., y_{n_k k})$. Since each of the L vectors is equally likely to be drawn, they should be an equal influence on the posterior density of θ. Thus the posterior density of θ is a mixture of the posterior densities corresponding the each of the vectors of length n, each with weight L^{-1}.

The form of the posterior density of θ is given by

$$p(\theta|y) = \sum_{k=1}^{L} p(\theta|k, y_k)p(k) \cdot L^{-1} \tag{3.21}$$

$$= \sum_{k=1}^{L} p(\theta|y_k) \cdot L^{-1} \tag{3.22}$$

$$= \sum_{k=1}^{L} \frac{p(\theta)p(y_k|\theta)}{p(y_k)} \cdot L^{-1} \tag{3.23}$$

$$= L^{-1}p(\theta) \sum_{k=1}^{L} \frac{p(y_k|\theta)}{p(y_k)} \tag{3.24}$$

where y is the collection of all the y_k vectors and each vector y_k has a number of n_k elements.

More specifically, using $\tilde{\sigma}$ and ξ instead of θ, the posterior density of $\tilde{\sigma}$ and ξ is given by

$$p(\tilde{\sigma}, \xi|y) \propto p(\tilde{\sigma})p(\xi)\left\{ \sum_{k=1}^{L} \frac{p(y_k|\tilde{\sigma}, \xi)}{p(y_k)} \right\}$$

$$\propto p(\tilde{\sigma})p(\xi)\left\{ \sum_{k=1}^{L} \prod_{i=1}^{n_k} \left[\frac{\mathrm{GP}(y_{ik}|\tilde{\sigma}, \xi)}{\int \int \mathrm{GP}(y_{ik}|\tilde{\sigma}, \xi)d\tilde{\sigma}d\xi} \right] \right\}$$

A general sampling scheme based on the Gibbs sampler should be as follows. Sample

k from $1, 2, ..., L$ with equal probability L^{-1} and obtain corresponding y_k. Given k, sample $\theta = (\tilde{\sigma}, \xi)$ from

$$p(\tilde{\sigma}, \xi | y_k) = \frac{p(\tilde{\sigma}, \xi) p(y_k | \tilde{\sigma}, \xi)}{p(y_k)} \propto p(\tilde{\sigma}, \xi) p(y_k | \tilde{\sigma}, \xi)$$

The Gibbs sampler is applied for this simulation, i.e., samples are drawn from the following conditional distributions,

$$p(\tilde{\sigma} | \xi, y_k) \propto p(\tilde{\sigma}) \times \prod_{i=1}^{n_k} \mathrm{GP}(y_{ik} | \tilde{\sigma}, \xi)$$

$$p(\xi | \tilde{\sigma}, y_k) \propto p(\xi) \times \prod_{i=1}^{n_k} \mathrm{GP}(y_{ik} | \tilde{\sigma}, \xi)$$

However, since L is large and the weight of each $p(\tilde{\sigma}, \xi | y_k)$ is the same in $p(\theta | y)$, then $\tilde{\sigma}$ and ξ are only sampled once for each y_k. The construction of a Gibbs sampler is explained in details in Gelman et al. (2003).

The Gibbs sampler uses Metropolis and Metropolis Hastings algorithms to sample from the posterior distributions of the GP parameters. These algorithms are adaptations of a random walk that uses an acceptance/rejection rule to converge to the specified target distributions (Gelman et al. (2003)). The posterior distribution for $\tilde{\sigma}$ is simulated using Metropolis Hastings step with the proposal density being a gamma distribution. The simulation for the posterior distribution of the ξ parameter depends on what type of prior distribution was used for the parameter. For a normal prior distribution, a Metropolis step is used to sample from the posterior distribution. Metropolis Hastings steps with a gamma and a beta proposal densities were used when sampling from the posterior distributions in the cases when the prior distributions are the negative gamma distribution and the negative beta distribution, respectively. The parameters of the proposal distributions are fine tuned in order to get the acceptance rate of the simulations approximately equal to 44%, to obtain optimal convergence (Gelman et al. (2003)).

Since there are 40,000 sets of POTs, 40,000 values are generated for the posterior distributions of the GP parameters. By doing this the uncertainty in the discharge rating curve and the sampling uncertainty have been merged into the MCMC algorithm for Bayesian inference for the GP parameters.

4. Results and discussions

In this section, the previously outlined methods are used for flood analysis on four rivers in Iceland. The rivers are Sanda in Thistilfjordur, Olfusa by Selfoss, Hvita by Kljafoss and Svarta in Skagafjordur. Two different types of models were used for the flood analysis: the block maxima model and the threshold model. These models are described in detail in Sections 3.3 and 3.4, respectively. The block maxima model uses the generalized extreme value distribution (GEV) and fits the distribution with the annual maximum values for each river. The threshold model uses peaks over threshold (POTs), i.e. the excess of discharge values over a predetermined threshold value, and fits the generalized Pareto distribution (GP) to the POTs. Two methods were used when determining the threshold value, namely the diagnostic based method (DBM) and the fixed frequency method (FFM). These two methods of choosing a threshold value are described in Section 3.4.2. For each river, the choice of threshold value, using the diagnostic based method, is explained using the graphs introduced in Section 3.4.2. Thus, three different models are used in the flood analysis, one block maxima model and two threshold models.

In theory, the three parameter GEV distribution and the two parameter GP distribution share the same parameter, namely the shape parameter, ξ. This parameter controls the tail behavior of the distributions and is of major importance when performing extreme value analysis. Within the Bayesian framework, three different kind of prior distributions are chosen for the shape parameter, two of which restrains the resulting posterior parameter and alters the final results of the flood analysis. The effect of restraining the shape parameters is investigated and compared to no restriction at all. The Bayesian methods of sampling from the posterior distributions for the block maxima model and the threshold model are described in Sections 3.3.3 and 3.4.5, respectively.

Furthermore, the effect of using discharge rating curves, to model the uncertainty in the extreme values, is investigated. Specifically, B-spline discharge rating curves when transforming measured water level into water discharge and the associated uncertainty.

The results are presented through figures and tables with a different set of figures and tables for every case of prior distribution for the shape parameter. The figures displayed in this section come from models where the uncertainty in the discharge

rating curve are merged together with the sampling uncertainty in the GEV or GP distribution parameters. Further details on the flood analysis can be found in appendices A, B, C, and D. That includes probability plots, quantile plots and density plots for all cases of prior distributions. The prior and posterior densities of all the parameters in the GEV and GP distributions are also displayed for all cases. Also, MCMC chains of all posterior parameters, and the prior and posterior distributions of the GEV and GP parameters when a discharge rating curve is not taken into account in the extreme analysis.

Table 4.1 shows a list of abbreviations regarding, figures and tables in the Result section. Every figure and table in the section is marked with some of these abbreviations and that explains which river the data belongs to and what kind of models were used to generate the results. For example, the text *(V064 BM w/DRC) Case 2* in the caption of a figure or a table, indicates that the data displayed comes from the river Olfusa (V064), a block maxima model was used (BM) with a neg-gamma prior distribution for the shape parameter (Case 2), and the uncertainty in the discharge rating curve was taken into account in the calculations (w/DRC).

Table 4.1: Abbreviations used to explain the origin of the data used to generate figures and tables

V064:	The river Olfusa: 64 is the number of the gauging station measuring the data
V066:	The river Hvita vid Kljafoss: 66 is the number of the gauging station measuring the data
V026:	The river Sanda in Thistilfjordur: 26 is the number of the gauging station measuring the data
V010:	The river Svarta in Skagafjordur: 10 is the number of the gauging station measuring the data
Case 1:	The shape parameter, ξ, was sampled using a normal prior distribution
Case 2:	The shape parameter, ξ, was sampled using a neg-gamma prior distribution
Case 3:	The shape parameter, ξ, was sampled using a neg-beta prior distribution
BM:	A block maxima model
TM DBM:	A threshold model using the diagnostic based method for determining the threshold value
TM FFM:	A threshold model using the fixed frequency method for determining the threshold value
w/DRC:	A discharge rating curve uncertainty was taken into account in the calculations
w/o DRC:	A discharge rating curve uncertainty was not taken into account in the calculations

4.1. Results for Olfusa

The discharge time series for Olfusa spans 57 years, from September 1950 to September 2007. The daily point estimates of water discharge are shown in Figure 4.1.

The relationship between water level and water discharge is found by applying the B-spline discharge rating curve, as discussed in Section 3.2, on the paired water level and water discharge data for the river. The B-spline discharge rating curve is shown in Figure 4.1.
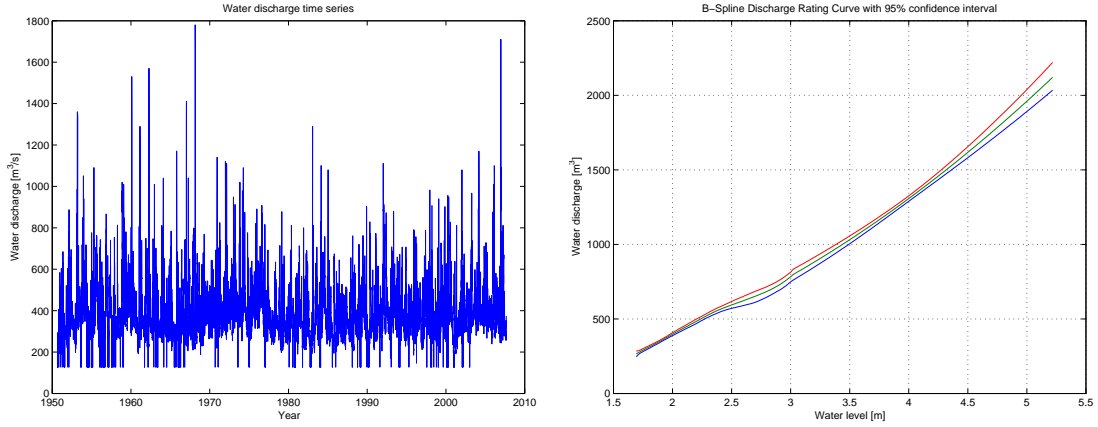
Figure 4.1: V064: Left panel: Water discharge time series. Right panel: B-spline Discharge Rating curve

4.1.1. Block maxima model

The annual maximum values used for the Block Maxima model are shown in Figure 4.2. It shows the discharge time series for the river with each annual maximum value visually highlighted with a star symbol. These values are point estimates of water discharge. The B-spline discharge rating curve (DRC) was applied to the annual maximum values to obtain the uncertainty in the estimates. Figure 4.3 shows how the discharge rating curve is used to estimate the uncertainty in the annual maximum values. In Figure 4.3 the highlighted annual maximum values from Figure 4.2 are fitted to the discharge rating curve and from that point it becomes manageable to estimate the uncertainty in the point estimate. This process is described in detail in section 3.3. Figure 4.3 shows the same water discharge time series as Figure 4.2 but also includes the 95% uncertainty interval for the annual maximum values.

The maximum annual values are fitted to the Generalized Extreme Value (GEV) distribution using a Markov Chain Monte Carlo scheme. The GEV distribution has three parameters, i.e., a location parameter μ, a scale parameter σ, and a shape paramter, ξ. The shape parameter is of special interest in our research and how it is effected by three different prior distributions. The three different cases of prior distributions for the ξ parameter in the GEV distribution are explained in detail in Section 3.3.2. The effect of the B-spline discharge rating curve on the flood analysis was also investigated. The construction of the B-spline discharge rating curve is discussed in Section 3.2 and the merging of the B-spline DRC with the GEV distribution, for the block maxima model, and the GP distribution, for the treshold model, is discussed in Sections 3.3 and 3.4, respectively.

The ways of checking the validation of the models are discussed in 2.2.2. Discussions on the development of the probability plots and the quantile plots can be found in
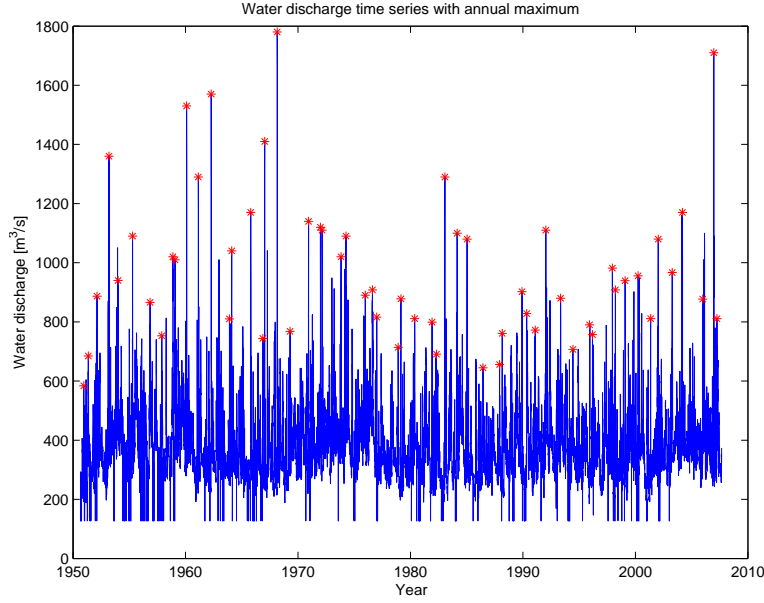
Figure 4.2: V064: Water discharge time series with annual maximum values
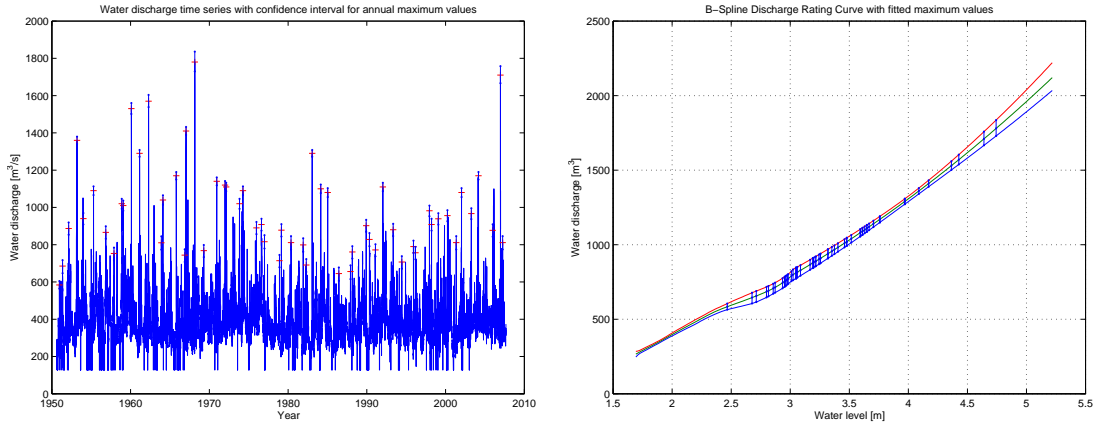
Figure 4.3: V064: Left panel: Water discharge time series with 95% posterior interval for extreme values. Right panel: B-spline discharge rating curve with fitted annual maximum values and their 95% posterior interval

Section 2.2.2. The return level plots and the plotting position of the empirical data on that plot, are discussed in Sections 2.2.1 and 2.2.2, respectively. The methods for conducting the Anderson-Darling test used to check the validity of the models are discussed in Section 2.2.2.
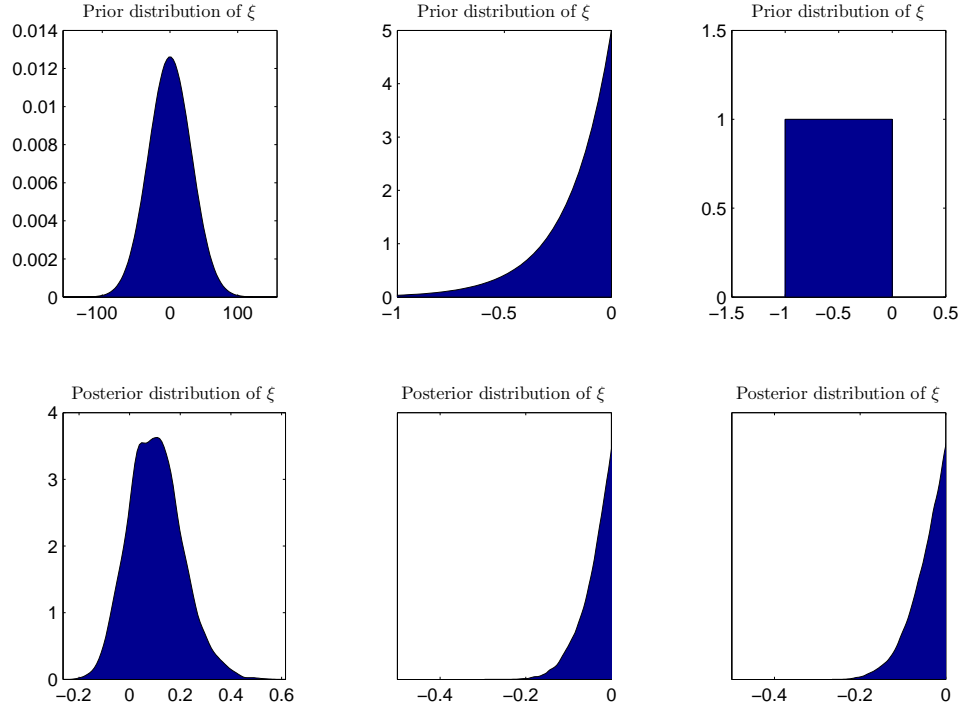
Figure 4.4: (V064 BM w/DRC): Prior and posterior distributions for the shape parameter (ξ) in the GEV distribution for all three cases of prior distributions. Case 1: left panels, Case 2: middle panels, Case 3: right panels.
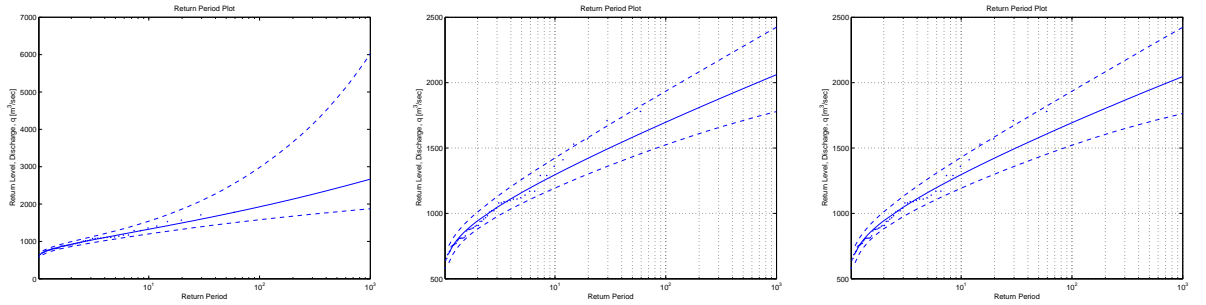
Figure 4.5: (V064 BM w/DRC): Return level plots for the block maxima model for all three cases of prior distributions. Case 1: left panel, Case 2: middle panel, Case 3: right panel.

Comparison between the three different cases of prior distribution for ξ

Figure 4.4 shows the prior distributions of ξ and their corresponding posterior distributions for all cases. Majority of the posterior distribution in Case 1 is positive and so constraining the posterior to only negative values has great influence on the results. Figure 4.5 show the return level plots for all three cases of prior distributions. Constraining the prior to negative values only, lowers the return levels and

Table 4.2: V064 BM: 100-year return levels of discharge (m^3/sec) for all three cases of prior distributions, calculated with and without a DRC

| | Block Extrema | | | | | |
| | With DRC | | | Without DRC | | |
Percentiles	Normal	Neg-Gamma	Neg-Beta	Normal	Neg-Gamma	Neg-Beta
2.5%	1581	1524	1521	1582	1529	1525
25%	1768	1632	1628	1772	1631	1628
50%	1927	1697	1693	1930	1695	1692
75%	2163	1772	1767	2148	1766	1765
97.5%	2980	1935	1935	2909	1926	1926
95% conf. int.	1399	410	414	1327	397	401

Figure 4.6: (V064 BM) Comparison of the 95% posterior interval of the 100-year return level of discharge, between the three cases of prior distributions, with DRC uncertainty (blue) and without DRC uncertainty (red).

makes the confidence interval narrower. This constriction has the effect that the data does not fit the model, as well as in Case 1.

Table 4.2 shows the 2.5%, 25%, 50%, 75%, and 97.5% percentiles of the 100-year return level for all three cases of prior distributions for the shape parameter, ξ. Figure 4.6 shows the 95% posterior interval of the 100-year return level for all three cases of prior distributions for the shape parameter, ξ, and the 2.5%, 50%, and 97.5% percentiles. The 95% posterior interval of the 100-year return level represents the uncertainty in the return level. Figure 4.6, shows how the uncertainty interval becomes smaller as the ξ value is restricted to negative value only.

Constraining the posterior density of ξ, to negative values only, by using negative prior distributions has a significant influence on the outcome of the posterior distributions and thus the resulting return levels. In the case where the prior distribution for the shape parameter is a normal distribution, the posterior distribution has more tendency to be positive than negative, having a mean value of 0.10 (see Table A.2). Constraining the priors has similar effects on the posteriors as eliminating the positive portion of the Case 1 posterior density. The negative part of the posterior density using the non-informative normal prior is similar to the posterior distributions resulting from the constraining priors. Since a higher value of ξ leads to thicker tail of the GEV distribution and hence larger return values, eliminating the positive portion of the ξ values reduces the return levels and the range for their 95% posterior intervals for high return periods. This reduction in the posterior densities of ξ, has the effect that the models in Cases 2 and 3, using the negative priors, do not fit the data as well as the model in Case 1.

Thus, constraining the ξ parameter to negative values only, has the effect that the median value of the 100-year return level becomes lower for both the negative gamma prior distribution (12% lower) and the negative beta prior distribution (13% lower). Furthermore, the uncertainty interval for the constraining prior distributions shrinks to approximately 26% of the uncertainty interval for the non-informative normal prior distribution.

Since majority of the posterior density when using the non-informative normal prior distribution, was positive, the median value of the 100-year return level is greater than the 97.5 percentiles for the 100-year return levels for the restricting prior distributions.

The effect of discharge rating curve uncertainty

The effect of merging the discharge rating curve uncertainty with the sampling uncertainty from the MCMC scheme has minor effect on the median value of the 100-year return levels and moderate effect on the 95% posterior intervals. This is shown in Table 4.2 and Figure 4.6. There is a change in the over all uncertainty for the 100-year return level, when adding the discharge rating curve uncertainty to the calculations. In Case 1, where the prior distribution is a normal distribution, the 95% posterior interval increases approximately 11%, when DRC uncertainty is taken into account. In Case 2, where the prior distribution is a negative gamma distribution, the 95% posterior interval increases approximately 3%, when DRC uncertainty is taken into account. In Case 3, where the prior distribution is a negative beta distribution, the 95% posterior interval increases approximately 1.5%, when DRC uncertainty is taken into account.

4.1.2. Threshold model

The first thing to do when using the threshold model is to choose the value of the threshold. A comb value of 5 was chosen in the threshold model for this river. As described in the Section 3.4.2, there are a few guidelines to be used when doing so. Figure 4.7 shows a mean residual life plot (MRLP) (green solid graph) (see Section 3.4.2) and it also shows how the number of peaks over threshold (POT) vary with respect to threshold value (blue solid graph). Furthermore, in the figure, the two vertical blue lines mark the interval where the number of POTs are, on one hand, equal to the number of years investigated in the data set (the right blue vertical line) and, on the other hand, where the number of POTs are equal to the number of years inspected times 2.5 (the left blue vertical line). One way to determine a threshold value is by looking at the MRLP and finding the smallest value where the plot becomes linear with respect to threshold.
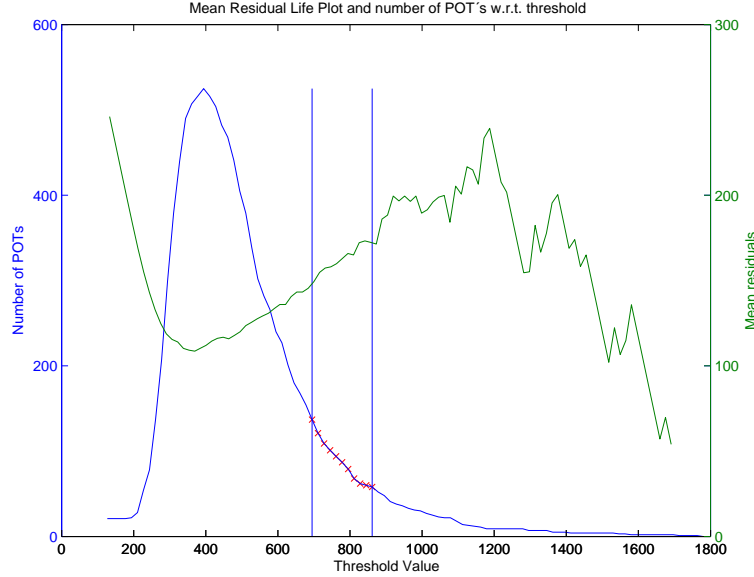
Figure 4.7: V064: Mean residual life plot and number of POTs as a function of threshold value

Figure 4.8, shows how the parameters of the ξ and σ^* change with respect to threshold value. As explained in Section 3.4.2, these two parameters should be constant for all values of threshold, larger than the smallest desired threshold value. In theory that is the ideal threshold value. All values below would skew the result of the flood analysis, due to too many values being used in the analysis. All threshold values above would leave to many extreme values out of the analysis, increasing the sampling uncertainty. The middle graphs in the figures are the median values of ξ and σ^*, w.r.t. threshold. The outer graphs represent the 95% confidence interval of the ξ and σ^* values. The aim is to find the lowest value of threshold, u_{low} where the a single value of ξ and σ^*, is inside the confidence interval, for all values of threshold,

larger than u_{low}. As is shown in Figure 4.8, the lowest threshold value where the same value of the parameters is inside the 95% confidence interval is not the same when looking at the two parameters. For σ^*, a threshold value of approximately 700 will produce a parameter inside for the 95% confidence interval of the above threshold values. For ξ, a threshold value of approximately 350 will produce a parameter inside for the 95% confidence interval of the above threshold values.
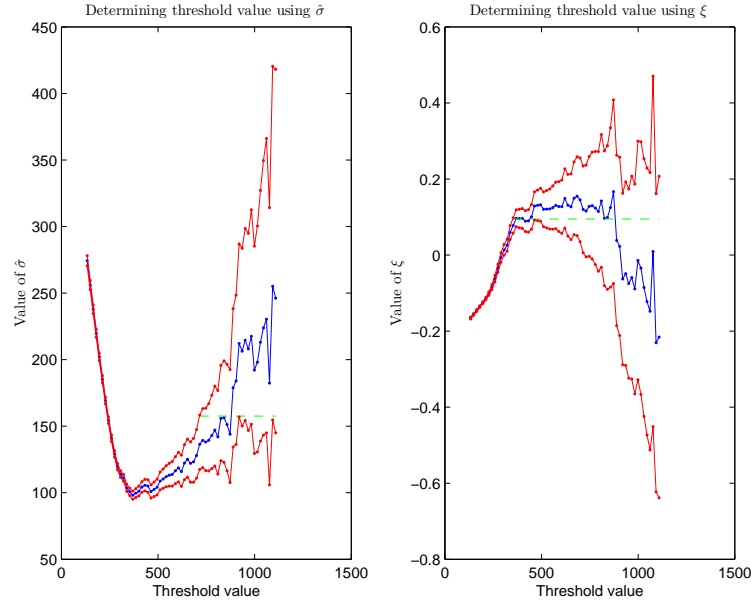
Figure 4.8: V064: Threshold approximation using the parameters σ^* and ξ

What can be inferred from these figures is a lower limit of $u_{low} = 700$. This lower limit comes from the estimation of the σ^* parameter w.r.t. threshold. The mean residual life plot suggests a threshold pick of approximately $u = 1000$ which would result in too few POTs and consequently a too large of a sample variance. Another guideline for choosing a threshold, was to choose it so the number of POTs in the range of $1 - 2.5$ times the number of years. The threshold chosen for this river was $u = 820$. That threshold value produces approximately 90 POTs, when using a comb value of 5, and it could be argued that the mean residual life plot is approximately linear for all higher threshold values.

Two different values for the threshold were used in the flood analysis. That is, one analysis using a threshold value of $u = 820$. And another analysis using the threshold value which produces as many POTs as there are years in the data set. That threshold value is $u = 862$. These two different methods for choosing the threshold will be referred to as the *diagnostic based method* (DBM) and the *fixed frequency method* (FFM), respectively.

When the threshold value has been chosen the B-spline rating curve was applied on the POTs to estimate the uncertainty in the extreme values. There after the comb

was used to further eliminate undesired values. The comb is used to minimize the correlation between extreme values used in the model. Some of the extreme values used in the model are possibly generated from point estimates of water discharge that are lower than the chosen threshold. As described in section 3.4, only values above the threshold will be used in the model so for point estimates close to the threshold value, the uncertainty vector describing the extreme value can be as large as having 40,000 elements used in the model or as small as having only 1 element.

4.1.3. Threshold model using diagnostic based methods (DBM) for determining the threshold value

The threshold model analysis of the data for Olfusa was continued using a threshold value of $u = 820$. In Figure 4.9 the POTs have been processed by the B-spline discharge rating curve to evaluate the uncertainty in the extreme values. In Figure 4.9 the POTs and their 95% posterior interval are shown with the water discharge time series along with the threshold value. As before, for some of the POTs, the full 40,000 set uncertainty vector will not be used in the analysis since there are values within those vectors that are below the threshold value. That has the effect that the number of POTs used to generate the posterior distributions for the GP parameter can vary from one iteration to the next.

Figure 4.9: V064: Left panel: Water discharge time series with 95% posterior interval for extreme values. Right panel: Discharge rating curve with fitted POT values

Comparison between the three different cases of prior distribution for ξ

Figure 4.10 shows the prior distributions of ξ and their corresponding posterior distributions for all cases. Majority of the posterior distribution in Case 1 is positive

4. Results and discussions

Figure 4.10: (V064 TM DBM w/DRC): Prior and posterior distributions for the shape parameter (ξ) in the GP distribution for all three cases of prior distributions. Case 1: left panels, Case 2: middle panels, Case 3: right panels.
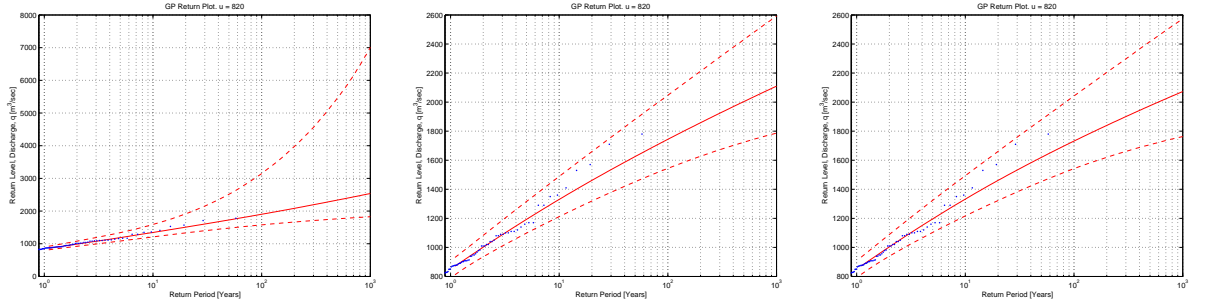
Figure 4.11: (V064 TM DBM w/DRC): Return level plots for the threshold model for all three cases of prior distributions. Case 1: left panel, Case 2: middle panel, Case 3: right panel.

and so constraining the posterior to only negative values has great influence on the results. Figure 4.11 show the return level plots for all three cases of prior distributions. Constraining the prior to negative values only, lowers the return levels and makes the confidence interval narrower. This constriction has the effect that the data does not fit the model, as well as in Case 1.

Table 4.3 shows the 2.5%, 25%, 50%, 75%, and 97.5% percentiles of the 100-year return level for all three cases of prior distributions for the shape parameter, ξ. Figure 4.12 shows the 95% posterior interval of the 100-year return level for all three cases of prior distributions for the shape parameter, ξ, and the 2.5%, 50%, and 97.5% percentiles. The 95% posterior interval of the 100-year return level represents the uncertainty in the return level. Figure 4.12, shows how the uncertainty interval becomes smaller as the ξ value is restricted to negative value only.

Table 4.3: V064 TM DBM: 100-year return levels of discharge (m³/sec), for all three cases of prior distributions, calculated with and without a DRC

Threshold model with threshold, u = 820						
	With DRC			Without DRC		
Percentiles	Normal	Neg-Gamma	Neg-Beta	Normal	Neg-Gamma	Neg-Beta
2.5%	1578	1544	1542	1594	1571	1566
25%	1750	1665	1655	1751	1689	1675
50%	1903	1744	1732	1889	1765	1748
75%	2147	1835	1823	2100	1852	1834
97.5%	3145	2047	2042	2960	2055	2035
95% conf. int.	1568	503	500	1366	483	469

Figure 4.12: (V064 TM DBM) Comparison of the 95% posterior interval of the 100-year return level of discharge, between the three cases of prior distributions, with DRC uncertainty (blue) and without DRC uncertainty (red).

Constraining the posterior density of ξ, to negative values only, by using negative prior distributions has a significant influence on the outcome of the posterior distributions and thus the resulting return levels. In the case where the prior distribution for the shape parameter is a normal distribution, the posterior distribution has more tendency to be positive than negative, having a mean value of 0.06 (see Table A.3). Constraining the priors has similar effects on the posteriors as eliminating the positive portion of Case 1 posterior density. The negative part of the posterior density using the non-informative normal prior is similar to the posterior distributions resulting from the constraining priors. Since a higher value of ξ leads to thicker tail of the GP distribution and hence larger return values, eliminating the positive por-

tion of the ξ values reduces the return levels and the range for their 95% posterior intervals for high return periods. This reduction in the posterior densities of ξ , has the effect that the models in Cases 2 and 3, using the negative priors, do not fit the data as well as the model in Case 1.

Thus, constraining the ξ parameter to negative values only, has the effect that the median value of the 100-year return level becomes lower for both cases of negative prior distributions for ξ. In the both case where the prior distribution is the negative the median value becomes approximately 10% lower. Furthermore, the uncertainty in Cases 2 and 3, where the priors are negative only, shrinks to approximately 30% of the uncertainty for Case 1, where the prior is non-informative.

The effect of discharge rating curve uncertainty

The effect of merging the discharge rating curve uncertainty with the sampling uncertainty from the MCMC scheme has minor effect on the median value of the 100-year return level. This is shown in Table 4.3 and Figure 4.12. There is a minor change in the over all uncertainty for the 100-year return level, when adding the discharge rating curve uncertainty to the calculations. In the Case 1, where the prior distribution is a normal distribution, the 95% posterior interval increases approximately 3%, when DRC uncertainty is taken into account. In the Case 2, where the prior distribution is a negative gamma distribution, the 95% posterior interval increases approximately 5%, when DRC uncertainty is taken into account. In the Case 3, where the prior distribution is a negative beta distribution, the 95% posterior interval increases approximately 7%, when DRC uncertainty is taken into account.

4.1.4. Threshold Model using the fixed frequency method (FFM) for determining the threshold value

With the fixed frequency method (FFM) a threshold is chosen so the number of point estimates of discharge that are above the threshold, after de-clustering, are equal to the number of years of data used in the analysis. For Olfusa, that leads to a threshold value of $u = 862$ with the total number of point estimates of discharge, greater than the threshold value, equal to 57. Figure 4.13 shows the B-spline discharge rating curve as well as the extreme values used in the analysis and their 95% uncertainty interval. Figure 4.13 shows the discharge time series of Olfusa along with the 95% discharge uncertainty vectors used in the model.
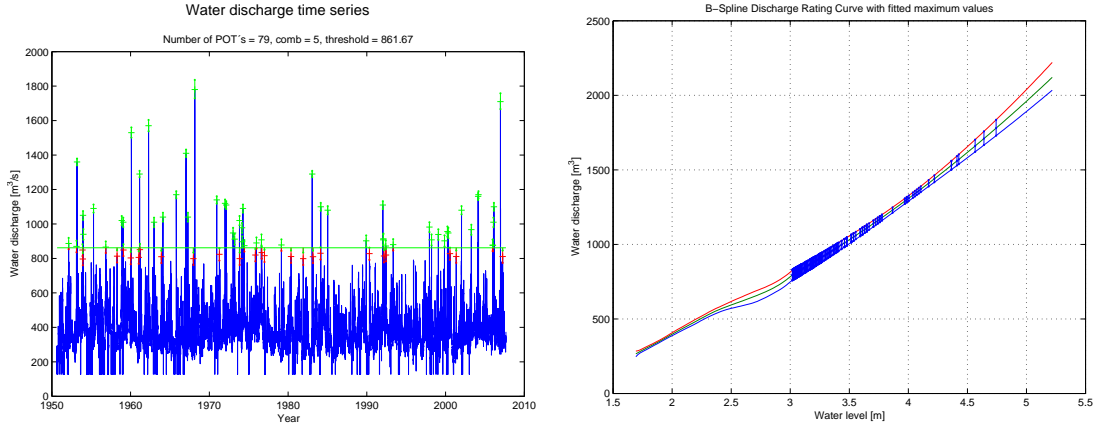
Figure 4.13: (V064 FFM): Right panel: Water discharge time series with 95% posterior interval for extreme values. Left panel: B-spline Discharge rating curve with fitted POT values

Comparison between the three different cases of prior distribution for ξ
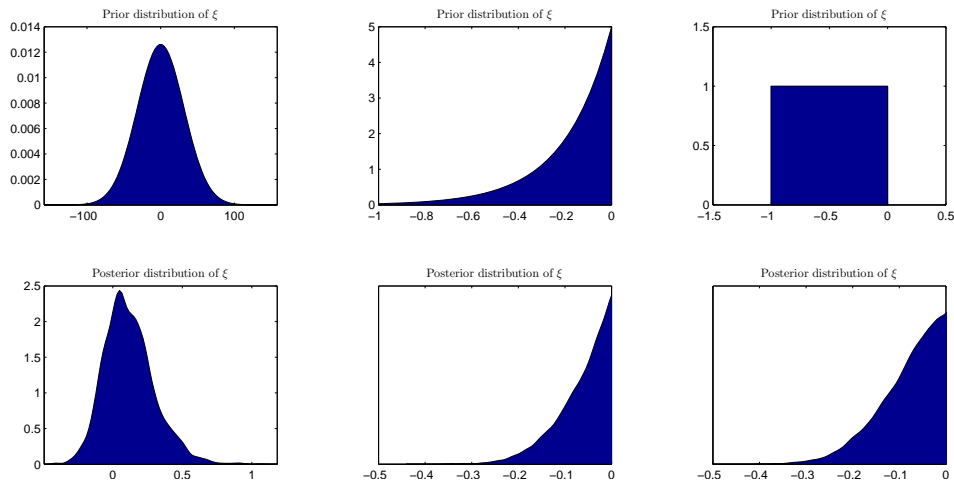
Figure 4.14: (V064 TM FFM w/DRC): Prior and posterior distributions for the shape parameter (ξ) in the GP distribution for all three cases of prior distributions. Case 1: left panels, Case 2: middle panels, Case 3: right panels.

Figure 4.14 shows the prior distributions of ξ and their corresponding posterior distributions for all cases. Majority of the posterior distribution in Case 1 is positive and so constraining the posterior to only negative values has great influence on the results. Figure 4.15 show the return level plots for all three cases of prior distributions. Constraining the prior to negative values only, lowers the return levels and makes the confidence interval narrower. This constriction has the effect that the data does not fit the model, as well as in Case 1.

4. Results and discussions
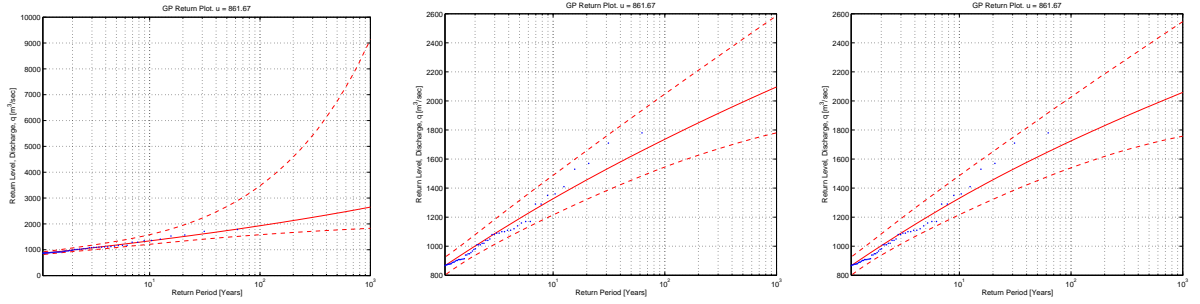
Figure 4.15: (V064 TM FFM w/DRC): Return level plots for the threshold model for all three cases of prior distributions. Case 1: left panel, Case 2: middle panel, Case 3: right panel.

Table 4.4: V064 TM FFM: 100-year return levels of discharge (m^3/sec), for all three cases of prior distributions, calculated with and without a DRC

Threshold model with threshold, u = 862						
	With DRC			Without DRC		
Percentiles	Normal	Neg-Gamma	Neg-Beta	Normal	Neg-Gamma	Neg-Beta
2.5%	1581	1545	1540	1601	1550	1547
25%	1762	1660	1650	1791	1661	1652
50%	1928	1736	1725	1978	1733	1722
75%	2204	1827	1811	2283	1815	1803
97.5%	3474	2048	2026	3653	2007	1994
95% conf. int.	1893	503	487	2052	457	447

Table 4.4 shows the 2.5%, 25%, 50%, 75%, and 97.5% percentiles of the 100-year return level for all three cases of prior distributions for the shape parameter, ξ. Figure 4.16 shows the 95% posterior interval of the 100-year return level for all three cases of prior distributions for the shape parameter, ξ, and the 2.5%, 50%, and 97.5% percentiles. The 95% posterior interval of the 100-year return level represents the uncertainty in the return level. Figure 4.16, shows how the uncertainty interval becomes smaller as the ξ value is restricted to negative value only.

Constraining the posterior density of ξ, to negative values only, by using negative prior distributions has a significant influence on the outcome of the posterior distributions and thus the resulting return levels. In the case where the prior distribution for the shape parameter is a normal distribution, the posterior distribution has more tendency to be positive than negative, having a mean value of 0.09 (see Table A.4). Constraining the priors has similar effects on the posteriors as eliminating the positive portion of the Case 1 posterior density. The negative part of the posterior density using the non-informative normal prior is similar to the posterior distributions resulting from the constraining priors. Since a higher value of ξ leads to thicker tail of the GP distribution and hence larger return values, eliminating the positive
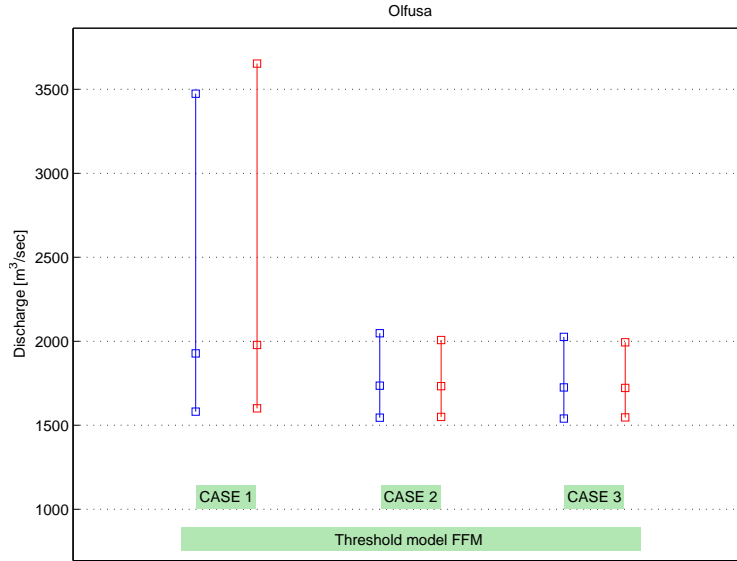
Figure 4.16: (V064 TM FFM) Comparison of the 95% posterior interval of the 100-year return level of discharge, between the three cases of prior distributions, with DRC uncertainty (blue) and without DRC uncertainty (red).

portion of the ξ values reduces the return levels and the range for their 95% posterior intervals for high return periods. This reduction in the posterior densities of ξ , has the effect that the models in Cases 2 and 3, using the negative priors, do not fit the data as well as the model in Case 1.

Thus, constraining the ξ parameter to negative values only, has the effect that the median value of the 100-year return level becomes significantly lower for both cases of negative prior distributions for ξ. In the both case where the prior distribution is the negative the median value becomes approximately 12% lower. Furthermore, the uncertainty in Cases 2 and 3, where the priors are negative only, shrinks to approximately 24% of the uncertainty for Case 1, where the prior is non-informative.

The effect of discharge rating curve uncertainty

The effect of merging the discharge rating curve uncertainty with the sampling uncertainty from the MCMC scheme has minor effect on the median value of the 100-year return level. This is shown in Table 4.4 and Figure 4.16. There is a change in the over all uncertainty for the 100-year return level, when adding the discharge rating curve uncertainty to the calculations. In Case 1, where the prior distribution is a normal distribution, the 95% posterior interval, surprisingly, decreases approximately 8%, when DRC uncertainty is taken into account. In Case 2, where the

prior distribution is a negative gamma distribution, the 95% posterior interval increases approximately 8%, when DRC uncertainty is taken into account. In Case 3, where the prior distribution is a negative beta distribution, the 95% posterior interval increases approximately 9%, when DRC uncertainty is taken into account.

4.1.5. Comparison between models

The models being compared are the block maxima model using the annual maximum values and two threshold models, one with the threshold value $u = 820$, found by using the diagnostic based method (DBM threshold model) and another one with a threshold value of $u = 862$, found by the fixed frequency method (FFM threshold model).

It can be argued that the extreme values used in the FFM threshold model are superior to those used in the block maxima model since they are not constricted to having one and only one extreme value per year, like the annual values used in the latter model. The argument is, that if the de-clustering of the POTs is successful and there is no correlation between the extremes, than the quality of the POTs gathered by using the FFM are at least, equal to that of the block maxima model. For that reason the comparison below will be between the block maxima model and the FFM threshold model, on one hand, and between the FFM threshold model and the DBM threshold model, on the other hand.
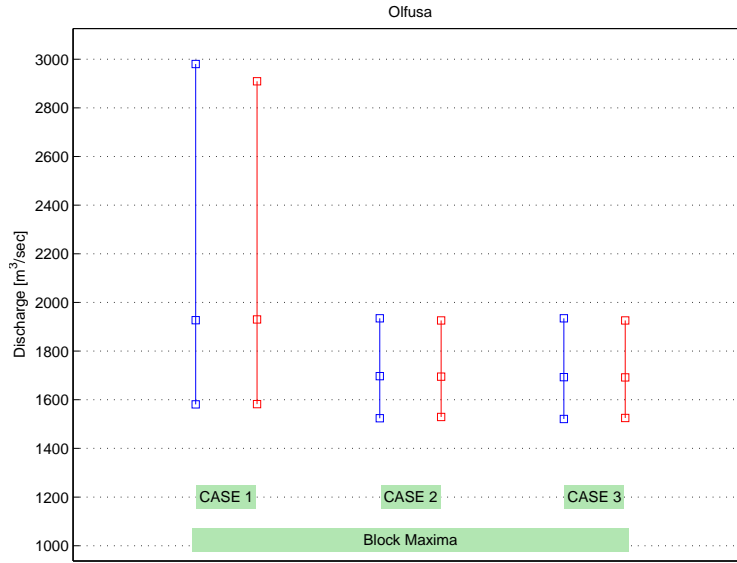

Figure 4.17: (V064) Comparison of the 95% posterior interval of the 100-year return level of discharge, between the three different models, with DRC uncertainty (blue) and without DRC uncertainty (red).

Block maxima model vs. FFM threshold model

Tables 4.2 and 4.4 show the percentiles for the 100-year return levels for the block maxima model and the FFM threshold model, respectively. Figure 4.17 shows the 95% posterior interval of the 100-year return level for the block maxima model and the FFM threshold model. Tables A.2 and A.4 show the percentiles of the posterior distributions for the GEV parameters for the Block maxima model and the GP parameters for the FFM Threshold model, respectively. The FFM threshold model uses approximately the same amount of extreme values as the block maxima model but the extremes used in the FFM threshold model are larger than those used in the block maxima model.

Looking at the 100-year return levels in Case 1 where the prior distribution for ξ is non-informative, the lower percentiles, 2.5%, 25%, and 50%, are very similar for both models. The higher percentiles, 75% and 97.5%, are larger for the FFM threshold model, hence the posterior interval is larger. The posterior densities for the Case 1 prior distributions for the block maxima model and the FFM threshold model are shown in Figure A.1 and Figure A.19, respectively.

The posterior density for the shape parameter, ξ, is wider in the FFM threshold model than in the block maxima model. The range of the 95% posterior interval for the parameter in the block maxima model is $[-0.09, 0.33]$ but $[-0.18, 0.48]$ for the FFM threshold model. The upper percentiles in the return level plots are particulary sensitive to high values of ξ which explains why the upper percentiles for the 100-year return levels are higher for the FFM threshold model than the block maxima model.

Cases 2 and 3 where the prior distribution for ξ is a negative gamma distribution and a negative beta distribution, respectively, do not fit the block maxima model well. A better fit comes when using the FFM threshold model. The median and the upper percentiles for the 100 year return level are larger in the FFM threshold model and provide a better fit for the extreme values used. The posterior interval for the return levels are too narrow in the block maxima model and the largest extremes deviate from the model.

DBM threshold model vs. FFM threshold model

Tables 4.3 and 4.4 show the percentiles for the 100-year return levels for the DBM threshold model and the FFM threshold model, respectively. Figure 4.17 shows the 95% posterior interval of the 100-year return level for the DBM threshold model and the FFM threshold model. Tables A.3 and A.4 show the percentiles of the posterior

distributions for the GP parameters for the DBM threshold model and the FFM threshold model, respectively.

By lowering the threshold from 862 to 820 the effective number of POTs increase from 53.85 to 64.95. Looking at the Case 1 prior distribution, these added extreme data have the effect of lowering the upper values of the posterior distribution for ξ. That leads to lower upper percentiles for the return level plot and thus smaller posterior interval. So, for this river, the added data used in the DBM threshold model lowered the upper percentiles for the 100 year return level and its posterior interval got smaller.

There is little difference between the two models when looking the results from the prior distributions in Cases 2 and 3. In both models, the negative gamma prior in Case 2 seems have the effect that the simulated values in the posterior distribution of ξ higher then for the negative beta prior in Case 3. That leads to higher return levels.

The Case 2 and Case 3 return levels produced by the FFM threshold model have narrower posterior intervals but the difference is minor. The median values for the return levels are almost identical for the DBM threshold model and the FFM threshold model.

4.2. Results for Hvita

The discharge time series for Hvita spans approximately 57 years, from July 1951 to September 2008. The daily point estimates of water discharge are shown in Figure 4.18
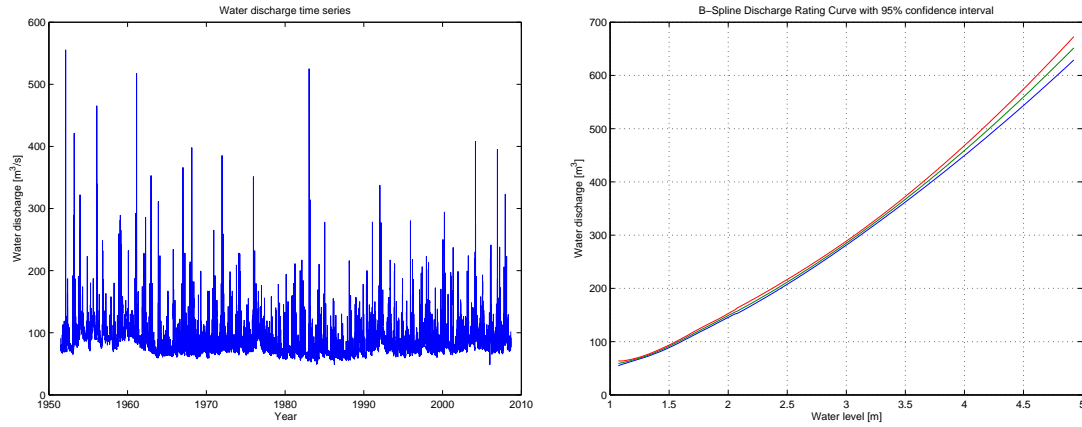
Figure 4.18: V066: Left panel: Water discharge time series. Right panel: B-spline Discharge Rating curve

The relationship between water level and water discharge is found by applying the B-spline discharge rating curve, as discussed in Section 3.2, on the paired water level and water discharge data for the river. The B-spline discharge rating curve is shown in Figure 4.18.

4.2.1. Block maxima model

The annual maximum values used for the Block Maxima model are shown in Figure 4.19. It shows the discharge time series for the river with each annual maximum value visually highlighted with a star symbol. These values are point estimates of water discharge. The B-spline discharge rating curve was applied on the annual maximum values to obtain the uncertainty in the estimates. Figure 4.20 shows how the discharge rating curve is used to estimate the uncertainty in the annual maximum values. In Figure 4.20 the highlighted annual maximum values from Figure 4.19 are fitted to the discharge rating curve and from that point it becomes manageable to estimate the uncertainty in the point estimate. This process is described in detail in Section 3.3. Figure 4.20 shows the same water discharge time series as Figure 4.19 but also includes the 95% uncertainty interval for the annual maximum values shown as well.
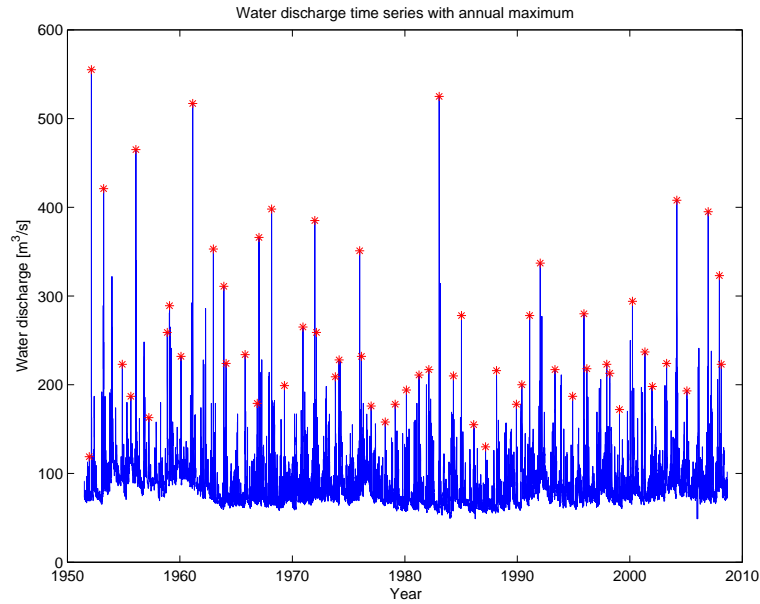
Figure 4.19: V066: Water discharge time series with annual maximum values

Comparison between the three different cases of prior distribution for ξ

Figure 4.21 shows the prior distributions of ξ and their corresponding posterior distributions for all cases. Majority of the posterior distribution in Case 1 is positive and so constraining the posterior to only negative values has great influence on the results. Figure 4.22 show the return level plots for all three cases of prior distributions. Constraining the prior to negative values only, lowers the return levels and makes the confidence interval narrower. This constriction has the effect that the data does not fit the model, as well as in Case 1.
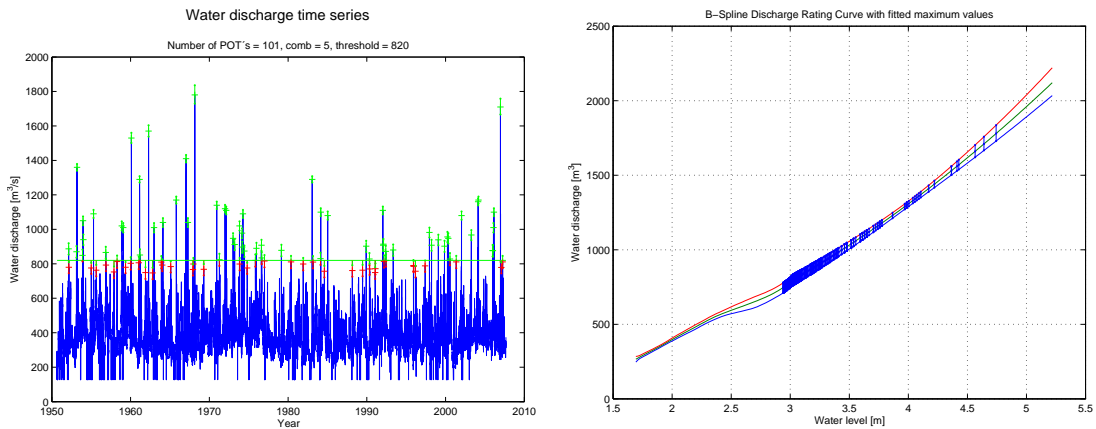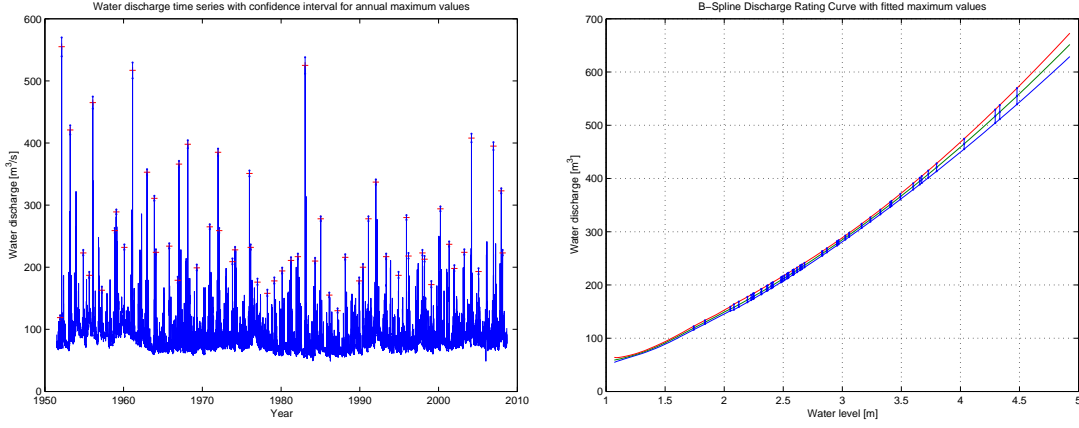
Figure 4.20: V066: Left panel: Water discharge time series with 95% posterior interval for extreme values. Right panel: B-spline discharge rating curve with fitted annual maximum values and their 95% posterior interval
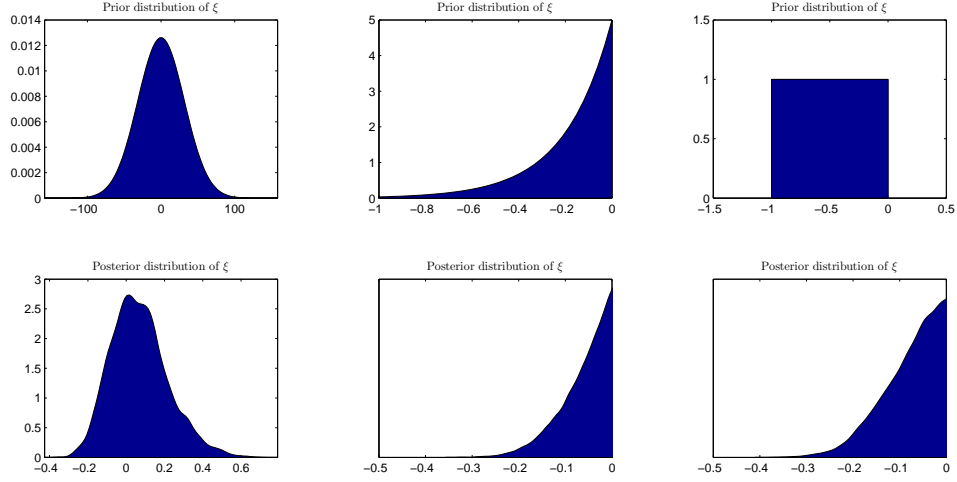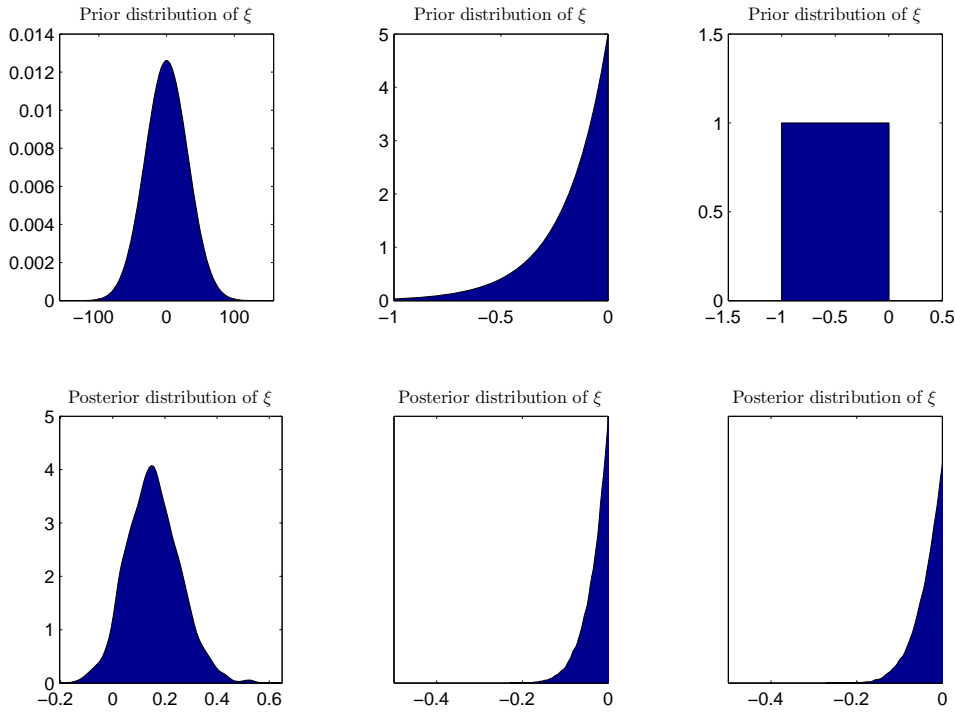

Figure 4.21: (V066 BM w/DRC): Prior and posterior distributions for the shape parameter (ξ) in the GEV distribution for all three cases of prior distributions. Case 1: left panels, Case 2: middle panels, Case 3: right panels.

Constraining the shape parameter to only negative values has a significant impact on the posterior density for that parameter. In the case where the prior distribution for the shape parameter is a normal distribution, the posterior distribution has more tendency to be positive than negative, having a mean value of 0.10 (see Table

4. Results and discussions
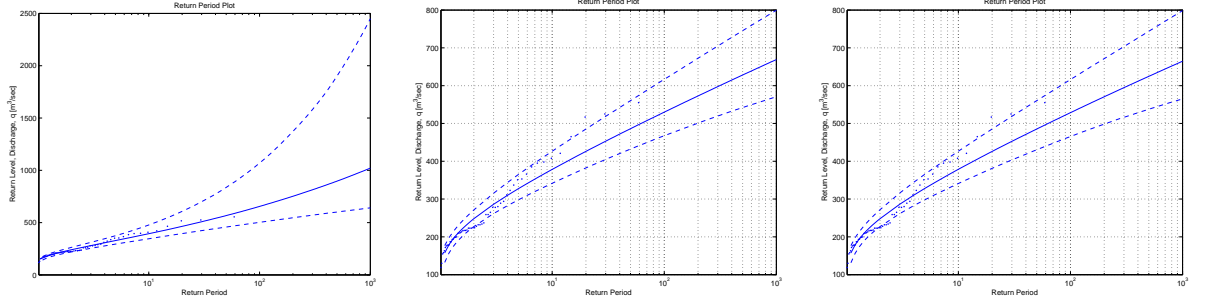
Figure 4.22: (V066 BM w/DRC): Return level plots for the block maxima model for all three cases of prior distributions. Case 1: left panel, Case 2: middle panel, Case 3: right panel.

Table 4.5: V066 BM: 100-year return levels of discharge (m^3/sec), for all three cases of prior distributions, calculated with and without a DRC

Block Extrema						
	With DRC			Without DRC		
Percentiles	Normal	Neg-Gamma	Neg-Beta	Normal	Neg-Gamma	Neg-Beta
2.5%	503	468	465	501	468	466
25%	587	506	504	585	506	505
50%	655	530	529	654	530	529
75%	753	557	555	750	557	556
97.5%	1069	617	616	1065	618	616
95% conf. int.	566	149	151	564	150	150

B.2). Constraining the priors has similar effects on the posteriors as eliminating the positive portion of the Case 1 posterior density. The negative part of the posterior density using the non-informative normal prior is similar to the posterior distributions resulting from the constraining priors. Since a higher value of ξ leads to thicker tail of the GEV distribution and hence larger return values, eliminating the positive portion of the ξ values reduces the return levels and the range for their 95% posterior intervals for high return periods. This reduction in the posterior densities of ξ, has the effect that the models in Cases 2 and 3, using the negative priors, do not fit the data as well as the model in Case 1.

Constraining the ξ parameter to negative values only as is done in Cases 2 and 3, has the effect that the median value of the 100-year return level becomes lower (20% lower for both Case 1 and Case 2). Furthermore, the uncertainty of the 100-year return level, for the two cases shrinks to approximately 25% of that of Case 1. By viewing the diagnostic plots in Figures B.4 and B.6, it seems that this reduction in posterior interval is too much for the data which do not fit the model.

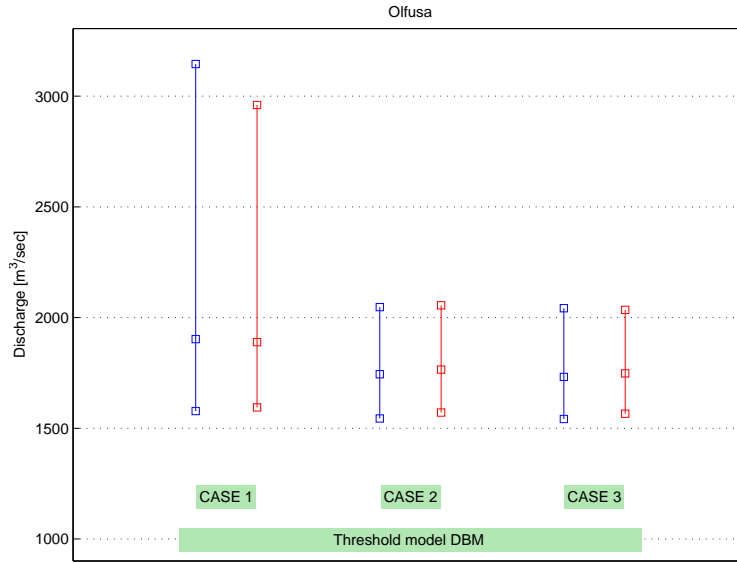Since majority of the posterior density when using the non-informative normal prior

Figure 4.23: (V066 BM) Comparison of the 95% posterior interval of the 100-year return level of discharge, between the three cases of prior distributions, with DRC uncertainty (blue) and without DRC uncertainty (red).

distribution, was positive, the median value of the 100-year return level is greater than the 97.5 percentiles for the 100-year return levels for the restricting prior distributions.

The effect of discharge rating curve uncertainty

The effect of merging the discharge rating curve uncertainty with the sampling uncertainty from the MCMC scheme has minor effect on the median value of the 100-year return levels and minor effect on the 95% posterior intervals. This is shown in Table 4.5 and Figure 4.23. There is a minor change in the over all uncertainty for the 100-year return level, when adding the discharge rating curve uncertainty to the calculations. In Case 1, where the prior distribution is a normal distribution, the increase of the 95% posterior interval is insignificant, i.e. less than 1%. In Case 2 where the prior distribution is a negative gamma distribution the 95% posterior interval becomes smaller. It is an insignificant change i.e. approximately 1% reduction in the size of the interval. In Case 3 where the prior distribution is a negative beta distribution the increase of the 95% posterior interval is approximately 2%.

4.2.2. Threshold model
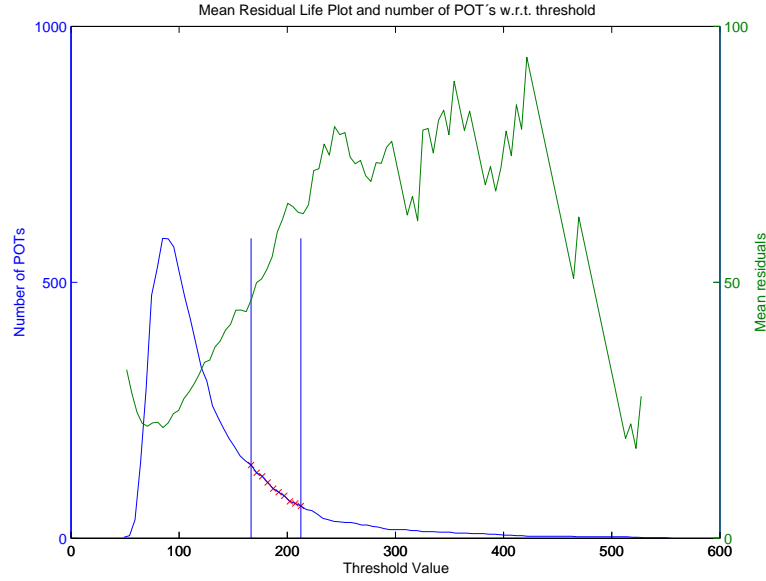
Figure 4.24: V066: Mean residual life plot and number of POTs as a function of threshold value

As is shown in Figure 4.25, the lowest threshold value where the same value of the parameters is inside the 95% confidence interval is not the same when looking at the two parameters. For σ^*, a threshold value of approximately 190 will produce a parameter inside for the 95% confidence interval of the above threshold values. For ξ, a threshold value of approximately 170 will produce a parameter inside for the 95% confidence interval of the above threshold values.

What can be inferred from Figure 4.25 is a lower limit of $u_{low} = 190$. This lower limit comes from the estimation of the σ^* parameter w.r.t. threshold. The mean residual life plot in Figure 4.24, suggests a threshold pick of approximately $u = 400$ which would result in too few POTs and consequently a too large of a sample variance. By disregarding the largest values of threshold, the mean residual life plot seems to behave linearly on the interval 200 to 400. Another guideline for choosing a threshold, was to choose it so the number of POTs in the range of $1 - 2.5$ times the number of years. The threshold chosen for this river was $u = 200$. That threshold value produces approximately 90 POTs, when using a comb value of 5, and it could be argued that the mean residual life plot is approximately linear for all higher threshold values.

Two different values for the threshold were used in the flood analysis. That is, one analysis using a threshold value of $u = 200$. And another analysis using the threshold value which produces as many POTs as there are years in the data set. That threshold value is $u = 213$. These two different methods for choosing the
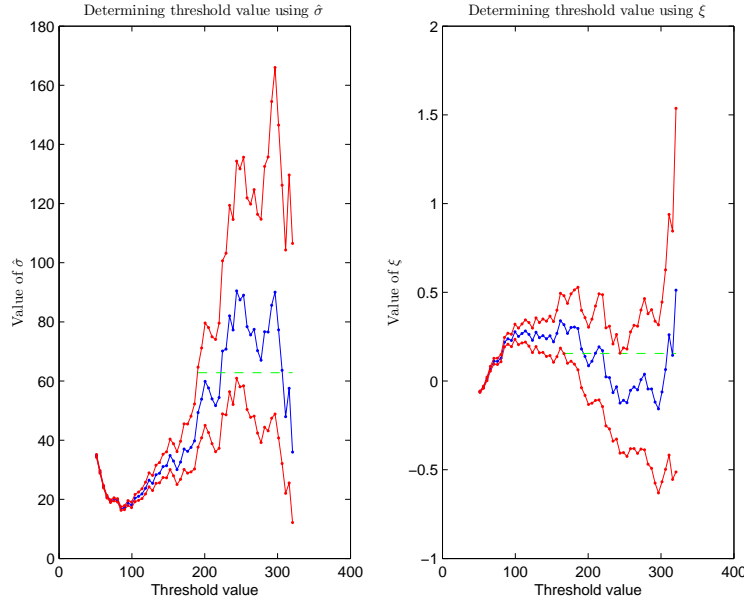
Figure 4.25: V066: Threshold approximation using the parameters σ^* and ξ

threshold will be referred to as the *diagnostic based method* (DBM) and the *fixed frequency method* (FFM), respectively.

4.2.3. Threshold model using diagnostic based methods (DBM) for determining the threshold value

The threshold model analysis of the data for Hvita was constructed using a threshold value of $u = 200$. In Figure 4.26 the POTs have been processed by the B-spline discharge rating curve to evaluate the uncertainty in the extreme values. In Figure 4.26 the POTs and their 95% posterior interval are shown with the water discharge time series along with the threshold value.

Comparison between the three different cases of prior distribution for ξ

Figure 4.27 shows the prior distributions of ξ and their corresponding posterior distributions for all cases. Majority of the posterior distribution in Case 1 is positive and so constraining the posterior to only negative values has great influence on the results. Figure 4.28 show the return level plots for all three cases of prior distributions. Constraining the prior to negative values only, lowers the return levels and makes the confidence interval narrower. This constriction has the effect that the data does not fit the model, as well as in Case 1. Figure 4.29, shows how the

4. Results and discussions
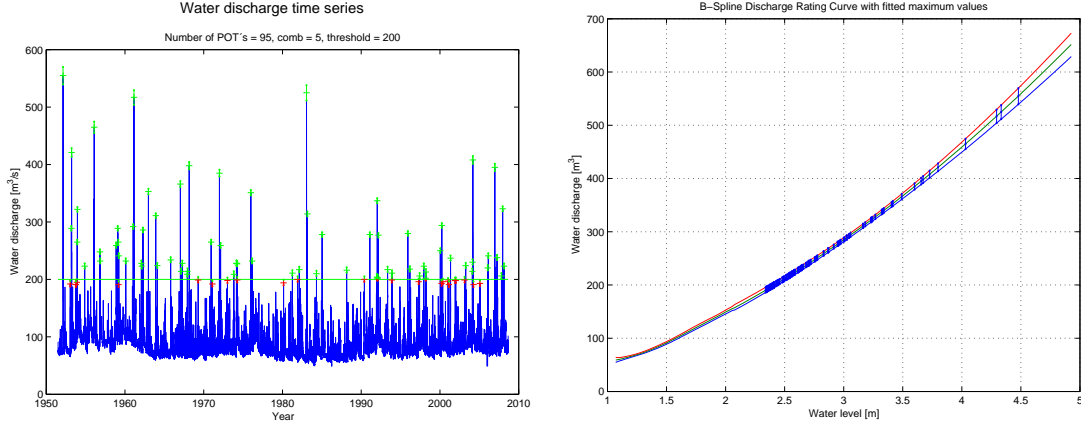
Figure 4.26: V066: Left panel: Water discharge time series with 95% posterior interval for extreme values. Right panel: Discharge rating curve with fitted POT values
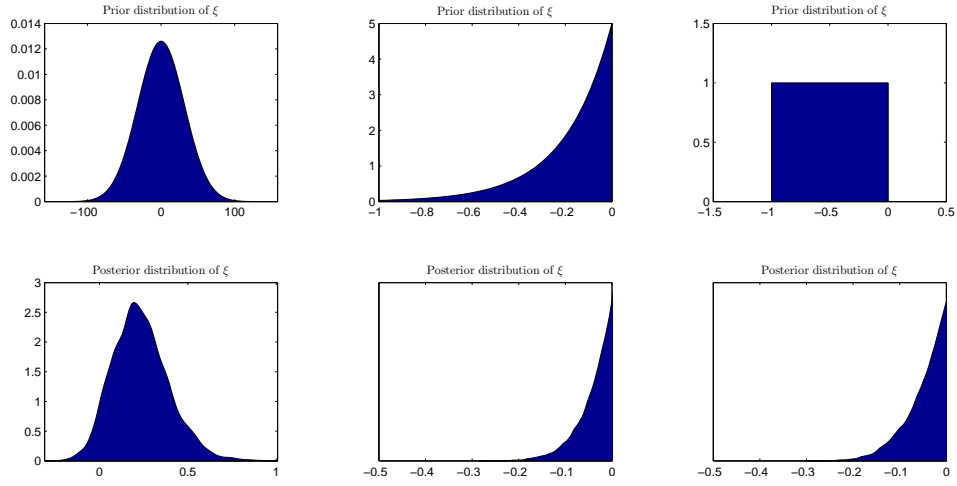
Figure 4.27: (V066 TM DBM w/DRC): Prior and posterior distributions for the shape parameter (ξ) in the GP distribution for all three cases of prior distributions. Case 1: left panels, Case 2: middle panels, Case 3: right panels.

uncertainty interval becomes smaller as the ξ value is restricted to negative value only.

In the case where the prior distribution for the shape parameter is a normal distribution, the posterior distribution has more tendency to be positive than negative, having a mean value of 0.22 (see Table B.3). Constraining the priors has similar effects on the posteriors as eliminating the positive portion of Case 1 posterior density. The negative part of the posterior density using the non-informative normal prior is similar to the posterior distributions resulting from the constraining priors. Since a higher value of ξ leads to thicker tail of the GP distribution and hence larger return values, eliminating the positive portion of the ξ values reduces the return

74
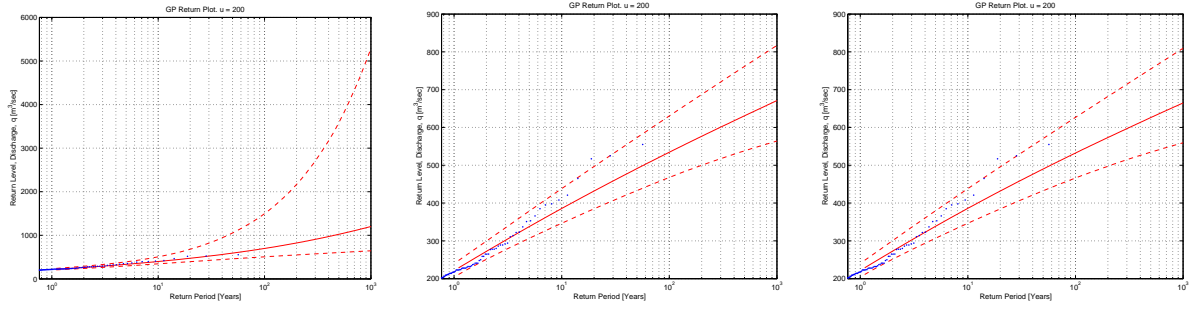
Figure 4.28: (V066 TM DBM w/DRC): Return level plots for the threshold model for all three cases of prior distributions. Case 1: left panel, Case 2: middle panel, Case 3: right panel.

Table 4.6: V066 TM DBM: 100-year return levels of discharge (m^3/sec), for all three cases of prior distributions, calculated with and without a DRC

Threshold model with threshold, u = 200						
	With DRC			Without DRC		
Percentiles	Normal	Neg-Gamma	Neg-Beta	Normal	Neg-Gamma	Neg-Beta
2.5%	507	468	466	503	473	472
25%	604	509	507	587	513	511
50%	699	534	532	668	538	536
75%	851	563	561	794	566	564
97.5%	1497	631	627	1299	631	628
95% conf. int.	990	163	161	797	158	156

levels and the range for their 95% posterior intervals for high return periods. This reduction in the posterior densities of ξ, has the effect that the models in Cases 2 and 3, using the negative priors, do not fit the data as well as the model in Case 1.

Thus, constraining the ξ parameter to negative values only, has the effect that the median value of the 100-year return level becomes lower for both cases of negative prior distributions for ξ. In the both case where the prior distribution is the negative the median value becomes approximately 26% lower. Furthermore, the uncertainty in Cases 2 and 3, where the priors are negative only, shrinks to approximately 40% of the uncertainty for Case 1, where the prior is non-informative.

The effect of discharge rating curve uncertainty

The effect of the discharge rating curve uncertainty on the 100-year return levels are shown in Table 4.6 and Figure 4.29. By merging the discharge rating curve uncertainty with the sampling uncertainty from the MCMC scheme, the median
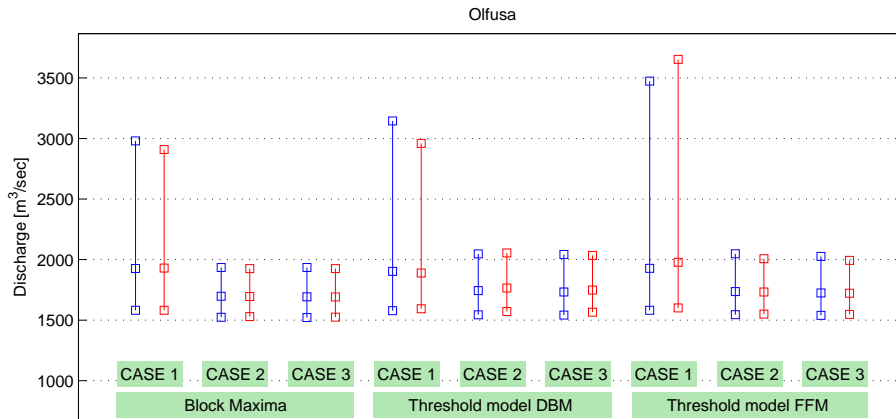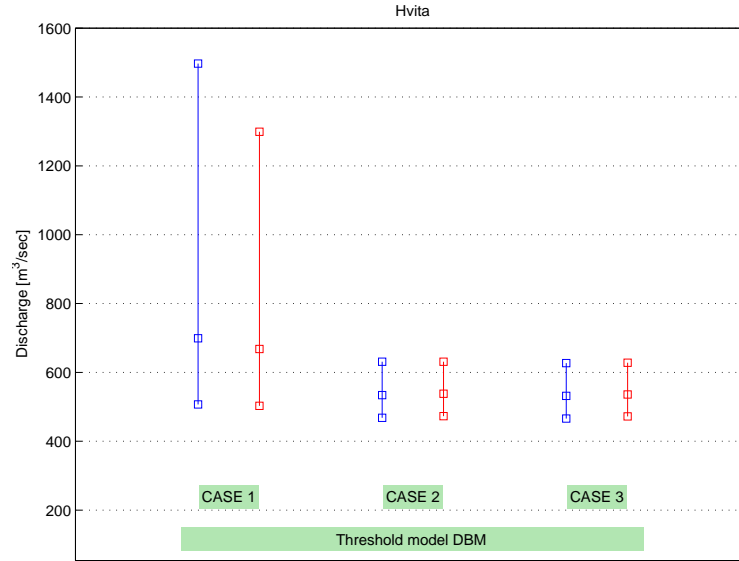
Figure 4.29: (V066 TM DBM) Comparison of the 95% posterior interval of the 100-year return level of discharge, between the three cases of prior distributions, with DRC uncertainty (blue) and without DRC uncertainty (red).

value of Case 1, where the ξ parameter is unrestrained, becomes approximately 5% larger. For Case 2 and Case 3, where the prior distribution for ξ is a negative gamma distribution, the median value becomes slightly lower, when the DRC uncertainty is taken into account.

The over all uncertainty in the 100-year return level increases when adding the discharge rating curve uncertainty to the calculations. In Case 1, where the prior distribution is a normal distribution the increase of the 95% posterior interval is approximately 24%. In Case 2, where the prior distribution is a negative gamma distribution the increase of the 95% posterior interval is approximately 3%. In Case 3, where the prior distribution is a negative beta distribution the increase of the 95% posterior interval is approximately 4%.

4.2.4. Threshold Model using the fixed frequency method (FFM) for determining the threshold value

With the fixed frequency method (FFM) a threshold is chosen so the number of point estimates of discharge that are above the threshold, after de-clustering, are equal to the number of years of data used in the analysis. For Hvita, that leads to a threshold value of $u = 213$ with the total number of point estimates of discharge, greater than the threshold value, equal to 57. Figure 4.30 shows the B-spline discharge rating

curve as well as the extreme values used in the analysis and their 95% uncertainty interval. Figure 4.30 shows the discharge time series of Hvita along with the 95% discharge uncertainty vectors used in the model.
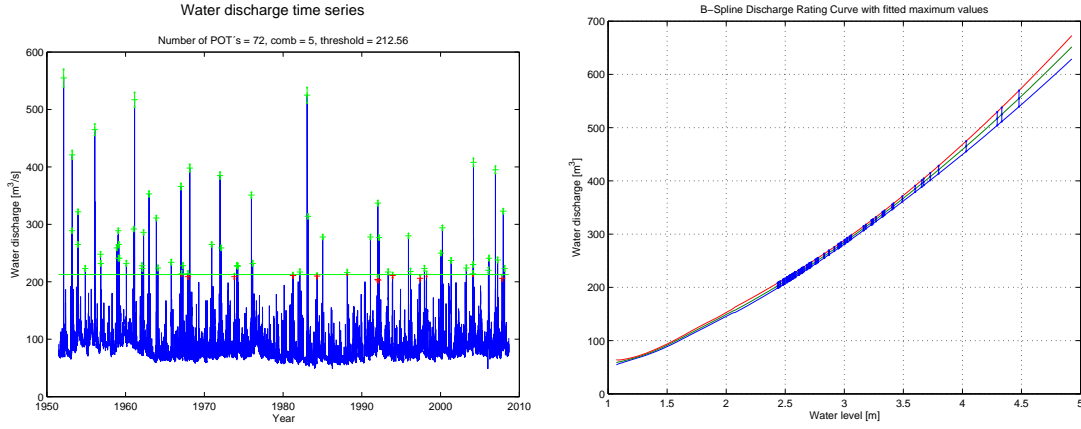
Figure 4.30: (V066 FFM): Right panel: Water discharge time series with 95% posterior interval for extreme values. Left panel: B-spline Discharge rating curve with fitted POT values

Comparison between the three different cases of prior distribution for ξ
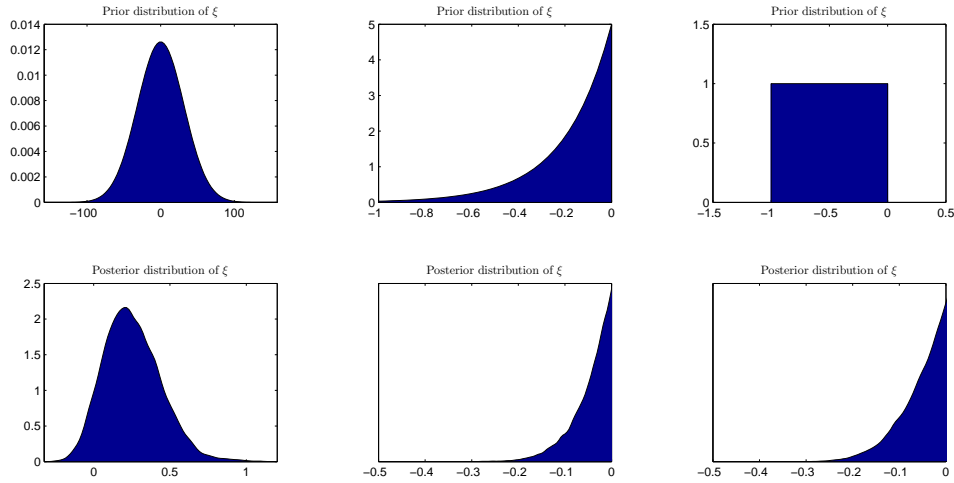
Figure 4.31: (V066 TM FFM w/DRC): Prior and posterior distributions for the shape parameter (ξ) in the GP distribution for all three cases of prior distributions. Case 1: left panels, Case 2: middle panels, Case 3: right panels.

Figure 4.31 shows the prior distributions of ξ and their corresponding posterior distributions for all cases. Majority of the posterior distribution in Case 1 is positive and so constraining the posterior to only negative values has great influence on

4. Results and discussions
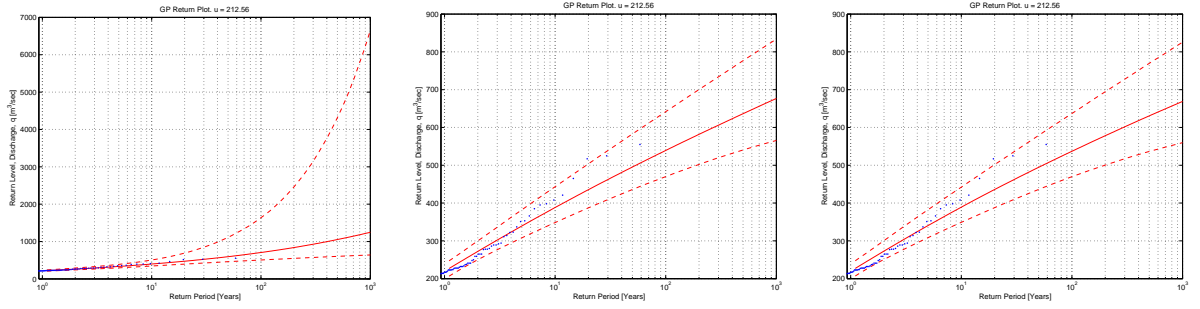
Figure 4.32: (V066 TM FFM w/DRC): Return level plots for the threshold model for all three cases of prior distributions. Case 1: left panel, Case 2: middle panel, Case 3: right panel.

Table 4.7: V066 TM FFM: 100-year return levels of discharge (m^3/sec), for all three cases of prior distributions, calculated with and without a DRC

Threshold model with threshold, u = 213						
	With DRC			Without DRC		
Percentiles	Normal	Neg-Gamma	Neg-Beta	Normal	Neg-Gamma	Neg-Beta
2.5%	506	470	470	508	471	471
25%	607	513	511	613	512	510
50%	707	539	537	718	538	535
75%	872	570	567	896	567	564
97.5%	1639	642	637	1718	632	630
95% conf. int.	1133	172	167	1210	161	159

the results. Figure 4.32 show the return level plots for all three cases of prior distributions. Constraining the prior to negative values only, lowers the return levels and makes the confidence interval narrower. This constriction has the effect that the data does not fit the model, as well as in Case 1.

Table 4.7 shows the 2.5%, 25%, 50%, 75%, and 97.5% percentiles of the 100-year return level for all three cases of prior distributions for the shape parameter, ξ. Figure 4.33 shows the 95% posterior interval of the 100-year return level for all three cases of prior distributions for the shape parameter, ξ, and the 2.5%, 50%, and 97.5% percentiles. The 95% posterior interval of the 100-year return level represents the uncertainty in the return level. Figure 4.33, shows how the uncertainty interval becomes smaller as the ξ value is restricted to negative value only.

Constraining the posterior density of ξ, to negative values only, by using negative prior distributions has a significant influence on the outcome of the posterior distributions and thus the resulting return levels. In the case where the prior distribution for the shape parameter is a normal distribution, the posterior distribution has more tendency to be positive than negative, having a mean value of 0.24 (see Table B.4).

Figure 4.33: (V066 TM FFM) Comparison of the 95% posterior interval of the 100-
year return level of discharge, between the three cases of prior distributions, with DRC
uncertainty (blue) and without DRC uncertainty (red).

Constraining the priors has similar effects on the posteriors as eliminating the pos-
itive portion of the Case 1 posterior density. The negative part of the posterior
density using the non-informative normal prior is similar to the posterior distribu-
tions resulting from the constraining priors. Since a higher value of ξ leads to thicker
tail of the GP distribution and hence larger return values, eliminating the positive
portion of the ξ values reduces the return levels and the range for their 95% posterior
intervals for high return periods. This reduction in the posterior densities of ξ, has
the effect that the models in Cases 2 and 3, using the negative priors, do not fit the
data as well as the model in Case 1.

Thus, constraining the ξ parameter to negative values only, has the effect that the
median value of the 100-year return level becomes lower for both cases of negative
prior distributions for ξ. In the both case where the prior distribution is the negative
the median value becomes approximately 27% lower. Furthermore, the uncertainty
in Cases 2 and 3, where the priors are negative only, shrinks to approximately 37%
of the uncertainty for Case 1, where the prior is non-informative.

The effect of discharge rating curve uncertainty

The effect of the discharge rating curve uncertainty on the 100-year return levels
are shown in Table 4.6 and Figure 4.29. By merging the discharge rating curve

uncertainty with the sampling uncertainty from the MCMC scheme, the median value of Case 1, where the ξ parameter is unrestrained, becomes approximately 5% larger. For Case 2 and Case 3, where the prior distribution for ξ is a negative gamma distribution, the median value becomes slightly lower, when the DRC uncertainty is taken into account.

The over all uncertainty in the 100-year return level changes when adding the discharge rating curve uncertainty to the calculations. In Case 1, where the prior distribution is a normal distribution, the 95% posterior interval, surprisingly, decreases approximately 6%, when DRC uncertainty is taken into account. In Case 2, where the prior distribution is a negative gamma distribution, the 95% posterior interval increases approximately 5%, when DRC uncertainty is taken into account. In Case 3, where the prior distribution is a negative beta distribution, the 95% posterior interval increases approximately 4%, when DRC uncertainty is taken into account.

4.2.5. Comparison between models

The models being compared are the block maxima model using the annual maximum values and two threshold models, one with the threshold value $u = 200$, found by using the diagnostic based method (DBM threshold model) and another one with a threshold value of $u = 213$, found by the fixed frequency method (FFM threshold model).

It can be argued that the extreme values used in the FFM threshold model are superior to those used in the block maxima model since they are not constricted to having one and only one extreme value per year, like the annual values used in the latter model. The argument is, that if the de-clustering of the POTs is successful and there is no correlation between the extremes, than the quality of the POTs gathered by using the FFM are at least, equal to that of the block maxima model. For that reason the comparison below will be between the block maxima model and the FFM threshold model, on one hand, and between the FFM threshold model and the DBM threshold model, on the other hand.

Block maxima model vs. FFM threshold model

Tables 4.5 and 4.7 show the percentiles for the 100-year return levels for the block maxima model and the FFM threshold model, respectively. Figure 4.34 shows the 95% posterior interval of the 100-year return level for the block maxima model and the FFM threshold model. Tables B.2 and B.4 show the percentiles of the posterior
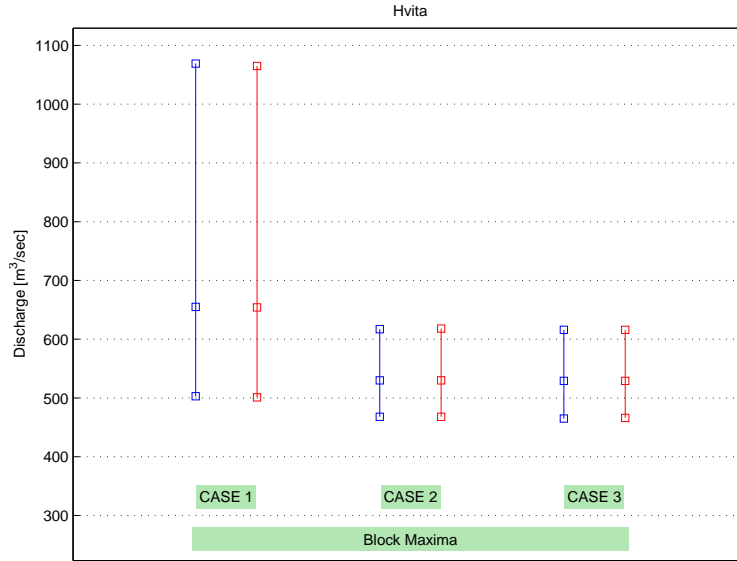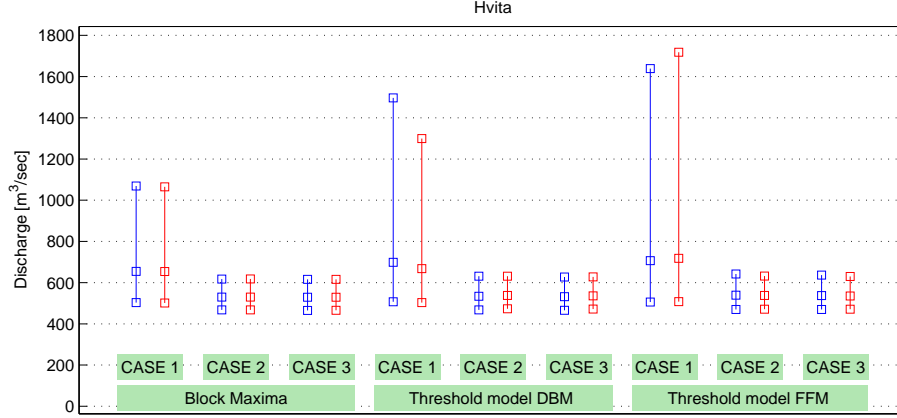
Figure 4.34: (V066) Comparison of the 95% posterior interval of the 100-year return level of discharge, between the three different models, with DRC uncertainty (blue) and without DRC uncertainty (red).

distributions for the GEV parameters for the Block maxima model and the GP parameters for the FFM Threshold model, respectively. The FFM threshold model uses approximately the same amount of extreme values as the block maxima model but the extremes used in the FFM threshold model are larger than those used in the block maxima model.

Looking at the 100-year return levels in Case 1 where the prior distribution for ξ is noninformative, the percentiles are considerably larger for the FFM threshold model than the block maxima model and hence the posterior interval is larger. The posterior densities for the Case 1 prior distributions for the block maxima model and the FFM threshold model are shown in Figure B.1 and Figure B.19, respectively.

The posterior density for the shape parameter, ξ, is wider in the FFM threshold model than in the block maxima model. The range of the 95% posterior interval for the parameter in the block maxima model is $[-0.04, 0.37]$ but $[-0.06, 0.65]$ for the FFM threshold model. The upper percentiles in the return level plots are particulary sensitive to high values of ξ which explains why the upper percentiles for the 100-year return levels are higher for the FFM threshold model than the block maxima model.

Cases 2 and 3 where the prior distribution for ξ is a negative gamma distribution and a negative beta distribution, respectively, do not provide a good fit in neither models. The constriction for posterior of ξ seems to be to excessive since a vast majority of its posterior density in Case 1 is positive.

DBM threshold model vs. FFM threshold model

Tables 4.6 and 4.7 show the percentiles for the 100-year return levels for the DBM threshold model and the FFM threshold model, respectively. Figure 4.34 shows the 95% posterior interval of the 100-year return level for the DBM threshold model and the FFM threshold model. Tables B.3 and B.4 show the percentiles of the posterior distributions for the GP parameters for the DBM threshold model and the FFM threshold model, respectively.

By lowering the threshold from 213 to 200 the effective number of POTs increase from 62.56 to 75.8. Looking at the Case 1 prior distribution, these added extreme data have the effect of lowering the upper values of the posterior distribution for ξ. That leads to lower upper percentiles for the return level plot and thus smaller posterior interval. So, for this river, the added data used in the DBM threshold model lowered the upper percentiles for the 100 year return level and its posterior interval got smaller.

There is little difference between the two models when looking the results from the prior distributions in Cases 2 and 3. In both models, the negative gamma prior in Case 2 seems have the effect that the simulated values in the posterior distribution of ξ are higher then for the negative beta prior in Case 3. That leads to higher return levels.

The return levels produced by the DBM threshold model have narrower posterior intervals than the FFM threshold model, but the difference is minor. The median values for the return levels are higher for the FFM threshold model than the DBM threshold model, but the difference is minor.

4.3. Results for Sanda

The discharge time series for Sanda spans approximately 43 years, from November 1965 to August 2008. The daily point estimates of water discharge are shown in Figure 4.35 The B-spline discharge rating curve is shown in Figure 4.35.
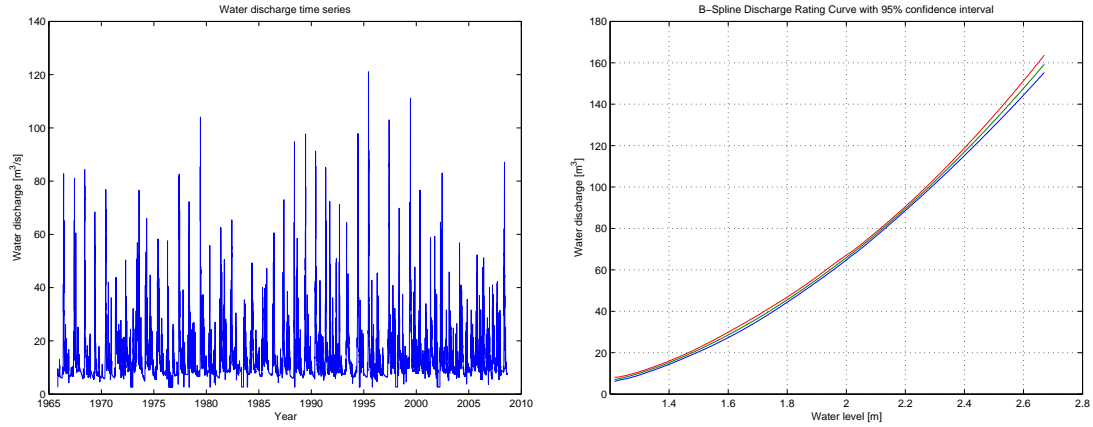
Figure 4.35: V026: Left panel: Water discharge time series. Right panel: B-spline Discharge Rating curve

4.3.1. Block maxima model

The annual maximum values used for the Block Maxima model are shown in Figure 4.36. Figure 4.37 shows how the discharge rating curve is used to estimate the uncertainty in the annual maximum values. In Figure 4.37 the highlighted annual maximum values from Figure 4.36 are fitted to the discharge rating curve. Figure 4.37 shows the same water discharge time series as Figure 4.36 but with the 95% uncertainty interval for the annual maximum values shown as well.
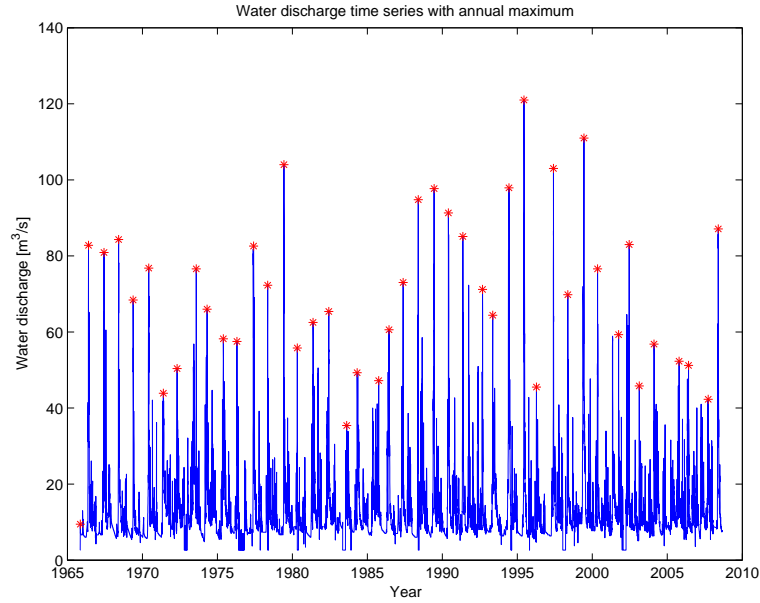
Figure 4.36: V026: Water discharge time series with annual maximum values

Figure 4.37: V026: Left panel: Water discharge time series with 95% posterior interval for extreme values. Right panel: B-spline discharge rating curve with fitted annual maximum values and their 95% posterior interval

Comparison between the three different cases of prior distribution for ξ

Figure 4.38: (V026 BM w/DRC): Prior and posterior distributions for the shape parameter (ξ) in the GEV distribution for all three cases of prior distributions. Case 1: left panels, Case 2: middle panels, Case 3: right panels.
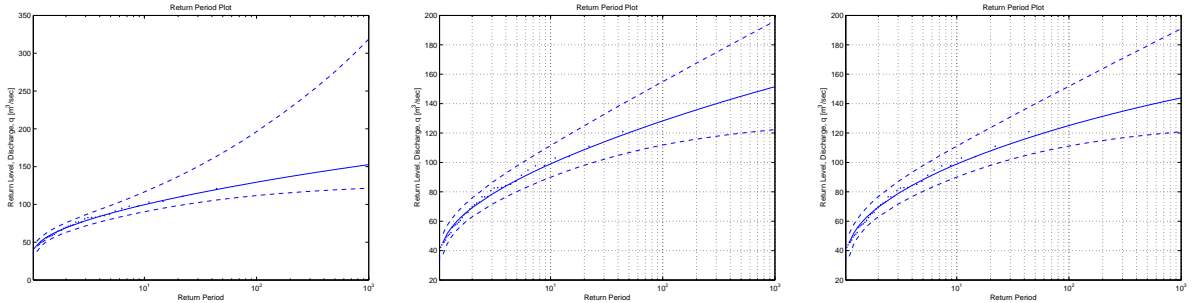
Figure 4.39: (V026 BM w/DRC): Return level plots for the block maxima model for all three cases of prior distributions. Case 1: left panel, Case 2: middle panel, Case 3: right panel.

Figure 4.38 shows the prior distributions of ξ and their corresponding posterior distributions for all cases. A big portion of of the posterior distribution in Case 1 is positive and so constraining the posterior to only negative values has great influence on the results. Figure 4.39 show the return level plots for all three cases of prior distributions. Constraining the prior to negative values only, lowers the return levels

Table 4.8: V026 BM: 100-year return levels of discharge (m^3/sec), for all three cases of prior distributions, calculated with and without a DRC

	Block Extrema					
	With DRC			Without DRC		
Percentiles	Normal	Neg-Gamma	Neg-Beta	Normal	Neg-Gamma	Neg-Beta
2.5%	112	112	111	112	112	111
25%	121	121	119	121	121	119
50%	129	128	125	130	128	125
75%	143	137	133	143	136	133
97.5%	196	155	152	198	154	151
95% conf. int.	85	43	41	86	42	40
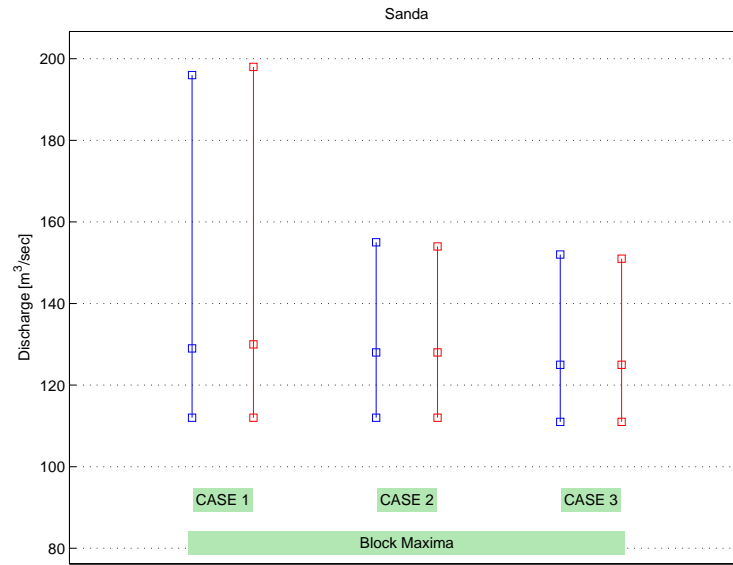
Figure 4.40: (V026 BM) Comparison of the 95% posterior interval of the 100-year return level of discharge, between the three cases of prior distributions, with DRC uncertainty (blue) and without DRC uncertainty (red).

and makes the confidence interval narrower. This constriction has the effect that the data does not fit the model, as well as in Case 1.

Constraining the posterior density of ξ, to negative values only, by using negative prior distributions has a significant influence on the outcome of the posterior distributions and thus the resulting return levels. In the case where the prior distribution for the shape parameter is a normal distribution, the posterior distribution has more tendency to be negative than positive, having a median value of -0.10 (see Table C.2). Constraining the priors has similar effects on the posteriors as eliminating the positive portion of the Case 1 posterior density. The negative part of the posterior

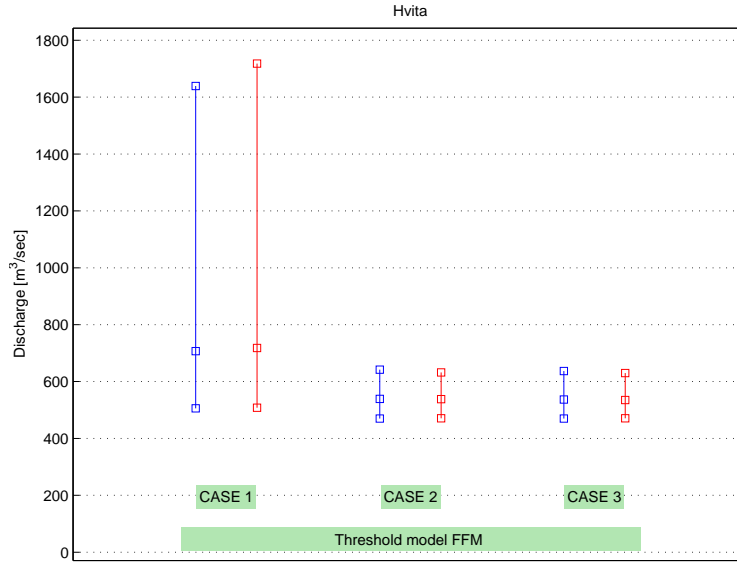density using the non-informative normal prior is similar to the posterior distributions resulting from the constraining priors. Since a higher value of ξ leads to thicker tail of the GEV distribution and hence larger return values, eliminating the positive portion of the ξ values reduces the return levels and the range for their 95% posterior intervals for high return periods. Since, the majority of the unrestricted, Case 1, posterior distribution of ξ is negative, the constriction to negative values only, as is done in Cases 2 and 3, does not have as drastic effect as it would, if the Case 1 posterior was more positive. Hence the, models in Cases 2 and 3 fit the data adequately, despite the restriction of ξ.

Constraining the ξ parameter to only negative values has the effect that the median value of the 100-year return level becomes lower for both the negative gamma prior distribution and the negative beta prior distribution. Furthermore, the uncertainty in the 100-year return level, for the constraining prior distributions in Cases 2 and 3, shrinks to approximately 45% of the uncertainty for Case 2 where the prior is non-informative.

The median value of the 100 year return level is lower in Case 3 where the prior distribution of ξ is negative beta then in Case 2 where the prior distribution is negative gamma. The reason for that is that the density of the gamma function is more condensed near the zero value while the beta distribution is uniform. The resulting posterior density of ξ, for Case 2 is therefor composed of higher values than the posterior density of ξ, in Case 3, leading to higher return levels.

The effect of discharge rating curve uncertainty

The effect of merging the discharge rating curve uncertainty with the sampling uncertainty from the MCMC scheme has minor effect on the median value of the 100-year return levels and minor effect on the 95% posterior intervals. This is shown in Table 4.8 and Figure 4.40. The change in the over all uncertainty for the 100-year return level, is minor, when adding the discharge rating curve uncertainty to the calculations. In Case 1, the range of the 95% confidence decreases when taking the DRC uncertainty into account, but the decrease is insignificant. In Case 2, the uncertainty interval is the same whether or not the DRC uncertainty into account. In Case 3, the uncertainty interval gets increases when taking the DRC uncertainty into account, but the increase is insignificant.

4.3.2. Threshold model
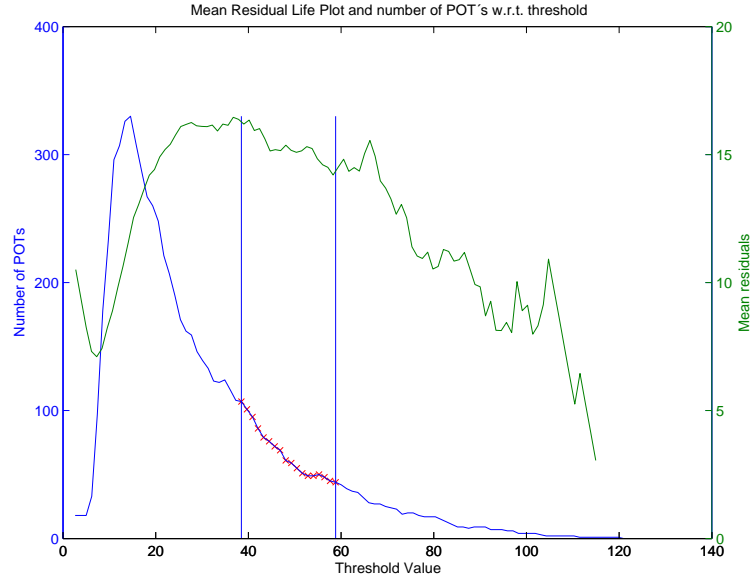
Figure 4.41: V026: Mean residual life plot and number of POTs as a function of threshold value

As is shown in Figure 4.42, the lowest threshold value where the same value of the parameters is inside the 95% confidence interval is not the same when looking at the two parameters. For σ^*, a threshold value of approximately 24 will produce a parameter inside for the 95% confidence interval of the above threshold values. For ξ, a threshold value of approximately 34 will produce a parameter inside for the 95% confidence interval of the above threshold values.

What can be inferred from these figures is a lower limit of $u_{low} = 34$. This lower limit comes from the estimation of the σ^* parameter w.r.t. threshold. The mean residual life plot could suggest a threshold pick of approximately $u = 30$. That being below the value of $u_{low} = 34$ a higher value for the threshold was chosen. The threshold chosen for this river was $u = 40$. That threshold value produces approximately 123 POTs when using a comb value of 5 and it could be argued that the mean residual life plot, in Figure 4.41, is approximately linear for all higher threshold values.

Two different values for the threshold were used in the flood analysis. That is, one analysis using a threshold value of $u = 40$, and another analysis using the threshold value which produces as many POTs as there are years in the data set. That threshold value is $u = 59$ These two different methods for choosing the threshold will be referred to as the *diagnostic based method* (DBM) and the *fixed frequency method* (FFM), respectively.
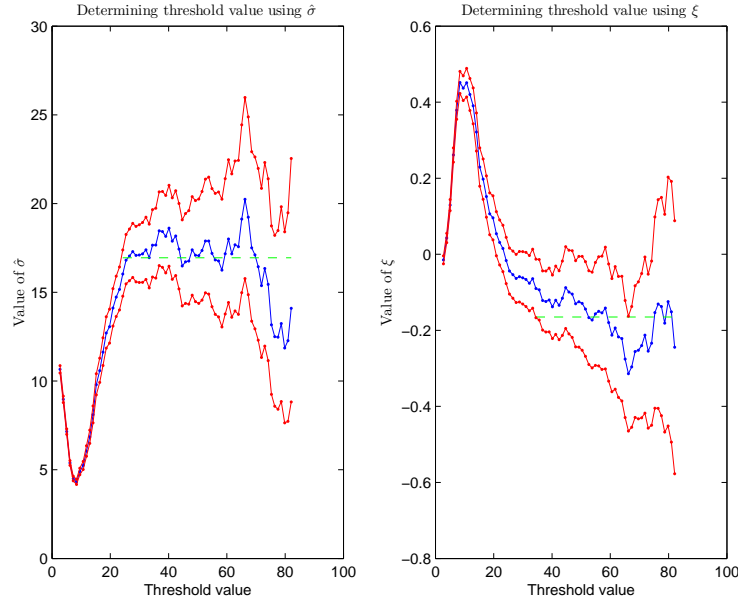
Figure 4.42: V026: Threshold approximation using the parameters σ^* and ξ

4.3.3. Threshold Model using diagnostic based methods (DBM) for determining the threshold value

The threshold model analysis of the data for Sanda was continued using a threshold value of $u = 40$. In Figure 4.43 the POTs have been processed by the B-spline discharge rating curve to evaluate the uncertainty in the extreme values. In Figure 4.43 the POTs and their 95% posterior interval are shown with the water discharge time series along with the threshold value.
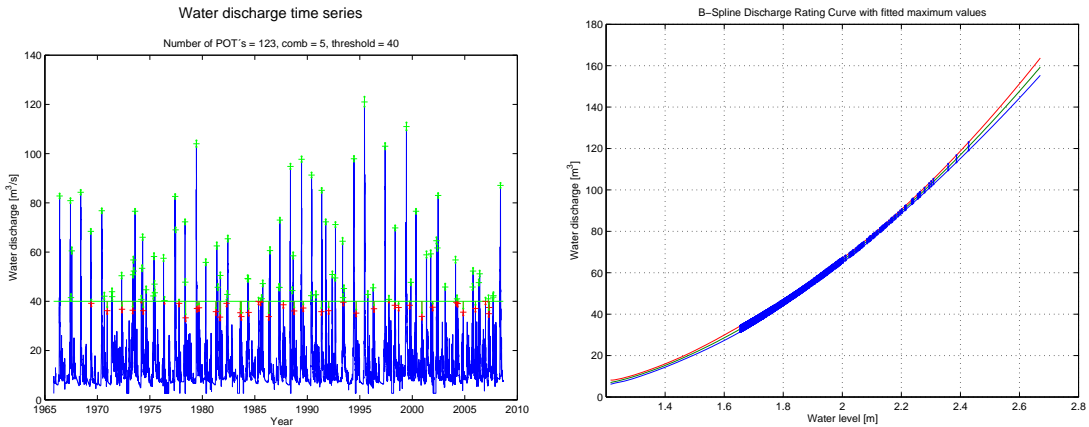
Figure 4.43: V026: Left panel: Water discharge time series with 95% posterior interval for extreme values. Right panel: Discharge rating curve with fitted POT values

4. Results and discussions

Comparison between the three different cases of prior distribution for ξ
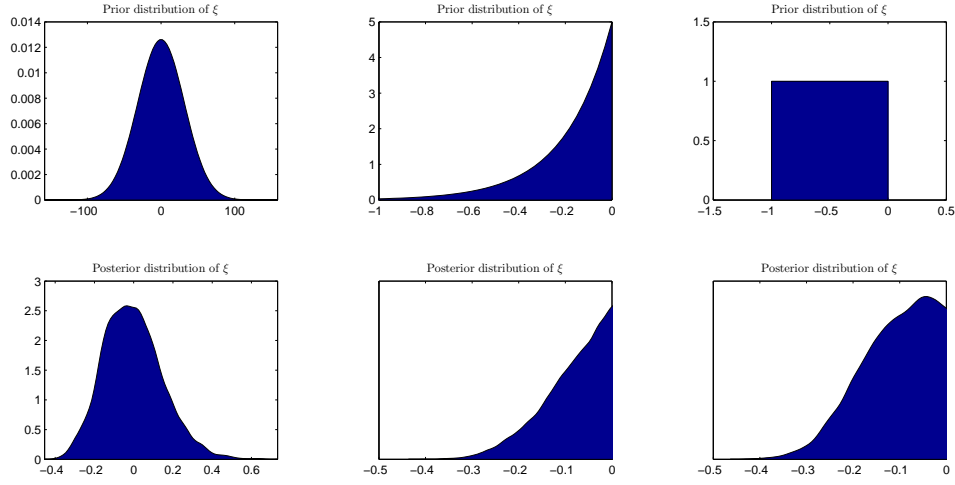
Figure 4.44: (V026 TM DBM w/DRC): Prior and posterior distributions for the shape parameter (ξ) in the GP distribution for all three cases of prior distributions. Case 1: left panels, Case 2: middle panels, Case 3: right panels.
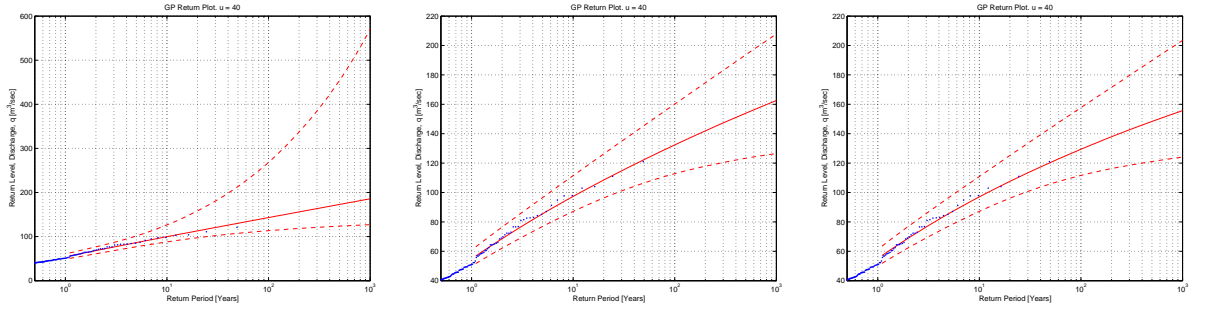
Figure 4.45: (V026 TM DBM w/DRC): Return level plots for the threshold model for all three cases of prior distributions. Case 1: left panel, Case 2: middle panel, Case 3: right panel.

Constraining the posterior density of ξ, to negative values only, by using negative prior distributions has a significant influence on the outcome of the posterior distributions and thus the resulting return levels. In the case where the prior distribution for the shape parameter is a normal distribution, the posterior distribution is more or less evenly distributed between positive and negative values, having a median value of -0.01 (see Table C.3). Constraining the priors has similar effects on the posteriors as eliminating the positive portion of Case 1 posterior density. The negative part of the posterior density using the non-informative normal prior is similar to the posterior distributions resulting from the constraining priors. Since a higher value of ξ leads to thicker tail of the GP distribution and hence larger return values, eliminating the positive portion of the ξ values reduces the return levels and the

Table 4.9: V026 TM DBM: 100-year return levels of discharge (m^3/sec), for all three cases of prior distributions, calculated with and without a DRC

Threshold model with threshold, u = 40						
	With DRC			Without DRC		
Percentiles	Normal	Neg-Gamma	Neg-Beta	Normal	Neg-Gamma	Neg-Beta
2.5%	113	113	112	114	113	112
25%	129	124	122	129	124	121
50%	143	132	129	143	132	129
75%	167	141	139	165	140	137
97.5%	268	160	158	248	157	155
95% conf. int.	155	47	46	134	44	43

Figure 4.46: (V026 TM DBM) Comparison of the 95% posterior interval of the 100-year return level of discharge, between the three cases of prior distributions, with DRC uncertainty (blue) and without DRC uncertainty (red).

range for their 95% posterior intervals for high return periods. This reduction in the posterior densities of ξ, has the effect that the models in Cases 2 and 3, using the negative priors, do not fit the data as well as the model in Case 1. Even so, majority of the unrestricted, Case 1, posterior distribution of ξ is negative, and thus the constriction to negative values only, as is done in Cases 2 and 3, does not have as drastic effect as it would, if the Case 1 posterior was more positive. Hence the, models in Cases 2 and 3 fit the data adequately, despite the restriction of ξ.

Thus, constraining the ξ parameter to negative values only, has the effect that the median value of the 100-year return level becomes lower for both cases of negative

prior distributions for ξ. In the both case where the prior distribution is the negative the median value becomes approximately 10% lower. Furthermore, the uncertainty in Cases 2 and 3, where the priors are negative only, shrinks to approximately 30% of the uncertainty for Case 1, where the prior is non-informative.

The effect of discharge rating curve uncertainty

The effect of merging the discharge rating curve uncertainty with the sampling uncertainty from the MCMC scheme has minor effect on the median value of the 100-year return level. This is shown in Table 4.9 and Figure 4.46. There is a change in the over all uncertainty for the 100-year return level, when adding the discharge rating curve uncertainty to the calculations. In Case 1, where the prior distribution is a normal distribution, the 95% posterior interval increases approximately 15%, when DRC uncertainty is taken into account. In Case 2, where the prior distribution is a negative gamma distribution, the 95% posterior interval increases approximately 10%, when DRC uncertainty is taken into account. In Case 3, where the prior distribution is a negative beta distribution, the 95% posterior interval increases approximately 7%, when DRC uncertainty is taken into account.

4.3.4. Threshold Model using the fixed frequency method (FFM) for determining the threshold value

With the rule of thumb (FFM) method a threshold is chosen so the number of point estimates of discharge that are above the threshold, after de-clustering, are equal to the number of years of data used in the analysis. For Sanda, that leads to a threshold value of $u = 59$ with the total number of point estimates of discharge, greater than the threshold value, equal to 43.

Comparison between the three different cases of prior distribution for ξ

Figure 4.48 shows the prior distributions of ξ and their corresponding posterior distributions for all cases. A big portion of of the posterior distribution in Case 1 is positive and so constraining the posterior to only negative values has great influence on the results. Figure 4.49 show the return level plots for all three cases of prior distributions. Constraining the prior to negative values only, lowers the return levels and makes the confidence interval narrower. This constriction has the effect that the data does not fit the model, as well as in Case 1.
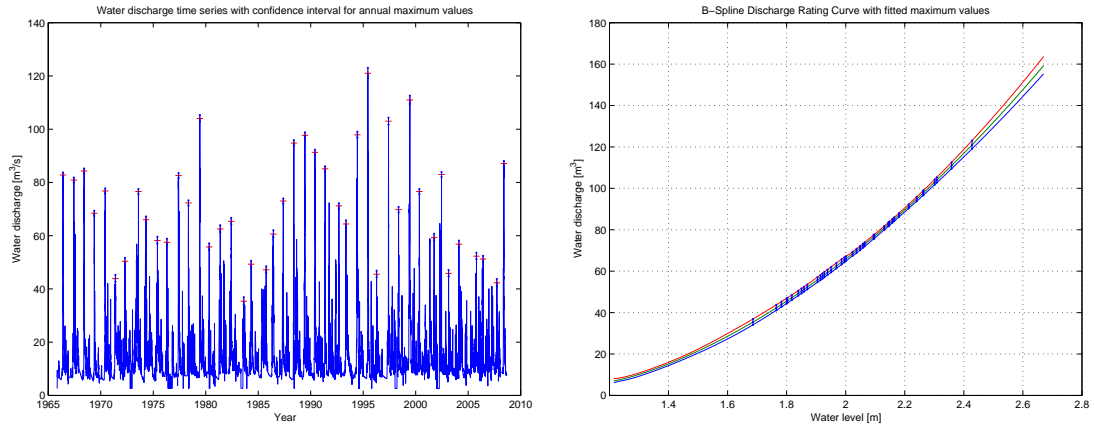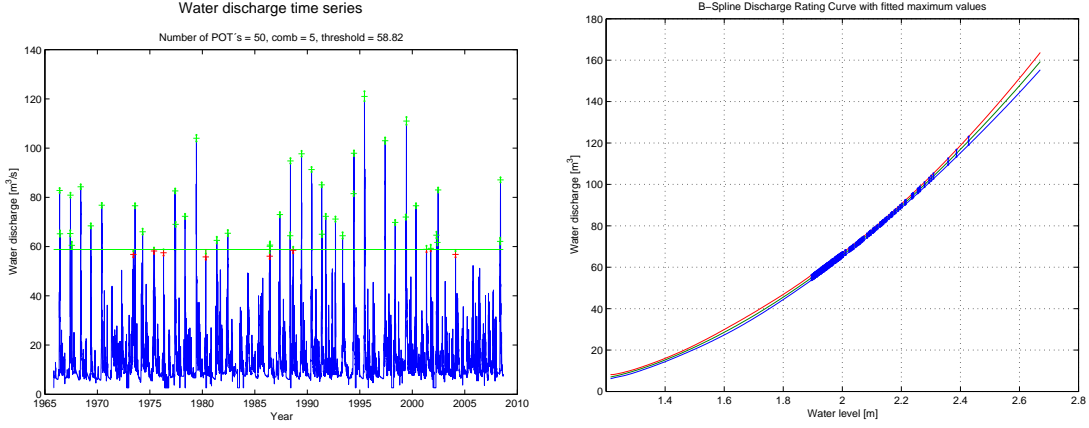
Figure 4.47: (V026 FFM): Right panel: Water discharge time series with 95% posterior interval for extreme values. Left panel: B-spline Discharge rating curve with fitted POT values
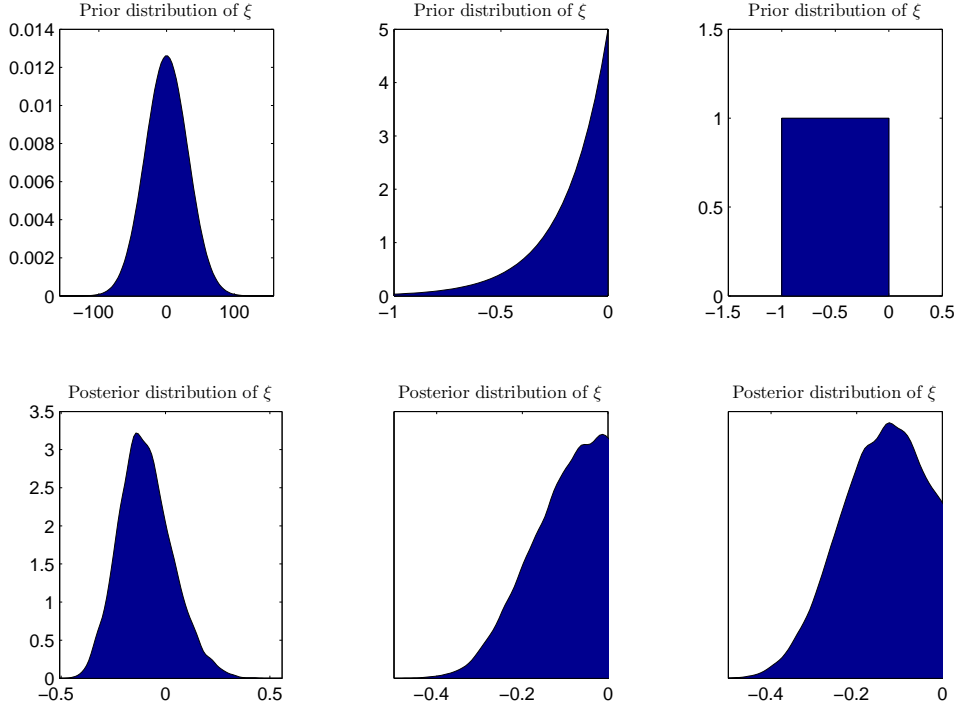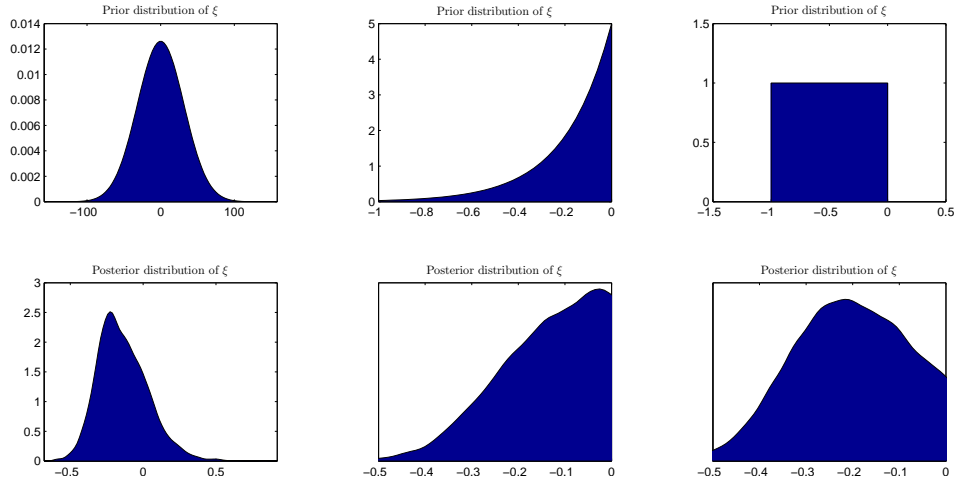

Figure 4.48: (V026 TM FFM w/DRC): Prior and posterior distributions for the shape parameter (ξ) in the GP distribution for all three cases of prior distributions. Case 1: left panels, Case 2: middle panels, Case 3: right panels.

Constraining the posterior density of ξ, to negative values only, by using negative prior distributions has a significant influence on the outcome of the posterior distributions and thus the resulting return levels. In the case where the prior distribution for the shape parameter is a normal distribution, the posterior distribution is more or less evenly distributed between positive and negative values, having a median value of -0.16 (see Table C.4). Constraining the priors has similar effects on the posteriors as eliminating the positive portion of the Case 1 posterior density. The negative part of the posterior density using the non-informative normal prior is similar to the posterior distributions resulting from the constraining priors. Since a higher value of ξ leads to thicker tail of the GP distribution and hence larger return

4. Results and discussions

Figure 4.49: (V026 TM FFM w/DRC): Return level plots for the threshold model for all three cases of prior distributions. Case 1: left panel, Case 2: middle panel, Case 3: right panel.

Table 4.10: V026 TM FFM: 100-year return levels of discharge (m^3/sec), for all three cases of prior distributions, calculated with and without a DRC

Threshold model with threshold, u = 59						
	With DRC			Without DRC		
Percentiles	Normal	Neg-Gamma	Neg-Beta	Normal	Neg-Gamma	Neg-Beta
2.5%	112	112	111	112	111	111
25%	120	120	118	120	120	118
50%	127	127	124	128	127	123
75%	141	136	131	141	136	131
97.5%	203	158	153	207	157	152
95% conf. int.	92	46	42	95	46	41

values, eliminating the positive portion of the ξ values reduces the return levels and the range for their 95% posterior intervals for high return periods. This reduction in the posterior densities of ξ, has the effect that the models in Cases 2 and 3, using the negative priors, do not fit the data as well as the model in Case 1. Even so, majority of the unrestricted, Case 1, posterior distribution of ξ is negative, and thus the constriction to negative values only, as is done in Cases 2 and 3, does not have as drastic effect as it would, if the Case 1 posterior was more positive. Hence the, models in Cases 2 and 3 fit the data adequately, despite the restriction of ξ.

Constraining the ξ parameter to negative values only, has the effect that the median value of the 100-year return level lowers a little for both cases of negative prior distributions for ξ. Furthermore, the uncertainty in Cases 2 and 3, where the priors are negative only, shrinks to approximately 48% and 45%, respectively, of the uncertainty for Case 1, where the prior is non-informative.
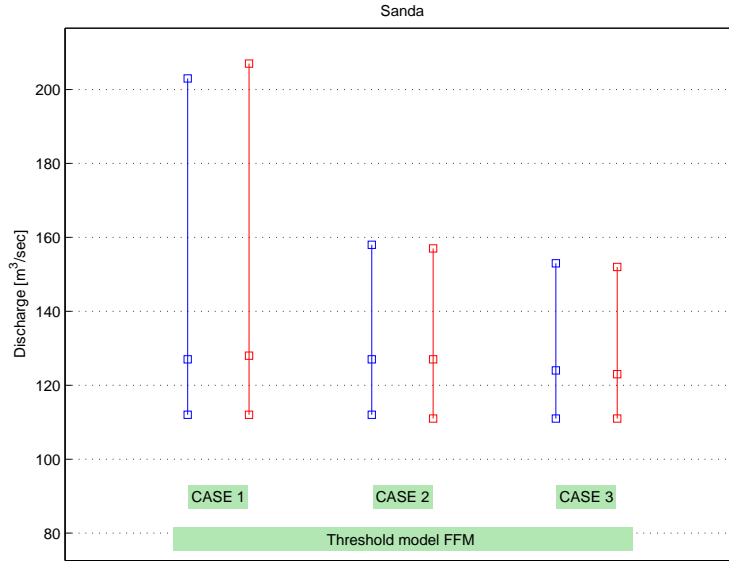
Figure 4.50: (V026 TM FFM) Comparison of the 95% posterior interval of the 100-year return level of discharge, between the three cases of prior distributions, with DRC uncertainty (blue) and without DRC uncertainty (red).

The effect of discharge rating curve uncertainty

The effect of merging the discharge rating curve uncertainty with the sampling uncertainty from the MCMC scheme has minor effect on the median value of the 100-year return level. This is shown in Table 4.10 and Figure 4.50. There is a change in the over all uncertainty for the 100-year return level, when adding the discharge rating curve uncertainty to the calculations. In Case 1, where the prior distribution is a normal distribution, the 95% posterior interval, surprisingly, decreases approximately 3%, when DRC uncertainty is taken into account. In Case 2, where the prior distribution is a negative gamma distribution, the 95% posterior interval increases approximately 4%, when DRC uncertainty is taken into account. In Case 3, where the prior distribution is a negative beta distribution, the 95% posterior interval increases approximately 4%, when DRC uncertainty is taken into account.

4.3.5. Comparison between models

The models being compared are the block maxima model using the annual maximum values and two threshold models, one with the threshold value $u = 40$, found by using the diagnostic based method (DBM threshold model) and another one with a threshold value of $u = 59$, found by the fixed frequency method (FFM threshold

model).

It can be argued that the extreme values used in the FFM threshold model are superior to those used in the block maxima model since they are not constricted to having one and only one extreme value per year, like the annual values used in the latter model. The argument is, that if the de-clustering of the POTs is successful and there is no correlation between the extremes, than the quality of the POTs gathered by using the FFM are at least, equal to that of the block maxima model. For that reason the comparison below will be between the block maxima model and the FFM threshold model, on one hand, and between the FFM threshold model and the DBM threshold model, on the other hand.
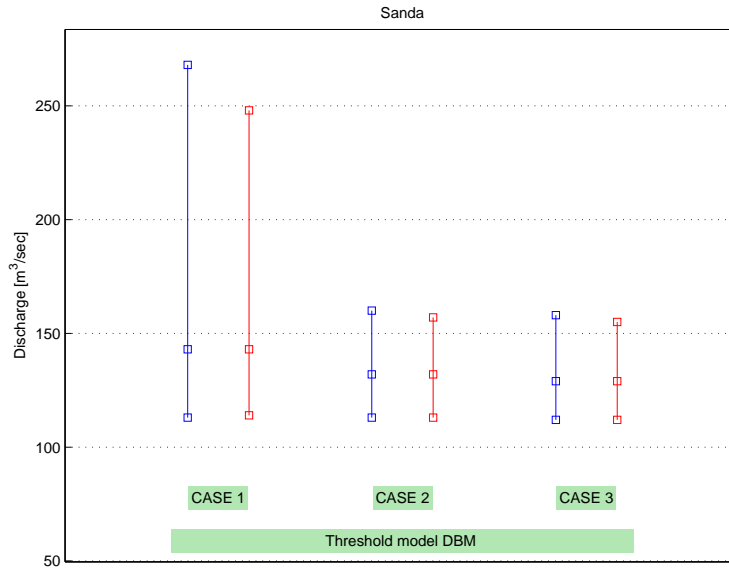

Figure 4.51: (V026) Comparison of the 95% posterior interval of the 100-year return level of discharge, between the three different models, with DRC uncertainty (blue) and without DRC uncertainty (red).

Block maxima model vs. FFM threshold model

Tables 4.8 and 4.10 show the percentiles for the 100-year return levels for the block maxima model and the FFM threshold model, respectively. Figure 4.51 shows the 95% posterior interval of the 100-year return level for the block maxima model and the FFM threshold model. Tables C.2 and C.4 show the percentiles of the posterior distributions for the GEV parameters for the Block maxima model and the GP parameters for the FFM Threshold model, respectively. The FFM threshold model uses approximately the same amount of extreme values as the block maxima model but the extremes used in the FFM threshold model are larger than those used in the block maxima model.

Looking at Case 1 where the prior distribution is noninformative, the 100-year return levels are similar when comparing the block maxima model and the FFM threshold model. However, the median value from the FFM threshold model is lower than

that of the block maxima model but the 95% posterior interval is larger. The wider interval is related to the fact that the interval for the posterior distribution of ξ is larger in the FFM threshold model than the block maxima model.

The range of the 95% posterior interval for the shape parameter in the block maxima model is $[-0.32, 0.19]$ but $[-0.43, 0.26]$ for the FFM threshold model. The upper percentiles in the return level plots are particulary sensitive to high values of ξ which explains why the upper percentiles for the 100-year return levels are higher for the FFM threshold model than the block maxima model.

Looking at Case 1 where the prior distribution for ξ is noninformative, the lower percentiles for the 100-year return level, 2.5%, 25%, and 50%, are very similar for both models. The higher percentiles, 75% and 97.5%, are larger for the FFM threshold model, hence the posterior interval is larger.

The posterior densities for the Case 1 prior distributions for the block maxima model and the FFM threshold model are shown in Figure C.1 and Figure C.19, respectively.

Both models provide a good fit for the data when constraining the posterior distributions of ξ with the prior distributions in Cases 1 and 2. The main difference between the models is that the posterior interval of the 100-year return level is larger in the FFM threshold model than the block maxima model. The 97.5% percentiles are larger for the FFM threshold model even though the median values are smaller.

DBM threshold model vs. FFM threshold model

Tables 4.9 and 4.10 show the percentiles for the 100-year return levels for the DBM threshold model and the FFM threshold model, respectively. Figure 4.51 shows the 95% posterior interval of the 100-year return level for the DBM threshold model and the FFM threshold model. Tables C.3 and C.4 show the percentiles of the posterior distributions for the GP parameters for the DBM threshold model and the FFM threshold model, respectively.

By lowering the threshold from 58.83 to 40 the effective number of POTs increase from 42.82 to 71.99. Looking at the Case 1 prior distribution, these added extreme data have the effect of increasing the upper values of the posterior distribution for ξ. That leads to higher percentiles for the return level plot and a larger posterior interval. So, for this river, the added data used in the DBM threshold model increased the upper percentiles for the 100 year return level and its posterior interval got larger.

In both models, the negative gamma prior in Case 2 seems have the effect that the

simulated values in the posterior distribution of ξ higher then for the negative beta prior in Case 3. That leads to slightly higher return levels.

The return levels produced by the FFM threshold model have narrower posterior intervals than the DBM threshold model but the difference is minor. The median values for the return levels are higher for the DBM threshold model than the FFM threshold model.

4.4. Results for Svarta

The discharge time series for Svarta spans 36 years, from September 1962 to August 1998. The daily point estimates of water discharge are shown in Figure 4.52
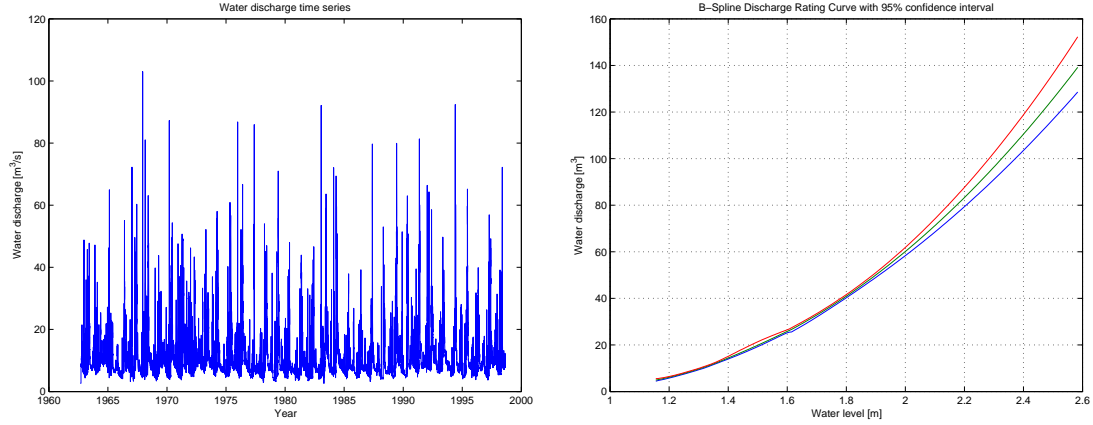
Figure 4.52: V010: Left panel: Water discharge time series. Right panel: B-spline Discharge Rating curve

The relationship between water level and water discharge is found by applying the B-spline discharge rating curve, as discussed in Section 3.2, on the paired water level and water discharge data for the river. The B-spline discharge rating curve is shown in Figure 4.52.

4.4.1. Block maxima model

The annual maximum values used for the Block Maxima model are shown in Figure 4.53. Figure 4.54 shows how the discharge rating curve is used to estimate the uncertainty in the annual maximum values. In Figure 4.54 the highlighted annual maximum values from Figure 4.53 are fitted to the discharge rating curve and from that point it becomes manageable to estimate the uncertainty in the point estimate. Figure 4.54 shows the same water discharge time series as Figure 4.53 but with the 95% uncertainty interval for the annual maximum values shown as well.
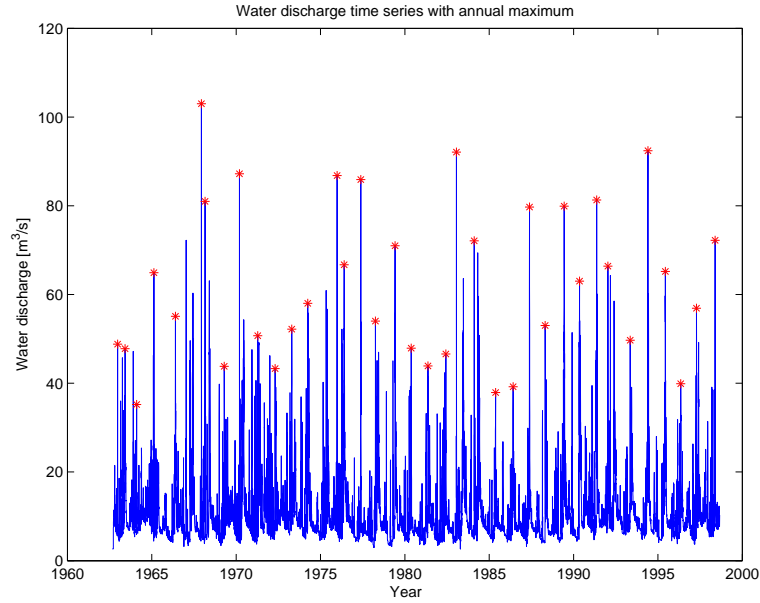
Figure 4.53: V010: Water discharge time series with annual maximum values

Figure 4.54: V010: Left panel: Water discharge time series with 95% posterior interval for extreme values. Right panel: B-spline discharge rating curve with fitted annual maximum values and their 95% posterior interval

Comparison between the three different cases of prior distribution for ξ

Figure 4.55: (V010 BM w/DRC): Prior and posterior distributions for the shape parameter (ξ) in the GEV distribution for all three cases of prior distributions. Case 1: left panels, Case 2: middle panels, Case 3: right panels.
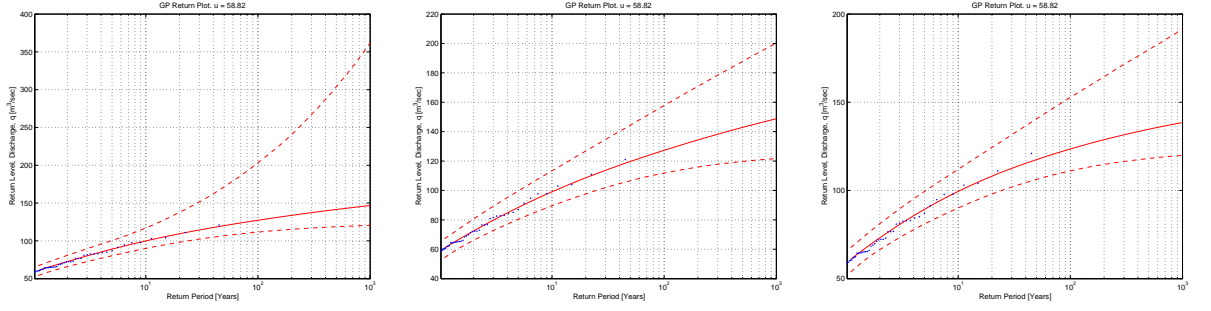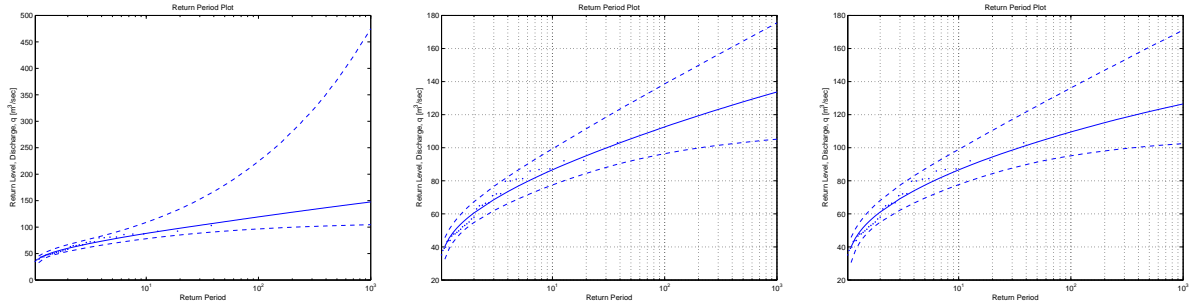

Figure 4.56: (V010 BM w/DRC): Return level plots for the block maxima model for all three cases of prior distributions. Case 1: left panel, Case 2: middle panel, Case 3: right panel.

Figure 4.55 shows the prior distributions of ξ and their corresponding posterior distributions for all cases. A big portion of posterior distribution in Case 1 is positive and therefore constraining the posterior to only negative values has great influence on the results. Figure 4.5 show the return level plots for all three cases of prior distributions. Constraining the prior to negative values only, lowers the return

4. Results and discussions

Table 4.11: *V010 BM: 100-year return levels of discharge (m^3/sec), for all three cases of prior distributions, calculated with and without a DRC*

| | Block Extrema | | | | | |
| | With DRC | | | Without DRC | | |
Percentiles	Normal	Neg-Gamma	Neg-Beta	Normal	Neg-Gamma	Neg-Beta
2.5%	97	96	95	98	97	97
25%	108	106	103	108	106	104
50%	120	113	110	120	113	110
75%	139	120	118	139	120	117
97.5%	225	139	136	225	138	134
95% conf. int.	128	42	41	127	40	38
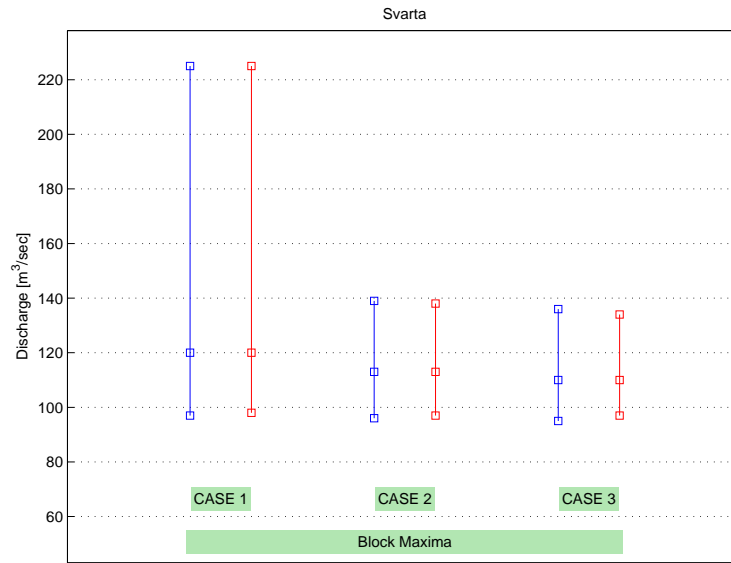
Figure 4.57: *(V010 BM) Comparison of the 95% posterior interval of the 100-year return level of discharge, between the three cases of prior distributions, with DRC uncertainty (blue) and without DRC uncertainty (red).*

levels and makes the confidence interval narrower. This constriction has the effect that the data does not fit the model, as well as in Case 1.

Constraining the posterior density of ξ, to negative values only, by using negative prior distributions has a significant influence on the outcome of the posterior distributions and thus the resulting return levels. In the case where the prior distribution for the shape parameter is a normal distribution, the posterior distribution has more tendency to be negative than positive, having a median value of -0.04 (see Table D.2). Constraining the priors has similar effects on the posteriors as eliminating the positive portion of the Case 1 posterior density. The negative part of the posterior

density using the non-informative normal prior is similar to the posterior distributions resulting from the constraining priors. Since a higher value of ξ leads to thicker tail of the GEV distribution and hence larger return values, eliminating the positive portion of the ξ values reduces the return levels and the range for their 95% posterior intervals for high return periods. This reduction in the posterior densities of ξ , has the effect that the models in cases 2 and 3, using the negative priors, do not fit the data as well as the model in Case 1. Even so, majority of the unrestricted, Case 1, posterior distribution of ξ is negative, and thus the constriction to negative values only, as is done in cases 2 and 3, does not have as drastic effect as it would, if the Case 1 posterior was more positive. Hence the, models in cases 2 and 3 fit the data adequately, despite the restriction of ξ.

The median value of the 100-year return level is lower in Case 3, where the prior distribution of ξ is negative beta then in Case 2, where the prior distribution is negative gamma. The reason for that is that the density of the gamma function is more condensed near the zero value while the beta distribution is uniform. The resulting posterior density of ξ, for Case 2 is therefor composed of higher values than the posterior density of ξ, in Case 3, leading to higher return levels.

Constraining the ξ parameter to only negative values has the effect that the median value of the 100-year return level becomes approximately 6% lower in Case 2 than Case 1, and approximately 9% lower in Case 3. Due to the negative prior distributions, the range of the 95% posterior interval for cases 2 and 3 shrinks to approximately 31% of the range of the posterior interval of Case 1.

The effect of discharge rating curve uncertainty

The effect of merging the discharge rating curve uncertainty with the sampling uncertainty from the MCMC scheme has minor effect on the median value of the 100-year return levels and moderate effect on the 95% posterior intervals. This is shown in Table 4.11 and Figure 4.57. The change in the over all uncertainty for the 100-year return level, is minor, when adding the discharge rating curve uncertainty to the calculations. In Case 1, range 95% posterior interval for the 100-year return level, increases insignificantly, or less than 1%. In Case 2, range 95% posterior interval for the 100-year return level, increases approximately 6%. In Case 3, range 95% posterior interval for the 100-year return level, increases approximately 11%.

4. Results and discussions

4.4.2. Threshold model
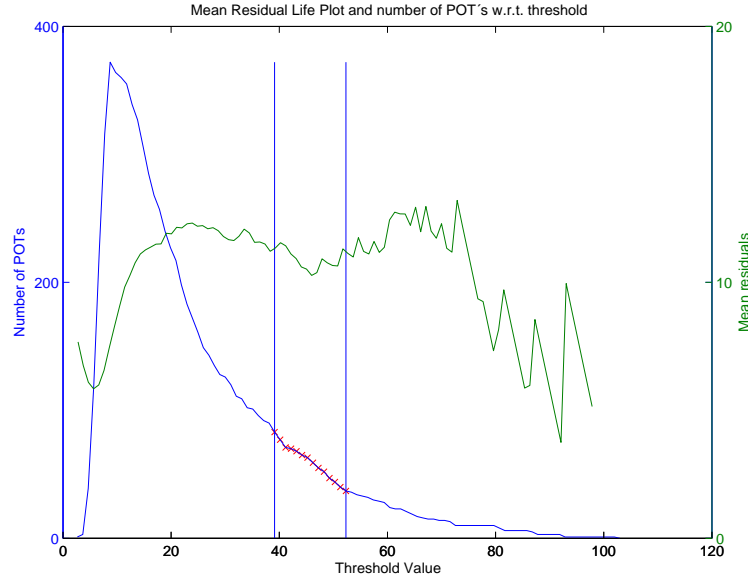
Figure 4.58: V010: Mean residual life plot and number of POTs as a function of threshold value

Figure 4.59, shows how the parameters of the ξ and σ^* change with respect to threshold value.

As is shown in Figure 4.59, the lowest threshold value where the same value of the parameters is inside the 95% confidence interval is approximately the same when looking at the two parameters. For σ^*, a threshold value of approximately 17 will produce a parameter inside for the 95% confidence interval of the above threshold values. For ξ, a threshold value of approximately 17 will produce a parameter inside for the 95% confidence interval of the above threshold values.

What can be inferred from these figures is a lower limit of $u_{low} = 17$. This lower limit comes from the estimation of both the σ^* parameter and the ξ parameter w.r.t. threshold. Disregarding the largest values, the mean residual life plot, in Figure 4.58, would suggest a threshold pick of approximately $u = 20$ but that would leave us with to many POTs. The threshold chosen for this river was $u = 40$. That threshold value produces 77 POTs when using a comb value of 5. Disregarding that the linearity does not hold for the largest threshold values, a threshold choice of $u = 40$ seems reasonable. The mean residual life plot, in Figure 4.58, is approximately linear on the interval $40 - 75$.

Two different values for the threshold were used in the flood analysis. That is, one analysis using a threshold value of $u = 40$, estimated using the methods described above. And another analysis using the threshold value which produces as many
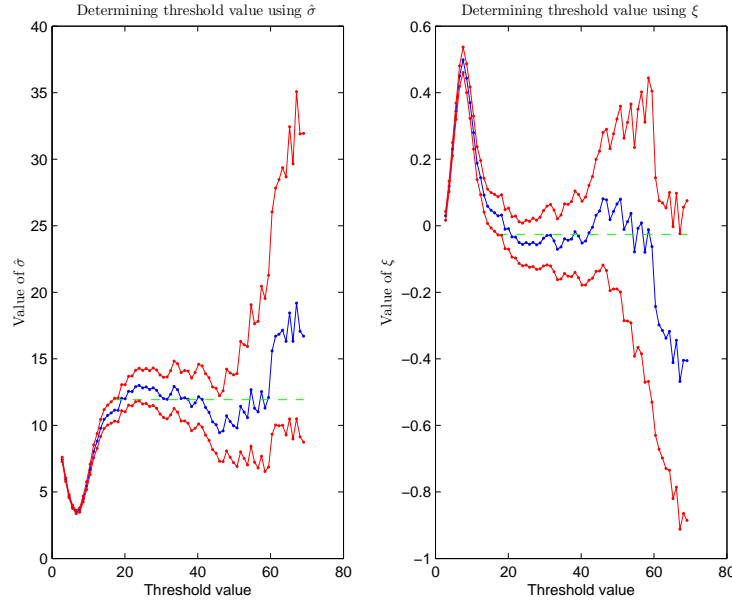
Figure 4.59: V010: Threshold approximation using the parameters σ^* and ξ

POTs as there are years in the data set. That threshold value is $u = 52$. These two different methods for choosing the threshold will be referred to as the *diagnostic based method* (DBM) and the *fixed frequency method* (FFM), respectively.

4.4.3. Threshold Model using diagnostic based methods (DBM) for determining the threshold value

The threshold model analysis of the data for Svarta was continued using a threshold value of $u = 40$. In Figure 4.60 the POTs have been processed by the B-spline discharge rating curve to evaluate the uncertainty in the extreme values. In Figure 4.60 the POTs and their 95% posterior interval are shown with the water discharge time series along with the threshold value.

Comparison between the three different cases of prior distribution for ξ

Figure 4.61 shows the prior distributions of ξ and their corresponding posterior distributions for all cases. A big portion of of the posterior distribution in Case 1 is positive and so constraining the posterior to only negative values has great influence on the results. Figure 4.62 show the return level plots for all three cases of prior distributions. Constraining the prior to negative values only, lowers the return levels and makes the confidence interval narrower. This constriction has the effect that
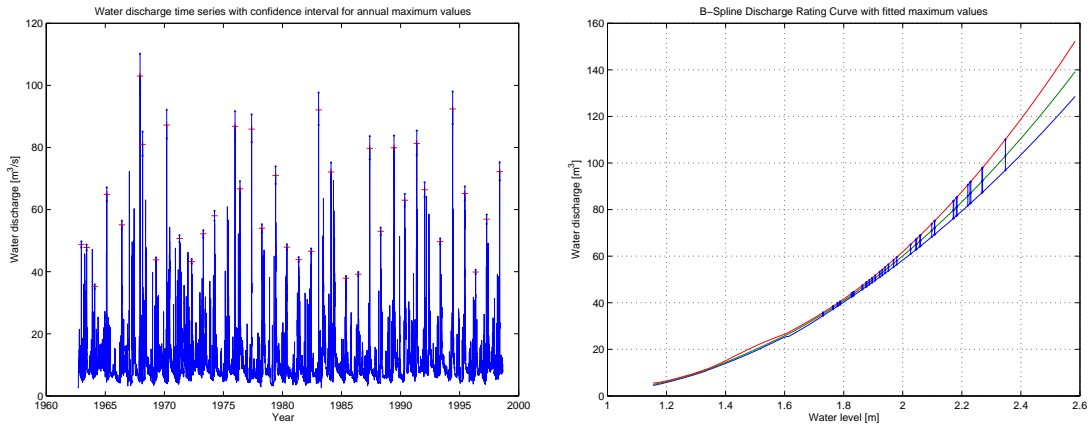
Figure 4.60: V010: Left panel: Water discharge time series with 95% posterior interval for extreme values. Right panel: Discharge rating curve with fitted POT values
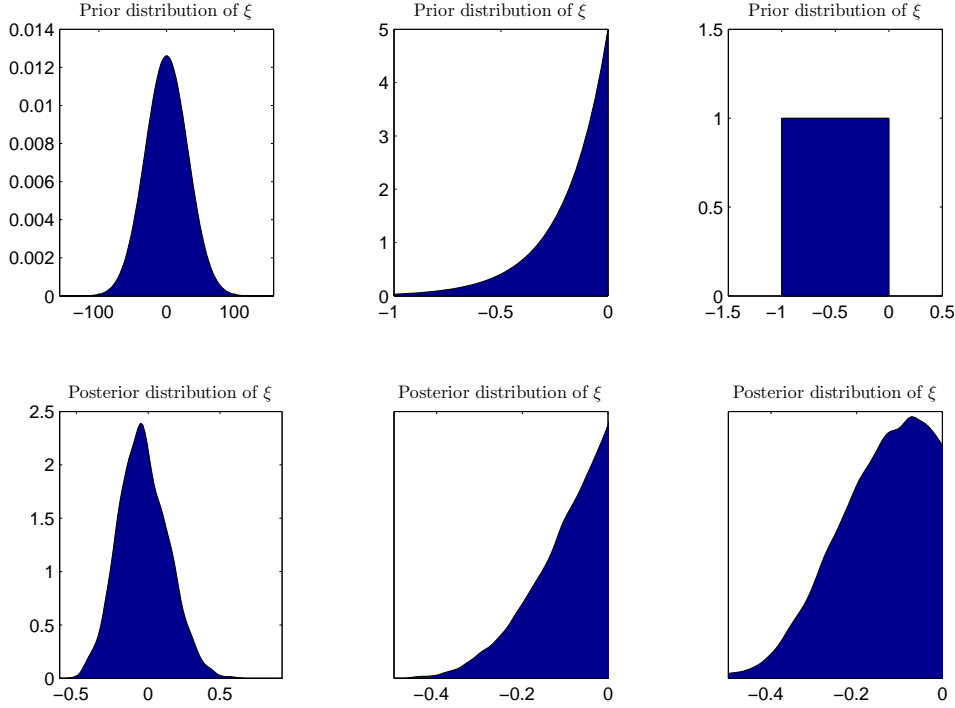

Figure 4.61: (V010 TM DBM w/DRC): Prior and posterior distributions for the shape parameter (ξ) in the GP distribution for all three cases of prior distributions. Case 1: left panels, Case 2: middle panels, Case 3: right panels.

the data does not fit the model, as well as in Case 1.

Constraining the posterior density of ξ, to negative values only, by using negative prior distributions has a significant influence on the outcome of the posterior distributions and thus the resulting return levels. In the case where the prior distribution for the shape parameter is a normal distribution, the posterior distribution has more tendency to be negative than positive, having a mean value of -0.24 (see Table D.3). Constraining the priors has similar effects on the posteriors as eliminating the positive portion of Case 1 posterior density. The negative part of the posterior density using the non-informative normal prior is similar to the posterior distributions resulting from the constraining priors. Since a higher value of ξ leads to thicker tail
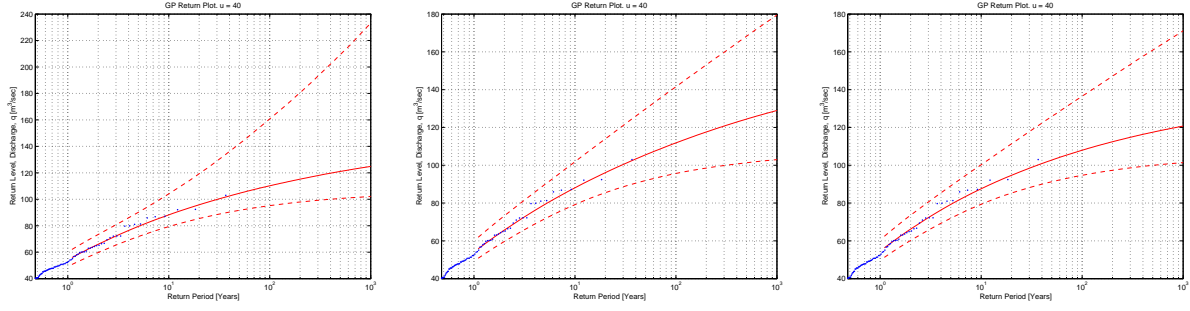
Figure 4.62: (V010 TM DBM w/DRC): Return level plots for the threshold model for all three cases of prior distributions. Case 1: left panel, Case 2: middle panel, Case 3: right panel.

Table 4.12: V010 TM DBM: 100-year return levels of discharge (m^3/sec), for all three cases of prior distributions, calculated with and without a DRC

Threshold model with threshold, u = 40						
	With DRC			Without DRC		
Percentiles	Normal	Neg-Gamma	Neg-Beta	Normal	Neg-Gamma	Neg-Beta
2.5%	95	96	95	96	97	96
25%	103	105	102	103	105	102
50%	110	112	108	110	112	107
75%	121	121	116	120	121	115
97.5%	161	142	137	161	140	135
95% conf. int.	66	46	42	64	43	39

of the GP distribution and hence larger return values, eliminating the positive portion of the ξ values reduces the return levels and the range for their 95% posterior intervals for high return periods. This reduction in the posterior densities of ξ , has the effect that the models in Cases 2 and 3, using the negative priors, do not fit the data as well as the model in Case 1. Even so, majority of the unrestricted, Case 1, posterior distribution of ξ is negative, and thus the constriction to negative values only, as is done in Cases 2 and 3, does not have as drastic effect as it would, if the Case 1 posterior was more positive. Hence the, models in Cases 2 and 3 fit the data adequately, despite the restriction of ξ.

Constraining the ξ parameter to negative values only, has the effect that the median value of the 100-year return level becomes higher in Case 2 compared to Case 1, but lower in Case 3 compared to Case 1. The reason for this is that the unrestricted posterior distribution for the ξ parameter in Case 1 is almost all negative and so is the median value. The Case 2 posterior distribution of ξ is constricted by the neg-gamma distribution which has the majority of is density close to the y-axis, leading to a higher median value than Case 1. The Case 3 posterior distribution of ξ is constricted by the neg-beta distribution which is a uniform distributin with

Figure 4.63: (V010 TM DBM) Comparison of the 95% posterior interval of the 100-year return level of discharge, between the three cases of prior distributions, with DRC uncertainty (blue) and without DRC uncertainty (red).

only negative values. The resulting posterior is essentially the same as the posterior for Case 1 except without its positive portion. Therefor the posterior median of ξ is larger for Case 3 than for Case 1. The uncertainties in Cases 2 and 3, where the priors are negative only, shrink to approximately 66% and 62% of the uncertainty for Case 1, respectively, where the prior is non-informative.

The effect of discharge rating curve uncertainty

The effect of merging the discharge rating curve uncertainty with the sampling uncertainty from the MCMC scheme has minor effect on the median value of the 100-year return level. This is shown in Table 4.12 and Figure 4.63. There is a minor change in the over all uncertainty for the 100-year return level, when adding the discharge rating curve uncertainty to the calculations. In Case 1, where the prior distribution is a normal distribution, the 95% posterior interval increases approximately 2%, when DRC uncertainty is taken into account. In Case 2, where the prior distribution is a negative gamma distribution, the 95% posterior interval increases approximately 5%, when DRC uncertainty is taken into account. In Case 3, where the prior distribution is a negative beta distribution, the 95% posterior interval increases approximately 9%, when DRC uncertainty is taken into account.

4.4.4. Threshold Model using the fixed frequency method (FFM) for determining the threshold value

For Svarta,the rule of thumb method (FFM), leads to a threshold value of $u = 52$ with the total number of point estimates of discharge, greater than the threshold value, equal to 36.
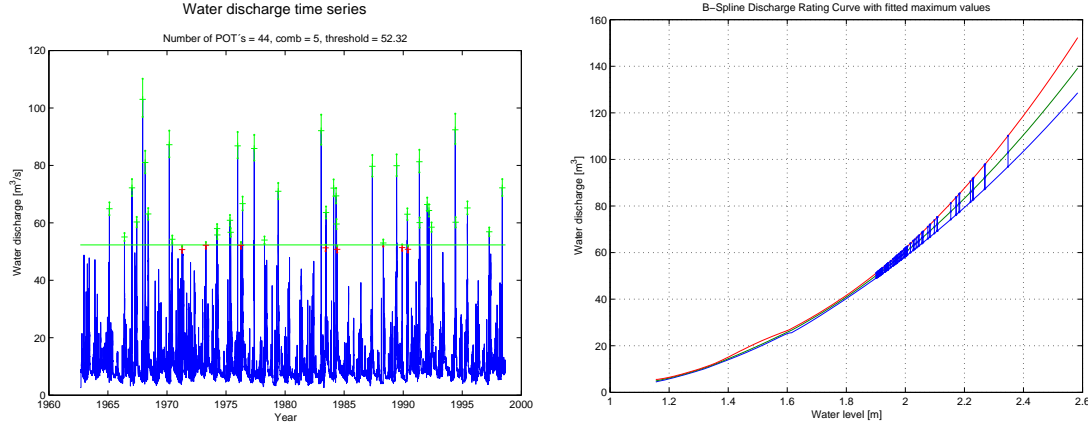
Figure 4.64: (V010 FFM): Right panel: Water discharge time series with 95% posterior interval for extreme values. Left panel: B-spline Discharge rating curve with fitted POT values

Comparison between the three different cases of prior distribution for ξ
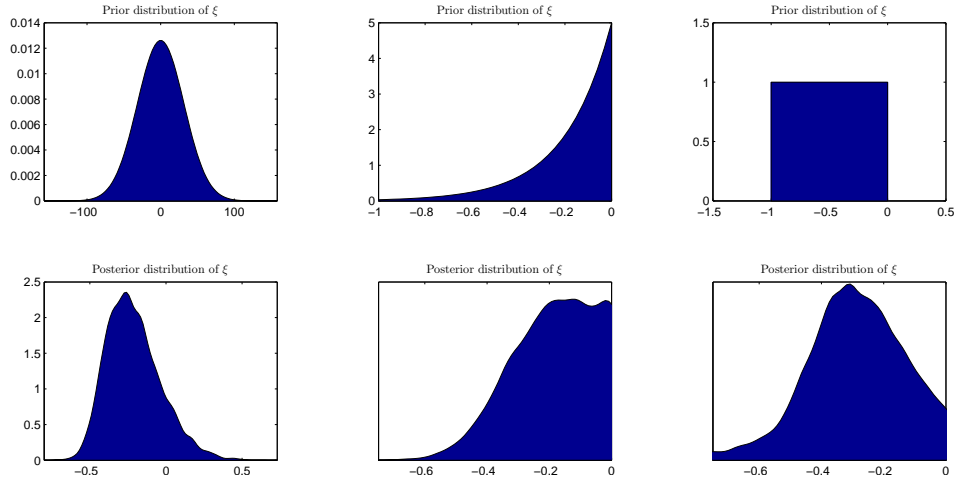
Figure 4.65: (V010 TM FFM w/DRC): Prior and posterior distributions for the shape parameter (ξ) in the GP distribution for all three cases of prior distributions. Case 1: left panels, Case 2: middle panels, Case 3: right panels.
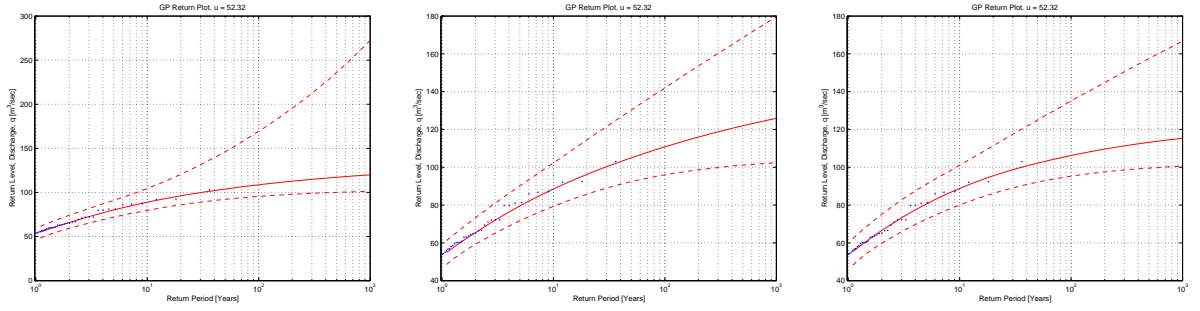
Figure 4.66: (V010 TM FFM w/DRC): Return level plots for the threshold model for all
   three cases of prior distributions. Case 1: left panel, Case 2: middle panel, Case 3: right
   panel.

*Table 4.13: V010 TM FFM: 100-year return levels of discharge (m^3/sec), for all
   three cases of prior distributions, calculated with and without a DRC*

Threshold model with threshold, u = 52						
	With DRC			Without DRC		
Percentiles	Normal	Neg-Gamma	Neg-Beta	Normal	Neg-Gamma	Neg-Beta
2.5%	95	96	95	97	98	97
25%	103	104	102	103	104	102
50%	109	111	106	108	110	106
75%	119	120	113	117	119	113
97.5%	169	142	135	160	142	134
95% conf. int.	74	46	40	63	44	36

Figure 4.65 shows the prior distributions of ξ and their corresponding posterior
distributions for all cases. A big portion of of the posterior distribution in Case 1 is
positive and so constraining the posterior to only negative values has great influence
on the results. Figure 4.66 show the return level plots for all three cases of prior
distributions. Constraining the prior to negative values only, lowers the return levels
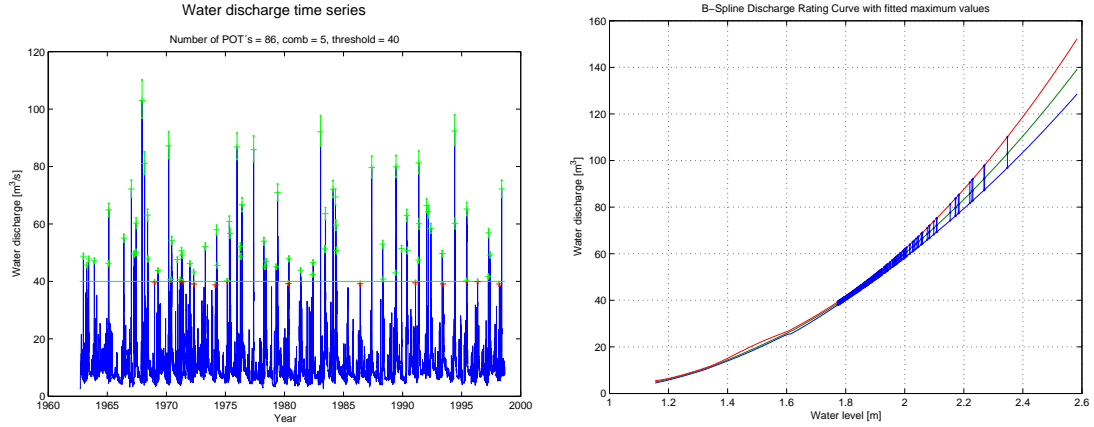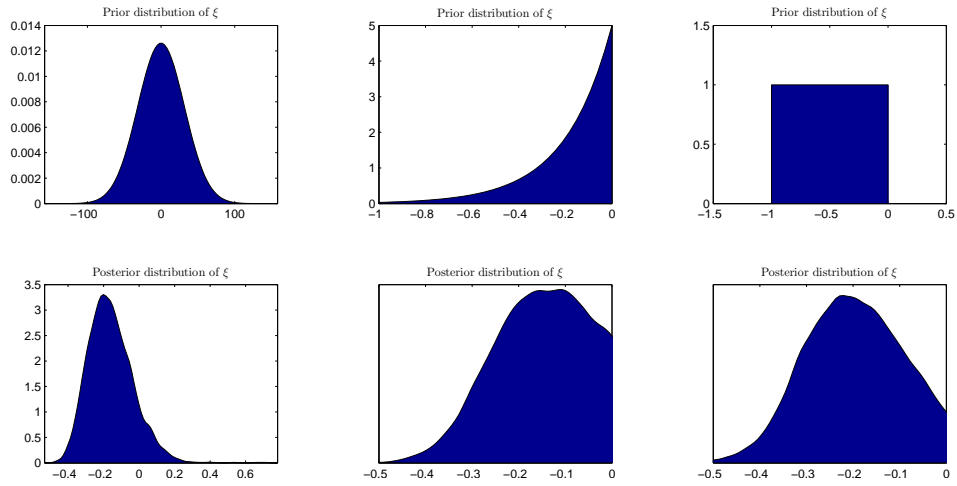and makes the confidence interval narrower. This constriction has the effect that
the data does not fit the model, as well as in Case 1.

Constraining the posterior density of ξ, to negative values only, by using negative
prior distributions has a significant influence on the outcome of the posterior distri-
butions and thus the resulting return levels. In the case where the prior distribution
for the shape parameter is a normal distribution, the posterior distribution has more
tendency to be positive than negative, having a mean value of -0.24 (see Table D.4).
Constraining the priors has similar effects on the posteriors as eliminating the pos-
itive portion of the Case 1 posterior density. The negative part of the posterior
density using the non-informative normal prior is similar to the posterior distribu-
tions resulting from the constraining priors. Since a higher value of ξ leads to thicker
tail of the GP distribution and hence larger return values, eliminating the positive
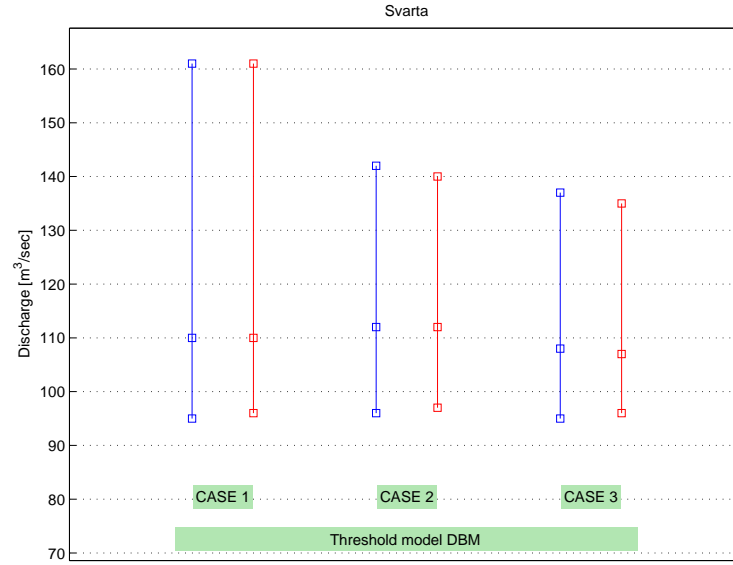
Figure 4.67: (V010 TM FFM) Comparison of the 95% posterior interval of the 100-year return level of discharge, between the three cases of prior distributions, with DRC uncertainty (blue) and without DRC uncertainty (red).

portion of the ξ values reduces the return levels and the range for their 95% posterior intervals for high return periods. This reduction in the posterior densities of ξ, has the effect that the models in Cases 2 and 3, using the negative priors, do not fit the data as well as the model in Case 1. Even so, majority of the unrestricted, Case 1, posterior distribution of ξ is negative, and thus the constriction to negative values only, as is done in Cases 2 and 3, does not have as drastic effect as it would, if the Case 1 posterior was more positive. Hence the, models in Cases 2 and 3 fit the data adequately, despite the restriction of ξ.

Constraining the ξ parameter to negative values only, has the effect that the median value of the 100-year return level becomes higher in Case 2 compared to Case 1, but lower in Case 3 compared to Case 1. The reason for this is that the unrestricted posterior distribution for the ξ parameter in Case 1 is almost all negative and so is the median value. The Case 2 posterior distribution of ξ is constricted by the neg-gamma distribution which has the majority of is density close to the y-axis, leading to a higher median value than Case 1. The Case 3 posterior distribution of ξ is constricted by the neg-beta distribution which is a uniform distributin with only negative values. The resulting posterior is essentially the same as the posterior for Case 1 except without its positive portion. Therefor the posterior median of ξ is larger for Case 3 than for Case 1. The uncertainties in Cases 2 and 3, where the priors are negative only, shrink to approximately 58% and 52% of the uncertainty for Case 1, respectively, where the prior is non-informative.

The effect of discharge rating curve uncertainty

The effect of merging the discharge rating curve uncertainty with the sampling uncertainty from the MCMC scheme has minor effect on the median value of the 100-year return level. This is shown in Table 4.13 and Figure 4.67. There is a change in the over all uncertainty for the 100-year return level, when adding the discharge rating curve uncertainty to the calculations. In Case 1, where the prior distribution is a normal distribution, the 95% posterior interval increases approximately 17%, when DRC uncertainty is taken into account. In Case 2, where the prior distribution is a negative gamma distribution, the 95% posterior interval increases approximately 14%, when DRC uncertainty is taken into account. In Case 3, where the prior distribution is a negative beta distribution, the 95% posterior interval increases approximately 11%, when DRC uncertainty is taken into account.

4.4.5. Comparison between models

The models being compared are the block maxima model using the annual maximum values and two threshold models, one with the threshold value $u = 40$, found by using the diagnostic based method (DBM threshold model) and another one with a threshold value of $u = 52$, found by the fixed frequency method (FFM threshold model).

It can be argued that the extreme values used in the FFM threshold model are superior to those used in the block maxima model since they are not constricted to having one and only one extreme value per year, like the annual values used in the latter model. The argument is, that if the de-clustering of the POTs is successful and there is no correlation between the extremes, than the quality of the POTs gathered by using the FFM are at least, equal to that of the block maxima model. For that reason the comparison below will be between the block maxima model and the FFM threshold model, on one hand, and between the FFM threshold model and the DBM threshold model, on the other hand.

Block maxima model vs. FFM threshold model

Tables 4.11 and 4.13 show the percentiles for the 100-year return levels for the block maxima model and the FFM threshold model, respectively. Figure 4.68 shows the 95% posterior interval of the 100-year return level for the block maxima model and the FFM threshold model. Tables D.2 and D.4 show the percentiles of the posterior distributions for the GEV parameters for the Block maxima model and the GP
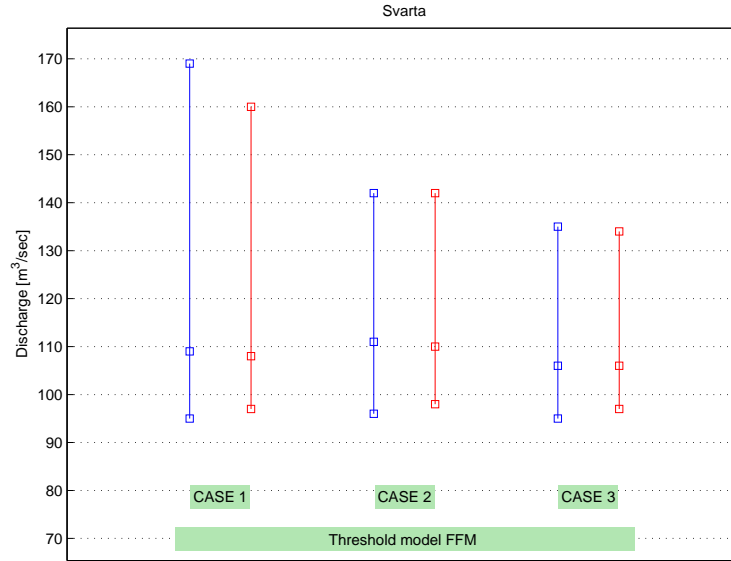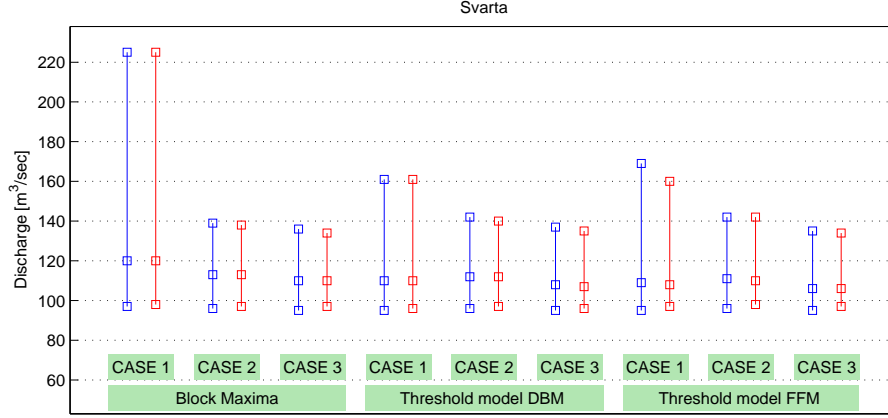
Figure 4.68: (V010) Comparison of the 95% posterior interval of the 100-year return level of discharge, between the three different models, with DRC uncertainty (blue) and without DRC uncertainty (red).

parameters for the FFM Threshold model, respectively. The FFM threshold model uses approximately the same amount of extreme values as the block maxima model but the extremes used in the FFM threshold model are larger than those used in the block maxima model.

In Case 1 where the prior distribution for ξ is noninformative, the posterior density of ξ takes higher values in the block maxima model than the FFM threshold model. Because of this, the return levels are higher for the block maxima model than the FFM threshold model.

In Cases 2 and 3 where the prior distributions of ξ constrains the posteriors to negative values only the difference in the return levels is small. The return levels are a bit higher for Case 2 where the ξ prior distribution is the negative gamma distribution. That is understandable since the Case 1 prior distribution is uniform but the Case 2 prior has the mass of its density closer to the value 0.

The posterior distributions of ξ has a much larger posterior interval when using the FFM threshold model compared to using the block maxima model. The range of the 95% posterior interval of the posterior density of ξ is $[-0.61, -0.05]$ using the Case 3 FFM threshold model compared to $[-0.38, -0.02]$ when using the Case 3 block maxima model. Despite this difference in the shape parameters the posterior interval of the return levels are very similar. This show how the return levels are much less sensitive to the changes in the shape parameter if the value of ξ is negative, compared to positive.

DBM threshold model vs. FFM threshold model

Tables 4.12 and 4.13 show the percentiles for the 100-year return levels for the DBM threshold model and the FFM threshold model, respectively. Figure 4.68 shows the 95% posterior interval of the 100-year return level for the DBM threshold model and the FFM threshold model. Tables D.3 and D.4 show the percentiles of the posterior distributions for the GP parameters for the DBM threshold model and the FFM threshold model, respectively.

By lowering the threshold from 52 to 40 the effective number of POTs increase from 37.77 to 76.48. Looking at the Case 1 prior distribution, these added extreme data have the effect of lowering the upper values of the posterior distribution for ξ. That leads to lower upper percentiles for the return level plot and thus smaller posterior interval. So, for this river, the added data used in the DBM threshold model lowered the upper percentiles for the 100 year return level and its posterior interval got smaller.

There is little difference between the two models when looking the results from Cases 2 and 3. In both models, the negative gamma prior in Case 2 seems have the effect that the simulated values in the posterior distribution of ξ higher then for the negative beta prior in Case 3. That leads to higher return levels.

In Cases 2 and 3, the return levels produced by the FFM threshold model have narrower posterior intervals but the difference is minor. The median values for the return levels are almost identical for the DBM threshold model and the FFM threshold model.

5. Conclusions and future research

A statistical model was constructed to perform flood analysis. The validity of this model was tested on four rivers in Iceland. One of the main novelty of the model was to combine the uncertainty in the discharge rating curve with the uncertainty in the flood analysis. The results show that, in general, this leads to a greater over-all uncertainty for the flood analysis. The confidence interval in the resulting return level plots become larger when the DRC uncertainty is taken into account. However, the difference is perhaps not as great as could be expected. For the rivers inspected the increase in the confidence interval for the 100-year return level is ranging from 0% to 15% depending on the river, and also depending on the model used for the analysis and which case of prior distribution used.

Three models were used to analyze the discharge data for each river. A block maxima model, which used annual maximum values of discharge to perform the flood analysis and two threshold models which used peaks over threshold (POT) to perform the analysis. The two threshold models used different threshold values in their analysis. In one of the threshold models, the diagnostic based method (DBM) was used to determine the threshold value and the other used the fixed frequency (FFM). These two methods for choosing the threshold are discussed in detail in Section 3.4.2.

Choosing which of the three models to use in the flood analysis is not a straight forward decision. There are advantages using the threshold model with the FFM threshold choice compared to the block maxima model. The number of extreme data used is the same in both models but if the de-clustering of the data is adequately done, the extremes used in the FFM threshold model should be at least, as good as the ones used in the block maxima model.

Using the diagnostic based method for determining the value of the threshold will always result in more POTs compared to the FFM method. Whether or not this increase in number of extremes enhances the results is different between rivers.

In most cases, choosing the DBM threshold model over the other two models would be recommended because it uses more extreme values in the analysis. We are confident that the diagnostic based method is superior to the fixed frequency method, for choosing a threshold, in three of the four rivers inspected. In the analysis for Olfusa, Hvita and Svarta, the DBM threshold model provided the best fit for the

data. However in the analysis for Sanda, the threshold value chosen is suspected to be to low and hence too many values were being regarded as extreme values.

Three different types of prior distributions for ξ were inspected. Case 1 used a noninformative prior for ξ, allowing the posterior distribution of ξ to take any value, and hence not constraining the parameter. Cases 2 and 3 used prior distributions for ξ which only had negative values and thus constraining the posterior of ξ to negative values only. The constriction in Cases 2 and 3 had a big effect on most of the rivers, compared to Case 1. The general difference between the using noninformative prior in Case 1 and using the informative priors in cases 2 and 3 is that the constrictions resulting from the informative priors makes the confidence intervals in the return period plots become smaller. The low end of the intervals is similar between all cases, but when the positive values of the posterior density for ξ is eliminated, which is essentially done when constraining the parameters to negative values, the return levels decrease accordingly. The restriction bounds the return levels, eliminating the exponential growth part resulting from the positive part of the ξ density. However, this comes at the expense of goodness of fit.

This expense is especially evident when looking at the rivers Olfusa and Hvita. For Olfusa the block maxima model was inadequate for Cases 2 and 3, and for Hvita these two cases were inadequate in all of the three models. The reason why the models performed worse in these two rivers than the other two, when constraining the shape parameter is simple: the change in ξ was to great compared to Case 1 where the shape parameter was unrestricted. For both of these rivers, a majority of the Case 1 posterior density of ξ was positive and therefore, constraining the parameter to negative values only was too much of an alteration and the data did not adequately fit the models. On the other hand, for the rivers Sanda and Svarta, the models provided a good fit for the data regardless of prior distributions used. That is because the majority of the Case 1 posterior density of ξ was already negative so the restraints in Cases 2 and 3 were not as big of shock as it was in the analysis of Olfusa and Hvita. Therefore it is concluded that this "one size fit all" approach for determining the prior distribution for ξ is not adequate in all cases.

A more elaborate approach to determine an informative prior distribution for the shape parameters could be to rely on the prior knowledge of an expert hydrologist. That approach would have to be examined specifically for each river. Through a general understanding of the discharge behavior of a particular river it is reasonable to hope that an expert hydrologist could have valuable information about extremal behavior. However, it is unlikely that prior beliefs could be adequately elicited directly in terms of the GEV or GP parameters. Therefore, an experts estimates of the median and 90% quantiles of a 100-year return level could be used to determine prior distributions for the parameters. This approach has been used in the past by Coles and Tawn (1996). Their work focused on extreme rainfall data but similar methods could be implemented in the flood analysis model.

Since the posterior distributions for the unrestricted shape parameter, ξ, is highly positive for some of the rivers inspected, it leads to the conclusion that the underlying distributions of the extreme values used in the analysis are not the same. It might therefore be beneficiary to investigate the underlying reasons for particular floods and conduct a flood analysis based on those reasons, for example, looking separately at summer and winter floods.

Using data on more rivers, the model constructed in this thesis, might be used to gain insight on the extreme behavior of rivers with regards to which type of river it is, i.e. whether the river is a glacier stream, a direct runoff stream or a springfed steam. Knowledge gained by such categorization of the rivers might be used for enhancing the choice of prior distributions used in the model.

5.1. Conclusions summary

- Difference between rivers: The results for Olfusa and Hvita are similar to each other, while the results for Sanda and Svarta are similar to each other. In the analysis for Olfusa and Hvita, the Case 1 posterior distributions of the shape parameter is highly positive, suggesting an unbounded tail of the extreme value distributions. That leads to high return levels and with large uncertainty intervals. In the analysis for Sanda and Svarta, the Case 1 posterior distributions of the shape parameter is largely negative, suggesting a bounded tail of the extreme value distributions. The return levels are therefore not as large as in Olfusa and Hvita and the uncertainty intervals are smaller.

- Difference between cases: Constricting the shape parameter to negative values only, as is done in Cases 2 and 3 lowers the return levels and decreases their uncertainties. That decrease in uncertainty comes at the expense of model fit. This is especially evident for the rivers Olfusa and Hvita, since the Case 1 posterior distributions for ξ is largely positive for those rivers. For Sanda and Svarta, the change between Case 1 on one hand and Cases 2 and 3 on the other hand, is not as great.

- Difference between models: The uncertainties in the return levels are smaller in the block maxima models than for the threshold models for all the rivers except for Svarta. The return level uncertainty the DBM threshold model is smaller than in the FFM threshold model for all the rivers except for Sanda.

- The effect of using DRC uncertainty: Using the DRC uncertainty in the calculations has the effect of increasing the over all uncertainty in the return levels for most of the models. However, in the FFM threshold model, the over all

5. Conclusions and future research

uncertainty decreases when adding the DRC uncertainty into the calculations for the rivers, Olfusa, Hvita, and Sanda.

118

References

S. Coles. *An introduction to statistical modeling of extreme values.* Springer series in statistics. Springer, 2001.

S. Coles and L. Pericchi. Anticipating catastrophes through extreme value modelling. *Journal of the Royal Statistical Society: Series C (Applied Statistics)*, 52(4):405–416, 2003.

S.G. Coles and J.A. Tawn. A bayesian analysis of extreme rainfall data. *Journal of the Royal Statistical Society. Series C (Applied Statistics)*, 45(4):pp. 463–478, 1996.

A.C. Davison and R.L. Smith. Models for exceedances over high thresholds. *Journal of the Royal Statistical Society. Series B (Methodological)*, 52(3):393–442, 1990.

R.A. Fisher and L.H. Tippett. On the estimation of the frequency distributions of the largest or smallest member of a sample. *Proc. Cambridge Phil. Soc.*, 24:180–190, 1928.

M. Frechet. Sur la loi de probabilite de l'ecart maximum. *Annales de la Societe Polonaise de Mathematique*, 6:93 − 116, 1927.

A. Gelman, J.B. Carlin, H.S. Stern, and D.B. Rubin. *Bayesian Data Analysis, Second Edition (Chapman & Hall/CRC Texts in Statistical Science).* Chapman and Hall/CRC, 2 edition, 2003.

B. Gnedenko. Sur la distribution limite du terme maximum d'une serie aleatoire. *The Annals of Mathematics*, 44(3):pp. 423–453, 1943.

E.J. Gumbel. *Statistics of extremes.* Columbia University Press, New York,, 1958.

B. Hrafnkelsson, K. Ingimarsson, S. Gardarsson, and A. Snorrason. Modeling discharge rating curves with bayesian b-splines. *Stochastic Environmental Research and Risk Assessment*, 26:1–20, 2012. ISSN 1436-3240.

A.F. Jenkinson. The frequency distribution of the annual maximum (or minimum) values of meteorological elements. *Quarterly Journal of the Royal Meteorological Society*, 81(348):158–171, 1955.

REFERENCES

MD. A. Karim and J.U. Chowdhury. A comparison of four distributions used in flood frequency analysis in bangladesh. *Hydrological Sciences Journal*, 40(1):55–66, 1995.

J. Lambie. Measurement of flow-velocity-area methods. In R. W. Herschy, editor, *Hydrometry: Principles and Practices*, number 2749 in Chichester, pages 1 – 52. John Wiley & Sons Ltd, UK, 1978.

L. Makkonen. Plotting Positions in Extreme Value Analysis. *Journal of Applied Meteorology and Climatology*, 45:334–340, 2006.

M. Mosley and A. McKerchar. Streamflow. In D. R. Maidment, editor, *Handbook of Hydrology*, number 2749, pages 8.1–8.39. McGraw Hill, New York, USA, 1993.

A.P. Øverleir and T. Reitan. Accounting for rating curve imprecision in flood frequency analysis using likelihood-based methods. *Journal of Hydrology*, 366(1-4): 89 – 100, 2009.

E. Parent and J. Bernier. Encoding prior experts judgments to improve risk analysis of extreme hydrological events via pot modeling. *Journal of Hydrology*, 283(1–4): 1 – 18, 2003.

J Pickands. Statistical inference using extreme order statistics. *Annals of Statistics*, 3(1):119–131, 1975.

D.S. Reis Jr. and J.R. Stedinger. Bayesian mcmc flood frequency analysis with historical information. *Journal of Hydrology*, 313(1–2):97 – 116, 2005.

R.D. Reiss and M. Thomas. *Statistical analysis of extreme values: with applications to insurance, finance, hydrology and other fields*. Birkhäuser, 2007.

R.L. Smith. Maximum likelihood estimation in a class of nonregular cases. *Biometrika*, 72(1):67 – 90, 1985.

R.L. Smith and J.C. Naylor. A comparison of maximum likelihood and bayesian estimators for the three-parameter weibull distribution. *Journal of the Royal Statistical Society Series C Applied Statistics*, 36(3):358–369, 1987.

M.A.J. Van Montfort and J.V. Witter. The generalized pareto distribution applied to rainfall depths. *Hydrological Sciences Journal*, 31(2):151–162, 1986.

R. von Mises. La distribution de la plus grande de n valeurs. In *Selected Papers, Volume II*, pages 271–294. Providence, RI, 1954.

W. Weibull. A statistical distribution function of wide applicability. *Journal of Applied Mechanics*, 18:293 – 297, 1951.

A. More details on the flood analysis for Olfusa

In this appendix, figures and tables that are relevant to the research but were not displayed in the main text of the paper, are displayed. That includes probability plots, quantile plots and density plots for all cases of prior distributions. The prior and posterior densities of all the parameters in the GEV and GP distributions are also displayed for all cases. The appendix also includes the sampled Markov chain Monte Carlo (MCMC) chains, used to construct the posterior distributions for the parameters of both the generalized extreme value distribution (GEV) and the generalized Pareto (GP) distribution. The samples are displayed both in figures, and in tables as quantiles for all the models with and without the inclusion discharge rating curve uncertainty. The histogram of the prior and posterior distribution and the diagnostic plots for the models are shown for all models without the inclusion of discharge rating curve uncertainty.

Table A.1 shows a list of abbreviations regarding the following figures and tables. Every figure and table in the appendix is marked with some of these abbreviations and that explains which river the data belongs to and what kind of models were used to generate the results. For example, the text *(V064 BM w/DRC) Case 2* in the caption of a figure or a table, indicates that the data displayed comes from the river Olfusa (V064), a block maxima model was used (BM) with a neg-gamma prior distribution for the shape parameter (Case 2), and the uncertainty in the discharge rating curve was taken into account in the calculations (w/DRC).

Table A.1: Abbreviations used to explain the origin of the data used to generate figures and tables

V064:	The river Olfusa: 64 is the number of the gauging station measuring the data
V066:	The river Hvita vid Kljafoss: 66 is the number of the gauging station measuring the data
V026:	The river Sanda i Thistilfjordur: 26 is the number of the gauging station measuring the data
V010:	The river Svarta in Skagafjordur: 10 is the number of the gauging station measuring the data
Case 1:	The shape parameter, ξ, was sampled using a normal prior distribution
Case 2:	The shape parameter, ξ, was sampled using a neg-gamma prior distribution
Case 3:	The shape parameter, ξ, was sampled using a neg-beta prior distribution
BM:	A block maxima model
TM DBM:	A threshold model using the diagnostic based method for determining the threshold value
TM FFM:	A threshold model using the fixed frequency method for determining the threshold value
w/DRC:	A discharge rating curve uncertainty was taken into account in the calculations
w/o DRC:	A discharge rating curve uncertainty was not taken into account in the calculations

A.1. V064: With discharge rating curve uncertainty

A.1.1. Block maxima model

Block maxima Model - Case 1: A normal prior distribution for the ξ parameter (BM w/DRC C1)

In Case 1, the prior distribution for ξ was chosen to be a normal distribution with a large variance, making it non-informative prior. The prior distribution for σ is a non-informative inv-χ^2 distribution and the prior distribution for μ is a normal distribution with large variance making it non-informative. So, in this case, the GEV parameters are not constricted in any way by their prior distributions. See

further details on the prior distributions in Section 3.3.2. The construction of the posterior distributions of all the parameters is discussed in Section 3.3.3. The prior and posterior distributions for the GEV parameters are shown in Figure A.1.
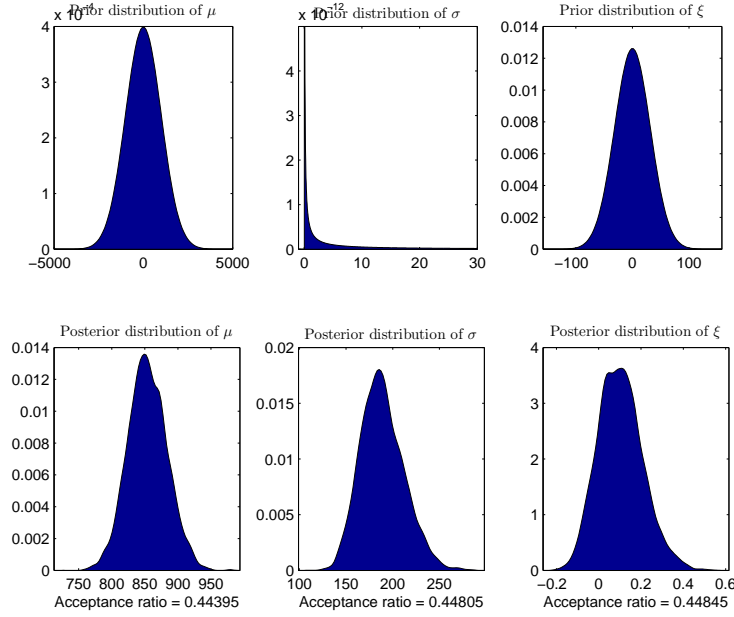

Figure A.1: (V064 BM w/DRC) CASE 1: Prior and posterior distributions for the GEV parameters

The simulated chains of posterior distributions for the GEV parameters are used to model the extreme behavior of the river. The simulated chains of the posterior distributions of the parameters are shown in Figure A.7 and their quantiles are shown in Table A.2.

Figure A.2 shows the return period plot for Olfusa as well as the quantile plot, the probability plot and the density plot. The Anderson-Darling p-value and the diagnostic plots in Figure A.2 are evaluated to check the validity of the model. The methods used for the model validation are discussed in Section 2.2.2.

The model is a good fit for the data, having an Anderson-Darling p-value of $p_B = 0.57$. Figure A.2 also indicates that the model fits the data reasonably well. The annual maximum values on the probability plot all lie close to the unit diagonal and the values are close to linear on the quantile plot. Plotting the annual maximum values on the return level plot also seem to indicate that the model fits the data well, since all the values are inside the 95% posterior interval of the return levels. Furthermore, the density plot indicates that the model is a good fit for the data since the histogram of the annual maximum values fit well inside the GEV probability density function.
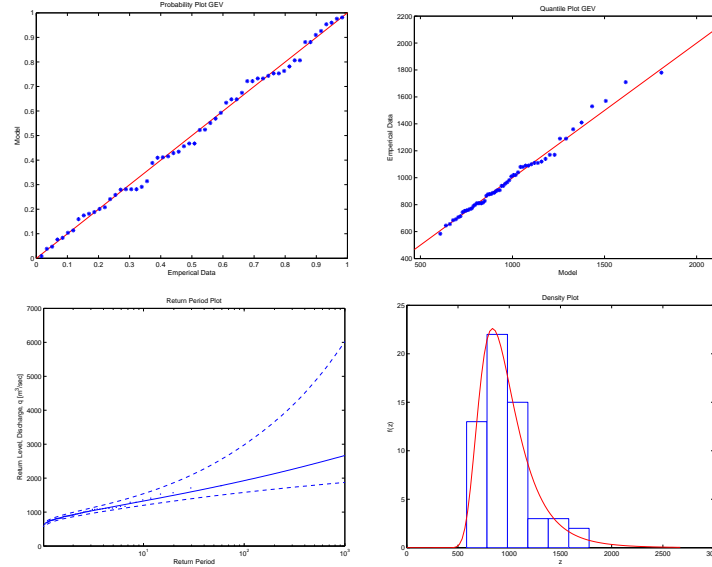
Figure A.2: (V064 BM w/DRC) CASE 1: Diagnostic plots for the block maxima model

Block Maxima Model - Case 2: A negative gamma prior distribution for the ξ parameter (BM w/DRC C2)

In Case 2, the prior distribution for ξ was chosen to be a negative gamma distribution. It contains only negative values having majority of the mass of the distribution is close to the y-axis. Therefore, in this case, the posterior density of the shape parameter of the GEV distribution is constricted to negative values only. The prior and posterior distributions for the GEV parameters are shown in Figure (A.3).

The simulated chains of the posterior distributions of the parameters are shown in Figure A.8 and their quantiles are shown in Table A.2.

Figure A.4 shows the return period plot for Olfusa as well as the quantile plot, the probability plot and the density plot. The Anderson-Darling p-value, $p_B = 0.49$, indicates that the model is a good fit for the data. The probability plot in Figure A.4 also indicates that the model fits the data reasonably well. The quantile plot, however, indicates that the data deviates from the model for the highest extreme values since it departs from linearity at those values. Similar deviation takes place when fitting the data to the return period plot. The largest values are inconsistent with the model. By looking at the histogram of the annual maximum values with the GEV density, the data seems to fit the model well. For a large majority of the data, the model seems to be a good fit. However, it does not adequately fit the behavior of the largest values which raises concerns as those are the values of most interest.
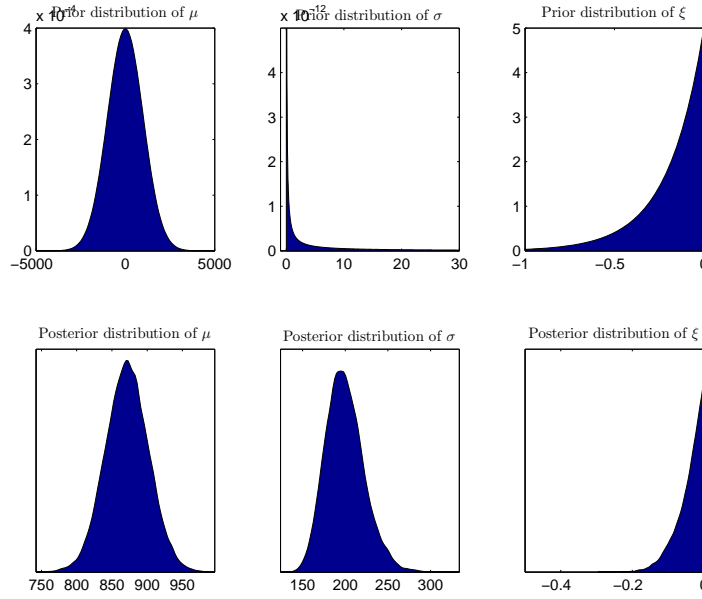
Figure A.3: (V064 BM w/DRC) CASE 2: Prior and posterior distributions for the GEV parameters

Block Maxima Model – Case 3: A negative beta prior distribution for the ξ parameter (BM w/DRC C3)

In Case 3, the prior distribution for ξ was chosen to be a negative beta distribution. It is a uniform distribution containing values on the interval $[-1; 0]$ Therefore, in this case, the posterior density of the shape parameter of the GEV distribution is constricted to negative values only. The prior and posterior distributions for the GEV parameters are shown in Figure (A.5).

The simulated chains of the posterior distributions of the parameters are shown in Figure A.9 and their quantiles are shown in Table A.2.

Figure A.6 shows the return period plot for Olfusa as well as the quantile plot, the probability plot and the density plot.

The results in this case, using the negative beta prior distribution for the ξ parameter are similar to the results, in Case 2 where the negative gamma prior distribution was used. The Anderson-Darling p-value of $p_B = 0.48$ indicates that the model is a good fit for the data. The probability plot in Figure A.6 also indicates that the model fits the data reasonably well. The quantile plot, however, indicates that the data deviate from the model for the highest extreme values since it departs from linearity at those values. Similar deviation takes place when fitting the data to the return period plot. The largest values are inconsistent with the model. By looking
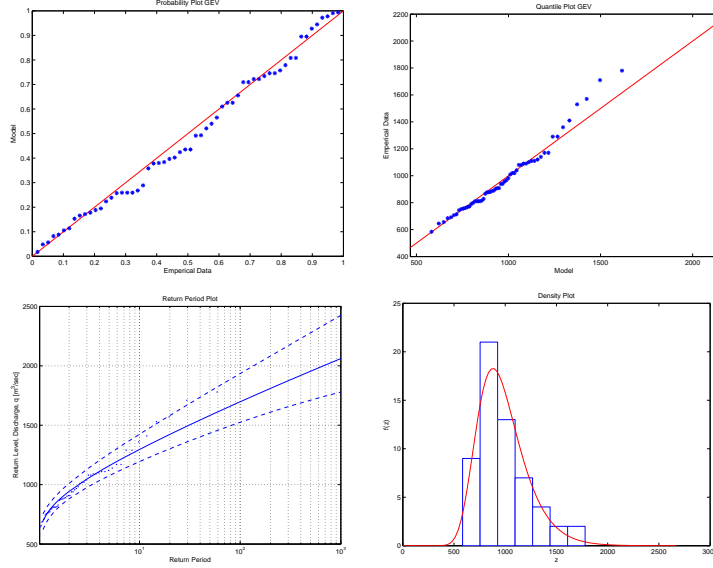
Figure A.4: (V064 BM w/DRC) CASE 2: Diagnostic plots for the block maxima model
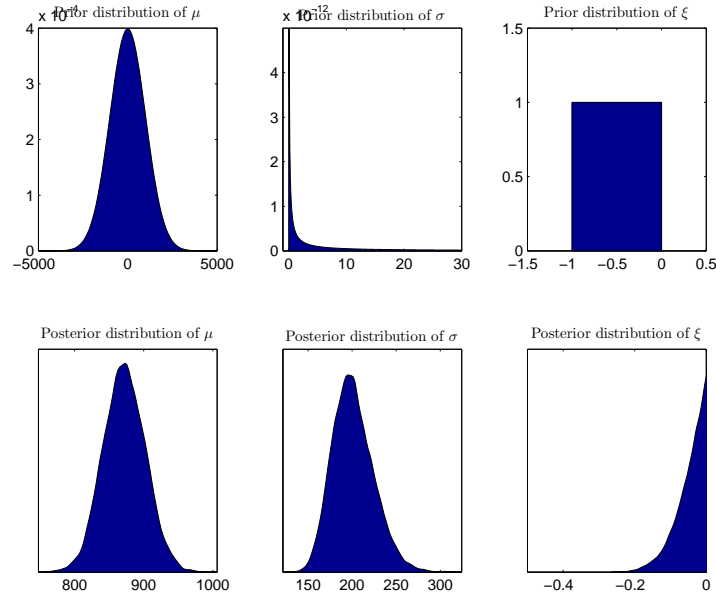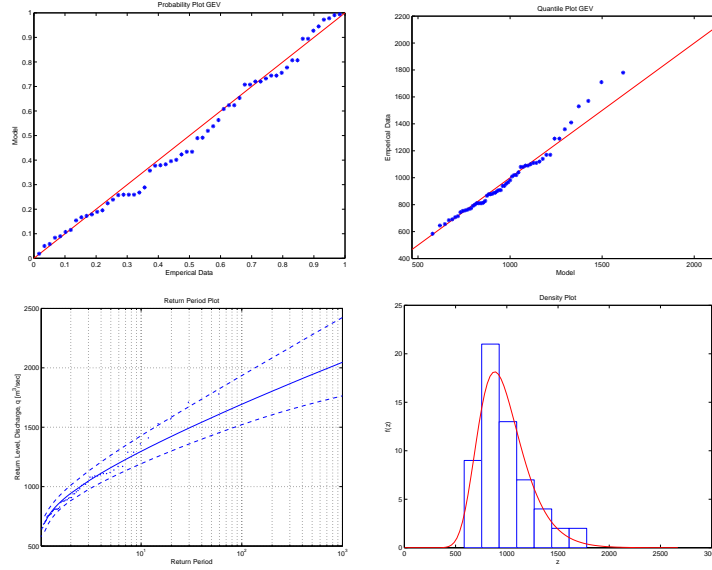

Figure A.5: (V064 BM w/DRC) CASE 3: Prior and posterior distributions for the GEV parameters

at the histogram of the annual maximum values with the GEV density, the data seems to fit the model well. For a large majority of the data, the model seems to be a good fit. However, it does not adequately fit the behavior of the largest values which raises concerns since those are the values of most interest.

Figure A.6: (V064 BM w/DRC) CASE 3: Diagnostic plots for the block maxima model

Block Maxima Model – Figures and tables displaying the posterior parameters of the GEV distribution

Table A.2: (V064 BM w/DRC): Percentiles for the posterior distributions of the GEV parameters, sampled using a MCMC iteration scheme, for all three cases of prior distributions, calculated with DRC uncertainty

Block Extrema with DRC
Percentiles for parameters in the GEV distribution

	Normal			Neg-Gamma			Neg-Beta		
	μ	σ	ξ	μ	σ	ξ	μ	σ	ξ
2.5%	798.56	148.46	-0.09	811.50	160.44	-0.14	813.74	160.65	-0.15
25%	835.14	173.12	0.02	850.98	183.85	-0.06	851.23	184.58	-0.07
50%	854.93	187.35	0.10	871.46	197.97	-0.03	871.78	199.36	-0.04
75%	875.49	203.32	0.17	891.84	213.52	-0.01	892.43	215.74	-0.02
97.5%	914.52	238.46	0.33	932.35	248.82	-0.00	932.34	251.83	-0.00
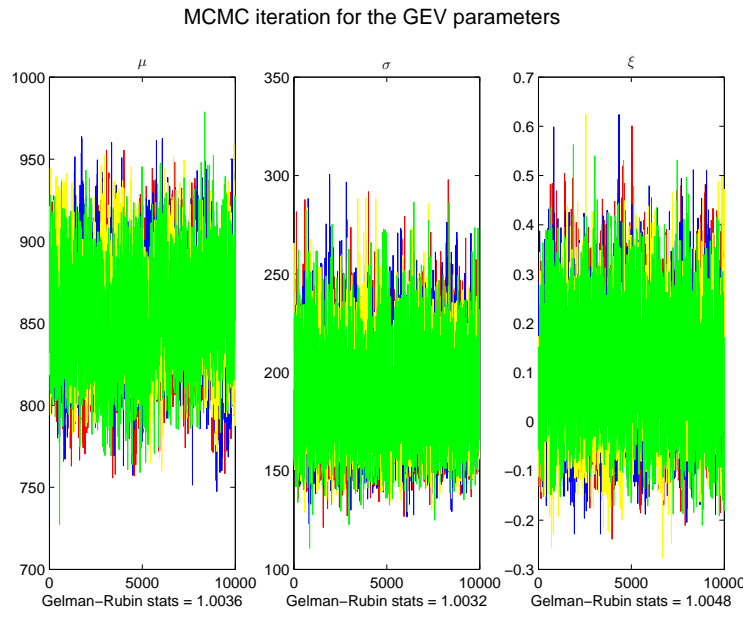
Figure A.7: (V064 BM w/DRC) Case 1: Markov chain Monte Carlo simulation for the parameters in the GEV distribution
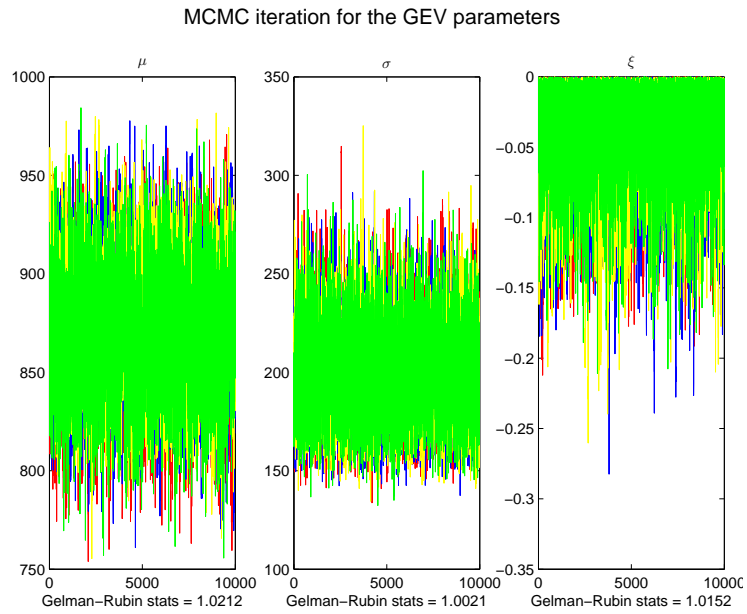
Figure A.8: (V064 BM w/DRC) Case 2: Markov chain Monte Carlo simulation for the parameters in the GEV distribution
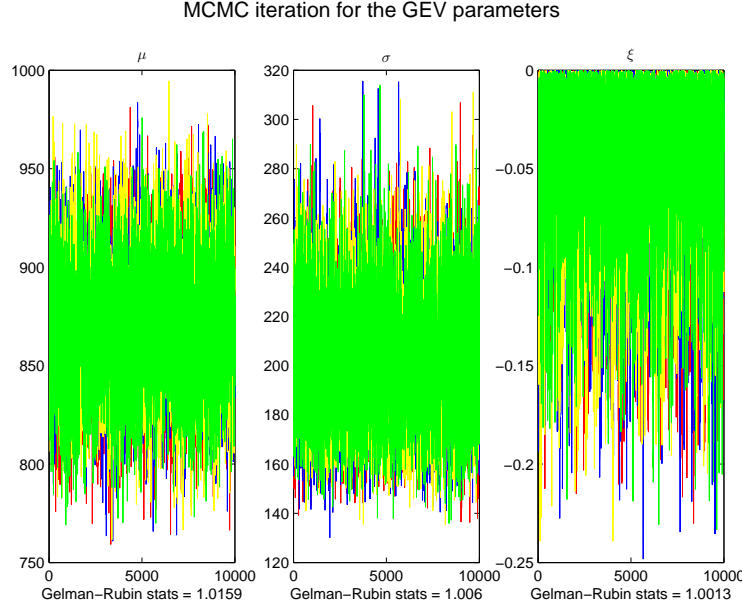
Figure A.9: (V064 BM w/DRC) Case 3: Markov chain Monte Carlo simulation for the parameters in the GEV distribution

A.1.2. Threshold model using the diagnostic based method (DBM) for determining the threshold value

Threshold model using diagnostic based methods for choosing a threshold- Case 1: A normal prior distribution for the ξ parameter (TM DBM w/DRC C1)

In Case 1, the prior distribution for ξ was chosen to be a normal distribution with a large variance, making it non-informative prior. The prior distribution for $\tilde{\sigma}$ is a non-informative inv-χ^2 distribution. So, in this case, the GP parameters are not constricted in any way by their prior distributions. The prior and posterior distributions for the GP parameters are shown in Figure A.10.

The model seems to be a good fit for the data, having an Anderson-Darling p-value of $p_B = 0.50$. The diagnostic plots in Figure A.11 also indicate that the model fits the data reasonably well. The annual maximum values on the probability plot all lie close to the unit diagonal and the points are close to linear on the quantile plot. Plotting the annual maximum values on the return level plot seem to indicate that the model fits the data well. The histogram of the POTs together with the GP density indicate that the model fits the POTs well. A big portion of the posterior density for the shape parameter is positive which has the effect that the upper percentiles for the return level increase exponentially on a logarithmic scale and thus become very large as return time increases.
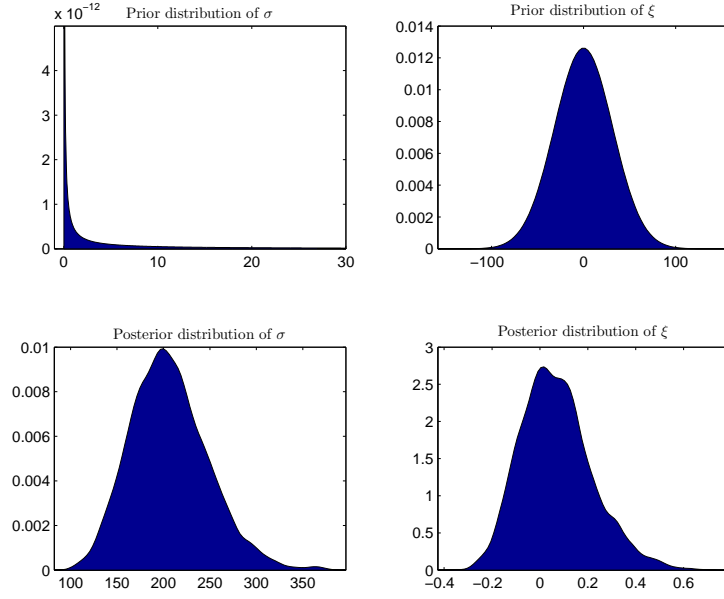
Figure A.10: (V064 TM DBM w/DRC) CASE 1: Prior and posterior distributions for the GP parameters
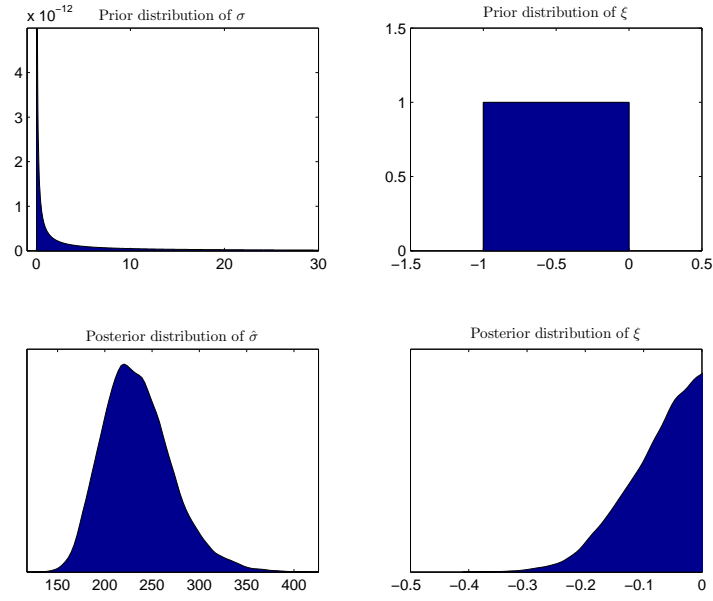
Threshold model using diagnostic based methods for choosing a threshold-Case 2: A negative gamma prior distribution for the ξ parameter (TM DBM w/DRC C2)

In Case 2, the prior distribution for ξ was chosen to be a negative gamma distribution. It contains only negative values having majority of the mass of the distribution is close to the y-axis. The prior distribution for $\tilde{\sigma}$ is a non-informative inv-χ^2 distribution. Therefore, in this case, the posterior density of the shape parameter of the GP distribution is constricted to negative values only. The prior and posterior distributions for the GP parameters are shown in Figure A.12.

The Anderson-Darling p-value of $p_B = 0.60$ indicates that the model is a good fit for the data. The probability plot in Figure A.13 also indicates that the model fits the data reasonably well. By looking at the histogram of the POTs and compare it to the probability density of the GP function, the model seems to fit the data well. The quantile plot however indicates that the POTs deviate from the model for the highest extreme values since it departs from linearity at those values. That does also seem to be the case when looking at the return level plot. For a large majority of the data, the model seems to be a good fit. However the largest POTs deviate from the model which raises concerns as those are the values of most interest.
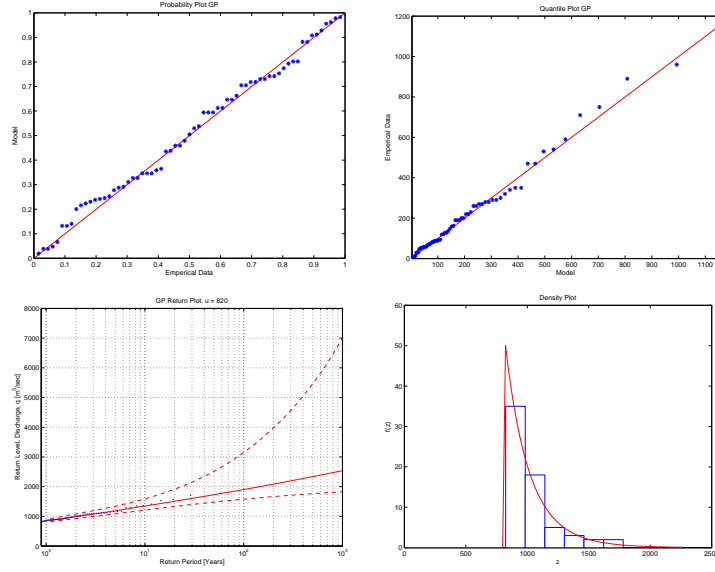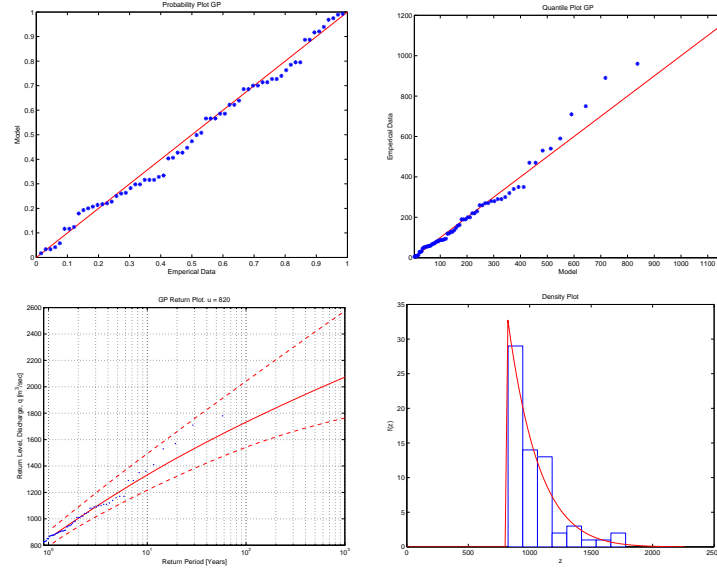
Figure A.11: (V064 TM DBM w/DRC) CASE 1: Diagnostic plots for the Threshold Model

Figure A.12: (V064 TM DBM w/DRC) CASE 2: Prior and posterior distributions for the GP parameters
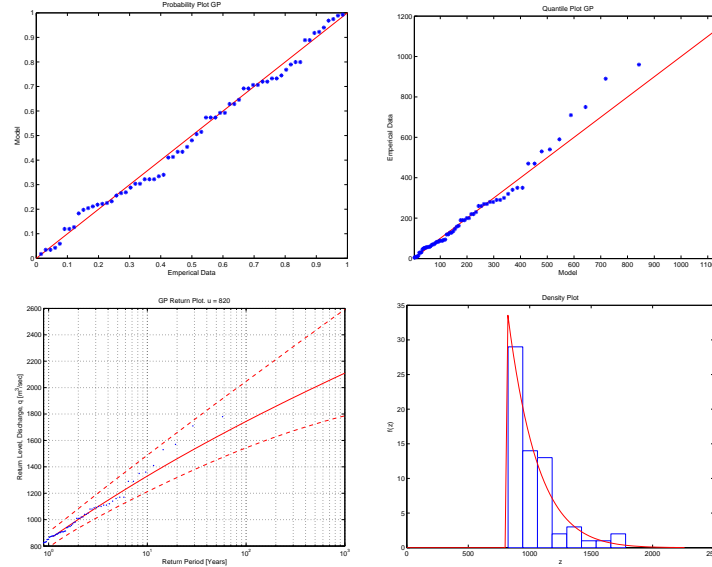
Figure A.13: (V064 TM DBM w/DRC) CASE 2: Diagnostic plots for the Threshold Model

Threshold model using diagnostic based methods for choosing a threshold- Case 3: A negative beta prior distribution for the ξ parameter (TM DBM w/DRC C3)

In Case 3, the prior distribution for ξ was chosen to be a negative beta distribution. It is a uniform distribution containing values on the interval $[-1; 0]$ The prior distribution for $\tilde{\sigma}$ is a non-informative inv-χ^2 distribution. Therefor, in this case, the posterior density of the shape parameter of the GEV distribution is constricted to negative values only. The prior and posterior distributions for the GP parameters are shown in Figure A.14.

The Anderson-Darling p-value of $p_B = 0.58$ indicates that the model is a good fit for the data. The probability plot in Figure A.15 also indicates that the model fits the data reasonably well. By looking at the histogram of the POTs and compare it to the probability density of the GP function, the model seems to fit the data well. The quantile plot however indicates that the POTs deviate from the model for the highest extreme values since it departs from linearity at those values. That is also the case when looking at the return level plot. For a large majority of the data, the model seems to be a good fit. However the largest POTs deviate from the model which raises concerns as those are the values of most interest.
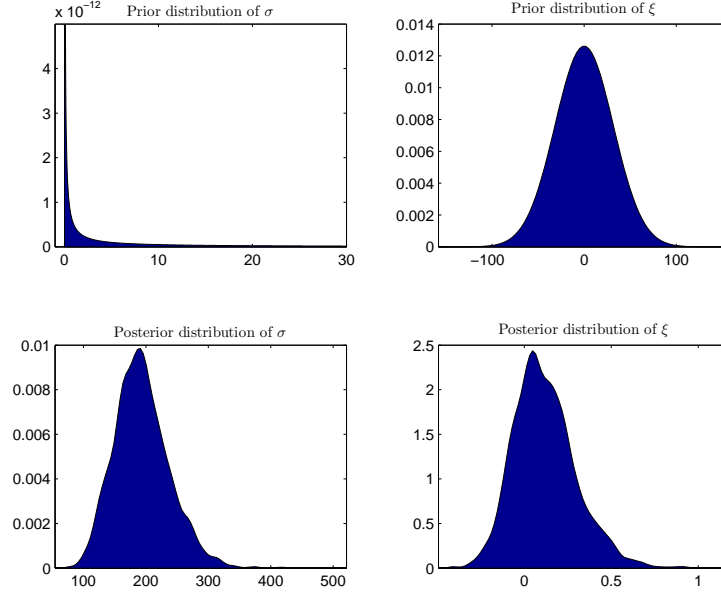
Figure A.14: (V064 TM DBM w/DRC) CASE 3: Prior and posterior distributions for the GP parameters

Threshold model using the diagnostic based method (DBM) for determining the threshold value - Figures and tables displaying the posterior parameters of the GP distribution

Figure A.15: (V064 TM DBM w/DRC) CASE 3: Diagnostic plots for the threshold model

Table A.3: (V064 TM DBM w/DRC): Percentiles for the posterior distributions of the GP parameters, sampled using a MCMC iteration scheme, for all three cases of prior distributions, calculated with DRC uncertainty

	Threshold model with DRC and u = 820					
	Percentiles for parameters in the GEV distribution					
	Normal		Neg-Gamma		Neg-Beta	
	σ	$\tilde{\xi}$	σ	$\tilde{\xi}$	σ	$\tilde{\xi}$
2.5%	131.96	-0.18	171.50	-0.19	174.47	-0.22
25%	173.58	-0.03	204.78	-0.09	208.96	-0.12
50%	200.18	0.06	226.22	-0.05	231.71	-0.07
75%	229.91	0.16	250.06	-0.02	257.19	-0.03
97.5%	298.03	0.40	304.82	-0.00	317.76	-0.00
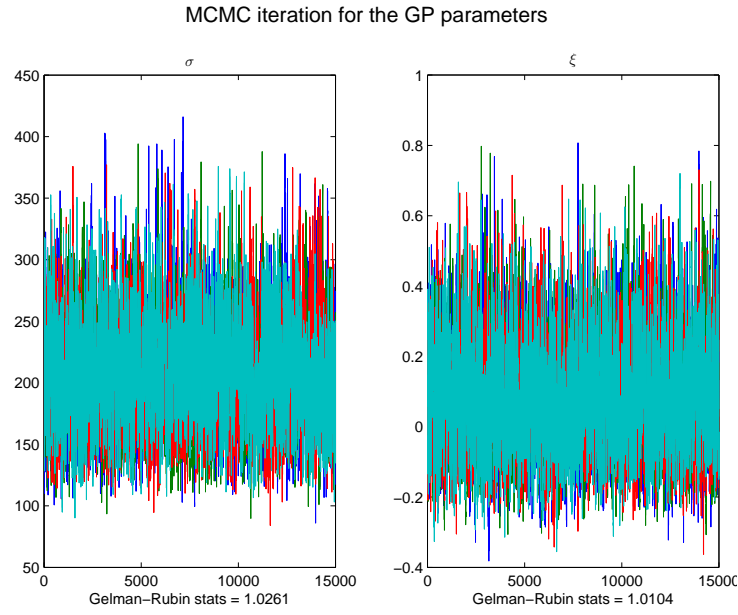
Figure A.16: (V064 TM DBM w/DRC) Case 1: Markov chain Monte Carlo simulation for the parameters in the GP distribution
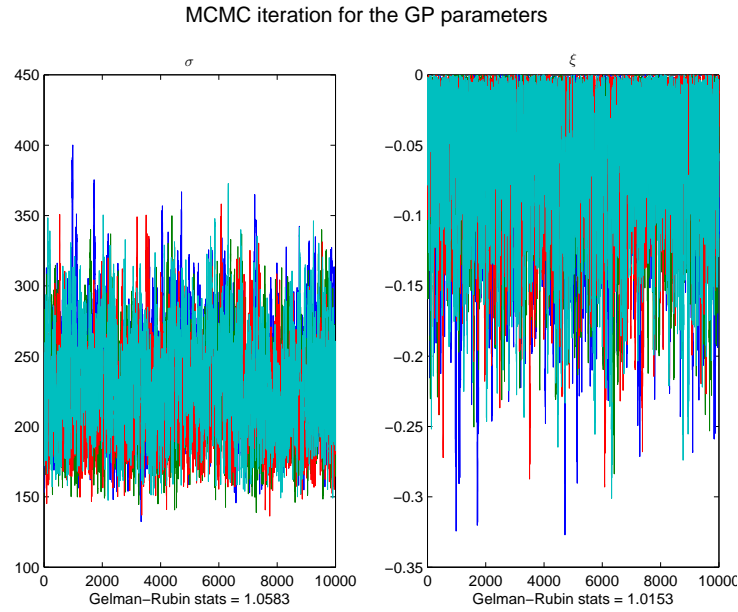
Figure A.17: (V064 TM DBM w/DRC) Case 2: Markov chain Monte Carlo simulation for the parameters in the GP distribution

MCMC iteration for the GP parameters
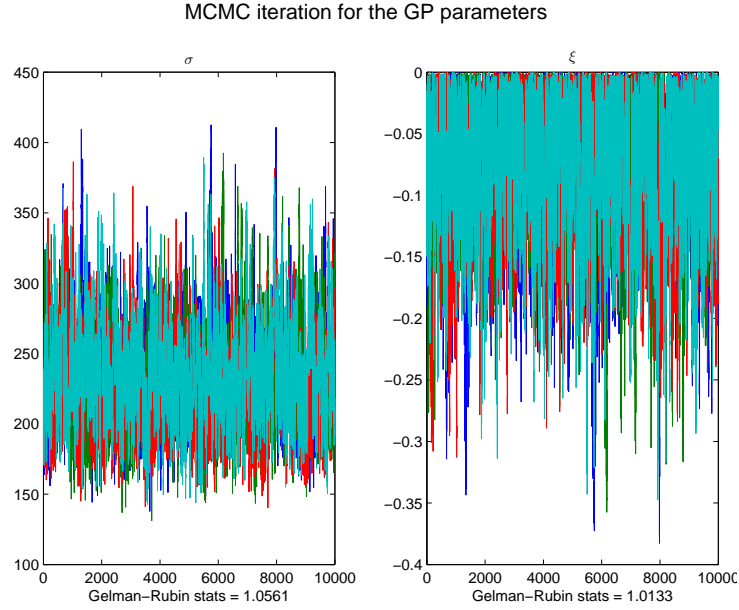
Figure A.18: (V064 TM DBM w/DRC) Case 3: Markov chain Monte Carlo simulation for the parameters in the GEV distribution

A.1.3. Threshold model using the fixed frequency method (FFM) for determining the threshold value

Threshold model using the fixed frequency method for choosing a threshold- Case 1: A normal prior distribution for the ξ parameter (TM FFM w/DRC C1)

In Case 1, the prior distribution for ξ was chosen to be a normal distribution with a large variance, making it non-informative prior. The prior distribution for $\tilde{\sigma}$ is a non-informative inv-χ^2 distribution. So, in this case, the GP parameters are not constricted in any way by their prior distributions. The prior and posterior distributions for the GP parameters are shown in Figure A.19.

The model seems to be a good fit for the data, with an Anderson-Darling p-value of $p_B = 0.50$. The diagnostic plots in Figure A.20 also indicate that the model fits the data well. The annual maximum values on the probability plot all lie close to the unit diagonal and the points are close to linear on the quantile plot. Comparison between the probability density of the GP distribution and the histogram of the POTs indicate a good model fit. Plotting the annual maximum values on the return level plot also seem to indicate that the model fits the data well.

Figure A.19: (V064 TM FFM w/DRC) CASE 1: Prior and posterior distributions for the GP parameters

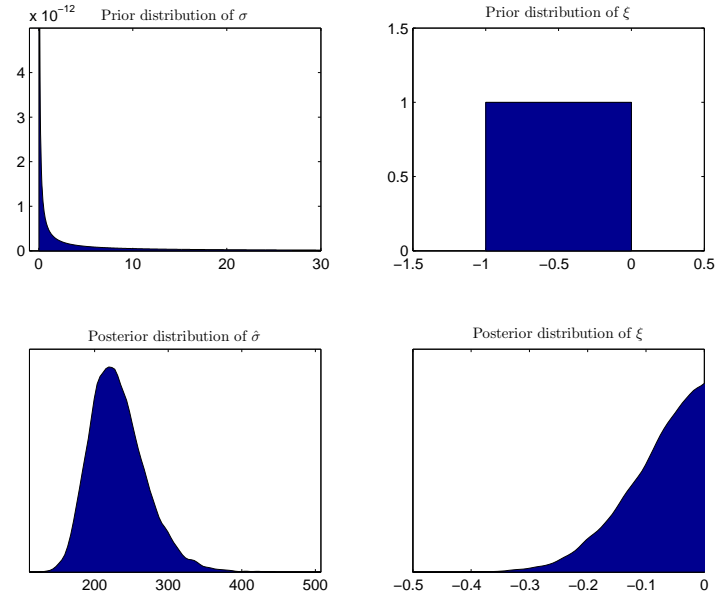## Threshold model using the fixed frequency method for choosing a threshold- Case 2: A negative gamma prior distribution for the ξ parameter (TM FFM w/DRC C2)

In Case 2, the prior distribution for ξ was chosen to be a negative gamma distribution. It contains only negative values having majority of the mass of the distribution is close to the y-axis. The prior distribution for $\tilde{\sigma}$ is a non-informative inv-χ^2 distribution. Therefore, in this case, the posterior density of the shape parameter of the GP distribution is constricted to negative values only. The prior and posterior distributions for the GP parameters are shown in Figure A.21.

The Anderson-Darling p-value of $p_B = 0.36$ indicates that the model is a reasonably good fit for the data. The probability plot in Figure A.22 also indicates that the model fits the data reasonably well. Comparison between the probability density of the GP distribution and the histogram of the POTs indicate a relatively good model fit. The quantile plot however indicates that the data deviate from the model for the highest extreme values since the highest values depart from linearity. By looking at the return level plot the model seems to fit the data reasonably well, even though the largest values tend to deviate from the median.
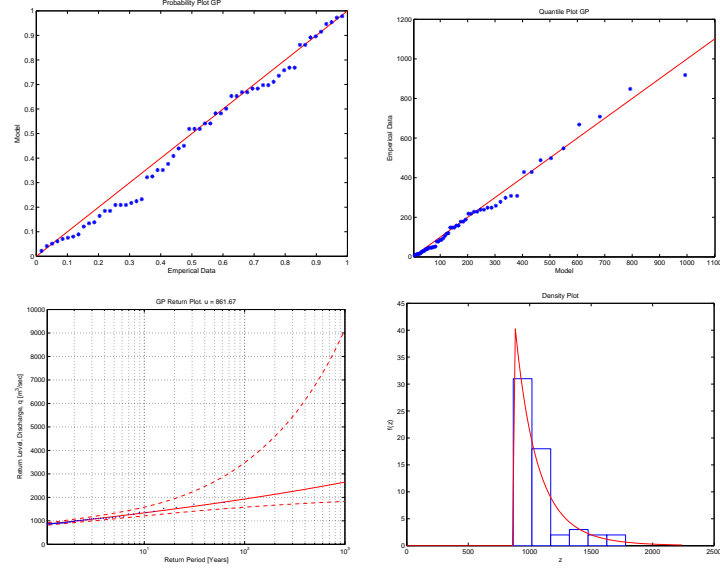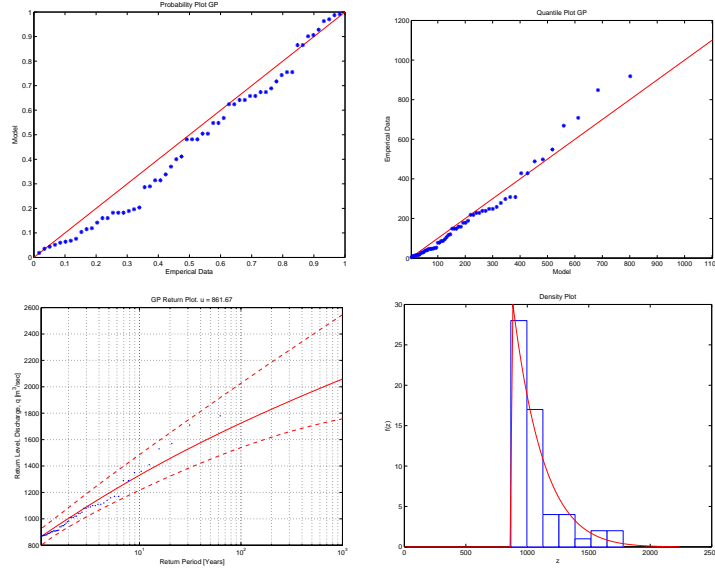
Figure A.20: (V064 TM FFM w/DRC) CASE 1: Diagnostic plots for the threshold model
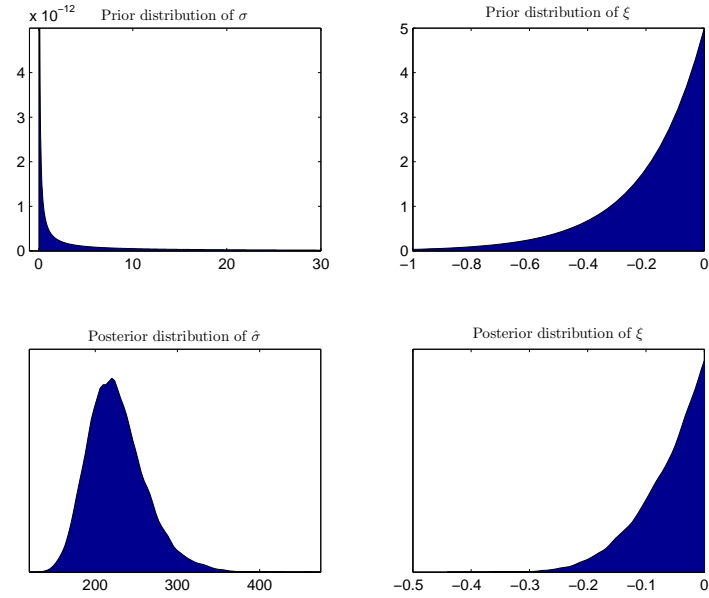
Figure A.21: (V064 TM FFM w/DRC) CASE 2: Prior and posterior distributions for the GP parameters
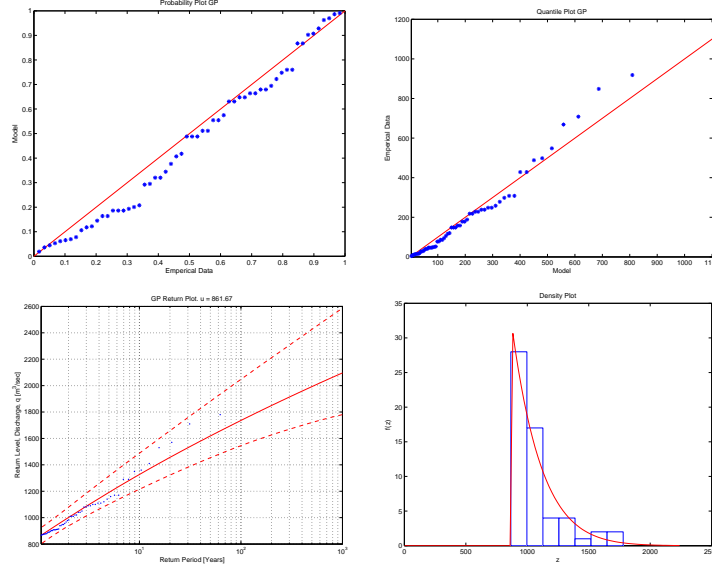
Figure A.22: (V064 TM FFM w/DRC) CASE 2: Diagnostic plots for the threshold model

Threshold model using the fixed frequency method for choosing a threshold- Case 3: A negative beta prior distribution for the ξ parameter (TM FFM w/DRC C3)

In Case 3, the prior distribution for ξ was chosen to be a negative beta distribution. It is a uniform distribution containing values on the interval $[-1; 0]$ The prior distribution for $\tilde{\sigma}$ is a non-informative inv-χ^2 distribution. Therefore, in this case, the posterior density of the shape parameter of the GEV distribution is constricted to negative values only. The prior and posterior distributions for the GP parameters are shown in Figure A.23.

The results from the negative beta prior distribution for the ξ parameter are almost identical to the results from the negative gamma prior distribution. The Anderson-Darling p-value, of $p_B = 0.32$, indicates that the model is a reasonably good fit for the data. The probability plot in Figure A.24 also indicates that the model fits the data reasonably well. Comparison between the probability density of the GP distribution and the histogram of the POTs indicate a relatively good model fit. The quantile plot however indicates that the data deviate from the model for the highest extreme values since the highest values depart from linearity. By looking at the return level plot the model seems to fit the data reasonably well, even though the largest values tend to deviate from the median.

Figure A.23: (V064 TM FFM w/DRC) CASE 3: Prior and posterior distributions for the GP parameters

Threshold model using the fixed frequency method (FFM) for determining the threshold value – Figures and tables displaying the posterior parameters of the GP distribution

Figure A.24: (V064 TM FFM w/DRC) CASE 3: Diagnostic plots for the threshold model

Table A.4: (V064 TM FFM w/DRC): Percentiles for the posterior distributions of the GP parameters, sampled using a MCMC iteration scheme, for all three cases of prior distributions, calculated with DRC uncertainty

|	Threshold model with DRC and u = 862					
	Percentiles for parameters in the GEV distribution					
	Normal		Neg-Gamma		Neg-Beta	
	σ	$\tilde{\xi}$	σ	$\tilde{\xi}$	σ	$\tilde{\xi}$
2.5%	122.80	-0.18	168.41	-0.20	170.46	-0.24
25%	165.69	-0.01	201.63	-0.10	205.18	-0.12
50%	191.41	0.09	222.82	-0.05	227.97	-0.07
75%	220.20	0.21	247.14	-0.02	254.52	-0.03
97.5%	287.16	0.48	307.85	-0.00	319.42	-0.00
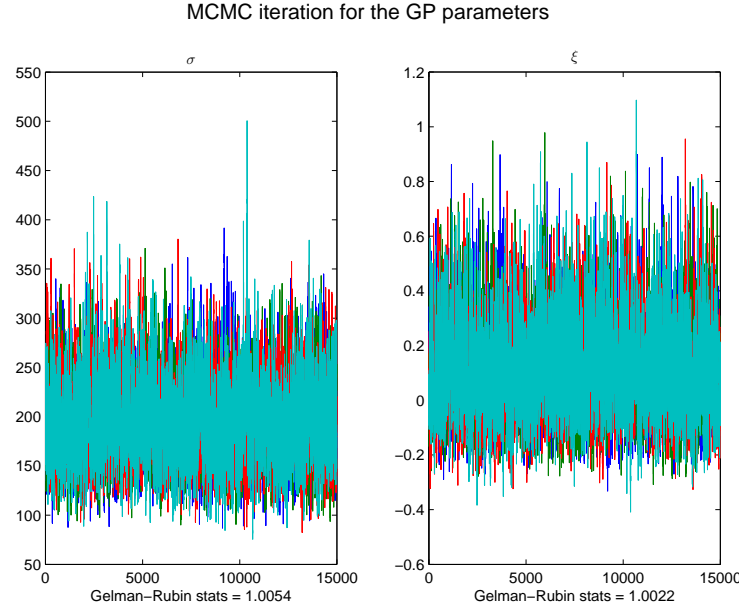
Figure A.25: (V064 TM FFM w/DRC) Case 1: Markov chain Monte Carlo simulation for the parameters in the GP distribution
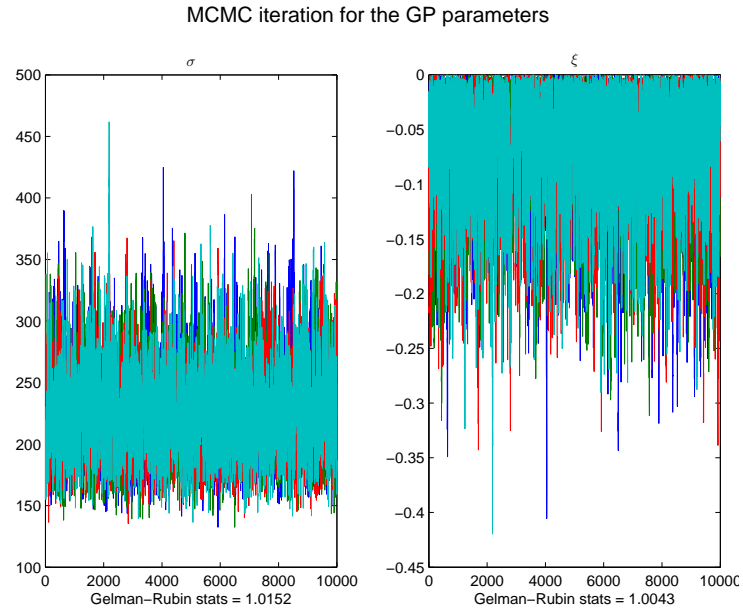
Figure A.26: (V064 TM FFM w/DRC) Case 2: Markov chain Monte Carlo simulation for the parameters in the GP distribution

MCMC iteration for the GP parameters

Figure A.27: (V064 TM FFM w/DRC) Case 3: Markov chain Monte Carlo simulation for the parameters in the GEV distribution

A.2. V064: Without discharge rating curve uncertainty

A.2.1. Block maxima model

Table A.5: (V064 BM w/o DRC): Percentiles for the posterior distributions of the GEV parameters, sampled using a MCMC iteration scheme, for all three cases of prior distributions, calculated without DRC uncertainty

	Block Extrema without DRC								
	Percentiles for parameters in the GEV distribution								
	Normal			Neg-Gamma			Neg-Beta		
	μ	σ	ξ	μ	σ	ξ	μ	σ	ξ
2.5%	807.04	150.23	-0.09	813.71	160.96	-0.13	814.91	161.60	-0.14
25%	838.59	172.86	0.03	850.41	183.43	-0.06	850.41	184.52	-0.07
50%	855.53	186.44	0.10	869.12	197.20	-0.03	869.53	199.09	-0.04
75%	872.73	201.63	0.17	887.48	212.27	-0.01	888.85	214.75	-0.02
97.5%	907.14	234.95	0.33	923.64	245.24	-0.00	926.33	249.79	-0.00

MCMC iteration for the GEV parameters
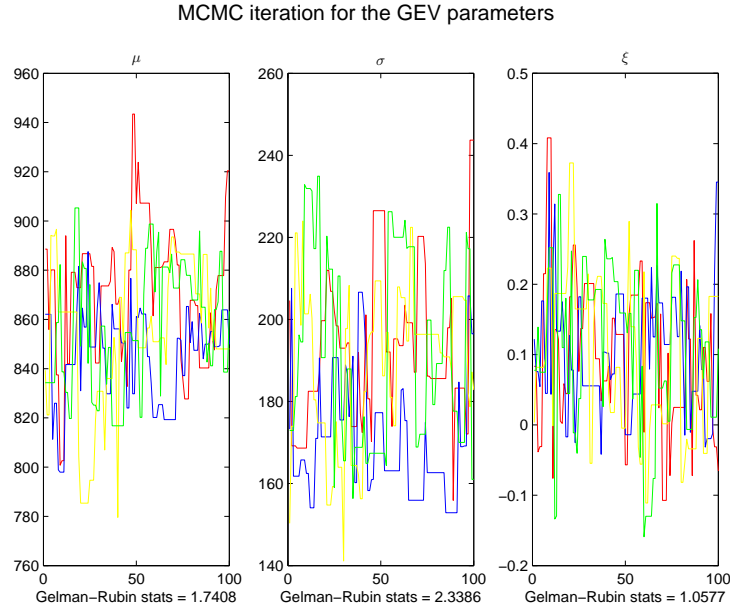
Figure A.28: (V064 BM w/o DRC) Case 1: Markov chain Monte Carlo simulation for the parameters in the GEV distribution
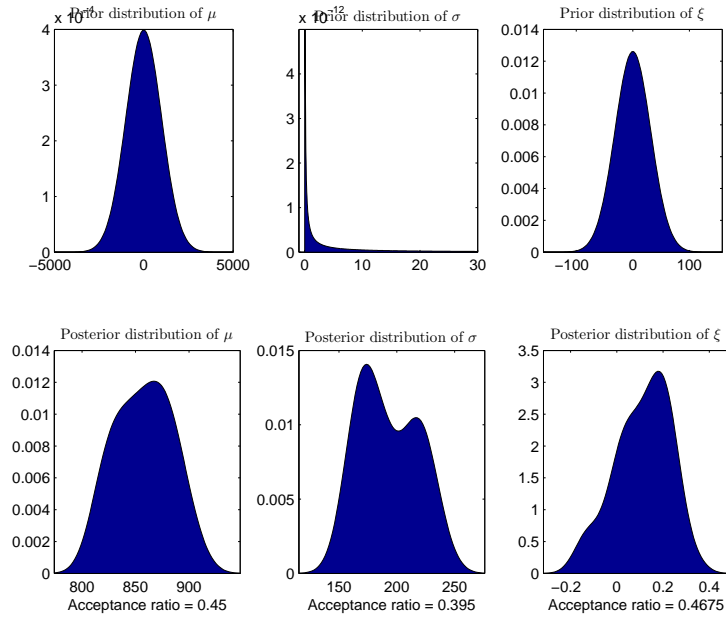
Figure A.29: (V064 BM w/o DRC) CASE 1: Prior and posterior distributions for the GEV parameters
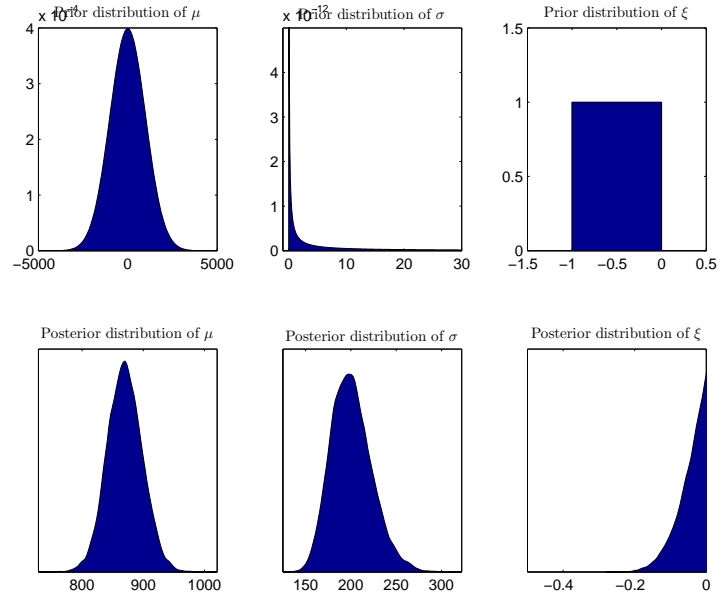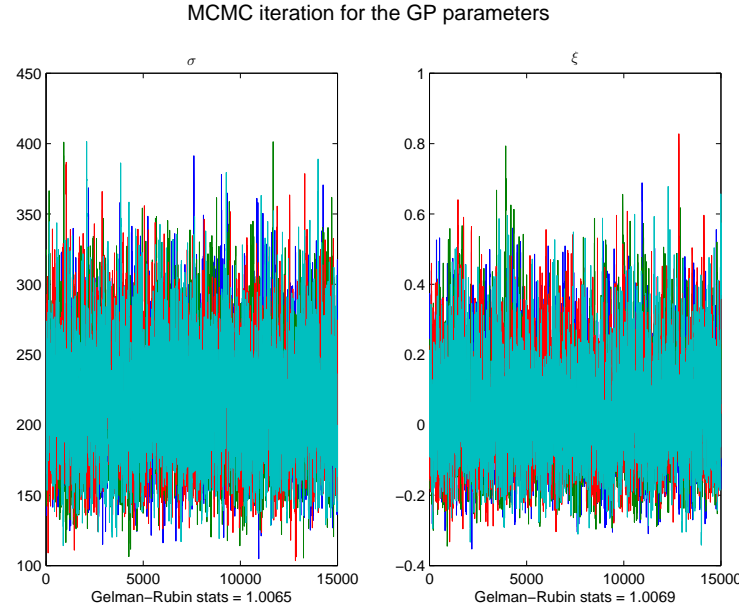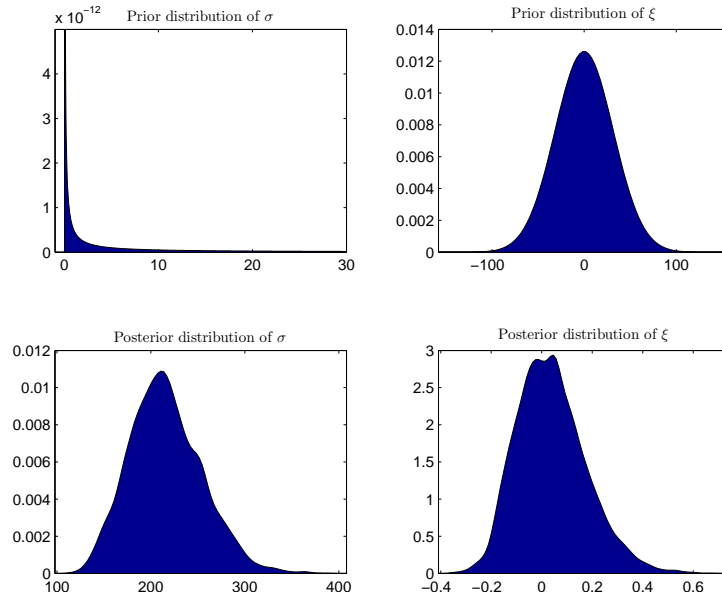
Figure A.30: (V064 BM w/o DRC) CASE 1: Diagnostic plots for the block maxima model

A.2.2. Threshold model using the diagnostic based method (DBM) for determining the threshold value

Table A.6: (V064 TM DBM w/o DRC): Percentiles for the posterior distributions of the GP parameters, sampled using a MCMC iteration scheme, for all three cases of prior distributions, calculated without DRC uncertainty

|	Threshold model with DRC and u = 820					
	Percentiles for parameters in the GEV distribution					
	Normal		Neg-Gamma		Neg-Beta	
	σ	$\tilde{\xi}$	σ	$\tilde{\xi}$	σ	$\tilde{\xi}$
2.5%	150.45	-0.20	182.60	-0.21	184.07	-0.24
25%	190.00	-0.06	215.16	-0.11	217.59	-0.13
50%	214.49	0.02	235.08	-0.06	238.38	-0.07
75%	241.66	0.12	258.05	-0.03	262.95	-0.04
97.5%	302.61	0.34	314.46	-0.00	322.53	-0.00
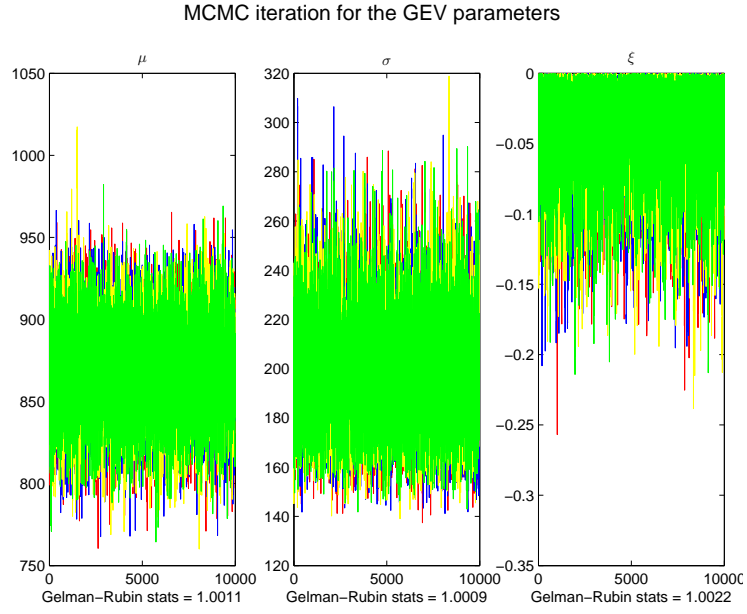
Figure A.31: (V064 BM w/o DRC) Case 2: Markov chain Monte Carlo simulation for the parameters in the GEV distribution
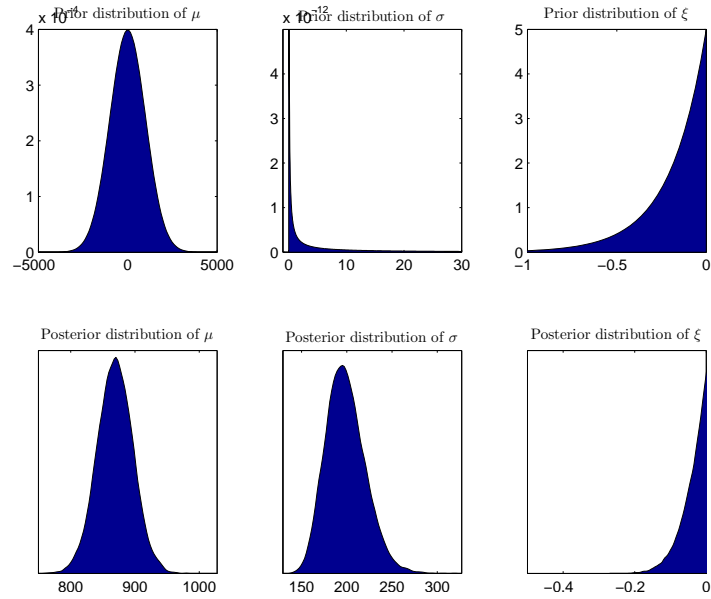
Figure A.32: (V064 BM w/o DRC) CASE 2: Prior and posterior distributions for the GEV parameters
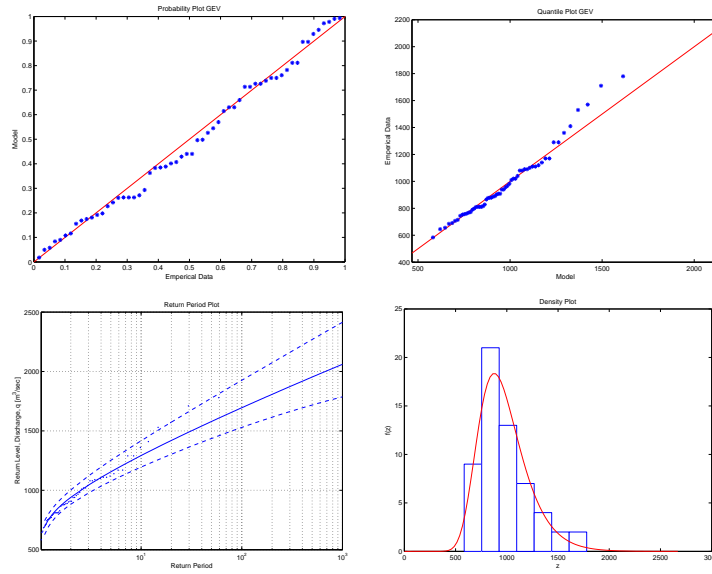
Figure A.33: (V064 BM w/o DRC) CASE 2: Diagnostic plots for the block maxima model
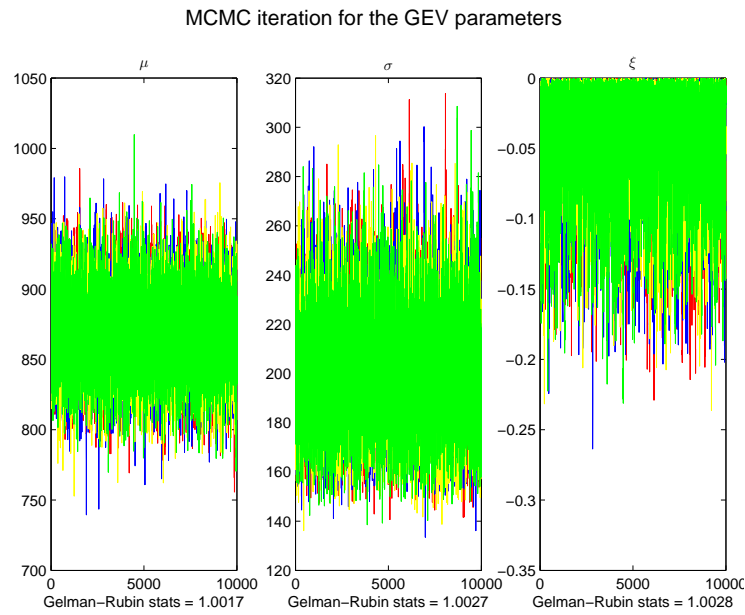
Figure A.34: (V064 BM w/o DRC) Case 3: Markov chain Monte Carlo simulation for the parameters in the GEV distribution

Figure A.35: (V064 BM w/o DRC) CASE 3: Prior and posterior distributions for the GEV parameters
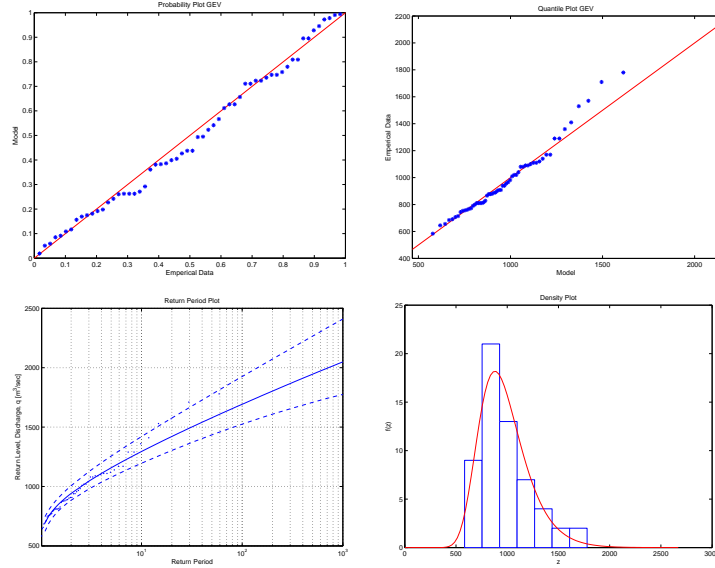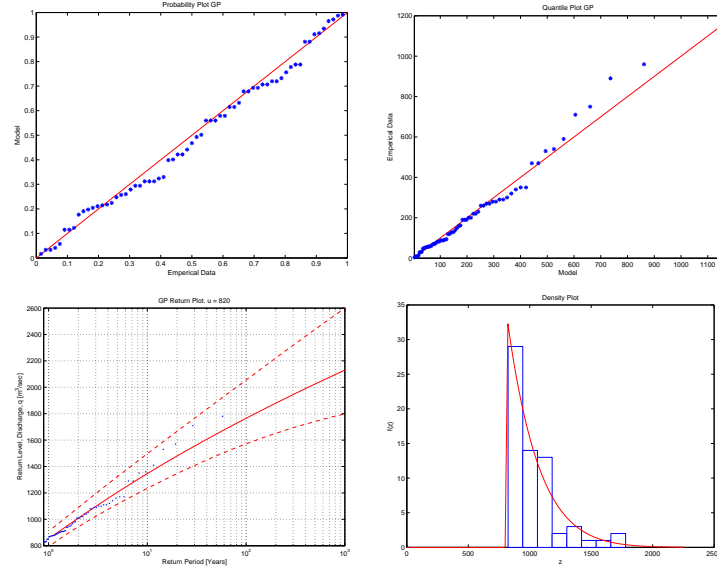

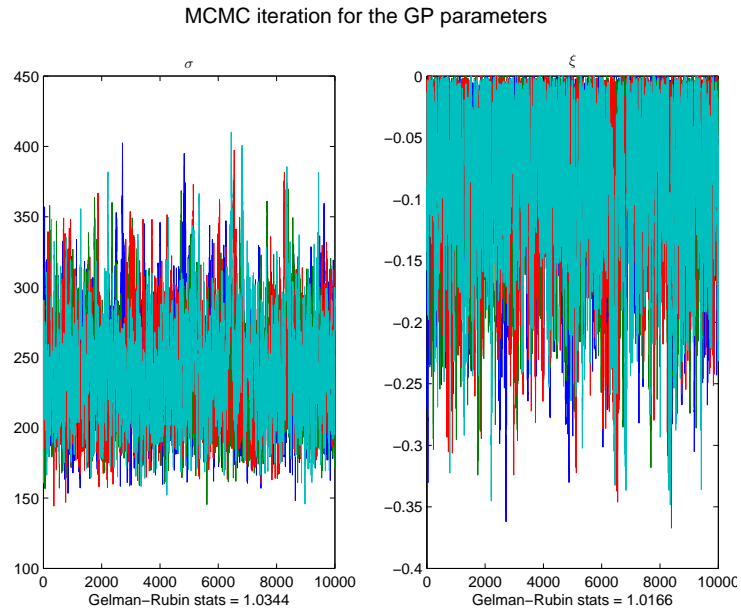*Figure A.36:* (V064 BM w/o DRC) CASE 3: Diagnostic plots for the block maxima model

Figure A.37: (V064 TM DBM w/o DRC) Case 1: Markov chain Monte Carlo simulation for the parameters in the GP distribution
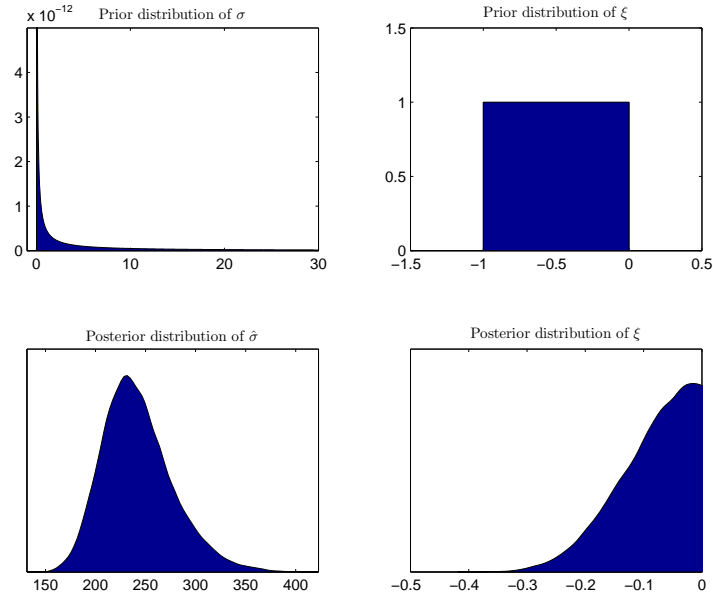

Figure A.38: (V064 TM DBM w/o DRC) CASE 1: Prior and posterior distributions for the GP parameters
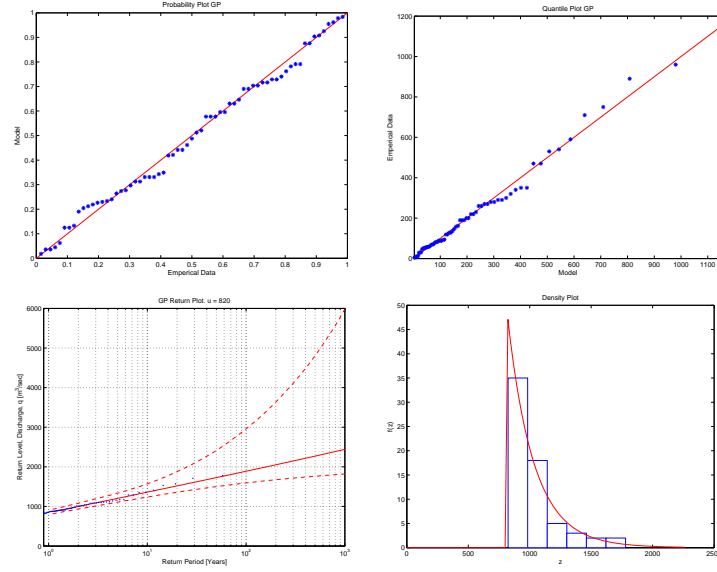
Figure A.39: (V064 TM DBM w/o DRC) CASE 1: Diagnostic plots for the threshold model

A.2.3. Threshold Model using the fixed frequency method (FFM) for determining the threshold value

Table A.7: (V064 TM FFM w/o DRC): Percentiles for the posterior distributions of the GP parameters, sampled using a MCMC iteration scheme, for all three cases of prior distributions, calculated without DRC uncertainty

|	Threshold model without DRC and u = 862					
	Percentiles for parameters in the GP distribution					
	Normal		Neg-Gamma		Neg-Beta	
	σ	$\tilde{\xi}$	σ	$\tilde{\xi}$	σ	$\tilde{\xi}$
2.5%	118.43	-0.15	165.83	-0.18	166.96	-0.22
25%	154.66	0.02	196.51	-0.09	199.35	-0.11
50%	178.07	0.13	215.10	-0.05	219.81	-0.06
75%	204.92	0.25	237.69	-0.02	243.73	-0.03
97.5%	264.17	0.51	288.96	-0.00	299.56	-0.00
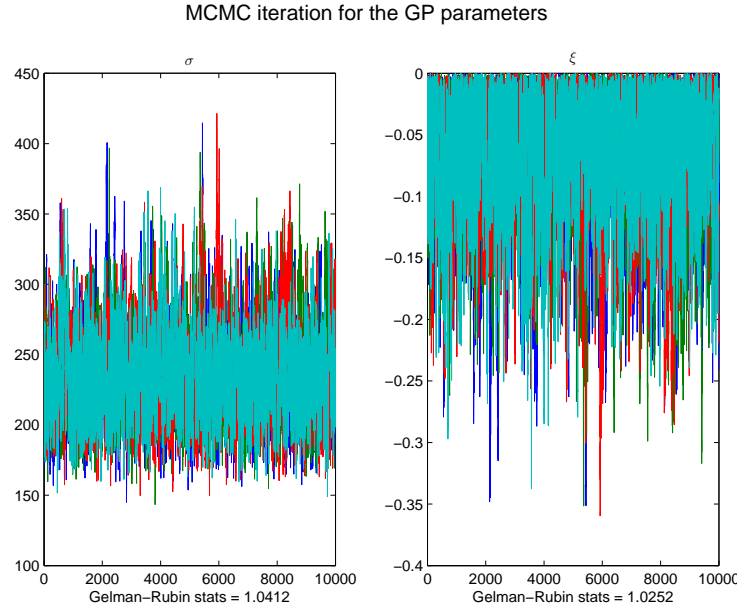
Figure A.40: (V064 TM DBM w/o DRC) Case 2: Markov chain Monte Carlo simulation for the parameters in the GP distribution
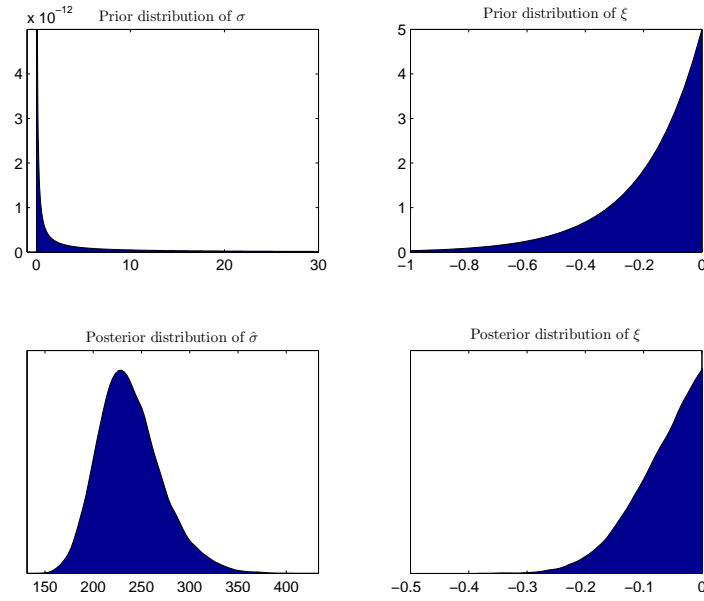
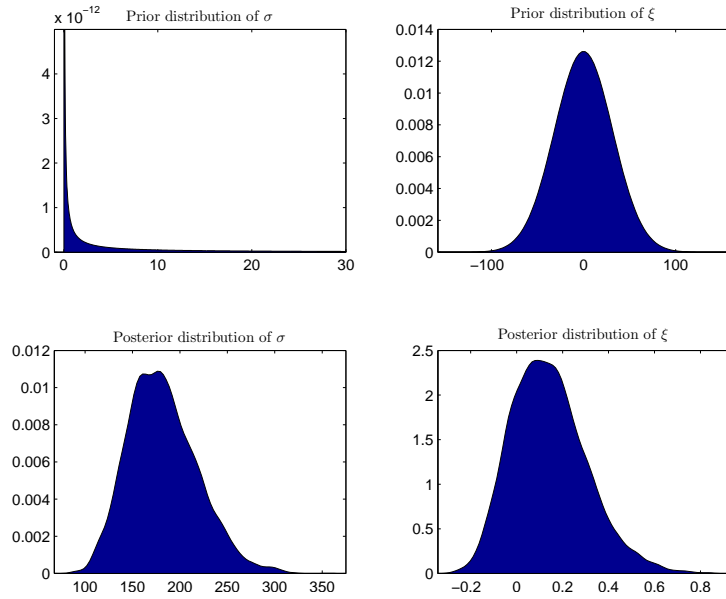*Figure A.41:* (V064 TM DBM w/o DRC) CASE 2: Prior and posterior distributions for the GP parameters
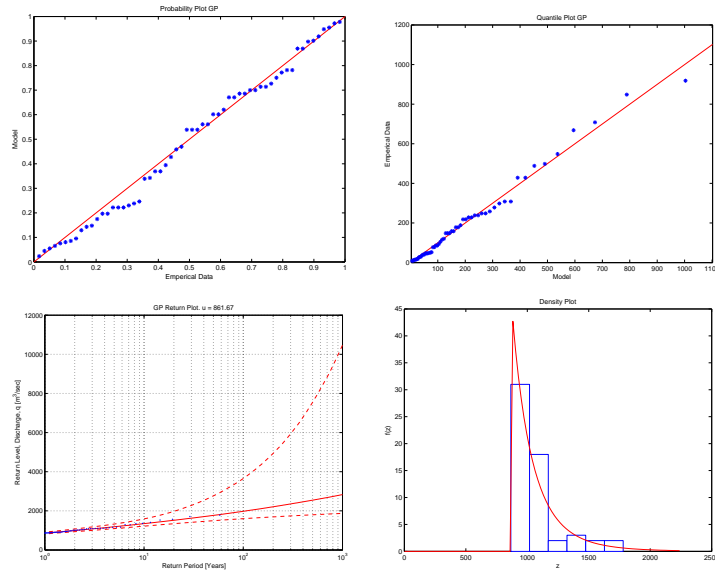
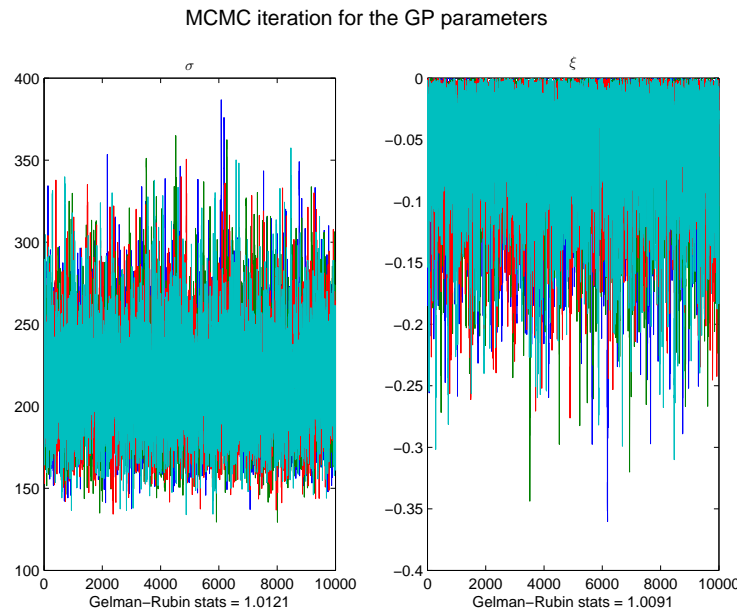Figure A.42: (V064 TM DBM w/o DRC) CASE 2: Diagnostic plots for the threshold model

Figure A.43: (V064 TM DBM w/o DRC) Case 3: Markov chain Monte Carlo simulation for the parameters in the GP distribution
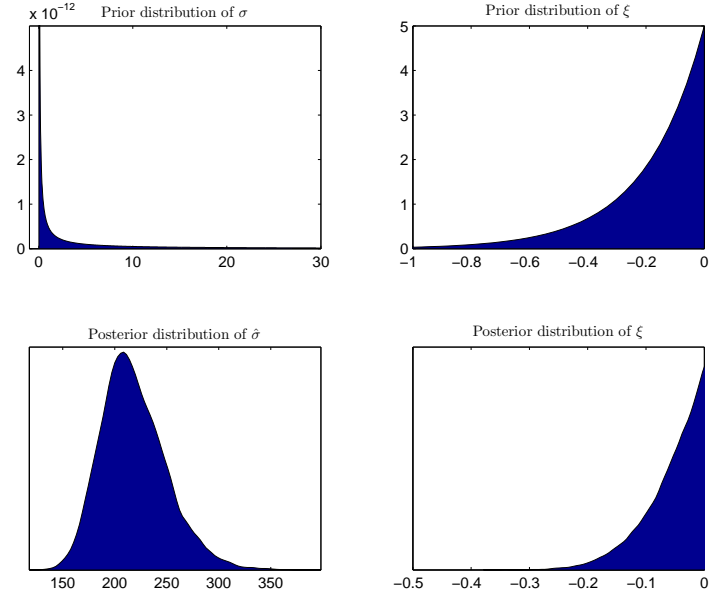
Figure A.44: (V064 TM DBM w/o DRC) CASE 3: Prior and posterior distributions for the GP parameters
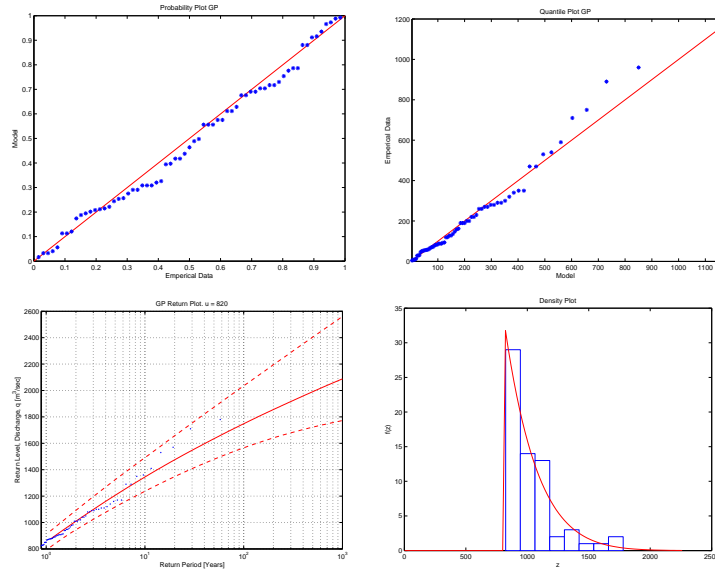
Figure A.45: (V064 TM DBM w/o DRC) CASE 3: Diagnostic plots for the threshold model
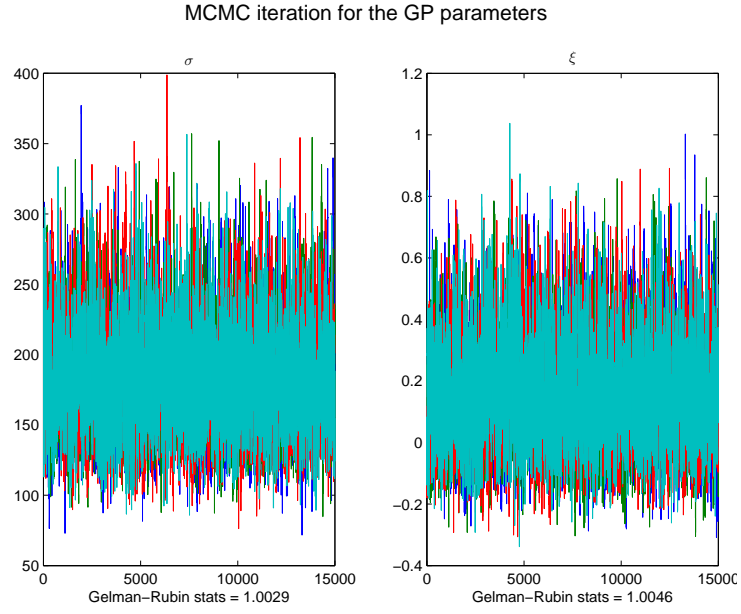
Figure A.46: (V064 TM FFM w/o DRC) Case 1: Markov chain Monte Carlo simulation for the parameters in the GP distribution

Figure A.47: (V064 TM FFM w/o DRC) CASE 1: Prior and posterior distributions for the GP parameters

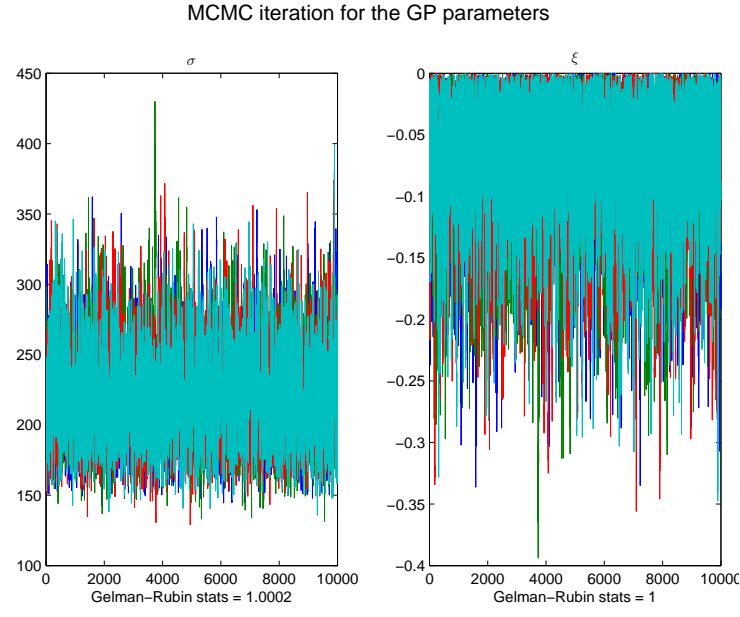*Figure A.48:* (V064 TM FFM w/o DRC) CASE 1: Diagnostic plots for the threshold model

Figure A.49: (V064 TM FFM w/o DRC) Case 2: Markov chain Monte Carlo simulation for the parameters in the GP distribution

Figure A.50: (V064 TM FFM w/o DRC) CASE 2: Prior and posterior distributions for the GP parameters
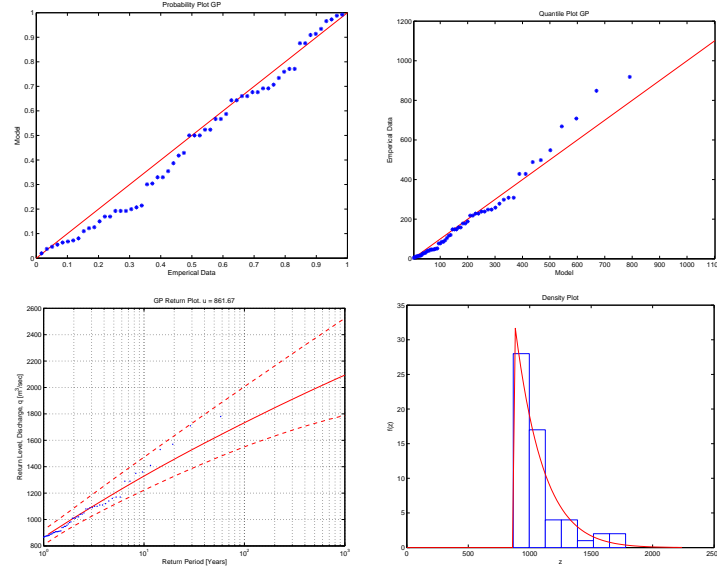
Figure A.51: (V064 TM FFM w/o DRC) CASE 2: Diagnostic plots for the threshold model

Figure A.52: (V064 TM FFM w/o DRC) Case 3: Markov chain Monte Carlo simulation for the parameters in the GP distribution
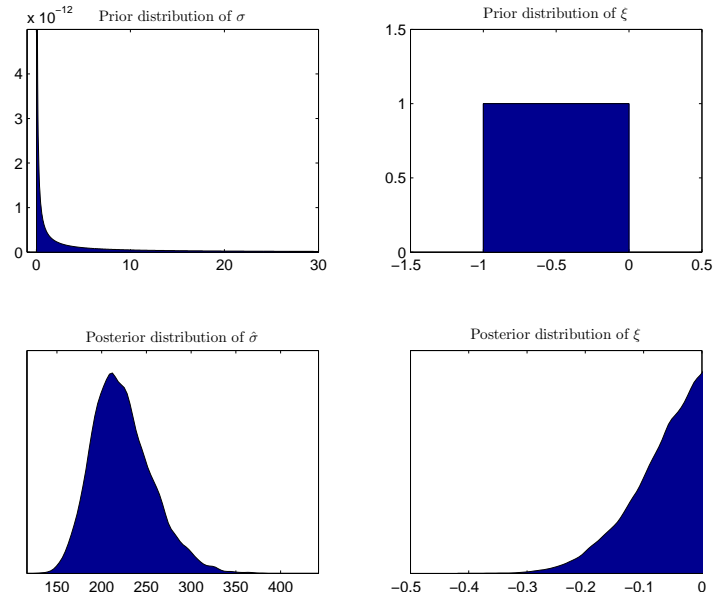

Figure A.53: (V064 TM FFM w/o DRC) CASE 3: Prior and posterior distributions for the GP parameters
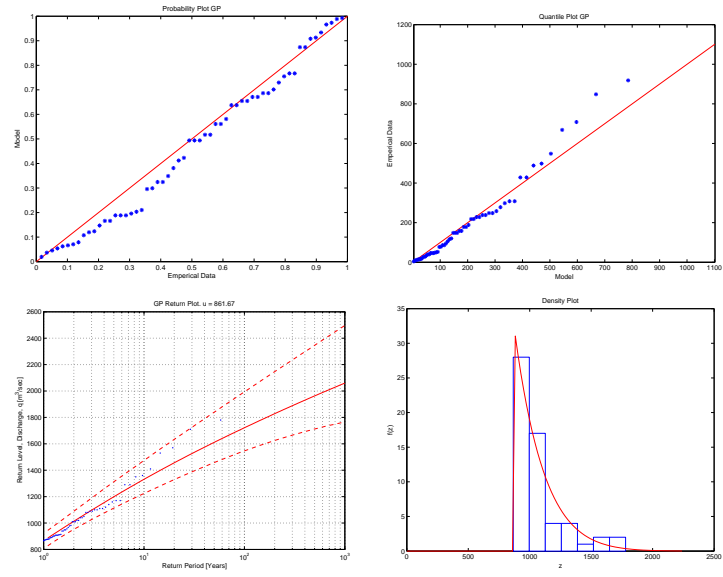
A. More details on the flood analysis for Olfusa

Figure A.54: (V064 TM FFM w/o DRC) CASE 3: Diagnostic plots for the threshold model

B. More details on the flood analysis for Hvita

In this appendix, figures and tables that are relevant to the research but were not displayed in the main text of the paper, are displayed. That includes probability plots, quantile plots and density plots for all cases of prior distributions. The prior and posterior densities of all the parameters in the GEV and GP distributions are also displayed for all cases. The appendix also includes the sampled Markov chain Monte Carlo (MCMC) chains, used to construct the posterior distributions for the parameters of both the generalized extreme value distribution (GEV) and the generalized Pareto (GP) distribution. The samples are displayed both in figures, and in tables as quantiles for all the models with and without the inclusion discharge rating curve uncertainty. The histogram of the prior and posterior distribution and the diagnostic plots for the models are shown for all models without the inclusion of discharge rating curve uncertainty.

Table B.1 shows a list of abbreviations regarding the following figures and tables. Every figure and table in the appendix is marked with some of these abbreviations and that explains which river the data belongs to and what kind of models were used to generate the results. For example, the text *(V066 BM w/DRC) Case 2* in the caption of a figure or a table, indicates that the data displayed comes from the river Hvita (V066), a block maxima model was used (BM) with a neg-gamma prior distribution for the shape parameter (Case 2), and the uncertainty in the discharge rating curve was taken into account in the calculations (w/DRC).

Table B.1: Abbreviations used to explain the origin of the data used to generate figures and tables

V066:	The river Hvita vid Kljafoss: 66 is the number of the gauging station measuring the data
Case 1:	The shape parameter, ξ, was sampled using a normal prior distribution
Case 2:	The shape parameter, ξ, was sampled using a neg-gamma prior distribution
Case 3:	The shape parameter, ξ, was sampled using a neg-beta prior distribution
BM:	A block maxima model
TM DBM:	A threshold model using the diagnostic based method for determining the threshold value
TM FFM:	A threshold model using the fixed frequency method for determining the threshold value
w/DRC:	A discharge rating curve uncertainty was taken into account in the calculations
w/o DRC:	A discharge rating curve uncertainty was not taken into account in the calculations

B.1. V066: With discharge rating curve uncertainty

B.1.1. Block maxima model

Block Maxima Model - Case 1: A normal prior distribution for the ξ parameter (BM w/DRC C1)

In Case 1, the prior distribution for ξ was chosen to be a normal distribution with a large variance, making it non-informative prior. The prior distribution for σ is a non-informative inv-χ^2 distribution and the prior distribution for μ is a normal distribution with large variance making it non-informative. So, in this case, the GEV parameters are not constricted in any way by their prior distributions. See further details on the prior distributions in Section 3.3.2. The construction of the posterior distribution of all the parameters is discussed in Section 3.3.3. The prior and posterior distributions for the GEV parameters are shown in Figure B.1.

The simulated chains of posterior distributions for the GEV parameters are used to model the extreme behavior of the river. The simulated chains of the posterior
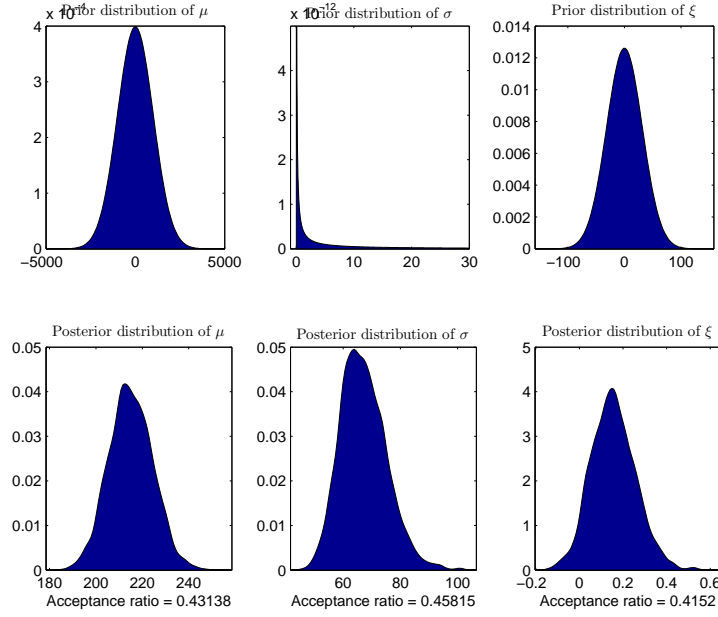
Figure B.1: (V066 BM w/DRC) CASE 1: Prior and posterior distributions for the GEV parameters

distributions of the parameters are shown in Figure B.7 and their quantiles are shown in Table B.2.

Figure B.2 shows the return period plot for Hvita as well as the quantile plot, the probability plot and the density plot. The Anderson-Darling p-value and the diagnostic plots in Figure B.2 are evaluated to check the validity of the model. The methods used for the model validation are discussed in Section 2.2.2.

The model is a reasonably good fit for the data, with an Anderson-Darling p-value of $p_B = 0.38$. Looking at the diagnostic plots in Figure B.2 a minor deviation from the unit diagonal is shown in the probability plot but despite that it indicates that the model fits the data reasonably well. The annual maximum value points on the quantile plot are close to linear indicating a good fit. Comparison between the probability density of the GEV distribution and the histogram of the POTs, indicates a good model fit. Plotting the annual maximum values on the return level plot also seem to indicate that the model fits the data well, since all the values are inside the 95% posterior interval of the return levels.
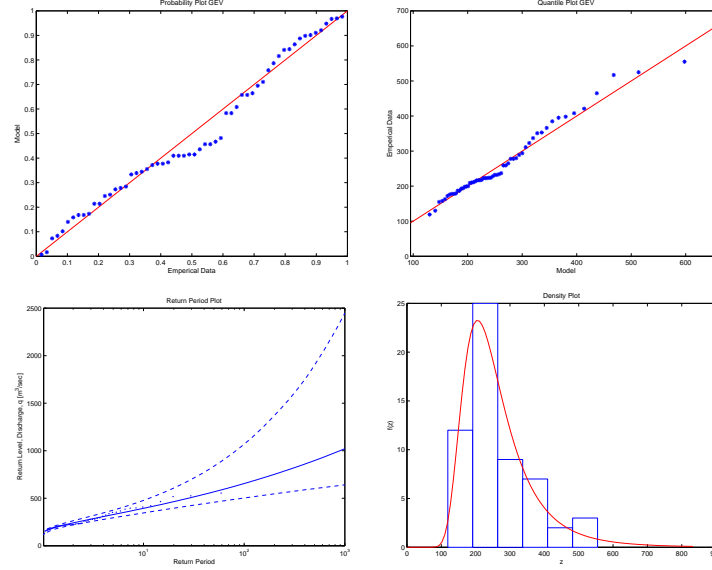
Figure B.2: (V066 BM w/DRC) CASE 1: Diagnostic plots for the block maxima model

Block Maxima Model - Case 2: A negative gamma prior distribution for the ξ parameter (BM w/DRC C2)

In Case 2, the prior distribution for ξ was chosen to be a negative gamma distribution. It contains only negative values having majority of the mass of the distribution is close to the y-axis. Therefore, in this case, the posterior density of the shape parameter of the GEV distribution is constricted to negative values only. The prior and posterior distributions for the GEV parameters are shown in Figure (B.3).

The simulated chains of the posterior distributions of the parameters are shown in Figure B.8 and their quantiles are shown in Table B.2.

Figure B.4 shows the return period plot for Hvita as well as the quantile plot, the probability plot and the density plot. Figure B.4 shows the diagnostic plots for the river. The Anderson-Darling p-value, of $p_B = 0.19$, indicates that the model is a reasonably good fit for the data. The probability plot in Figure B.4 deviates from the unit diagonal for few of the data points. The quantile plot deviates from linearity at the largest data point indicating an inadequate fit to the model. Comparison between the probability density of the GP distribution and the histogram of the POTs, indicates that the model does not fit the data well as there are more POTs having values around 200 than the model anticipates. There are also to more POTs having values around 550 than the model predicts. Furthermore, the data points deviate from the expected values in the return period plot indicating an inadequate fit to the model.
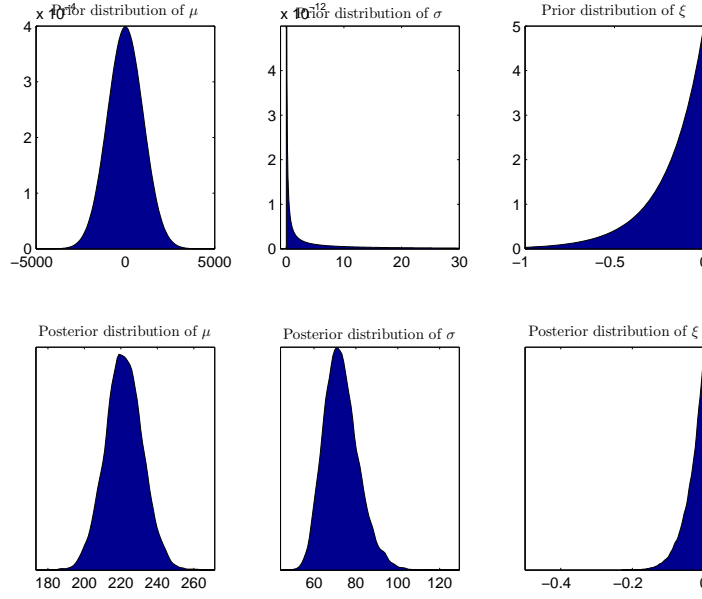
Figure B.3: (V066 BM w/DRC) CASE 2: Prior and posterior distributions for the GEV parameters

Block Maxima Model - Case 3: A negative beta prior distribution for the ξ parameter (BM w/DRC C3)

In Case 3, the prior distribution for ξ was chosen to be a negative beta distribution. It is a uniform distribution containing values on the interval $[-1; 0]$ Therefore, in this case, the posterior density of the shape parameter of the GEV distribution is constricted to negative values only. The prior and posterior distributions for the GEV parameters are shown in Figure (B.5).

The simulated chains of the posterior distributions of the parameters are shown in Figure B.9 and their quantiles are shown in Table B.2.

Figure B.6 shows the return period plot for Hvita as well as the quantile plot, the probability plot and the density plot.

Figure B.6 shows a diagnostic plots for the river for case 3, when the prior distribution for the ξ parameter is a negative beta distribution. The results are similar to the results from Case 2. The Anderson-Darling p-value of $p_B = 0.19$ indicates that the model is a reasonably good fit for the data. The probability plot in Figure B.6 deviates from the unit diagonal for few of the data points. The quantile plot deviates from linearity at the largest data point indicating an inadequate fit to the model. Comparison between the probability density of the GEV distribution and the histogram of the POTs indicates that the model does not fit the data well as
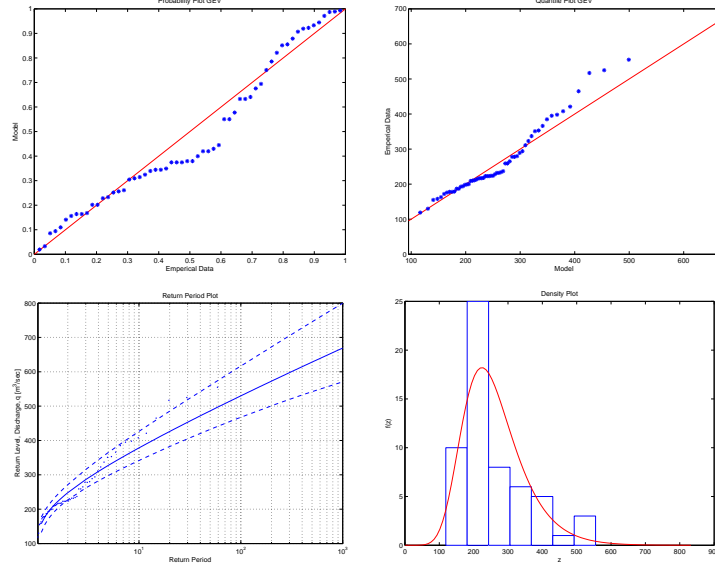
Figure B.4: (V066 BM w/DRC) CASE 2: Diagnostic plots for the block maxima model
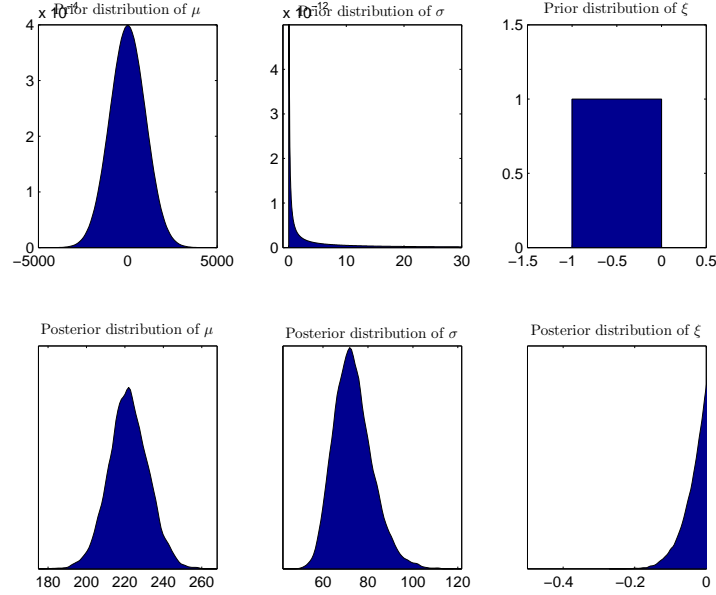
Figure B.5: (V066 BM w/DRC) CASE 3: Prior and posterior distributions for the GEV parameters

there are more POTs having values around 200 than the model anticipates. There are also to more POTs having values around 550 than the model predicts. Furthermore, the data points deviate from the expected values in the return period plot indicating an inadequate fit to the model.
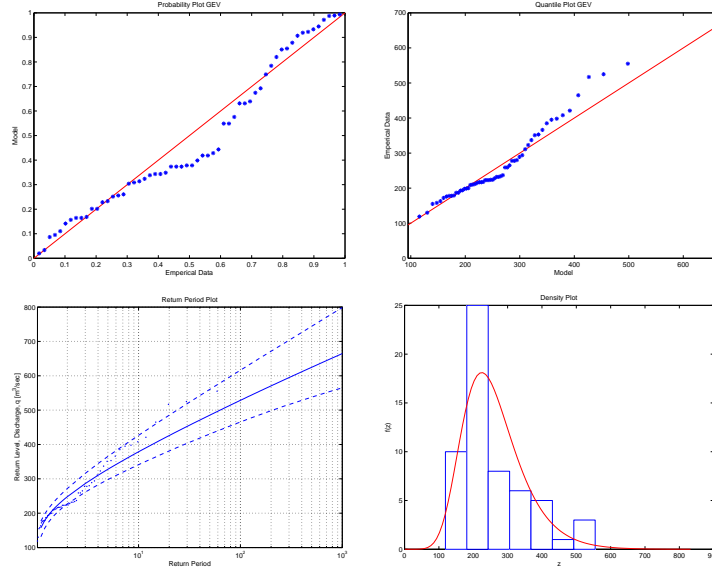
Figure B.6: (V066 BM w/DRC) CASE 3: Diagnostic plots for the block maxima model

Block Maxima Model – Figures and tables displaying the posterior parameters of the GEV distribution

Table B.2: (V066 BM w/DRC): Percentiles for the posterior distributions of the GEV parameters, sampled using a MCMC iteration scheme, for all three cases of prior distributions, calculated with DRC uncertainty

	Normal			Neg-Gamma			Neg-Beta		
	μ	σ	ξ	μ	σ	ξ	μ	σ	ξ
2.5%	197.00	53.28	-0.04	201.62	58.95	-0.11	201.72	58.80	-0.12
25%	208.83	61.72	0.09	214.86	67.17	-0.05	215.17	67.35	-0.06
50%	215.13	66.81	0.15	221.57	72.36	-0.03	221.73	72.67	-0.03
75%	221.65	72.46	0.22	228.47	78.09	-0.01	228.69	78.59	-0.01
97.5%	234.01	84.75	0.37	242.08	91.57	-0.00	242.69	92.45	-0.00

Block Extrema with DRC
Percentiles for parameters in the GEV distribution

MCMC iteration for the GEV parameters
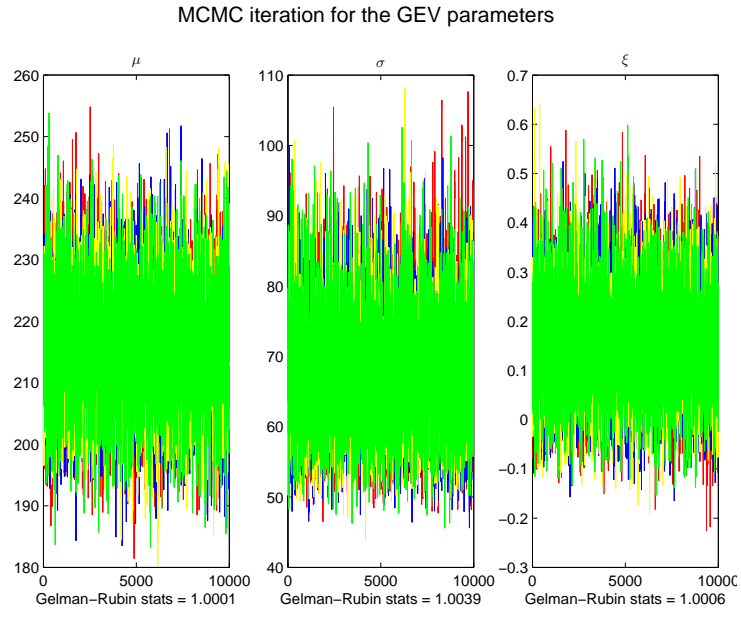
Figure B.7: (V066 BM w/DRC) Case 1: Markov chain Monte Carlo simulation for the parameters in the GEV distribution

MCMC iteration for the GEV parameters
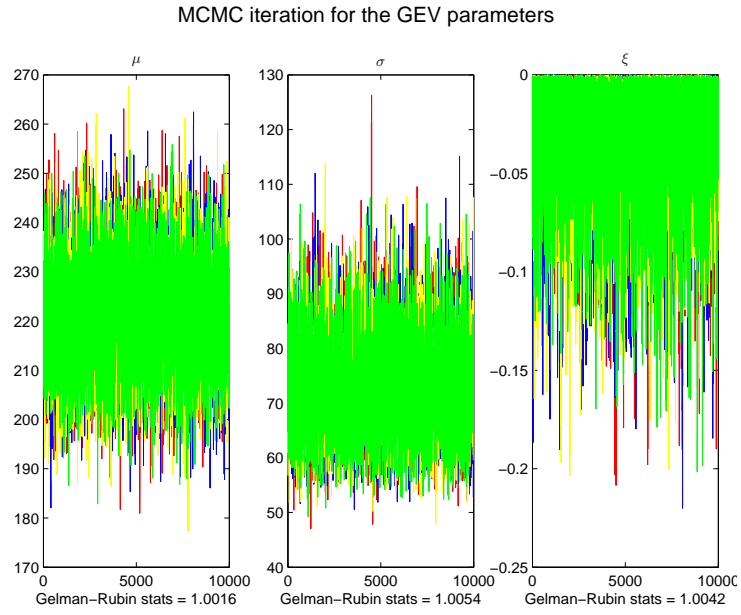
Figure B.8: (V066 BM w/DRC) Case 2: Markov chain Monte Carlo simulation for the parameters in the GEV distribution
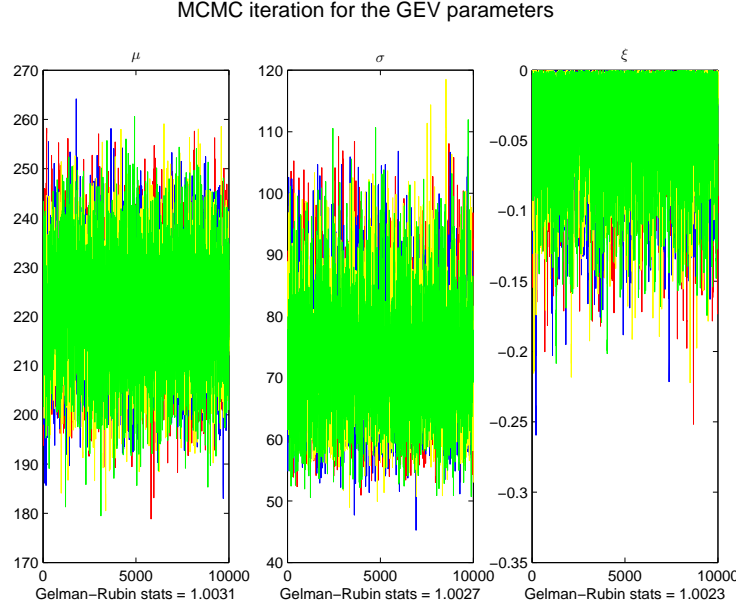
Figure B.9: (V066 BM w/DRC) Case 3: Markov chain Monte Carlo simulation for the parameters in the GEV distribution

B.1.2. Threshold model using the diagnostic based method (DBM) for determining the threshold value

Threshold model using diagnostic based methods for choosing a threshold-Case 1: A normal prior distribution for the ξ parameter (TM DBM w/DRC C1)

In Case 1, the prior distribution for ξ was chosen to be a normal distribution with a large variance, making it non-informative prior. The prior distribution for $\tilde{\sigma}$ is a non-informative inv-χ^2 distribution. So, in this case, the GP parameters are not constricted in any way by their prior distributions. The prior and posterior distributions for the GP parameters are shown in Figure B.10.

The model seems to be a reasonably good fit for the data, having an Anderson-Darling p-value of $p_B = 0.45$. The diagnostic plots in Figure B.11 indicates that the model fits the data well. The probability plot is close to the unit diagonal for all the data points. The data points are close to being linear in the quantile plot and they fit well in the return period plot.
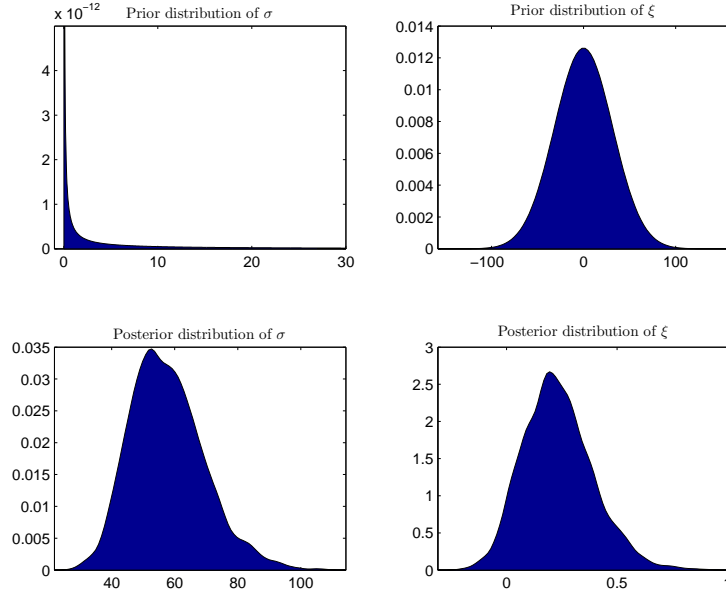
Figure B.10: (V066 TM DBM w/DRC) CASE 1: Prior and posterior distributions for the GP parameters

Threshold model using diagnostic based methods for choosing a threshold-Case 2: A negative gamma prior distribution for the ξ parameter (TM DBM w/DRC C2)

In Case 2, the prior distribution for ξ was chosen to be a negative gamma distribution. It contains only negative values having majority of the mass of the distribution is close to the y-axis. The prior distribution for $\tilde{\sigma}$ is a non-informative inv-χ^2 distribution. Therefore, in this case, the posterior density of the shape parameter of the GP distribution is constricted to negative values only. The prior and posterior distributions for the GP parameters are shown in Figure B.12.

Figure B.13 shows a diagnostic plots for the model. The Anderson-Darling p-value of $p_B = 0.26$ indicates that the model is a reasonably good fit for the data. The probability plot in Figure B.13 deviates from the unit diagonal for few of the data points. The quantile plot deviates from linearity at the largest data point indicating an inadequate fit to the model. Furthermore, the data points deviate from the expected values in the return period plot indicating an inadequate fit to the model.
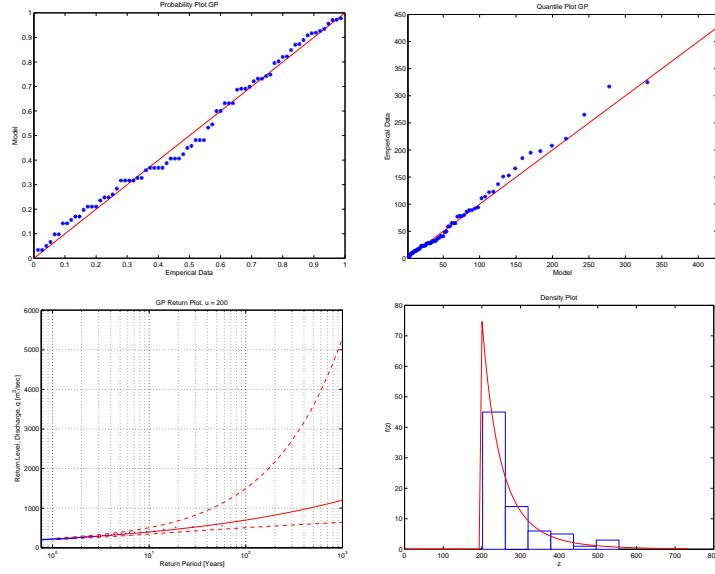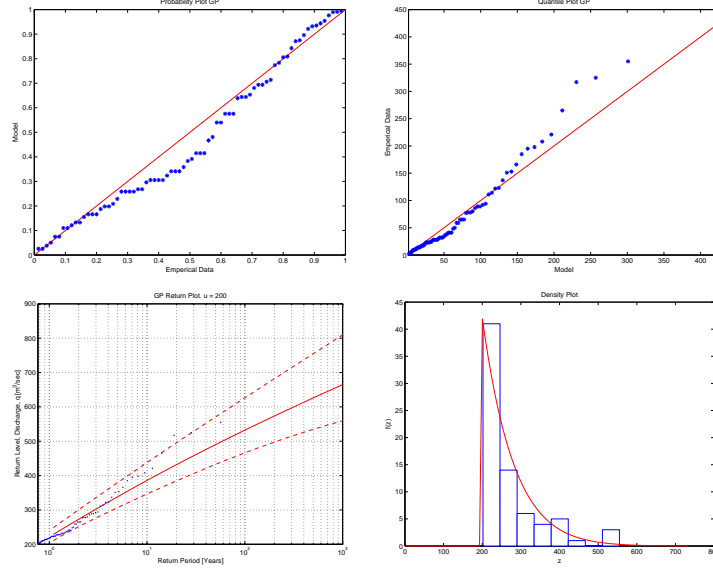
Figure B.11: (V066 TM DBM w/DRC) CASE 1: Diagnostic plots for the Threshold Model
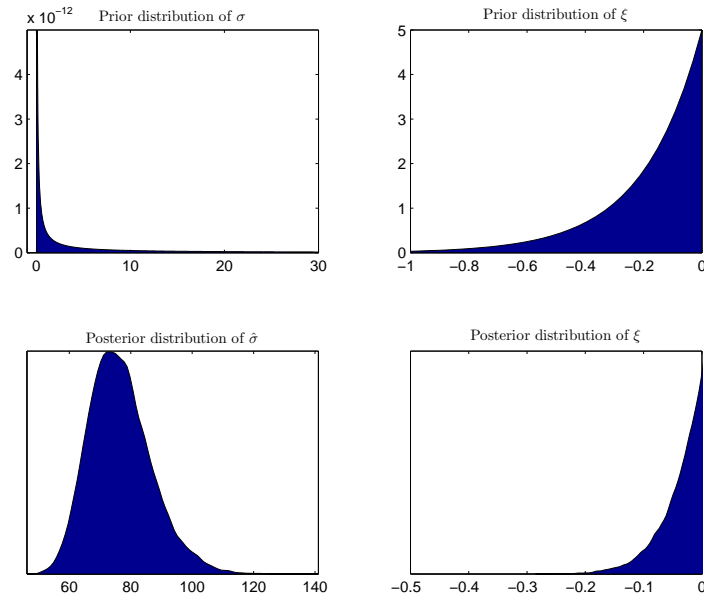
Figure B.12: (V066 TM DBM w/DRC) CASE 2: Prior and posterior distributions for the GP parameters
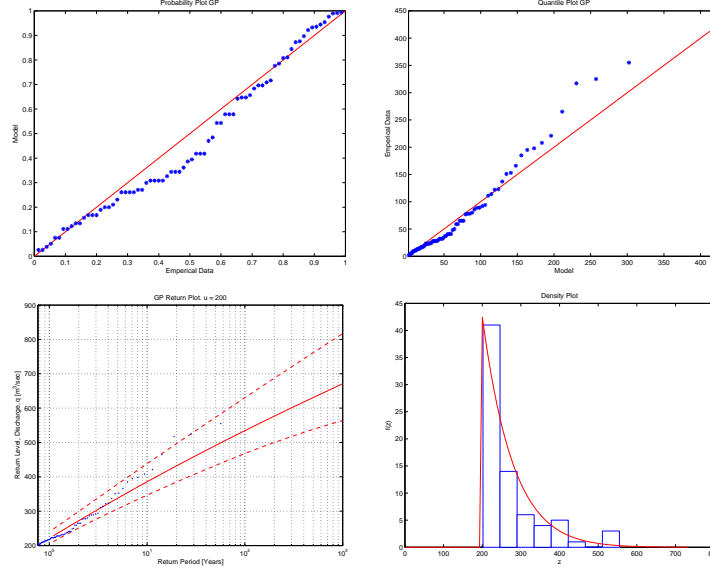
Figure B.13: (V066 TM DBM w/DRC) CASE 2: Diagnostic plots for the Threshold Model

Threshold model using diagnostic based methods for choosing a threshold- Case 3: A negative beta prior distribution for the ξ parameter (TM DBM w/DRC C3)

In Case 3, the prior distribution for ξ was chosen to be a negative beta distribution. It is a uniform distribution containing values on the interval $[-1; 0]$ The prior distribution for $\tilde{\sigma}$ is a non-informative inv-χ^2 distribution. Therefor, in this case, the posterior density of the shape parameter of the GEV distribution is constricted to negative values only. The prior and posterior distributions for the GP parameters are shown in Figure B.14.

Figure B.15 shows a diagnostic plots for the model for case 3, when the prior distribution for the ξ parameter is a negative beta distribution. The results are almost identical to case 2.

The Anderson-Darling p-value of $p_B = 0.25$ indicates that the model is a reasonably good fit for the data. The probability plot in Figure B.15 deviates from the unit diagonal for few of the data points. The quantile plot deviates from linearity at the largest data point indicating an inadequate fit to the model. Furthermore, the data points deviate from the expected values in the return period plot indicating an inadequate fit to the model.
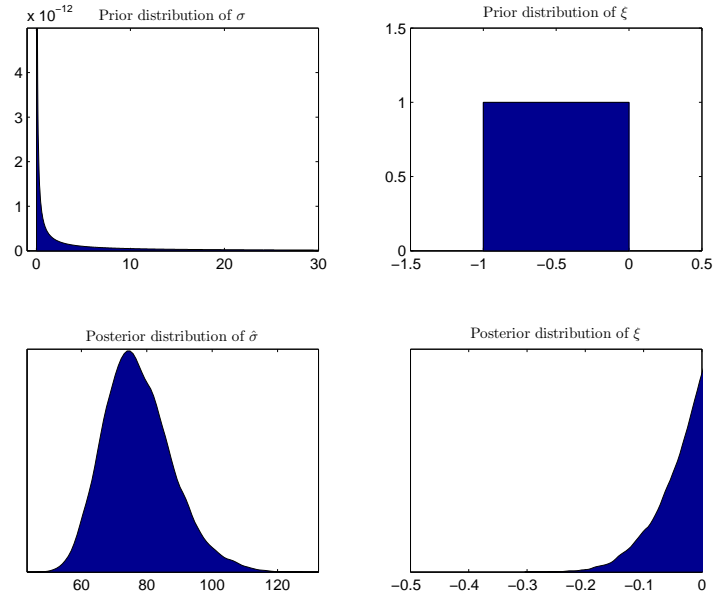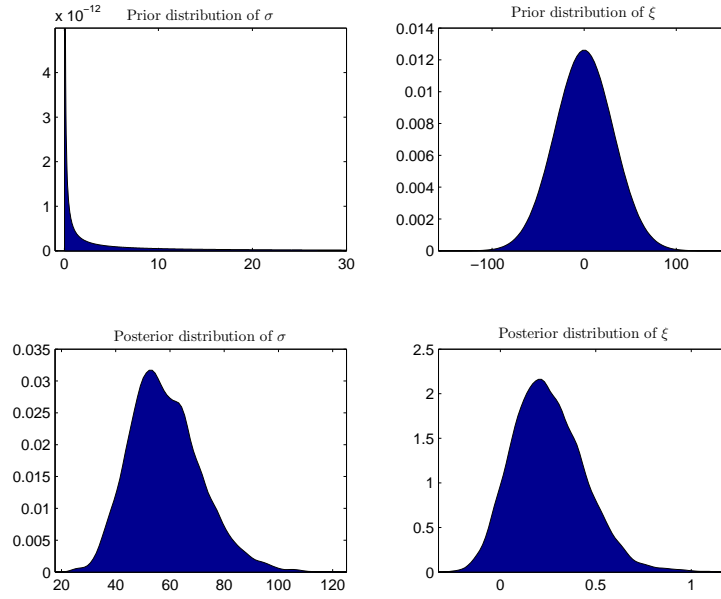
Figure B.14: (V066 TM DBM w/DRC) CASE 3: Prior and posterior distributions for the GP parameters

Threshold model using the diagnostic based method (DBM) for determining the threshold value - Figures and tables displaying the posterior parameters of the GP distribution

Figure B.15: (V066 TM DBM w/DRC) CASE 3: Diagnostic plots for the threshold model

Table B.3: (V066 TM DBM w/DRC): Percentiles for the posterior distributions of the GP parameters, sampled using a MCMC iteration scheme, for all three cases of prior distributions, calculated with DRC uncertainty

	Threshold model with DRC and u = 200					
	Percentiles for parameters in the GEV distribution					
	Normal		Neg-Gamma		Neg-Beta	
	σ	$\tilde{\xi}$	σ	$\tilde{\xi}$	σ	$\tilde{\xi}$
2.5%	37.67	-0.05	59.38	-0.14	59.74	-0.16
25%	49.23	0.12	69.32	-0.06	70.13	-0.07
50%	56.75	0.22	75.67	-0.03	76.51	-0.04
75%	64.90	0.34	82.76	-0.01	83.91	-0.02
97.5%	83.88	0.58	99.61	-0.00	100.85	-0.00
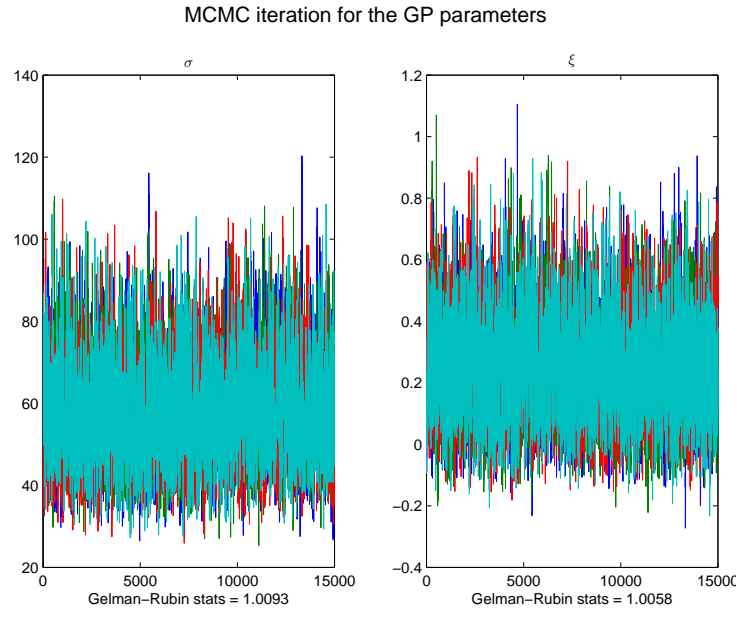
Figure B.16: (V066 TM DBM w/DRC) Case 1: Markov chain Monte Carlo simulation for the parameters in the GP distribution
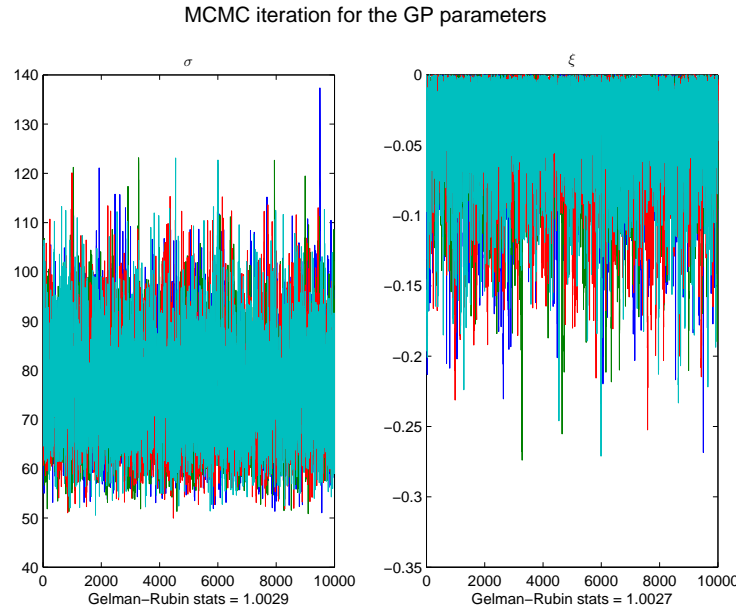
Figure B.17: (V066 TM DBM w/DRC) Case 2: Markov chain Monte Carlo simulation for the parameters in the GP distribution
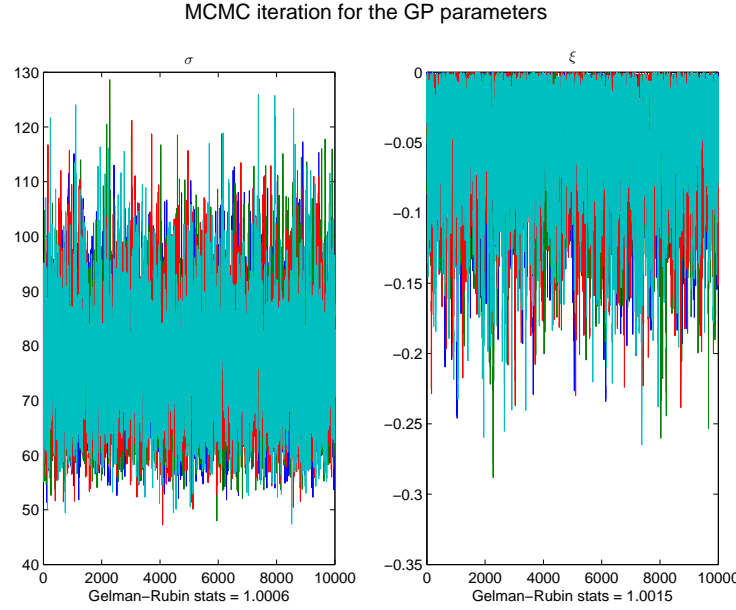
Figure B.18: (V066 TM DBM w/DRC) Case 3: Markov chain Monte Carlo simulation for the parameters in the GEV distribution

B.1.3. Threshold model using the fixed frequency method (FFM) for determining the threshold value

Threshold model using the fixed frequency method for choosing a threshold- Case 1: A normal prior distribution for the ξ parameter (TM FFM w/DRC C1)

In Case 1, the prior distribution for ξ was chosen to be a normal distribution with a large variance, making it non-informative prior. The prior distribution for $\tilde{\sigma}$ is a non-informative inv-χ^2 distribution. So, in this case, the GP parameters are not constricted in any way by their prior distributions. The prior and posterior distributions for the GP parameters are shown in Figure B.19.

The model seems to be a reasonably good fit for the data, with an Anderson-Darling p-value of $p_B = 0.46$. The diagnostic plots in Figure B.11 indicates that the model fits the data well. The probability plot is close to the unit diagonal for all the data points. Comparison between the probability density of the GP distribution and the histogram of the POTs indicate a good model fit. The data points are close to being linear in the quantile plot and they fit well in the return period plot.

Figure B.19: (V066 TM FFM w/DRC) CASE 1: Prior and posterior distributions for the GP parameters

Threshold model using the fixed frequency method for choosing a threshold- Case 2: A negative gamma prior distribution for the ξ parameter (TM FFM w/DRC C2)

In Case 2, the prior distribution for ξ was chosen to be a negative gamma distribution. It contains only negative values having majority of the mass of the distribution is close to the y-axis. The prior distribution for $\tilde{\sigma}$ is a non-informative inv-χ^2 distribution. Therefore, in this case, the posterior density of the shape parameter of the GP distribution is constricted to negative values only. The prior and posterior distributions for the GP parameters are shown in Figure B.21.

Figure B.13 shows a diagnostic plots for the model. The Anderson-Darling p-value of $p_B = 0.09$ raises concerns whether the model is adequate in emulating the data. The probability plot in Figure B.13 deviates from the unit diagonal for some of the data points. Comparison between the probability density of the GP distribution, and the histogram of the POTs, raises some doubt about the accuracy of the model since the number of values for each range represented by the bars in the Figure do not seem to gradually get fewer with increasing POT values, as would be expected, but instead there are for example more POTs having values around 550 then there are POTs with values around 500. The quantile plot deviates from linearity at the largest data point indicating an inadequate fit to the model. Furthermore, the data points deviate from the expected values in the return period plot indicating an inadequate fit to the model.
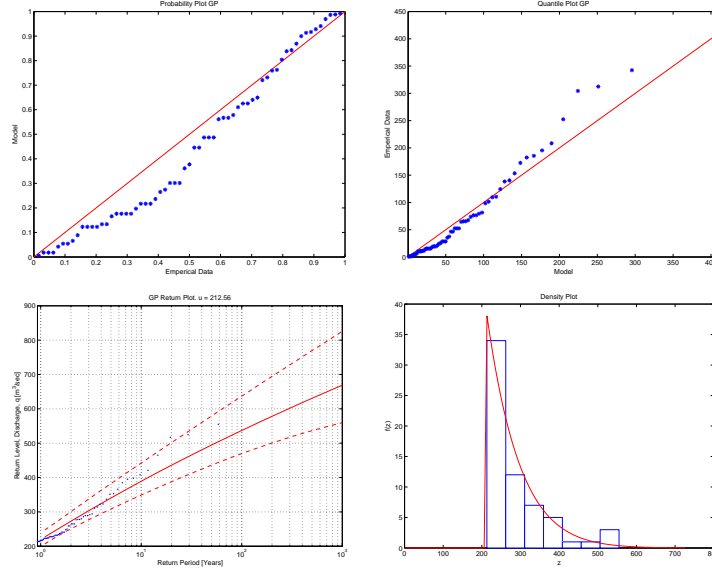
Figure B.20: (V066 TM FFM w/DRC) CASE 1: Diagnostic plots for the Threshold Model

Figure B.21: (V066 TM FFM w/DRC) CASE 2: Prior and posterior distributions for the GP parameters
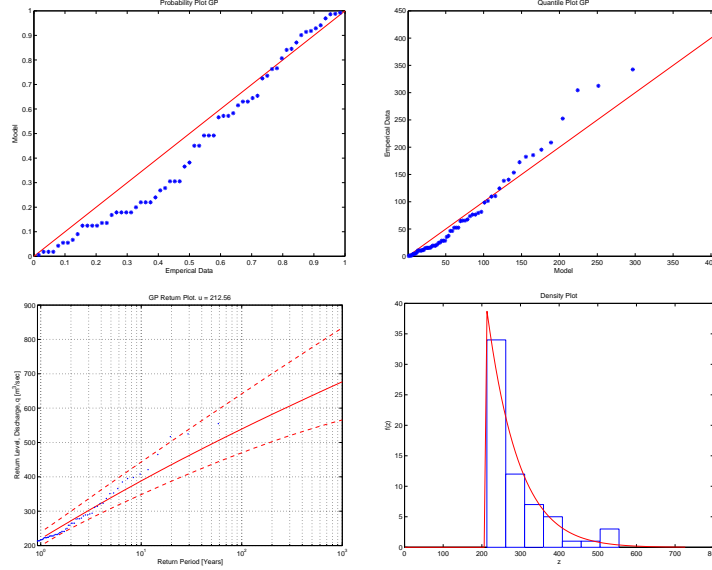
Figure B.22: (V066 TM FFM w/DRC) CASE 2: Diagnostic plots for the Threshold Model

Threshold model using the fixed frequency method for choosing a threshold- Case 3: A negative beta prior distribution for the ξ parameter (TM FFM w/DRC C3)

In Case 3, the prior distribution for ξ was chosen to be a negative beta distribution. It is a uniform distribution containing values on the interval $[-1; 0]$ The prior distribution for $\tilde{\sigma}$ is a non-informative inv-χ^2 distribution. Therefore, in this case, the posterior density of the shape parameter of the GEV distribution is constricted to negative values only. The prior and posterior distributions for the GP parameters are shown in Figure B.23.

Figure B.15 shows a diagnostic plots for the model for case 3, when the prior distribution for the ξ parameter is a negative beta distribution. The results are almost identical to case 2.

The Anderson-Darling p-value of $p_B = 0.09$ raises concerns whether the model is adequate in emulating the data. The probability plot in Figure B.15 deviates from the unit diagonal for few of the data points. Comparison between the probability density of the GP distribution and the histogram of the POTs, raises some doubt about the accuracy of the model since the number of values for each range represented by the bars in the figure do not seem to gradually get fewer with increasing POT values, as would be expected, but instead there are for example more POTs having values around 550 then there are POTs with values around 500. The quantile plot deviates from linearity at the largest data point indicating an inadequate fit to

Figure B.23: (V066 TM FFM w/DRC) CASE 3: Prior and posterior distributions for the GP parameters

the model. Furthermore, the data points deviate from the expected values in the return period plot indicating an inadequate fit to the model.

Threshold model using the fixed frequency method (FFM) for determining the threshold value - Figures and tables displaying the posterior parameters of the GP distribution

Figure B.24: (V066 TM FFM w/DRC) CASE 3: Diagnostic plots for the Threshold Model

Table B.4: (V066 TM FFM w/DRC): Percentiles for the posterior distributions of the GP parameters, sampled using a MCMC iteration scheme, for all three cases of prior distributions, calculated with DRC uncertainty

	Threshold model with DRC and u = 213					
	Percentiles for parameters in the GEV distribution					
	Normal		Neg-Gamma		Neg-Beta	
	σ	$\tilde{\xi}$	σ	$\tilde{\xi}$	σ	$\tilde{\xi}$
2.5%	36.73	-0.06	60.33	-0.16	60.52	-0.18
25%	48.94	0.13	70.89	-0.07	71.79	-0.08
50%	56.95	0.24	77.62	-0.04	78.87	-0.05
75%	65.85	0.37	85.31	-0.02	87.10	-0.02
97.5%	86.71	0.65	103.42	-0.00	106.32	-0.00
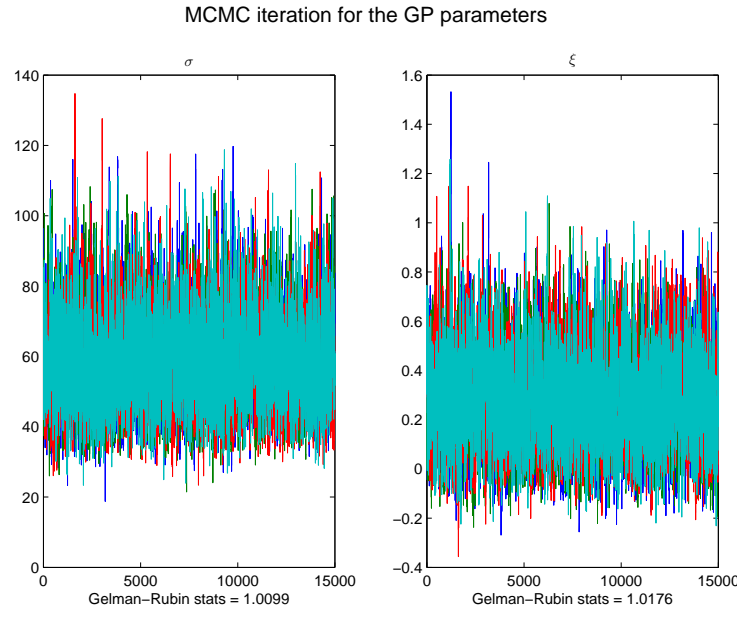
Figure B.25: (V066 TM FFM w/DRC) Case 1: Markov chain Monte Carlo simulation for the parameters in the GP distribution
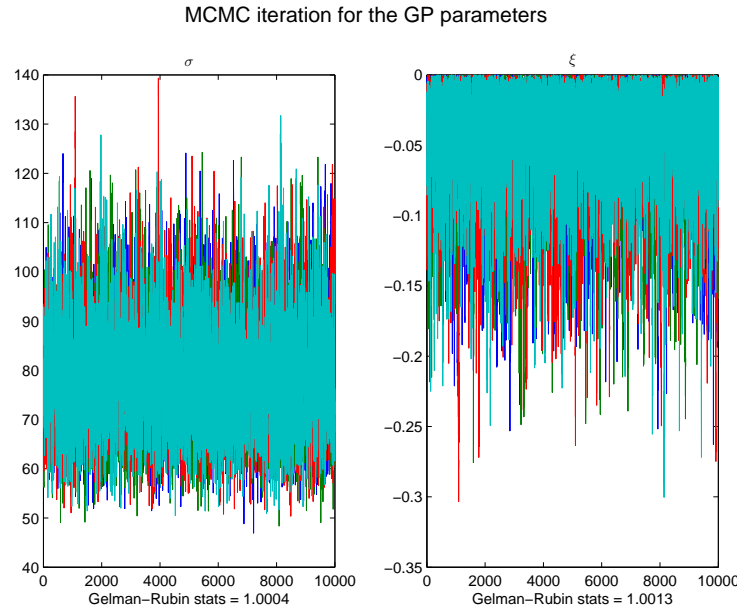
Figure B.26: (V066 TM FFM w/DRC) Case 2: Markov chain Monte Carlo simulation for the parameters in the GP distribution

MCMC iteration for the GP parameters

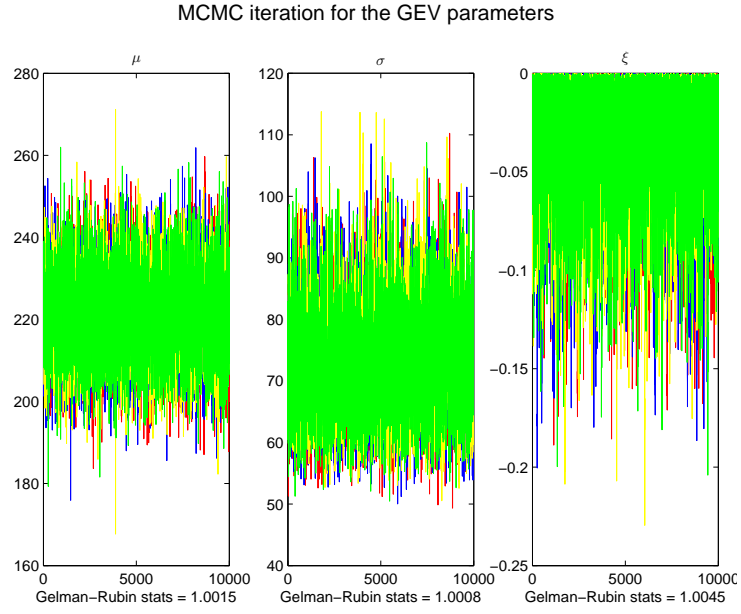*Figure B.27:* (V066 TM FFM w/DRC) Case 3: Markov chain Monte Carlo simulation for the parameters in the GEV distribution

B.2. V066: Without discharge rating curve uncertainty

B.2.1. Block maxima model

Table B.5: (V066 BM w/o DRC): Percentiles for the posterior distributions of the GEV parameters, sampled using a MCMC iteration scheme, for all three cases of prior distributions, calculated without DRC uncertainty

	Block Extrema without DRC								
	Percentiles for parameters in the GEV distribution								
	Normal			Neg-Gamma			Neg-Beta		
	μ	σ	ξ	μ	σ	ξ	μ	σ	ξ
2.5%	197.25	53.38	-0.04	202.20	59.05	-0.11	202.14	59.02	-0.13
25%	208.86	61.64	0.08	214.78	67.25	-0.05	214.92	67.55	-0.06
50%	214.73	66.65	0.15	221.57	72.37	-0.03	221.65	72.95	-0.03
75%	221.07	72.20	0.22	228.51	78.04	-0.01	228.63	78.94	-0.01
97.5%	233.77	84.47	0.37	241.76	90.82	-0.00	242.46	92.10	-0.00
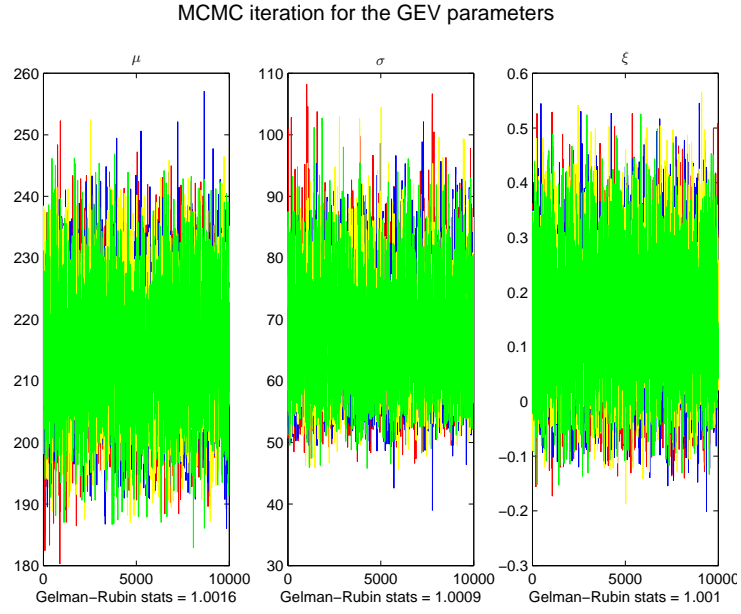
Figure B.28: (V066 BM w/o DRC) Case 1: Markov chain Monte Carlo simulation for the parameters in the GEV distribution
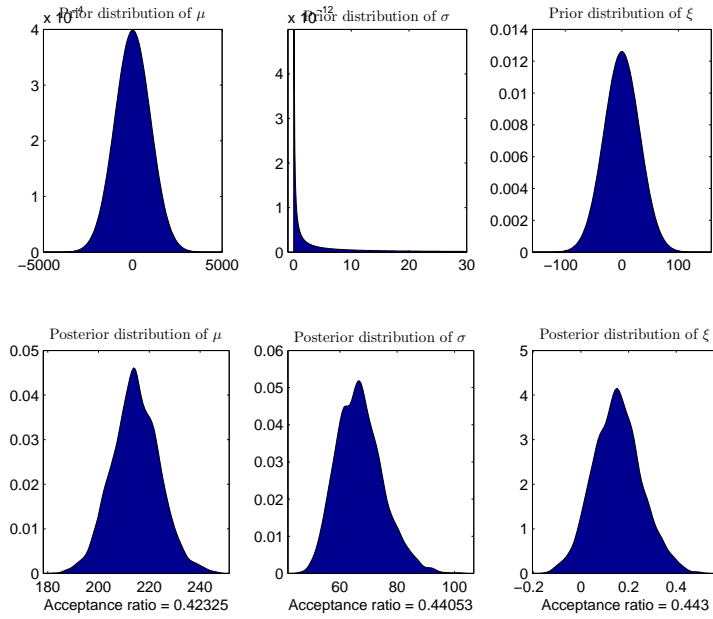
Figure B.29: (V066 BM w/o DRC) CASE 1: Prior and posterior distributions for the GEV parameters
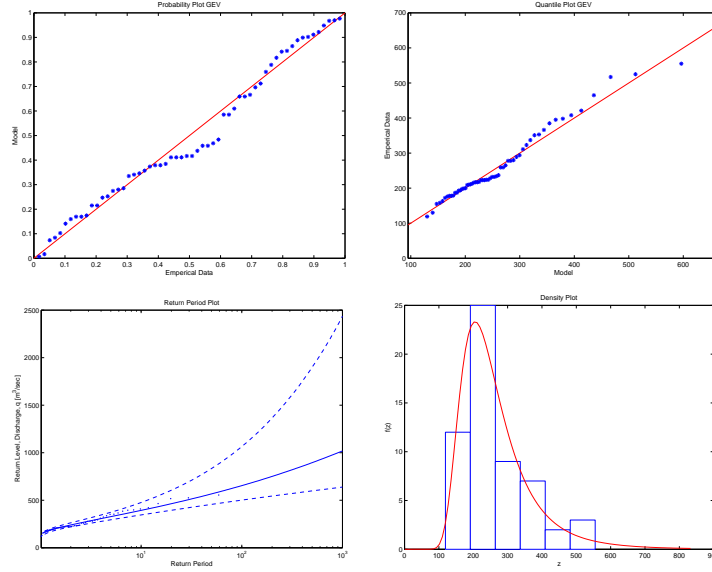
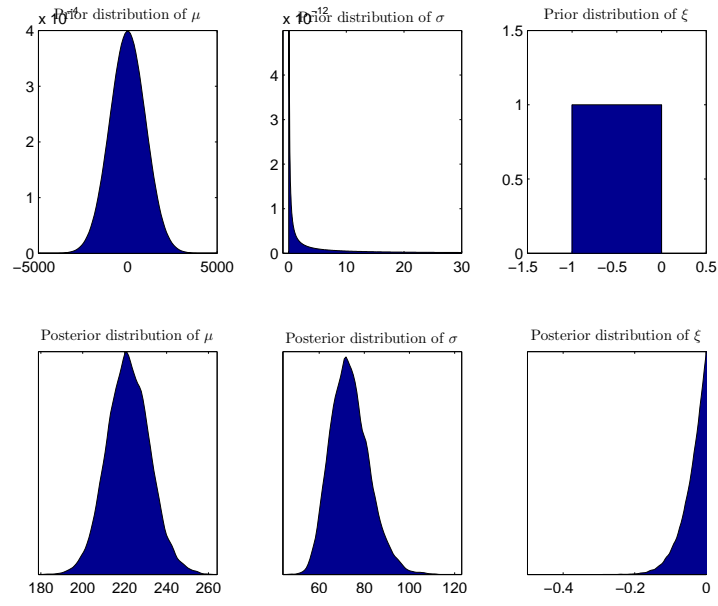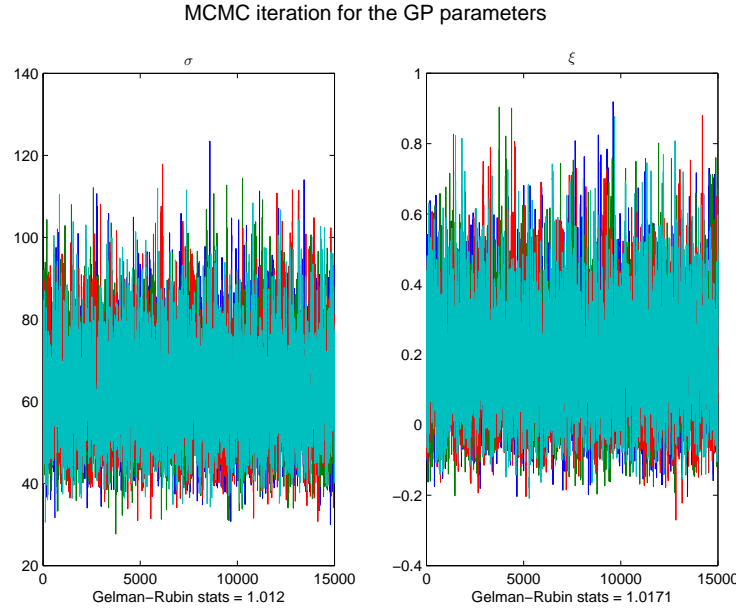*Figure B.30:* (V066 BM w/o DRC) CASE 1: Diagnostic plots for the block maxima model

B.2.2. Threshold model using the diagnostic based method (DBM) for determining the threshold value

Table B.6: (V066 TM DBM w/o DRC): Percentiles for the posterior distributions of the GP parameters, sampled using a MCMC iteration scheme, for all three cases of prior distributions, calculated without DRC uncertainty

	Threshold model with DRC and u = 200					
	Percentiles for parameters in the GEV distribution					
	Normal		Neg-Gamma		Neg-Beta	
	σ	$\tilde{\xi}$	σ	$\tilde{\xi}$	σ	$\tilde{\xi}$
2.5%	42.55	-0.07	61.48	-0.14	62.18	-0.16
25%	54.21	0.07	71.26	-0.06	72.11	-0.08
50%	61.70	0.17	77.17	-0.03	78.56	-0.04
75%	69.95	0.28	84.13	-0.01	85.79	-0.02
97.5%	88.22	0.51	100.06	-0.00	102.27	-0.00

Figure B.31: (V066 BM w/o DRC) Case 2: Markov chain Monte Carlo simulation for the parameters in the GEV distribution
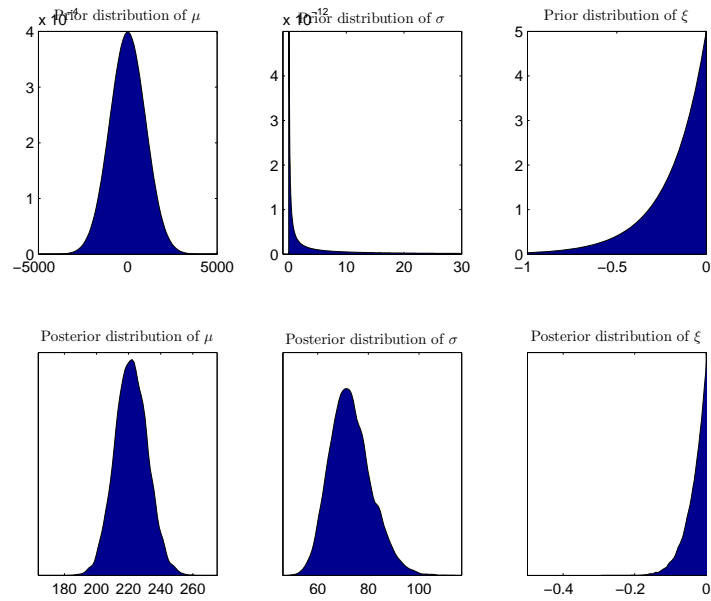
Figure B.32: (V066 BM w/o DRC) CASE 2: Prior and posterior distributions for the GEV parameters
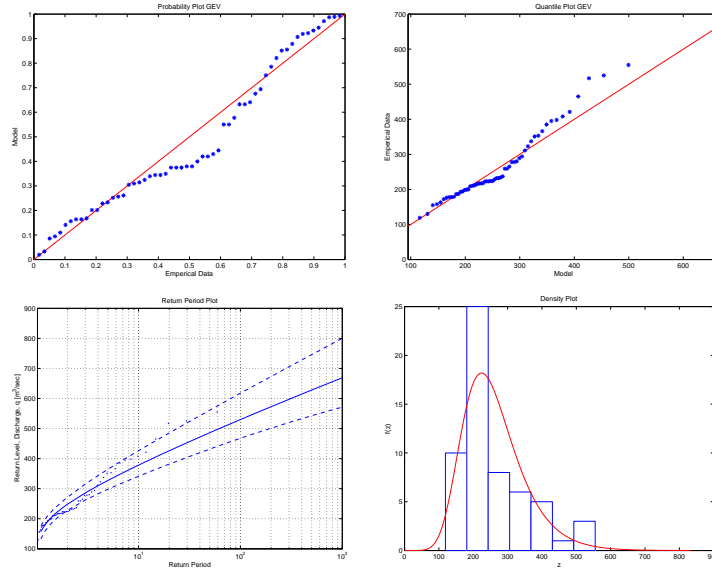
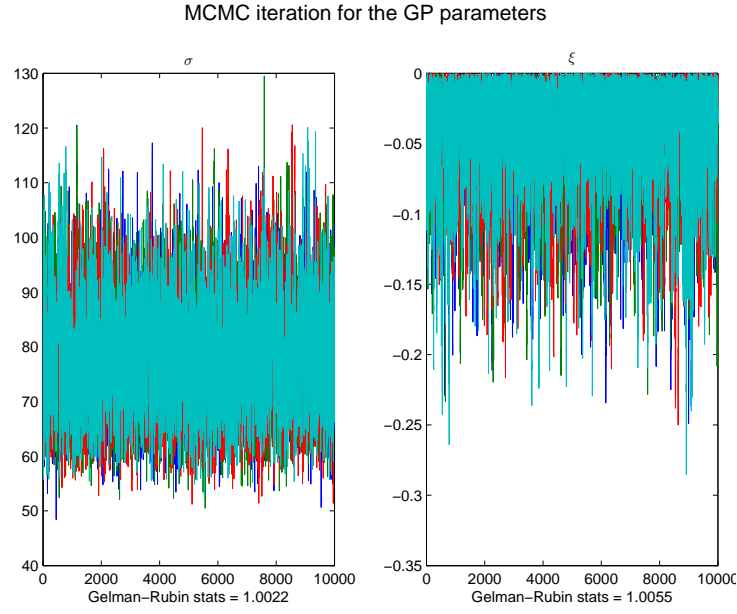*Figure B.33:* (V066 BM w/o DRC) CASE 2: Diagnostic plots for the block maxima model
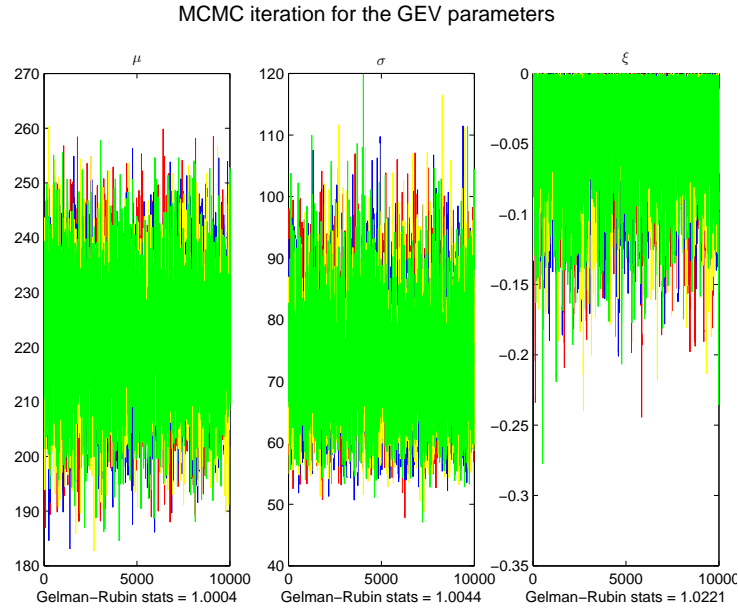
Figure B.34: (V066 BM w/o DRC) Case 3: Markov chain Monte Carlo simulation for the parameters in the GEV distribution

Figure B.35: (V066 BM w/o DRC) CASE 3: Prior and posterior distributions for the GEV parameters
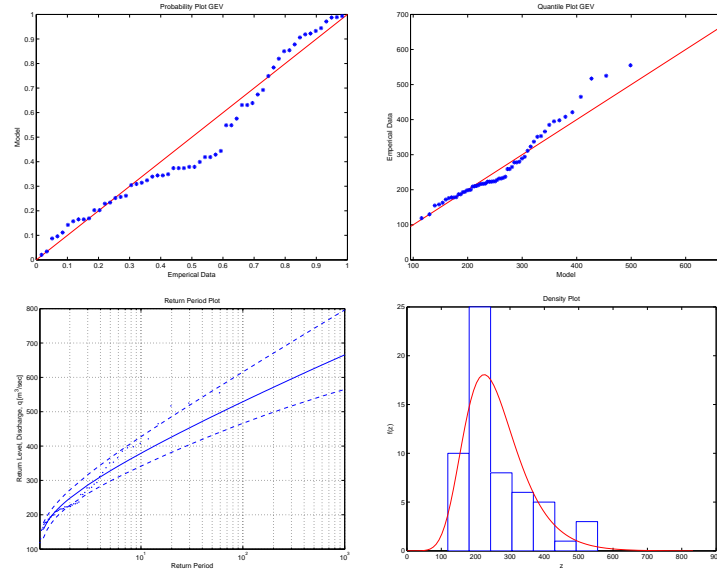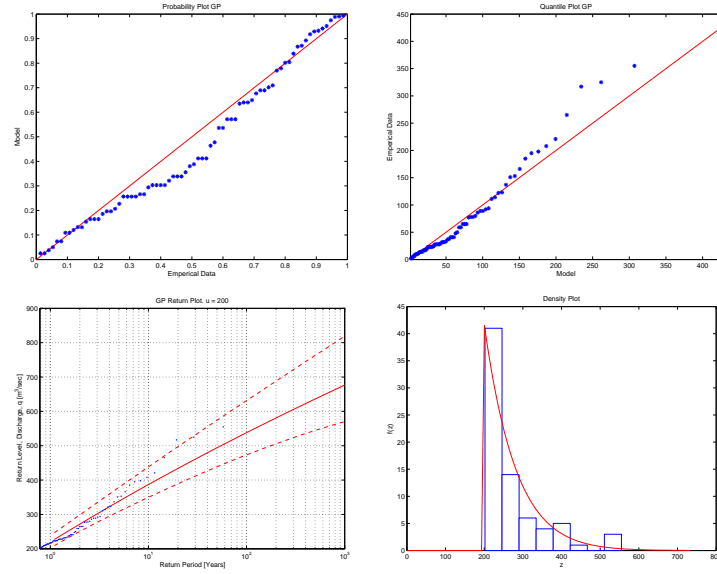

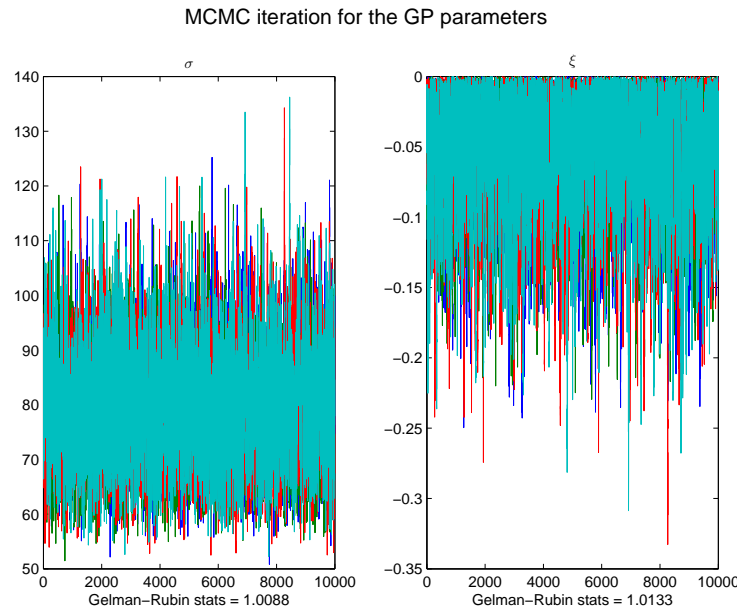*Figure B.36:* (V066 BM w/o DRC) CASE 3: Diagnostic plots for the block maxima model

Figure B.37: (V066 TM DBM w/o DRC) Case 1: Markov chain Monte Carlo simulation for the parameters in the GP distribution
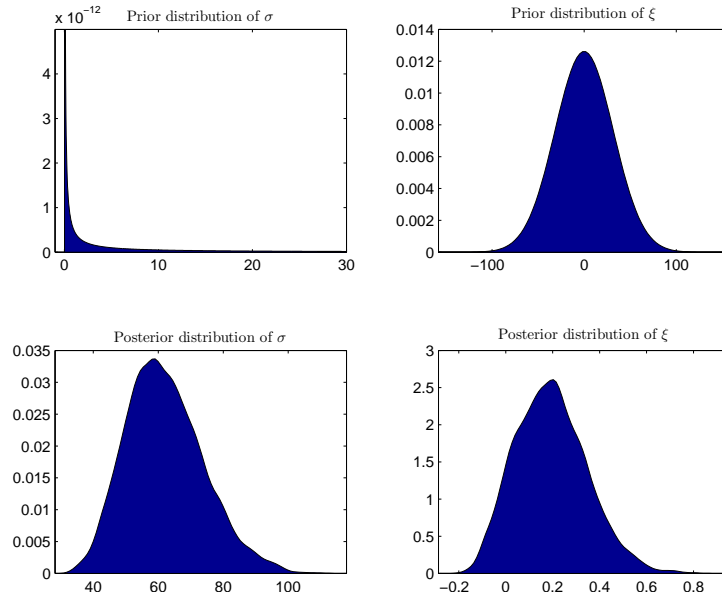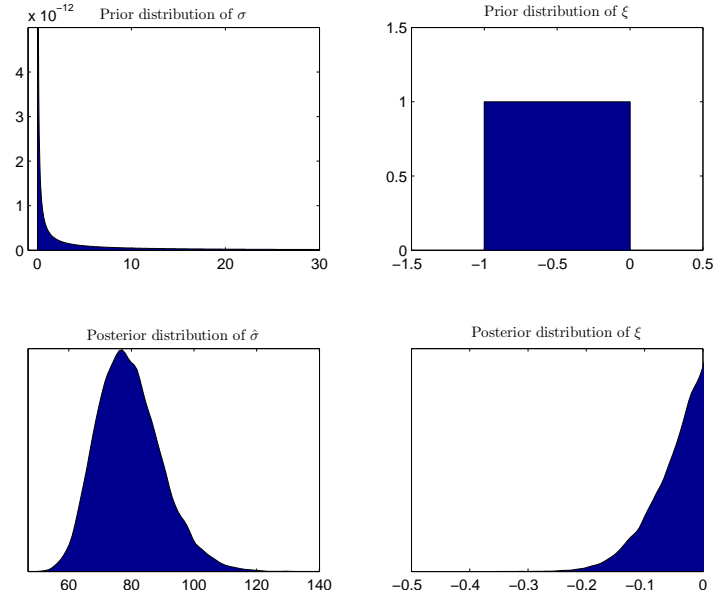

Figure B.38: (V066 TM DBM w/o DRC) CASE 1: Prior and posterior distributions for the GP parameters
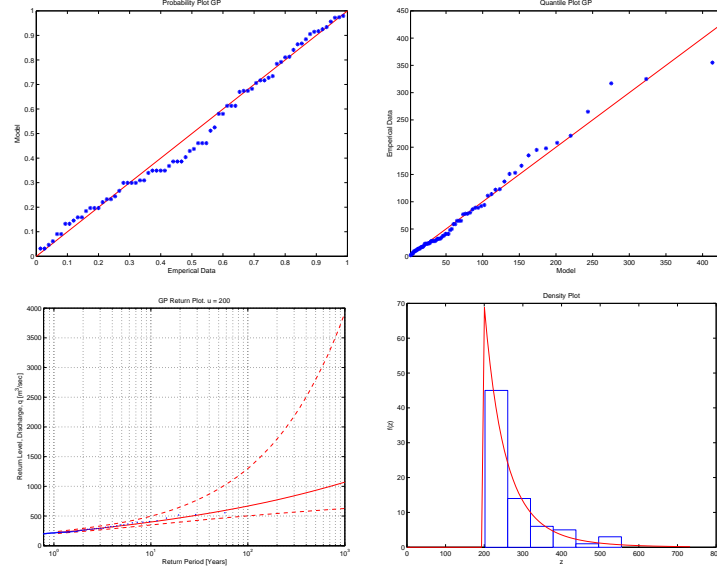
Figure B.39: (V066 TM DBM w/o DRC) CASE 1: Diagnostic plots for the threshold model

B.2.3. Threshold model using the fixed frequency method (FFM) for determining the threshold value

Table B.7: (V066 TM FFM w/o DRC): Percentiles for the posterior distributions of the GP parameters, sampled using a MCMC iteration scheme, for all three cases of prior distributions, calculated without DRC uncertainty

|	Threshold model without DRC and u = 213					
	Percentiles for parameters in the GP distribution					
	Normal		Neg-Gamma		Neg-Beta	
	σ	$\tilde{\xi}$	σ	$\tilde{\xi}$	σ	$\tilde{\xi}$
2.5%	34.99	-0.05	59.79	-0.15	60.14	-0.18
25%	47.33	0.14	70.27	-0.07	70.89	-0.08
50%	55.38	0.26	76.90	-0.03	77.75	-0.04
75%	64.51	0.39	84.04	-0.02	85.61	-0.02
97.5%	84.95	0.68	101.09	-0.00	104.36	-0.00

Figure B.40: (V066 TM DBM w/o DRC) Case 2: Markov chain Monte Carlo simulation for the parameters in the GP distribution
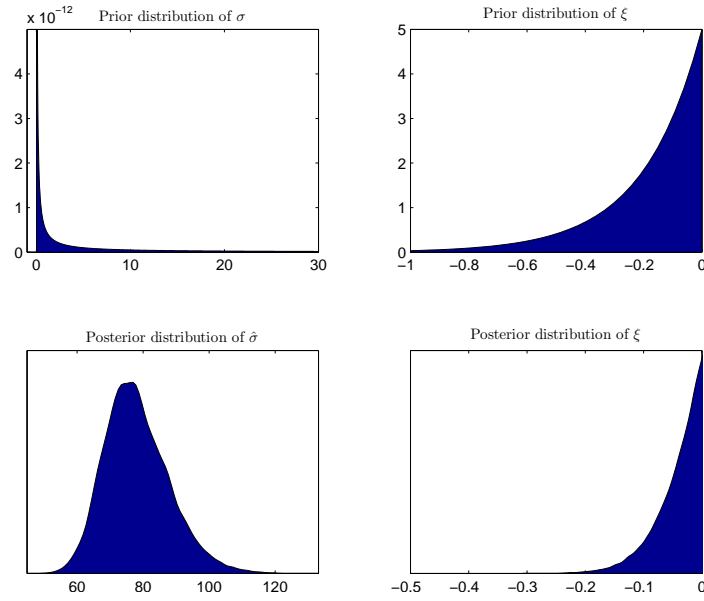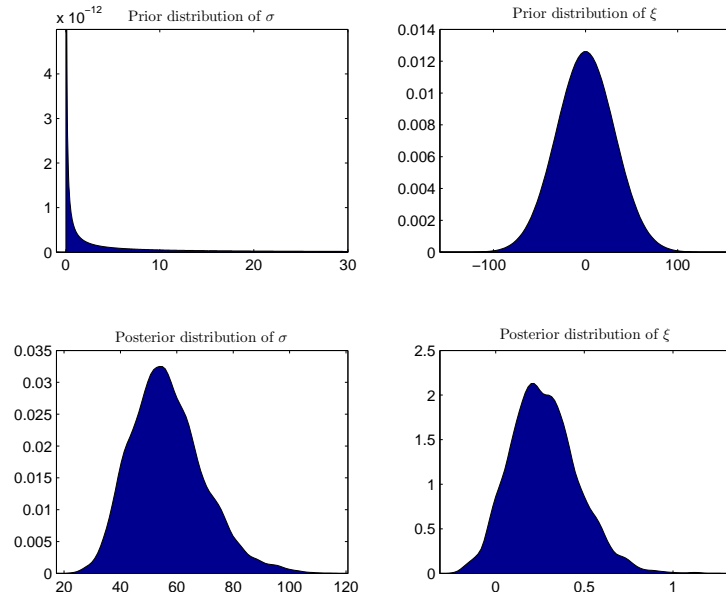

Figure B.41: (V066 TM DBM w/o DRC) CASE 2: Prior and posterior distributions for the GP parameters
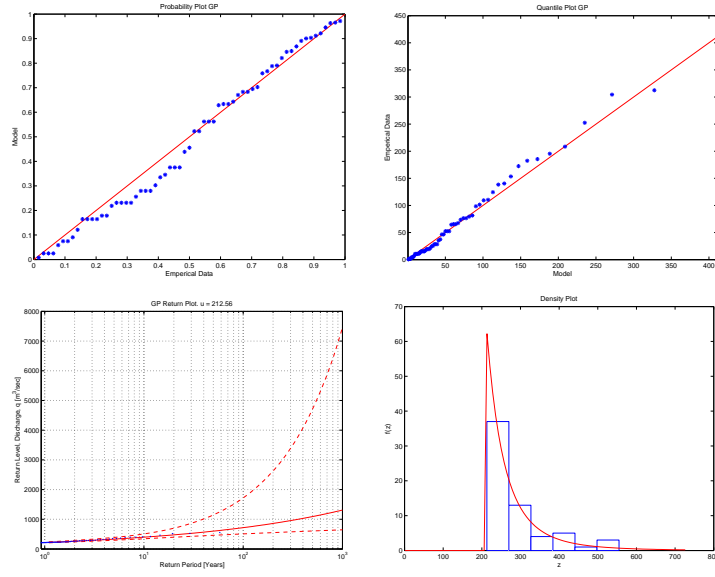
Figure B.42: (V066 TM DBM w/o DRC) CASE 2: Diagnostic plots for the threshold model

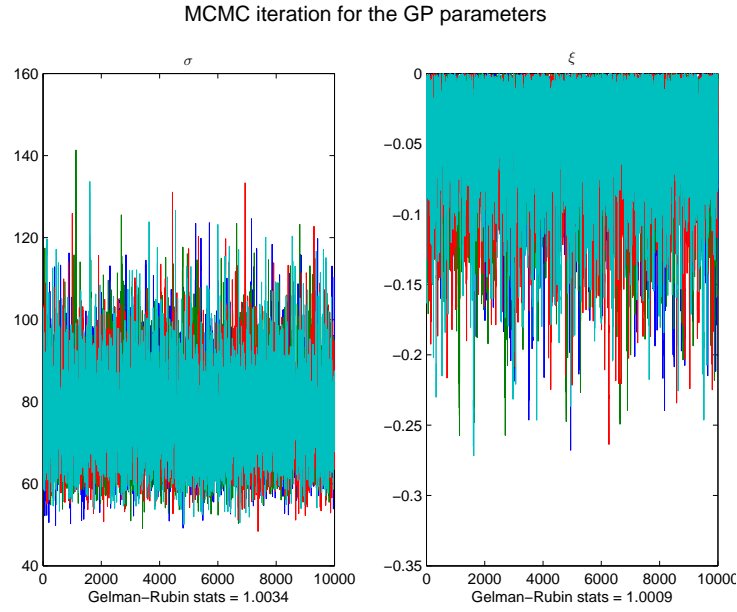*Figure B.43:* (V066 TM DBM w/o DRC) Case 3: Markov chain Monte Carlo simulation for the parameters in the GP distribution

Figure B.44: (V066 TM DBM w/o DRC) CASE 3: Prior and posterior distributions for the GP parameters
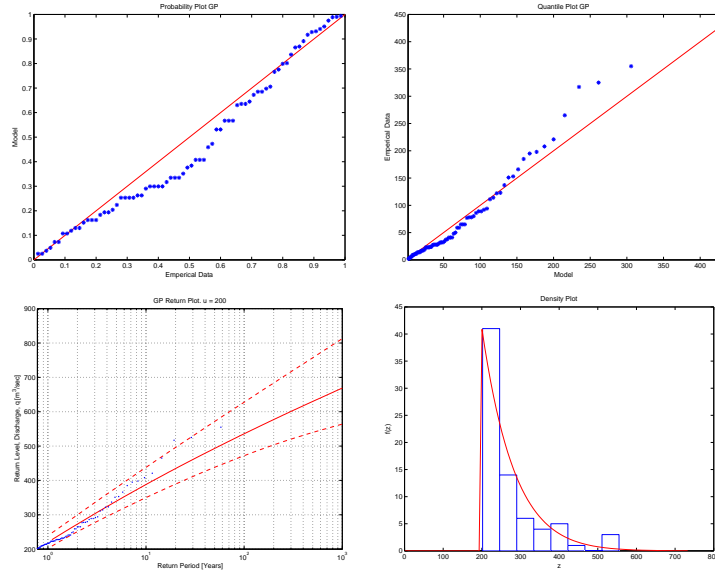
Figure B.45: (V066 TM DBM w/o DRC) CASE 3: Diagnostic plots for the threshold model
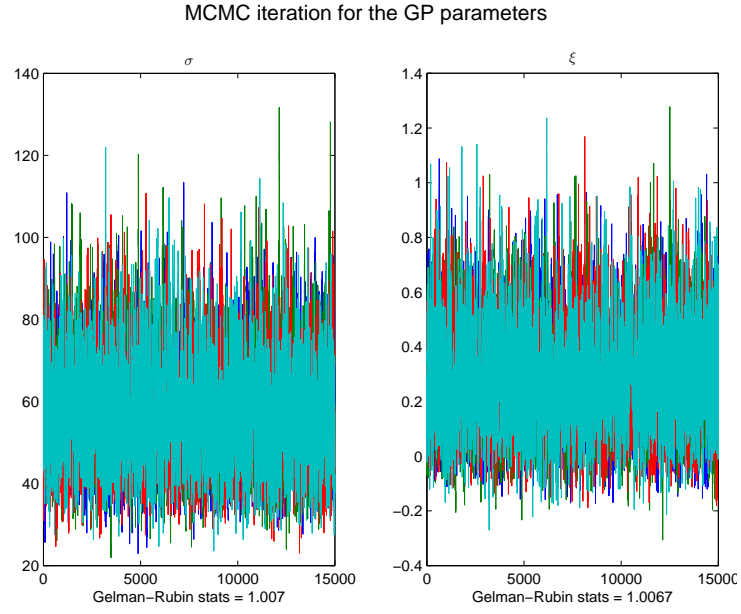
Figure B.46: (V066 TM FFM w/o DRC) Case 1: Markov chain Monte Carlo simulation for the parameters in the GP distribution
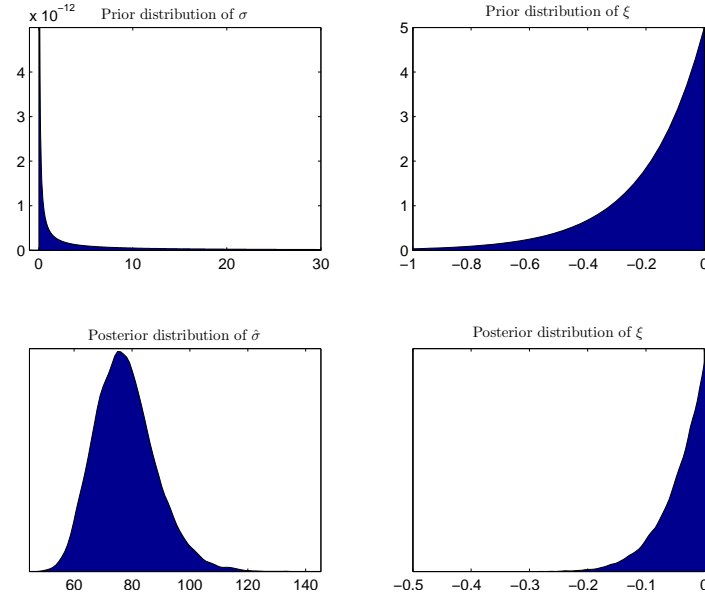

Figure B.47: (V066 TM FFM w/o DRC) CASE 1: Prior and posterior distributions for the GP parameters
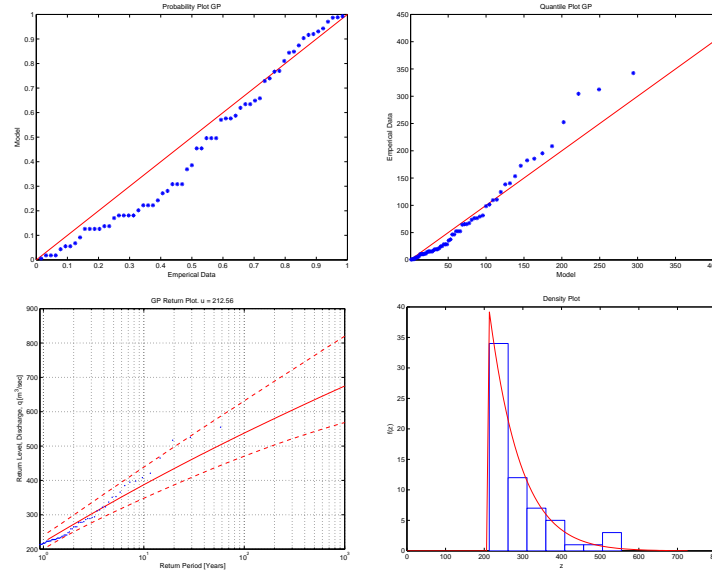
Figure B.48: (V066 TM FFM w/o DRC) CASE 1: Diagnostic plots for the threshold model

Figure B.49: (V066 TM FFM w/o DRC) Case 2: Markov chain Monte Carlo simulation for the parameters in the GP distribution

Figure B.50: (V066 TM FFM w/o DRC) CASE 2: Prior and posterior distributions for the GP parameters

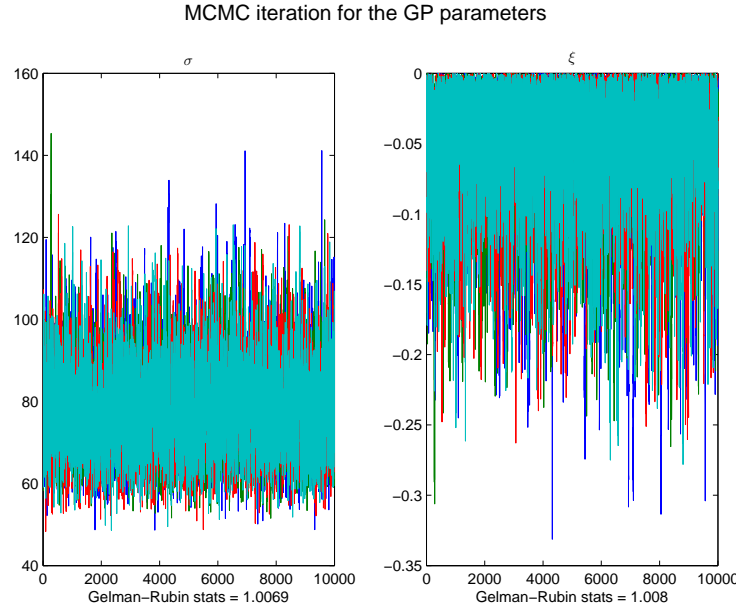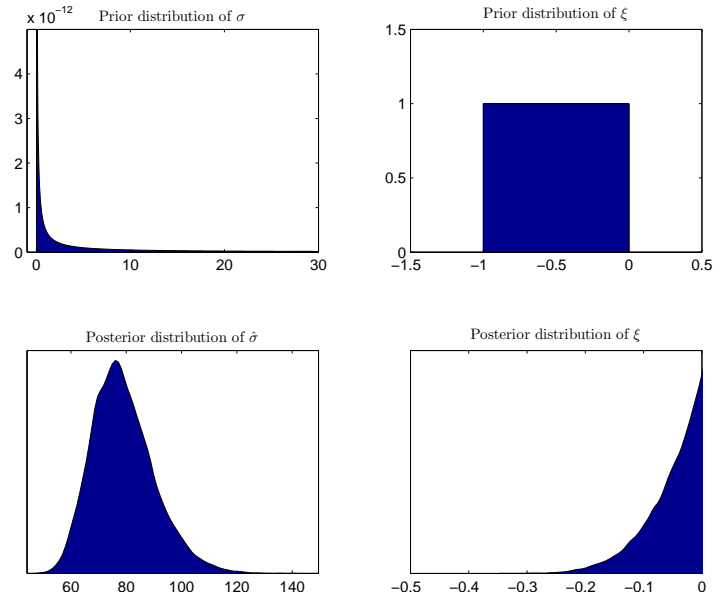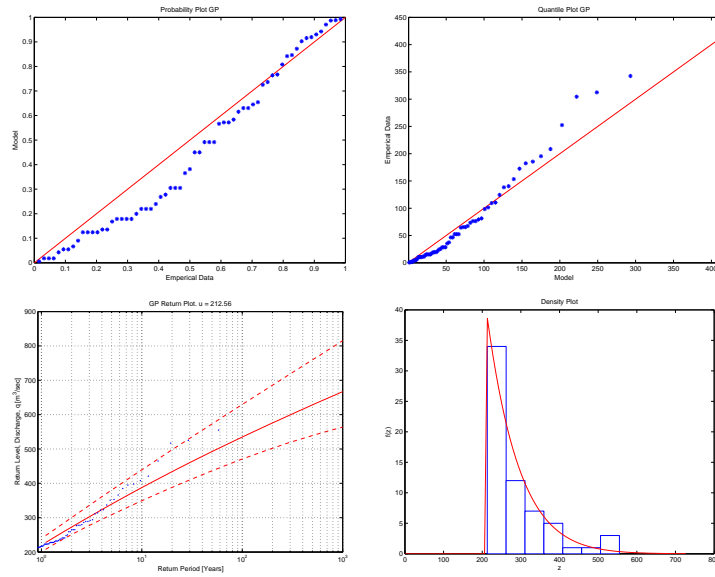*Figure B.51:* (V066 TM FFM w/o DRC) CASE 2: Diagnostic plots for the threshold model

MCMC iteration for the GP parameters

Figure B.52: (V066 TM FFM w/o DRC) Case 3: Markov chain Monte Carlo simulation for the parameters in the GP distribution

Figure B.53: (V066 TM FFM w/o DRC) CASE 3: Prior and posterior distributions for the GP parameters

195

Figure B.54: (V066 TM FFM w/o DRC) CASE 3: Diagnostic plots for the threshold model

C. More details on the flood analysis for Sanda

In this appendix, figures and tables that are relevant to the research but were not displayed in the main text of the paper, are displayed. That includes probability plots, quantile plots and density plots for all cases of prior distributions. The prior and posterior densities of all the parameters in the GEV and GP distributions are also displayed for all cases. The appendix also includes the sampled Markov chain Monte Carlo (MCMC) chains, used to construct the posterior distributions for the parameters of both the generalized extreme value distribution (GEV) and the generalized Pareto (GP) distribution. The samples are displayed both in figures, and in tables as quantiles for all the models with and without the inclusion discharge rating curve uncertainty. The histogram of the prior and posterior distribution and the diagnostic plots for the models are shown for all models without the inclusion of discharge rating curve uncertainty.

Table C.1 shows a list of abbreviations regarding the following figures and tables. Every figure and table in the appendix is marked with some of these abbreviations and that explains which river the data belongs to and what kind of models were used to generate the results. For example, the text *(V026 BM w/DRC) Case 2* in the caption of a figure or a table, indicates that the data displayed comes from the river Sanda (V026), a block maxima model was used (BM) with a neg-gamma prior distribution for the shape parameter (Case 2), and the uncertainty in the discharge rating curve was taken into account in the calculations (w/DRC).

Table C.1: Abbreviations used to explain the origin of the data used to generate figures and tables

V026:	The river Sanda i Thistilfjordur: 26 is the number of the gauging station measuring the data
Case 1:	The shape parameter, ξ, was sampled using a normal prior distribution
Case 2:	The shape parameter, ξ, was sampled using a neg-gamma prior distribution
Case 3:	The shape parameter, ξ, was sampled using a neg-beta prior distribution
BM:	A block maxima model
TM DBM:	A threshold model using the diagnostic based method for determining the threshold value
TM FFM:	A threshold model using the fixed frequency method for determining the threshold value
w/DRC:	A discharge rating curve uncertainty was taken into account in the calculations
w/o DRC:	A discharge rating curve uncertainty was not taken into account in the calculations

C.1. V026: With discharge rating curve uncertainty

C.1.1. Block maxima model

Block Maxima Model - Case 1: A normal prior distribution for the ξ parameter (BM w/DRC C1)

In Case 1, the prior distribution for ξ was chosen to be a normal distribution with a large variance, making it non-informative prior. The prior distribution for σ is a non-informative inv-χ^2 distribution and the prior distribution for μ is a normal distribution with large variance making it non-informative. So, in this case, the GEV parameters are not constricted in any way by their prior distributions. See further details on the prior distributions in Section 3.3.2. The construction of the posterior distribution of all the parameters is discussed in Section 3.3.3. The prior and posterior distributions for the GEV parameters are shown in Figure C.1

The simulated chains of posterior distributions for the GEV parameters are used to model the extreme behavior of the river. The simulated chains of the posterior
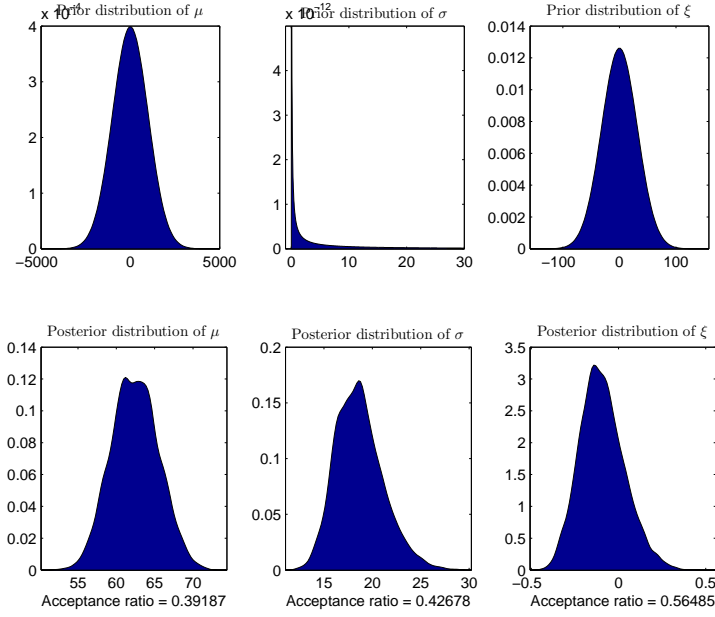
Figure C.1: (V026 BM w/DRC) CASE 1: Prior and posterior distributions for the GEV parameters

distributions of the parameters are shown in Figure C.7 and their quantiles are shown in Table C.2.

Figure C.2 shows the return period plot for Sanda as well as the quantile plot, the probability plot and the density plot. The Anderson-Darling p-value and the diagnostic plots in Figure C.2 are evaluated to check the validity of the model. The methods used for the model validation are discussed in Section 2.2.2.

The model seems to be a good fit for the data, having an Anderson-Darling p-value of $p_B = 0.61$. The diagnostic plots in Figure C.2 also indicate that the model fits the data well. The annual maximum value points on the probability plot all lie close to the unit diagonal and the points are close to linear on the quantile plot, which is both an indication to a good fit. Comparison between the probability density of the GEV distribution and the histogram of the POTs indicates a good model fit. Plotting the annual maximum values on the return level plot also seem to indicate that the model fits the data well, since all the values are inside the 95% posterior interval of the return levels.
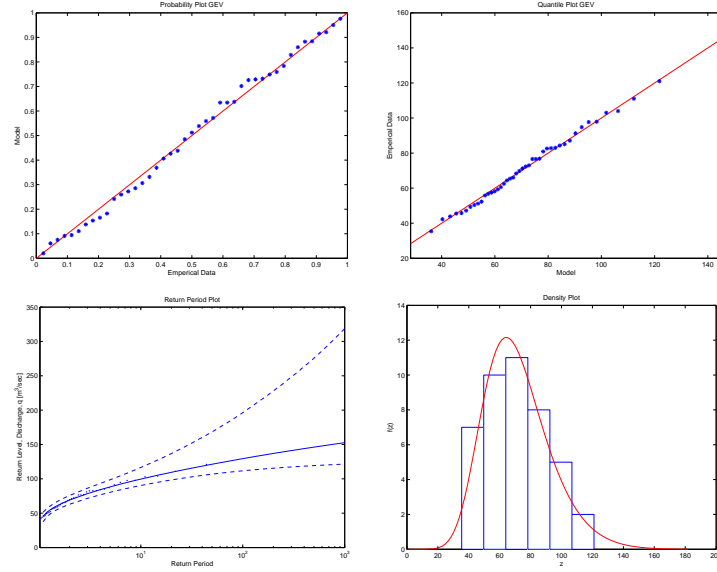
Figure C.2: (V026 BM w/DRC) CASE 1: Diagnostic plots for the block maxima model

Block Maxima Model - Case 2: A negative gamma prior distribution for the ξ parameter (BM w/DRC C2)

In Case 2, the prior distribution for ξ was chosen to be a negative gamma distribution. It contains only negative values having majority of the mass of the distribution is close to the y-axis. Therefore, in this case, the posterior density of the shape parameter of the GEV distribution is constricted to negative values only. The prior and posterior distributions for the GEV parameters are shown in Figure (C.3).

The simulated chains of the posterior distributions of the parameters are shown in Figure C.8 and their quantiles are shown in Table C.2.

Figure C.4 shows the return period plot for Sanda as well as the quantile plot, the probability plot and the density plot. The model seems to be a good fit for the data, having an Anderson-Darling p-value of $p_B = 0.63$. The diagnostic plots in Figure C.4 also indicate that the model fits the data reasonably well. The annual maximum value points on the probability plot all lie close to the unit diagonal and the points are close to linear on the quantile plot. Comparison between the probability density of the GP distribution and the histogram of the POTs indicates a good model fit. Plotting the annual maximum values on the return level plot also seem to indicate that the model fits the data well.
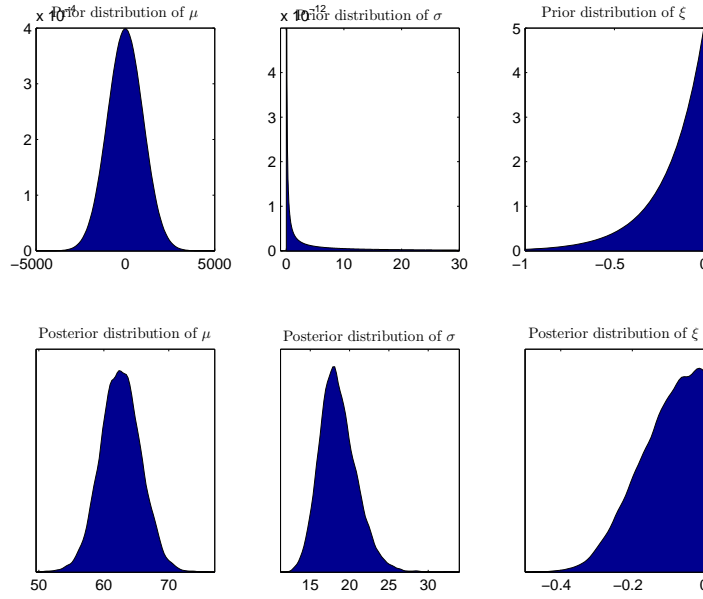
Figure C.3: (V026 BM w/DRC) CASE 2: Prior and posterior distributions for the GEV
   parameters

Block Maxima Model - Case 3: A negative beta prior distribution for the ξ parameter (BM w/DRC C3)

In Case 3, the prior distribution for ξ was chosen to be a negative beta distribution. It is a uniform distribution containing values on the interval $[-1; 0]$ Therefore, in this case, the posterior density of the shape parameter of the GEV distribution is constricted to negative values only. The prior and posterior distributions for the GEV parameters are shown in Figure (C.5).

The simulated chains of the posterior distributions of the parameters are shown in Figure C.9 and their quantiles are shown in Table C.2.

Figure C.6 shows the return period plot for Sanda as well as the quantile plot, the probability plot and the density plot.

The model seems to be a good fit for the data, having an Anderson-Darling p-value of $p_B = 0.60$. The diagnostic plots in Figure C.6 also indicate that the model fits the data well. The annual maximum values on the probability plot all lie close to the unit diagonal and the points are close to linear on the quantile plot, both indicating a good model fit. Comparison between the probability density of the GEV distribution and the histogram of the POTs indicates a good model fit. Plotting the annual maximum values on the return level plot also seem to indicate that the model fits the data well, since all the values are inside the 95% posterior interval of the
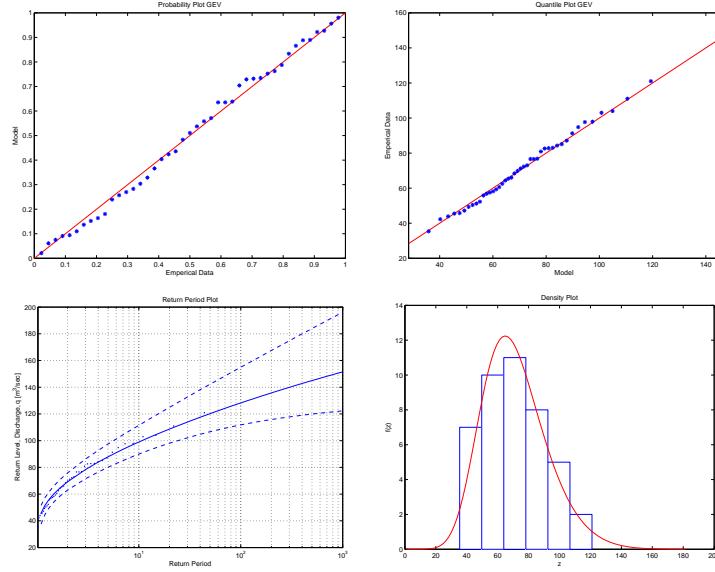
Figure C.4: (V026 BM w/DRC) CASE 2: Diagnostic plots for the block maxima model
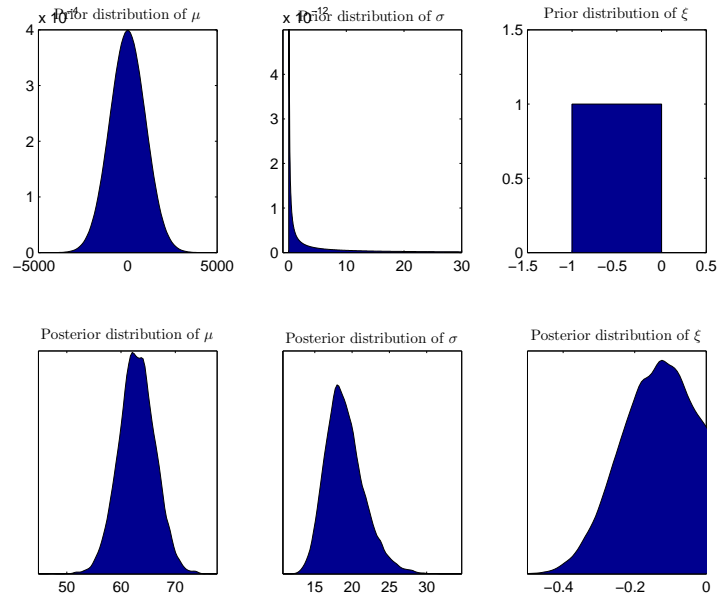

Figure C.5: (V026 BM w/DRC) CASE 3: Prior and posterior distributions for the GEV
   parameters

return levels.

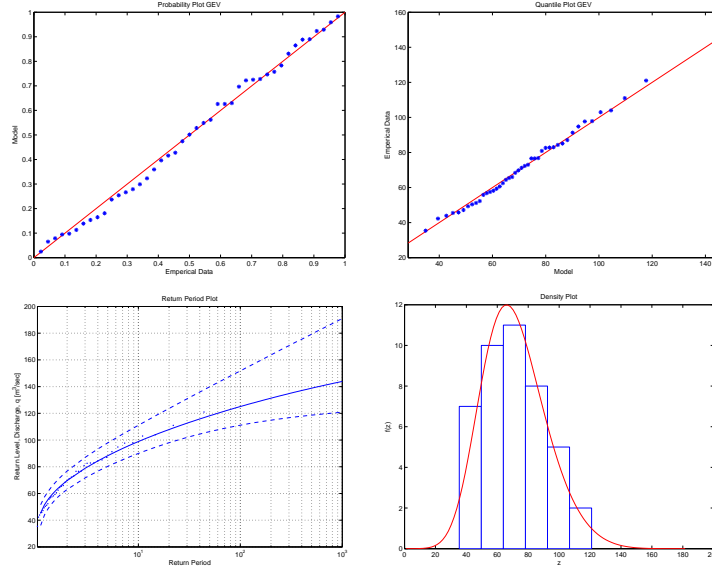## Block Maxima Model - Figures and tables displaying the posterior parameters of the GEV distribution

*Figure C.6:* (V026 BM w/DRC) CASE 3: Diagnostic plots for the block maxima model

Table C.2: (V026 BM w/DRC): Percentiles for the posterior distributions of the GEV parameters, sampled using a MCMC iteration scheme, for all three cases of prior distributions, calculated with DRC uncertainty

	Block Extrema with DRC								
	Percentiles for parameters in the GEV distribution								
	Normal			Neg-Gamma			Neg-Beta		
	μ	σ	ξ	μ	σ	ξ	μ	σ	ξ
2.5%	56.67	14.38	-0.32	56.55	14.56	-0.30	56.48	14.79	-0.35
25%	60.38	16.87	-0.18	60.52	16.92	-0.17	60.77	17.24	-0.21
50%	62.42	18.42	-0.10	62.57	18.32	-0.10	62.92	18.74	-0.14
75%	64.48	20.16	-0.01	64.64	19.98	-0.05	65.14	20.54	-0.08
97.5%	68.49	24.16	0.19	68.65	23.70	-0.00	69.37	24.93	-0.01

C. More details on the flood analysis for Sanda
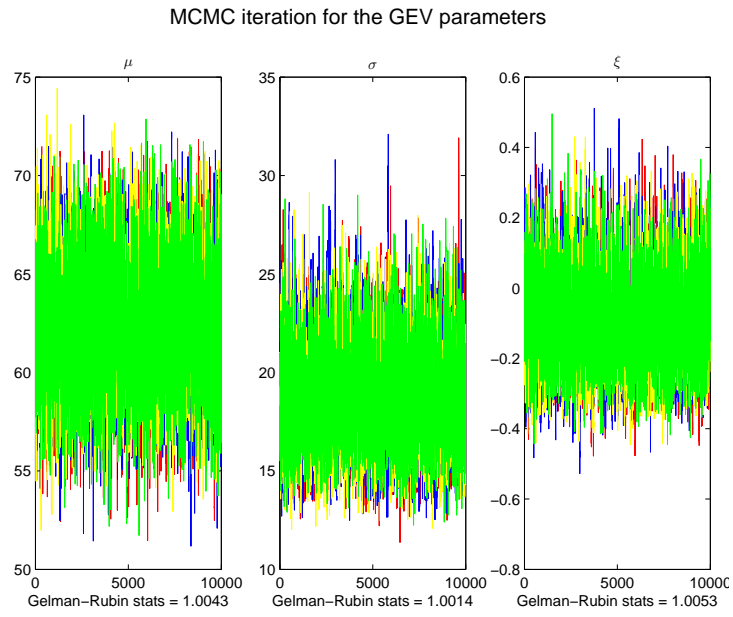
Figure C.7: (V026 BM w/DRC) Case 1: Markov chain Monte Carlo simulation for the parameters in the GEV distribution
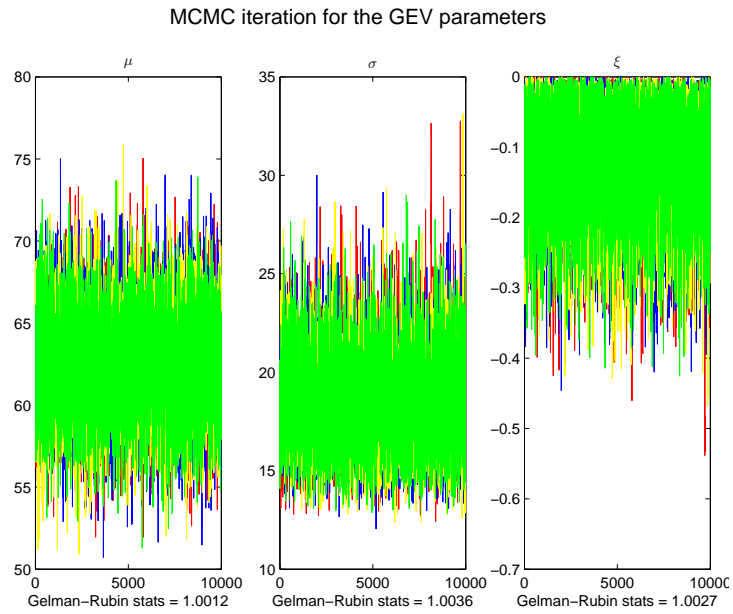
Figure C.8: (V026 BM w/DRC) Case 2: Markov chain Monte Carlo simulation for the parameters in the GEV distribution

MCMC iteration for the GEV parameters
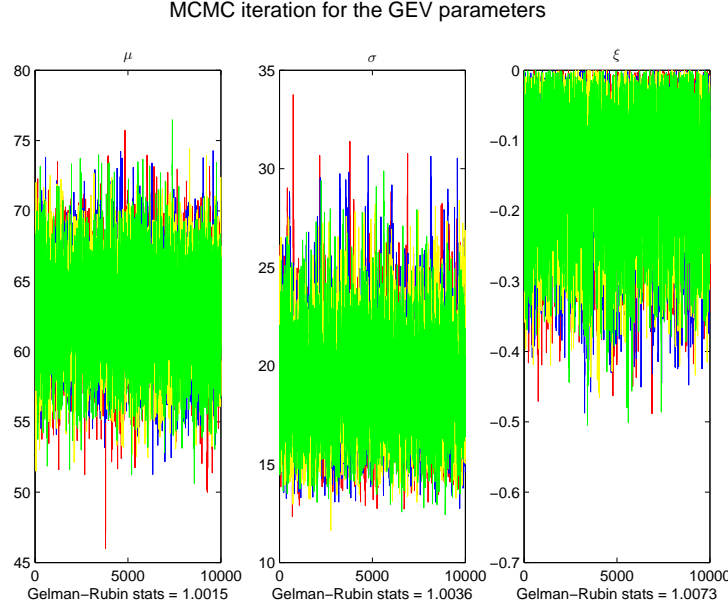
Figure C.9: (V026 BM w/DRC) Case 3: Markov chain Monte Carlo simulation for the parameters in the GEV distribution

C.1.2. Threshold model using the diagnostic based method (DBM) for determining the threshold value

Threshold model using diagnostic based methods for choosing a threshold-Case 1: A normal prior distribution for the ξ parameter (TM DBM w/DRC C1)

In Case 1, the prior distribution for ξ was chosen to be a normal distribution with a large variance, making it non-informative prior. The prior distribution for $\tilde{\sigma}$ is a non-informative inv-χ^2 distribution. So, in this case, the GP parameters are not constricted in any way by their prior distributions. The prior and posterior distributions for the GP parameters are shown in Figure C.10.

The model seems to be a reasonably good fit for the data, having an Anderson-Darling p-value of $p_B = 0.30$. The diagnostic plots in Figure C.11 also indicate that the model fits the data reasonably well. The annual maximum value points on the probability plot lie close to the unit diagonal with only minor exceptions. The points are close to linear on the quantile plot except a slight deviation for the largest values. Comparison between the probability density of the GP distribution and the histogram of the POTs indicates a good model fit. Plotting the annual maximum values on the return level plot also seem to indicate that the model fits the data well.
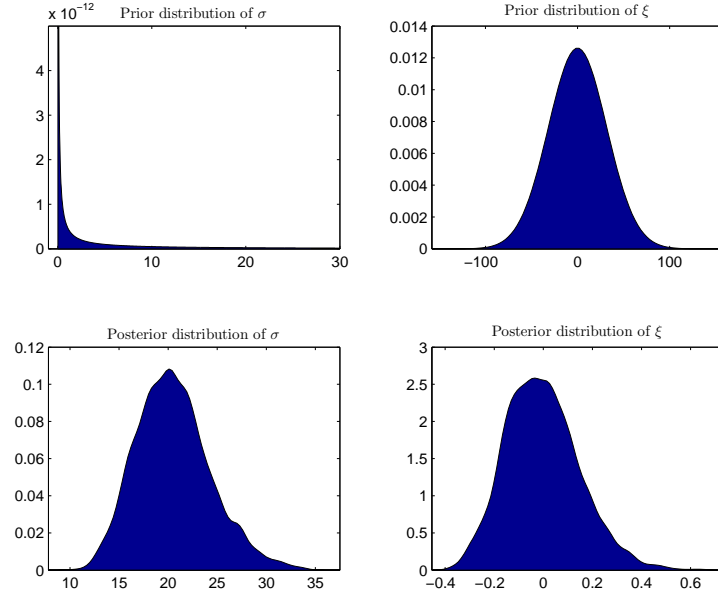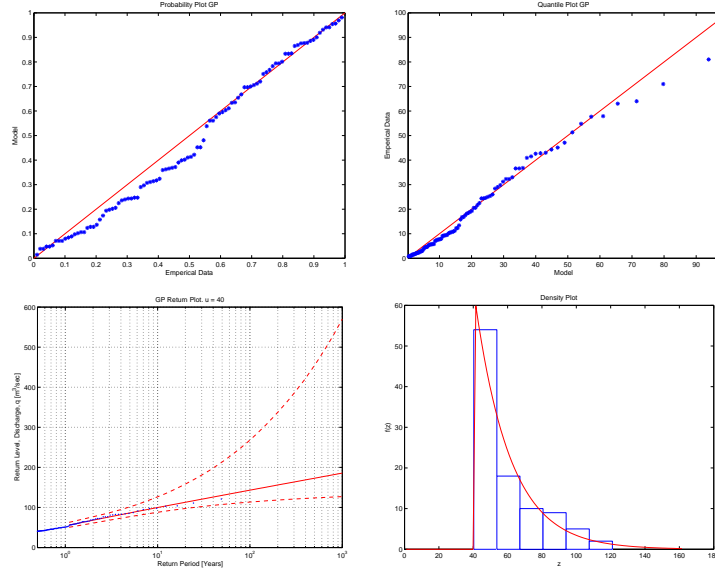
Figure C.10: (V026 TM DBM w/DRC) CASE 1: Prior and posterior distributions for the GP parameters
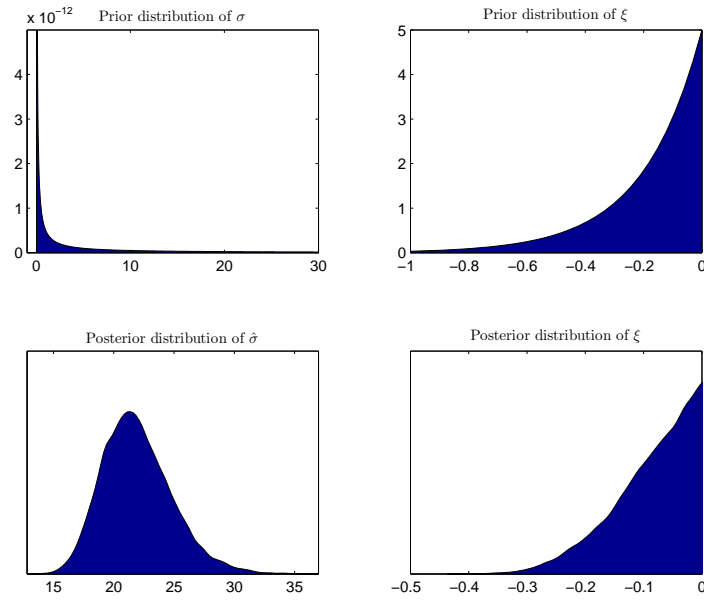
Threshold model using diagnostic based methods for choosing a threshold-Case 2: A negative gamma prior distribution for the ξ parameter (TM DBM w/DRC C2)

In Case 2, the prior distribution for ξ was chosen to be a negative gamma distribution. It contains only negative values having majority of the mass of the distribution is close to the y-axis. The prior distribution for $\tilde{\sigma}$ is a non-informative inv-χ^2 distribution. Therefore, in this case, the posterior density of the shape parameter of the GP distribution is constricted to negative values only. The prior and posterior distributions for the GP parameters are shown in Figure C.12.

The model seems to be a reasonably good fit for the data, having an Anderson-Darling p-value of $p_B = 0.22$. The diagnostic plots in Figure C.13 also indicate that the model fits the data reasonably well. The annual maximum value points on the probability plot lie close to the unit diagonal with only minor exceptions. The points are close to linear on the quantile plot indicating a good fit. Comparison between the probability density of the GP distribution and the histogram of the POTs indicates a good model fit. Plotting the annual maximum values on the return level plot also seem to indicate that the model fits the data well.
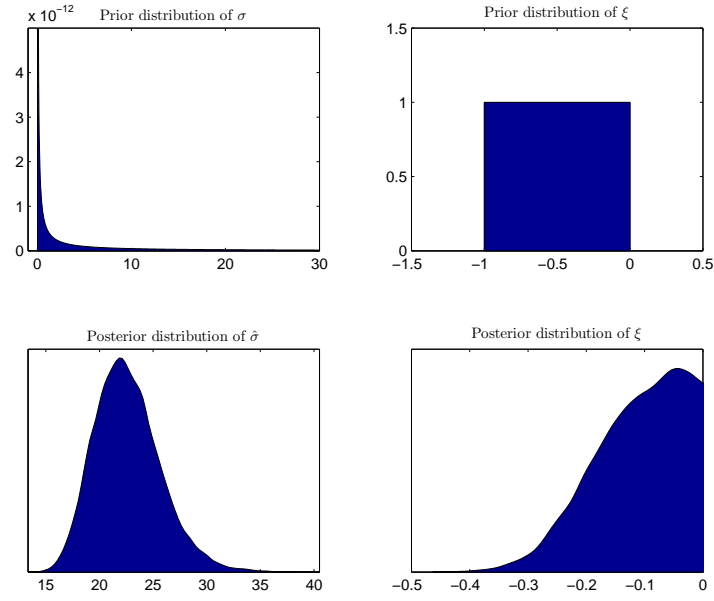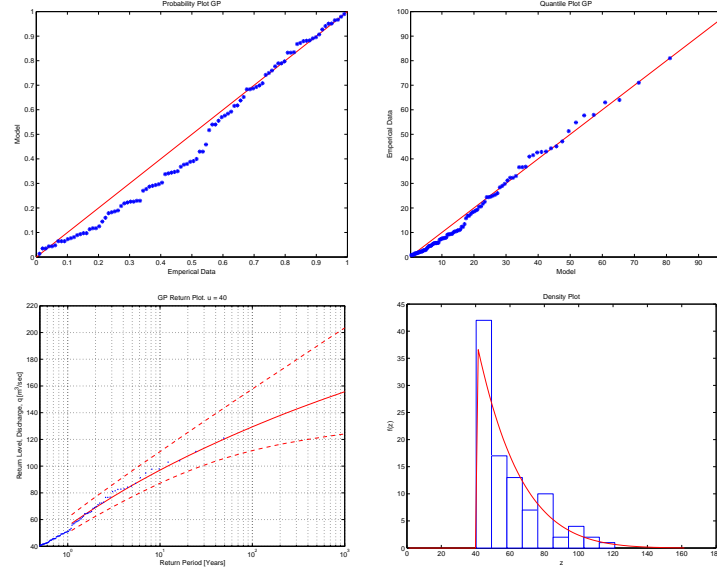
Figure C.11: (V026 TM DBM w/DRC) CASE 1: Diagnostic plots for the Threshold Model

Figure C.12: (V026 TM DBM w/DRC) CASE 2: Prior and posterior distributions for the GP parameters
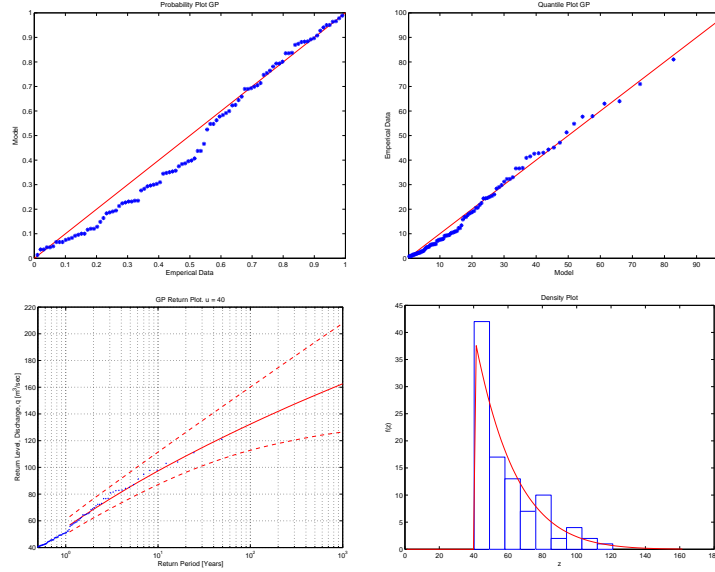
Figure C.13: (V026 TM DBM w/DRC) CASE 2: Diagnostic plots for the Threshold Model

Threshold model using diagnostic based methods for choosing a threshold-Case 3: A negative beta prior distribution for the ξ parameter (TM DBM w/DRC C3)

In Case 3, the prior distribution for ξ was chosen to be a negative beta distribution. It is a uniform distribution containing values on the interval $[-1; 0]$ The prior distribution for $\tilde{\sigma}$ is a non-informative inv-χ^2 distribution. Therefor, in this case, the posterior density of the shape parameter of the GEV distribution is constricted to negative values only. The prior and posterior distributions for the GP parameters are shown in Figure C.14.

The model seems to be a reasonably good fit for the data, having an Anderson-Darling p-value of $p_B = 0.18$. The diagnostic plots in Figure C.13 also indicate that the model fits the data reasonably well. The annual maximum value points on the probability plot lie close to the unit diagonal with only minor exceptions. The points are close to linear on the quantile plot indicating a good fit. Comparison between the probability density of the GP distribution and the histogram of the POTs indicates a good model fit. Plotting the annual maximum values on the return level plot also seem to indicate that the model fits the data well.

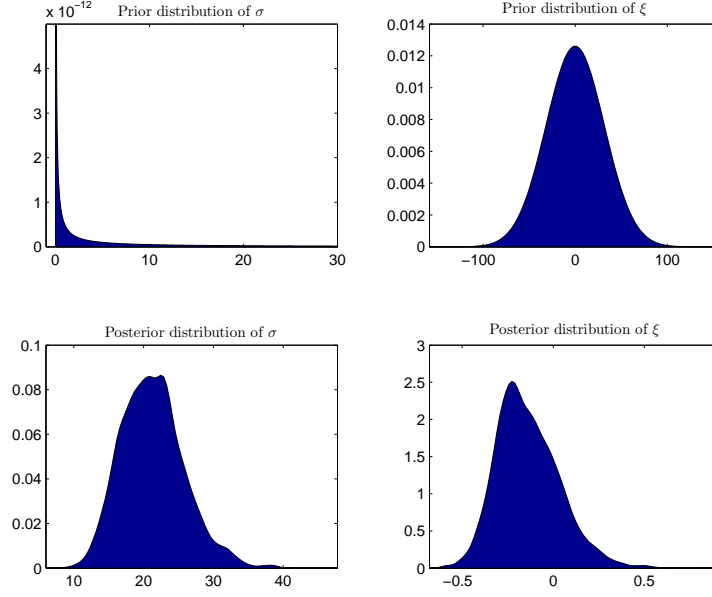*Figure C.14:* (V026 TM DBM w/DRC) CASE 3: Prior and posterior distributions for the GP parameters

Threshold model using the diagnostic based method (DBM) for determining the threshold value - Figures and tables displaying the posterior parameters of the GP distribution

Figure C.15: (V026 TM DBM w/DRC) CASE 3: Diagnostic plots for the threshold model

Table C.3: (V026 TM DBM w/DRC): Percentiles for the posterior distributions of the GP parameters, sampled using a MCMC iteration scheme, for all three cases of prior distributions, calculated with DRC uncertainty

	Threshold model with DRC and u = 40 Percentiles for parameters in the GEV distribution					
	Normal		Neg-Gamma		Neg-Beta	
	σ	$\tilde{\xi}$	σ	$\tilde{\xi}$	σ	$\tilde{\xi}$
2.5%	13.89	-0.26	17.10	-0.25	17.42	-0.28
25%	17.77	-0.11	19.89	-0.13	20.42	-0.16
50%	20.23	-0.01	21.68	-0.07	22.34	-0.10
75%	22.81	0.09	23.69	-0.03	24.46	-0.05
97.5%	28.45	0.33	28.48	-0.00	29.44	-0.01
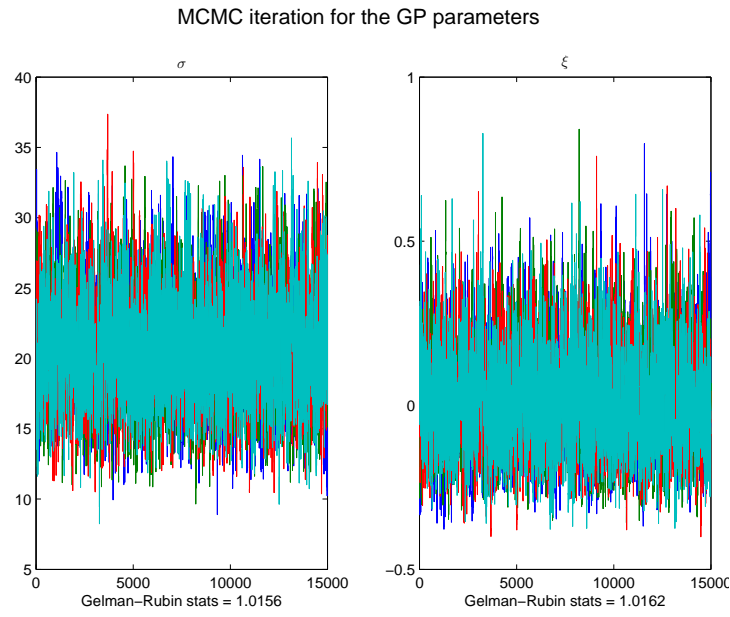
Figure C.16: (V026 TM DBM w/DRC) Case 1: Markov chain Monte Carlo simulation for the parameters in the GP distribution
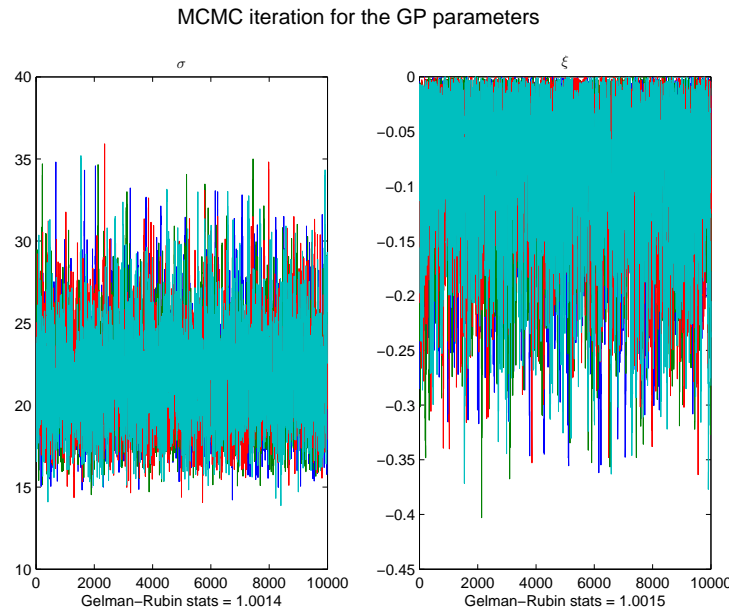
Figure C.17: (V026 TM DBM w/DRC) Case 2: Markov chain Monte Carlo simulation for the parameters in the GP distribution

MCMC iteration for the GP parameters
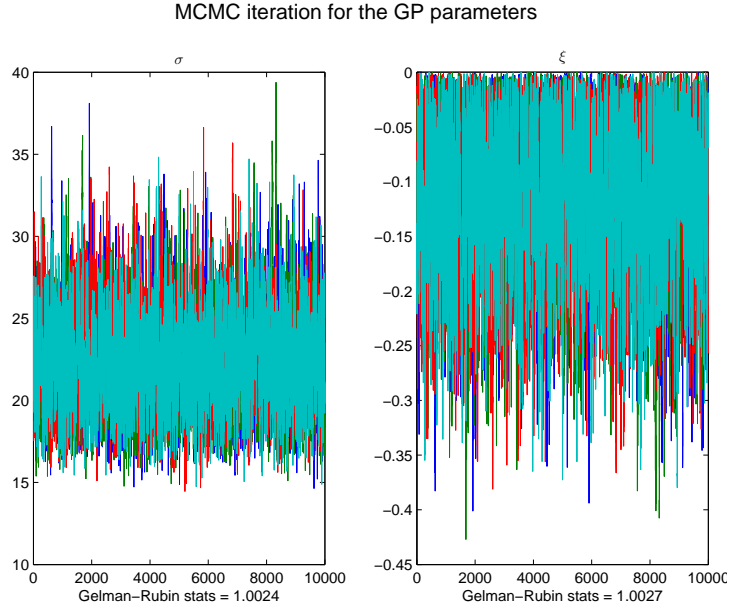
Figure C.18: (V026 TM DBM w/DRC) Case 3: Markov chain Monte Carlo simulation
for the parameters in the GEV distribution

C.1.3. Threshold model using the fixed frequency method (FFM) for determining the threshold value

Threshold model using the fixed frequency method for choosing a threshold- Case 1: A normal prior distribution for the ξ parameter (TM FFM w/DRC C1)

In Case 1, the prior distribution for ξ was chosen to be a normal distribution with a large variance, making it non-informative prior. The prior distribution for $\tilde{\sigma}$ is a non-informative inv-χ^2 distribution. So, in this case, the GP parameters are not constricted in any way by their prior distributions. The prior and posterior distributions for the GP parameters are shown in Figure C.19.

The model seems to be a good fit for the data, having an Anderson-Darling p-value of $p_B = 0.63$. The diagnostic plots in Figure C.20 also indicate that the model fits the data reasonably well. The annual maximum value points on the probability plot lie close to the unit diagonal. The points are close to linear on the quantile plot indicating a good fit. Comparison between the probability density of the GP distribution and the histogram of the POTs indicate a good model fit. Plotting the annual maximum values on the return level plot also seem to indicate that the model fits the data well.

Figure C.19: (V026 TM FFM w/DRC) CASE 1: Prior and posterior distributions for the GP parameters

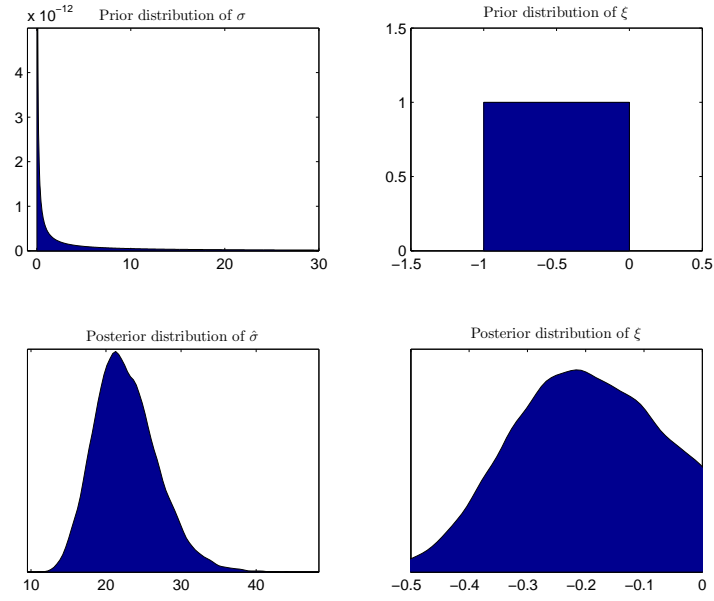## Threshold model using the fixed frequency method for choosing a threshold- Case 2: A negative gamma prior distribution for the ξ parameter (TM FFM w/DRC C2)

In Case 2, the prior distribution for ξ was chosen to be a negative gamma distribution. It contains only negative values having majority of the mass of the distribution is close to the y-axis. The prior distribution for $\tilde{\sigma}$ is a non-informative inv-χ^2 distribution. Therefore, in this case, the posterior density of the shape parameter of the GP distribution is constricted to negative values only. The prior and posterior distributions for the GP parameters are shown in Figure C.21.

The model seems to be a good fit for the data, having an Anderson-Darling p-value of $p_B = 0.69$. The diagnostic plots in Figure C.22 also indicate that the model fits the data reasonably well. The annual maximum value points on the probability plot lie close to the unit diagonal. The points are close to linear on the quantile plot indicating a good fit. Comparison between the probability density of the GP distribution and the histogram of the POTs indicate a good model fit. Plotting the annual maximum values on the return level plot also seem to indicate that the model fits the data well.
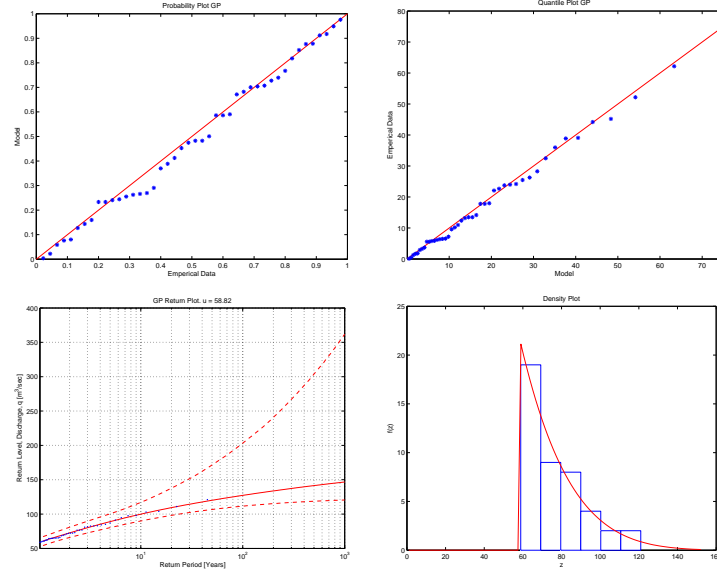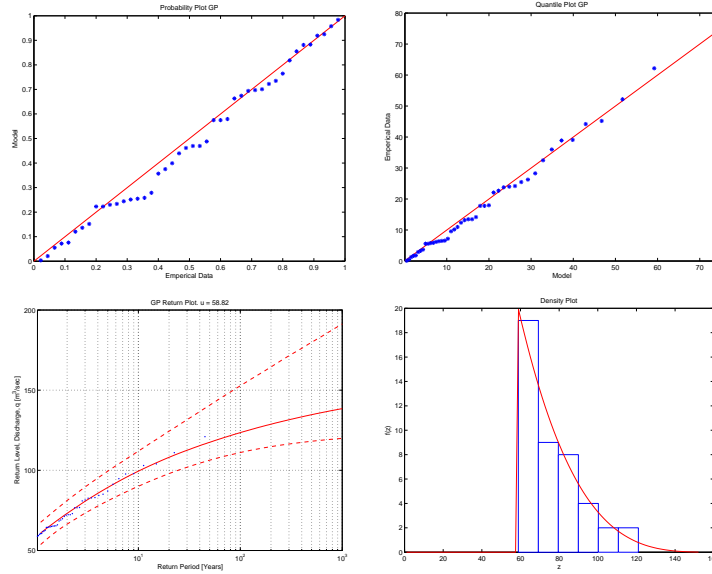
Figure C.20: (V026 TM FFM w/DRC) CASE 1: Diagnostic plots for the Threshold Model
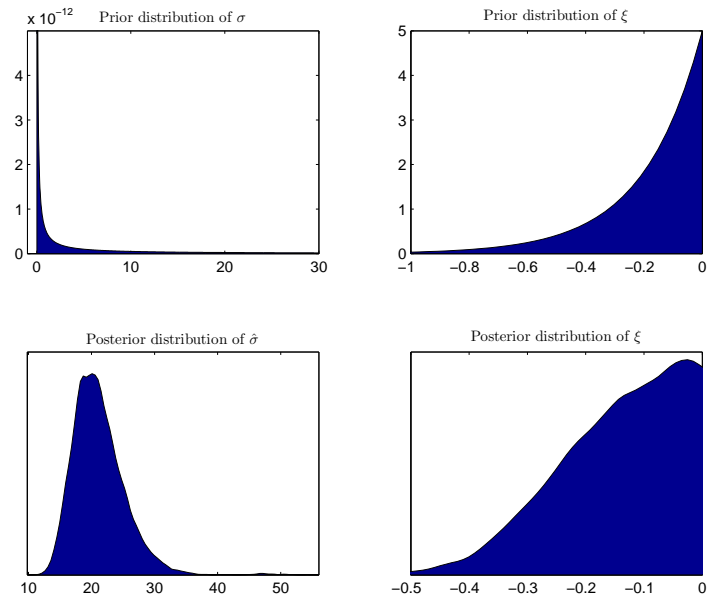
Figure C.21: (V026 TM FFM w/DRC) CASE 2: Prior and posterior distributions for the GP parameters
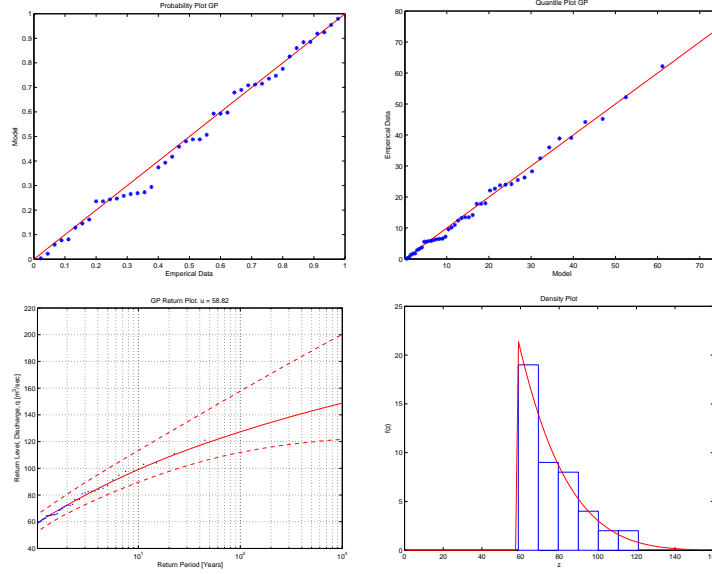
Figure C.22: (V026 TM FFM w/DRC) CASE 2: Diagnostic plots for the Threshold Model

Threshold model using the fixed frequency method for choosing a threshold- Case 3: A negative beta prior distribution for the ξ parameter (TM FFM w/DRC C3)

In Case 3, the prior distribution for ξ was chosen to be a negative beta distribution. It is a uniform distribution containing values on the interval $[-1; 0]$ The prior distribution for $\tilde{\sigma}$ is a non-informative inv-χ^2 distribution. Therefore, in this case, the posterior density of the shape parameter of the GEV distribution is constricted to negative values only. The prior and posterior distributions for the GP parameters are shown in Figure C.23.

The model seems to be a good fit for the data, having an Anderson-Darling p-value of $p_B = 0.65$. The diagnostic plots in Figure C.24 also indicate that the model fits the data reasonably well. The annual maximum value points on the probability plot lie close to the unit diagonal. The points are close to linear on the quantile plot indicating a good fit. Comparison between the probability density of the GP distribution and the histogram of the POTs indicate a good model fit. Plotting the annual maximum values on the return level plot also seem to indicate that the model fits the data well.

Figure C.23: (V026 TM FFM w/DRC) CASE 3: Prior and posterior distributions for the GP parameters

Threshold model using the fixed frequency method (FFM) for determining the threshold value - Figures and tables displaying the posterior parameters of the GP distribution

Figure C.24: (V026 TM FFM w/DRC) CASE 3: Diagnostic plots for the threshold model

Table C.4: (V026 TM FFM w/DRC): Percentiles for the posterior distributions of the GP parameters, sampled using a MCMC iteration scheme, for all three cases of prior distributions, calculated with DRC uncertainty

	Threshold model with DRC and u = 59					
	Percentiles for parameters in the GEV distribution					
	Normal		Neg-Gamma		Neg-Beta	
	σ	$\tilde{\xi}$	σ	$\tilde{\xi}$	σ	$\tilde{\xi}$
2.5%	13.40	-0.43	14.90	-0.39	15.60	-0.44
25%	18.01	-0.27	18.32	-0.22	19.76	-0.30
50%	21.05	-0.16	20.63	-0.13	22.34	-0.21
75%	24.28	-0.03	23.35	-0.06	25.31	-0.12
97.5%	31.87	0.26	30.33	-0.01	32.06	-0.02
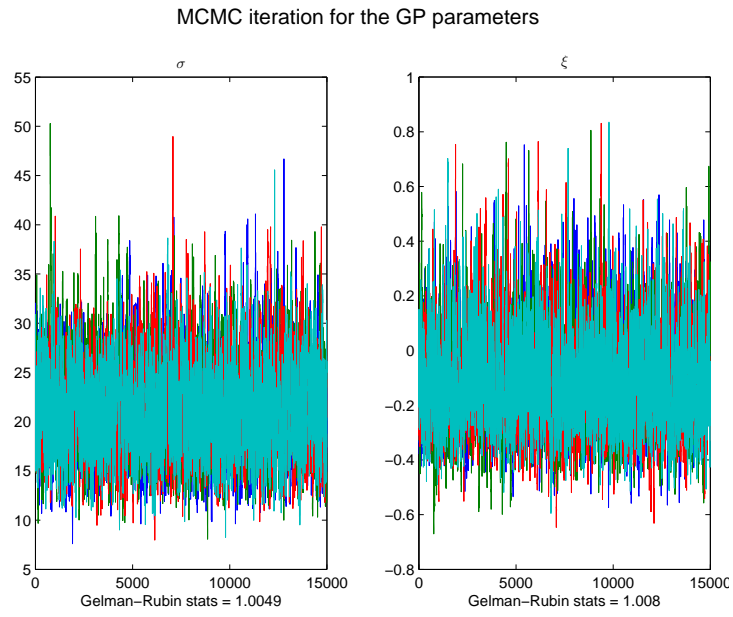
Figure C.25: (V026 TM FFM w/DRC) Case 1: Markov chain Monte Carlo simulation for the parameters in the GP distribution
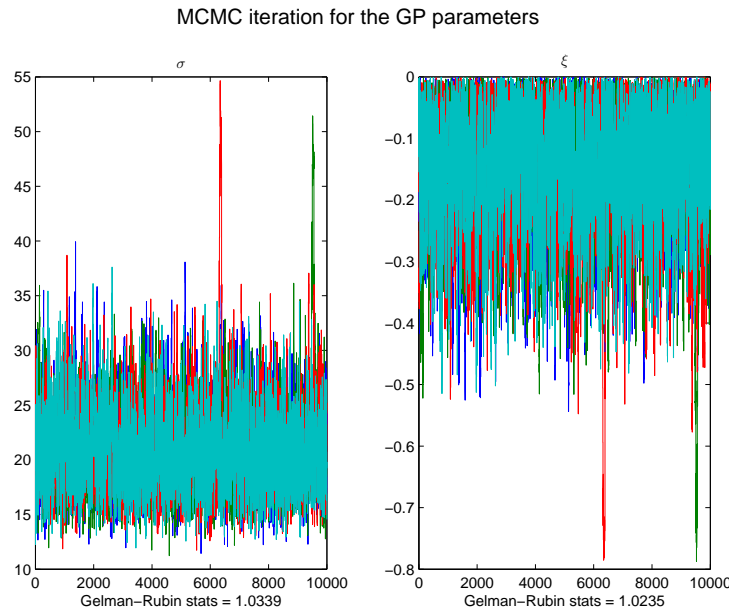
Figure C.26: (V026 TM FFM w/DRC) Case 2: Markov chain Monte Carlo simulation for the parameters in the GP distribution

MCMC iteration for the GP parameters
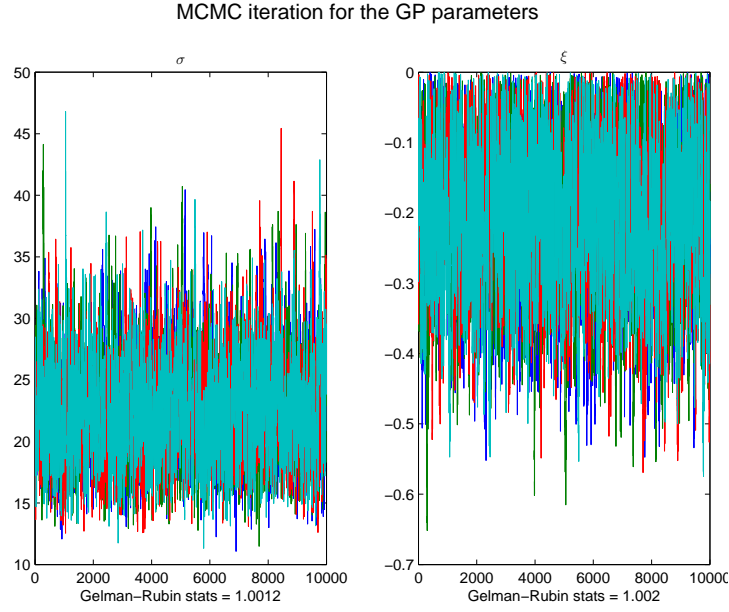
Figure C.27: (V026 TM FFM w/DRC) Case 3: Markov chain Monte Carlo simulation for the parameters in the GEV distribution

C.2. V026: Without discharge rating curve uncertainty

C.2.1. Block maxima model

Table C.5: (V026 BM w/o DRC): Percentiles for the posterior distributions of the GEV parameters, sampled using a MCMC iteration scheme, for all three cases of prior distributions, calculated without DRC uncertainty

|	Block Extrema without DRC								
	Percentiles for parameters in the GEV distribution								
	Normal			Neg-Gamma			Neg-Beta		
	μ	σ	ξ	μ	σ	ξ	μ	σ	ξ
2.5%	56.62	14.46	-0.32	56.43	14.65	-0.30	56.79	14.84	-0.34
25%	60.41	16.87	-0.18	60.41	16.90	-0.17	60.80	17.20	-0.21
50%	62.37	18.39	-0.10	62.49	18.32	-0.10	62.87	18.68	-0.14
75%	64.43	20.11	-0.01	64.56	19.94	-0.05	65.03	20.37	-0.08
97.5%	68.35	24.25	0.19	68.65	23.79	-0.01	69.22	24.59	-0.01

MCMC iteration for the GEV parameters
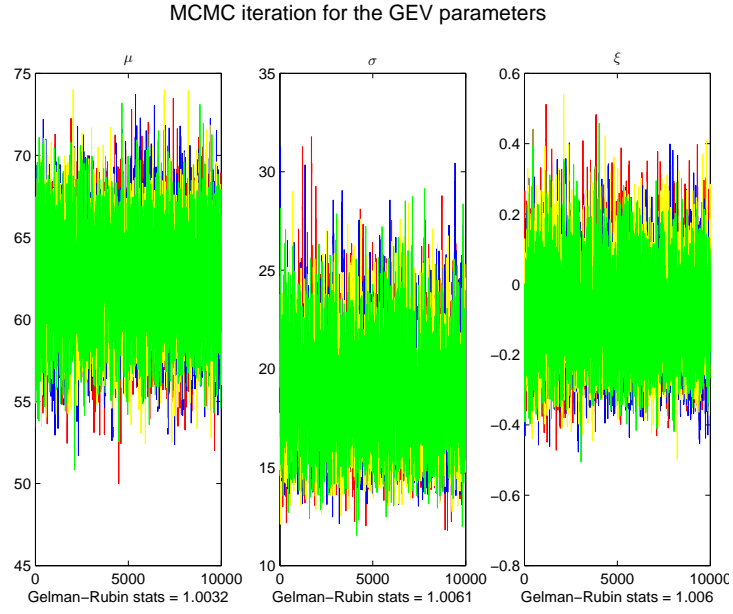
Figure C.28: (V026 BM w/o DRC) Case 1: Markov chain Monte Carlo simulation for the parameters in the GEV distribution
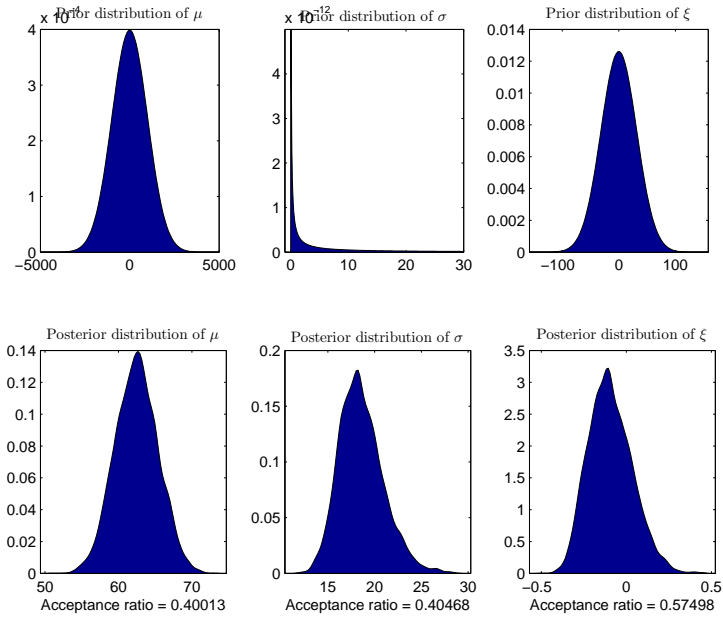
Figure C.29: (V026 BM w/o DRC) CASE 1: Prior and posterior distributions for the GEV parameters
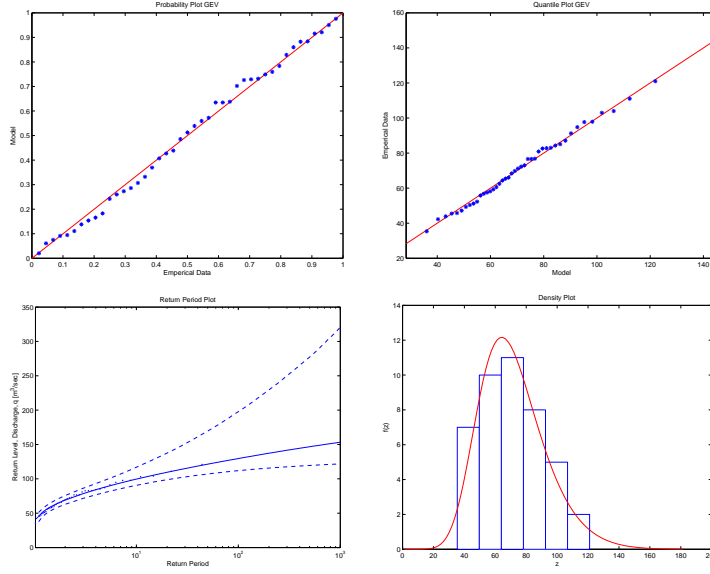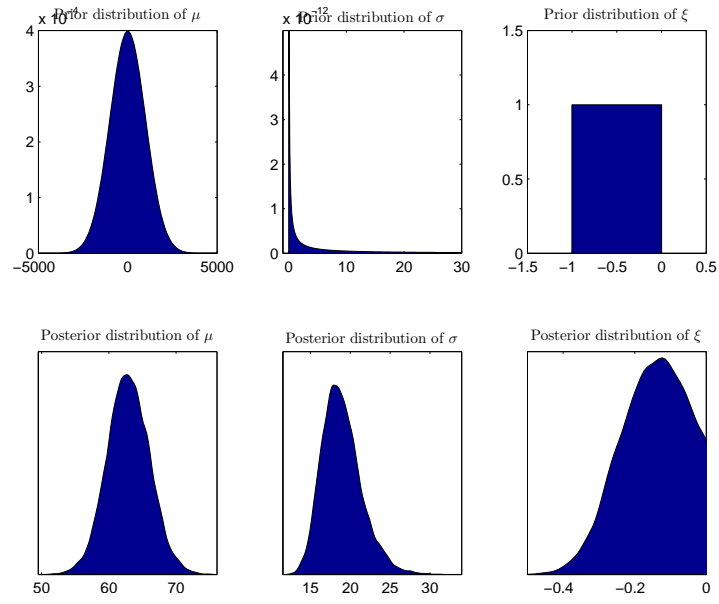
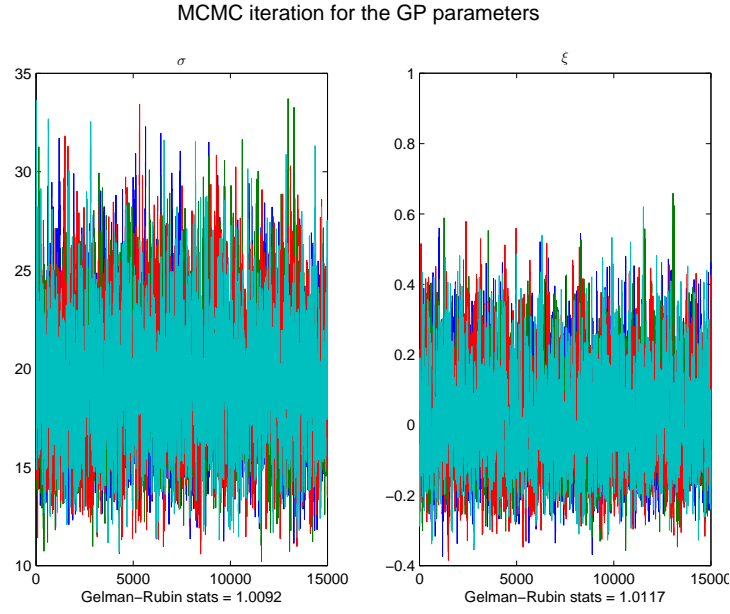*Figure C.30:* (V026 BM w/o DRC) CASE 1: Diagnostic plots for the block maxima model

C.2.2. Threshold model using the diagnostic based method (DBM) for determining the threshold value

Table C.6: (V026 TM DBM w/o DRC): Percentiles for the posterior distributions of the GP parameters, sampled using a MCMC iteration scheme, for all three cases of prior distributions, calculated without DRC uncertainty

	Threshold model with DRC and u = 40					
	Percentiles for parameters in the GEV distribution					
	Normal		Neg-Gamma		Neg-Beta	
	σ	$\tilde{\xi}$	σ	$\tilde{\xi}$	σ	$\tilde{\xi}$
2.5%	13.85	-0.23	16.65	-0.22	16.83	-0.25
25%	17.28	-0.09	19.07	-0.11	19.54	-0.15
50%	19.22	-0.00	20.58	-0.07	21.16	-0.09
75%	21.37	0.09	22.27	-0.03	23.02	-0.04
97.5%	26.28	0.29	26.26	-0.00	27.32	-0.00
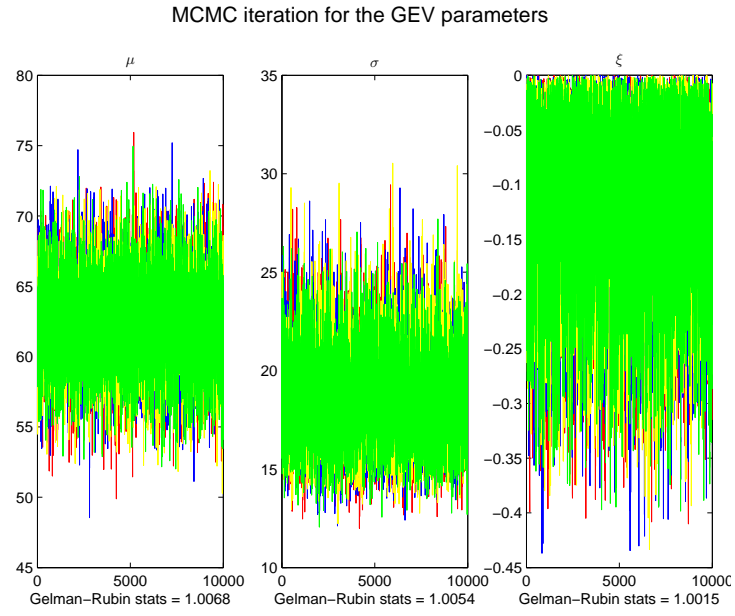
Figure C.31: (V026 BM w/o DRC) Case 2: Markov chain Monte Carlo simulation for the parameters in the GEV distribution
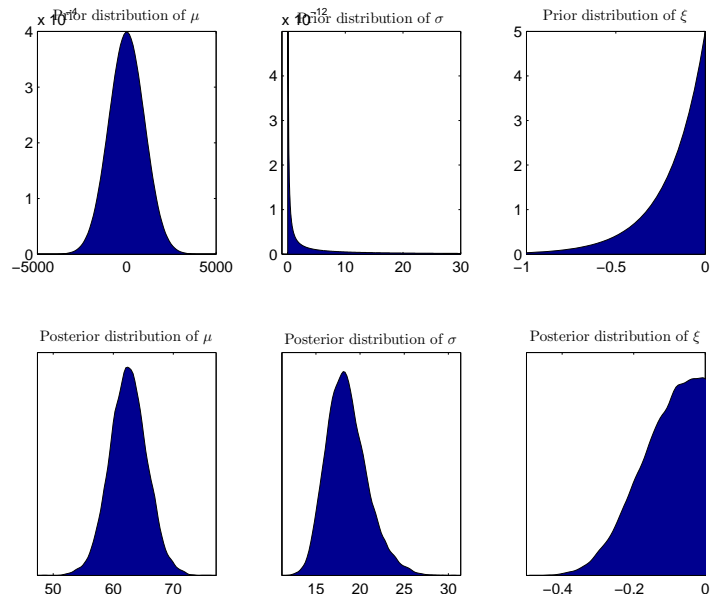
Figure C.32: (V026 BM w/o DRC) CASE 2: Prior and posterior distributions for the GEV parameters
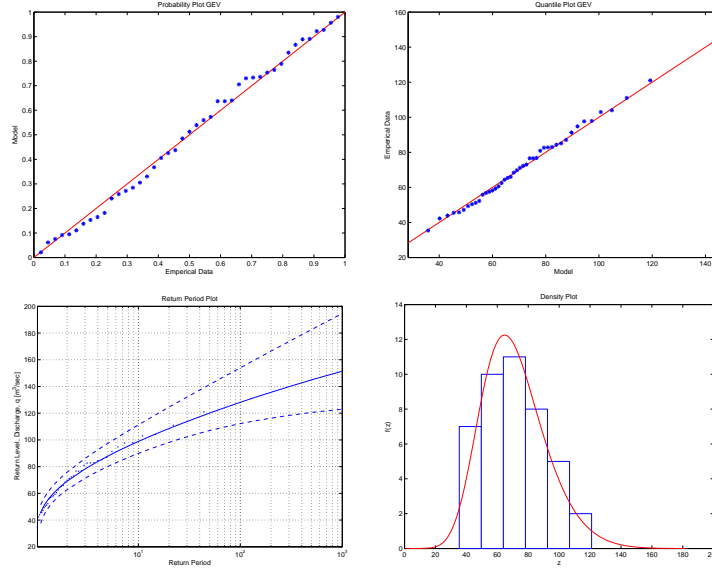
Figure C.33: (V026 BM w/o DRC) CASE 2: Diagnostic plots for the block maxima model
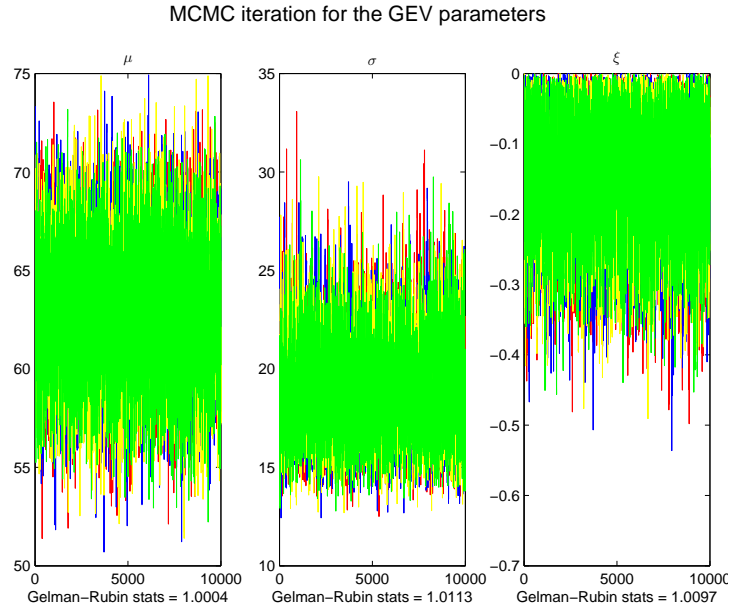
Figure C.34: (V026 BM w/o DRC) Case 3: Markov chain Monte Carlo simulation for the parameters in the GEV distribution
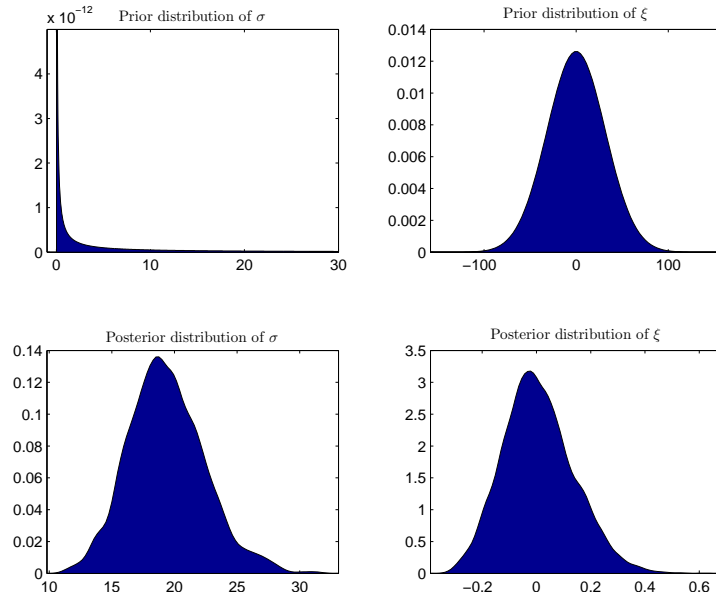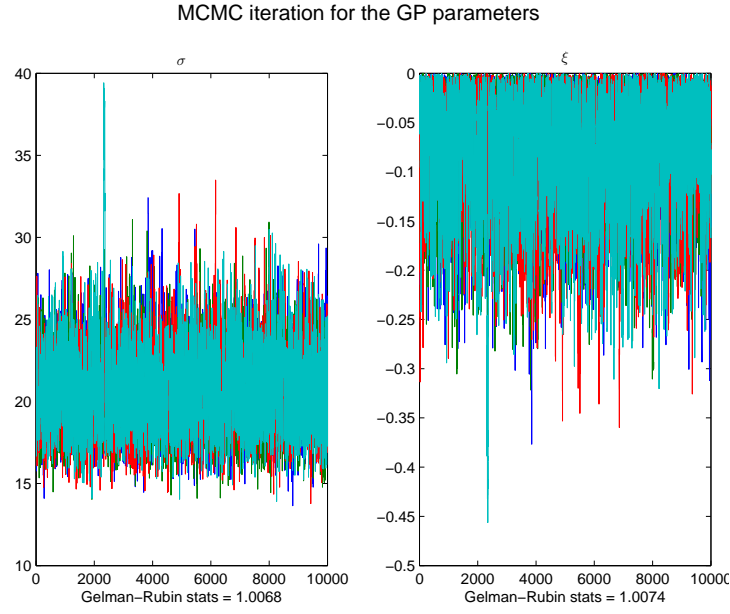
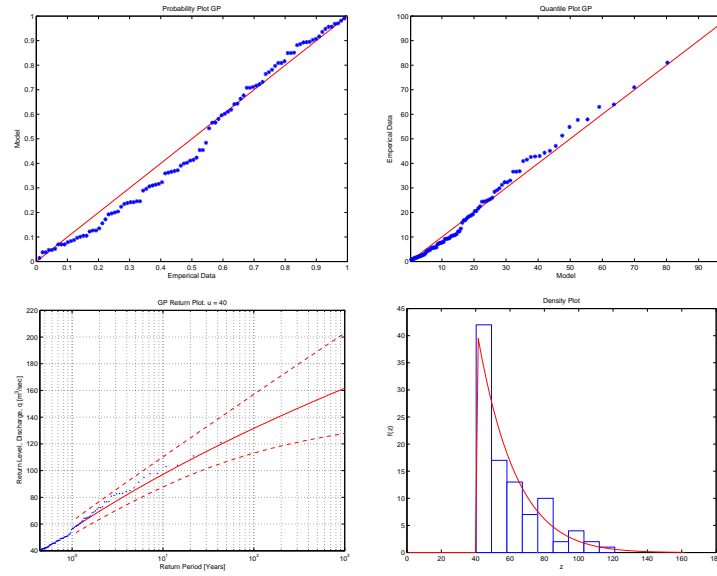*Figure C.35:* (V026 BM w/o DRC) CASE 3: Prior and posterior distributions for the GEV parameters
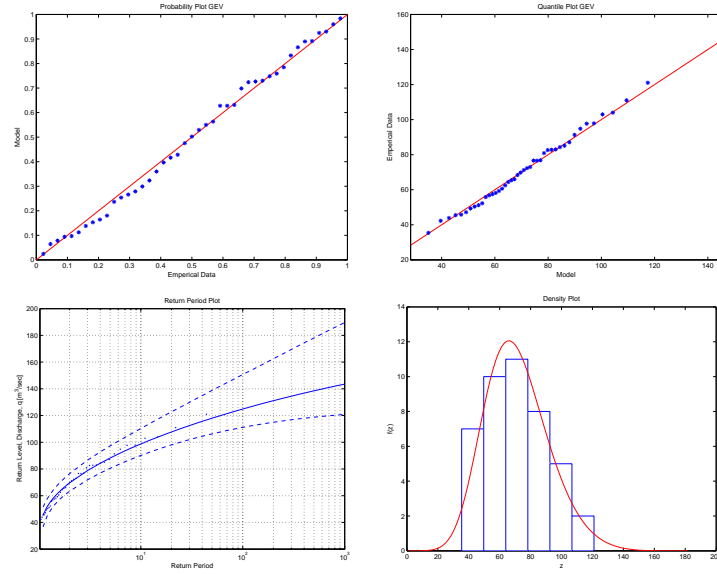
Figure C.36: (V026 BM w/o DRC) CASE 3: Diagnostic plots for the block maxima model
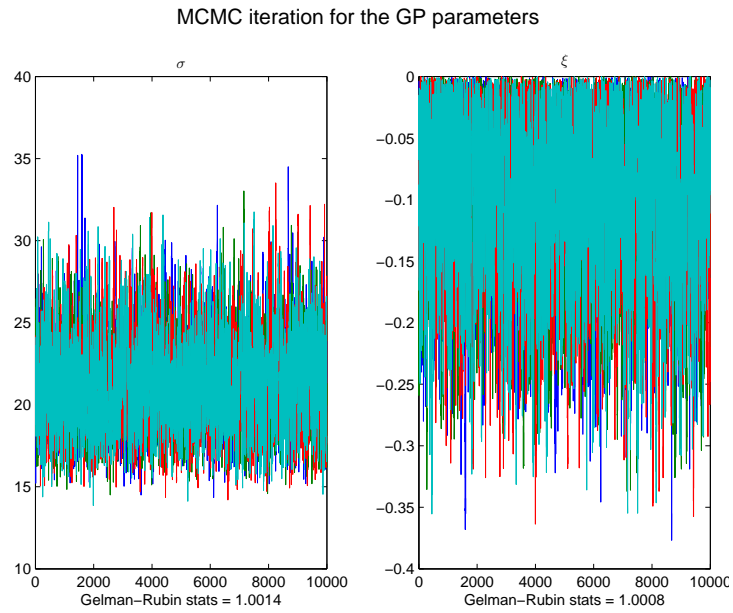
MCMC iteration for the GP parameters

Figure C.37: (V026 TM DBM w/o DRC) Case 1: Markov chain Monte Carlo simulation for the parameters in the GP distribution
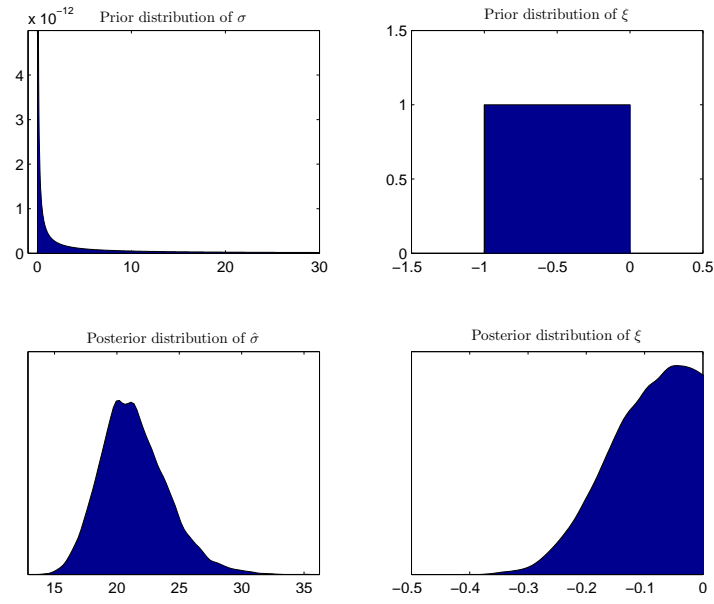

Figure C.38: (V026 TM DBM w/o DRC) CASE 1: Prior and posterior distributions for the GP parameters
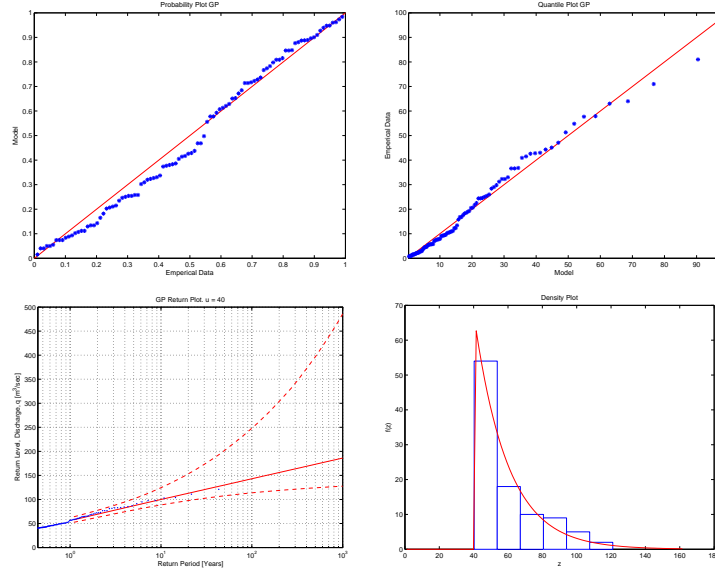
Figure C.39: (V026 TM DBM w/o DRC) CASE 1: Diagnostic plots for the threshold model

C.2.3. Threshold model using the fixed frequency method (FFM) for determining the threshold value

Table C.7: (V026 TM FFM w/o DRC): Percentiles for the posterior distributions of the GP parameters, sampled using a MCMC iteration scheme, for all three cases of prior distributions, calculated without DRC uncertainty

|	Threshold model without DRC and u = 59					
	Percentiles for parameters in the GP distribution					
	Normal		Neg-Gamma		Neg-Beta	
	σ	$\tilde{\xi}$	σ	$\tilde{\xi}$	σ	$\tilde{\xi}$
2.5%	12.81	-0.40	14.64	-0.37	15.15	-0.44
25%	17.42	-0.24	18.10	-0.21	18.98	-0.28
50%	20.15	-0.13	20.23	-0.13	21.58	-0.19
75%	23.17	-0.02	22.83	-0.06	24.56	-0.11
97.5%	29.69	0.28	29.03	-0.01	31.56	-0.01

Figure C.40: (V026 TM DBM w/o DRC) Case 2: Markov chain Monte Carlo simulation for the parameters in the GP distribution
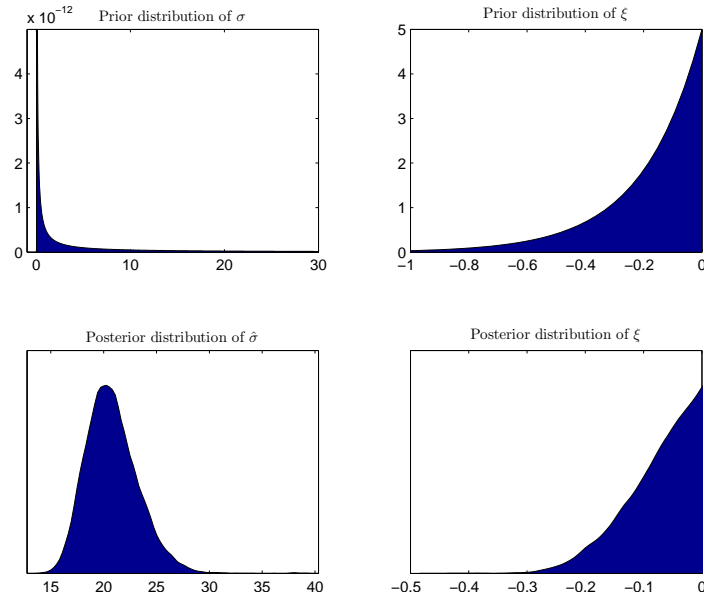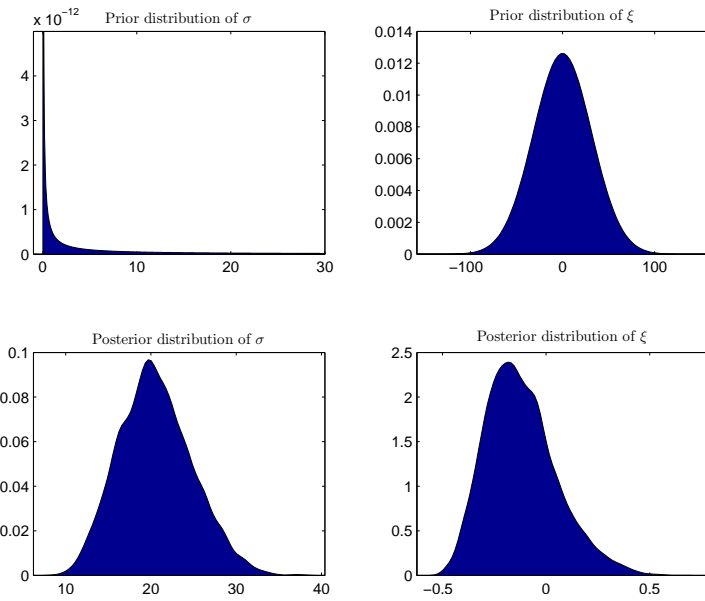

Figure C.41: (V026 TM DBM w/o DRC) CASE 2: Prior and posterior distributions for the GP parameters
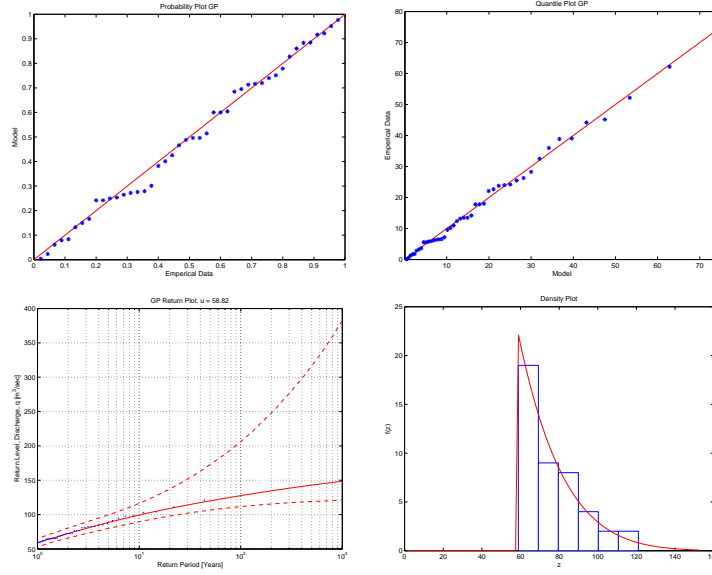
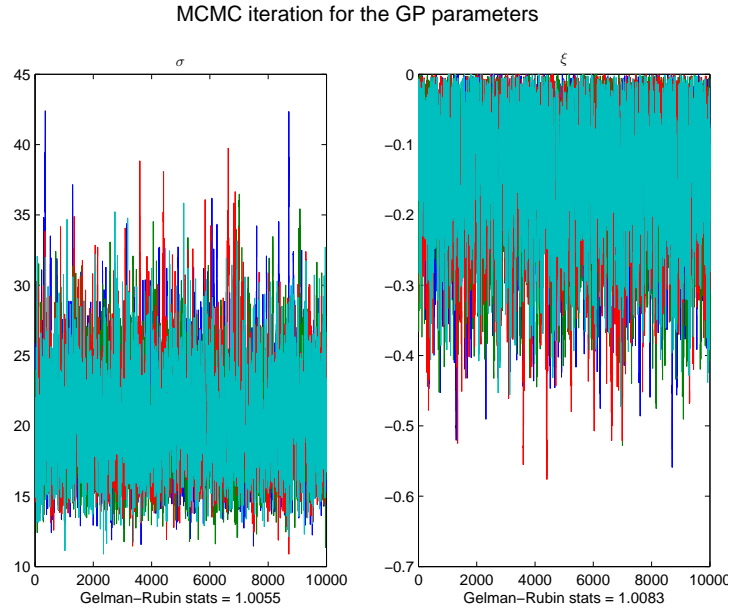*Figure C.42:* (V026 TM DBM w/o DRC) CASE 2: Diagnostic plots for the threshold model

Figure C.43: (V026 TM DBM w/o DRC) Case 3: Markov chain Monte Carlo simulation for the parameters in the GP distribution
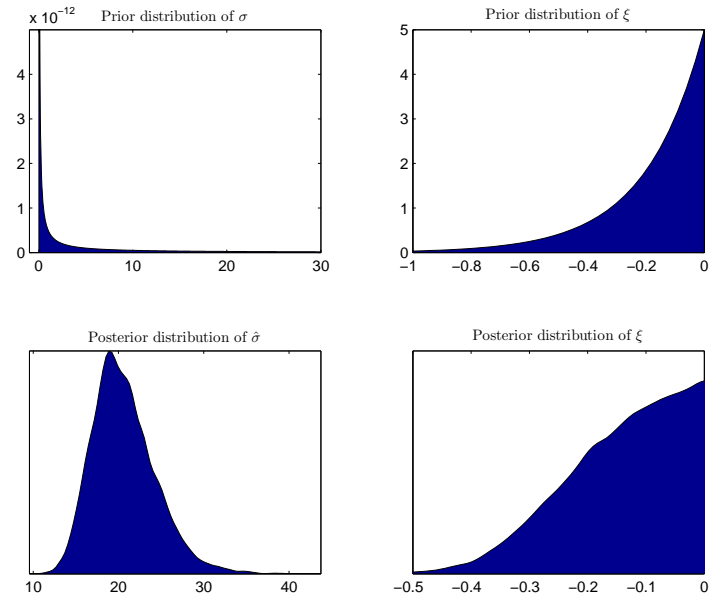
Figure C.44: (V026 TM DBM w/o DRC) CASE 3: Prior and posterior distributions for the GP parameters
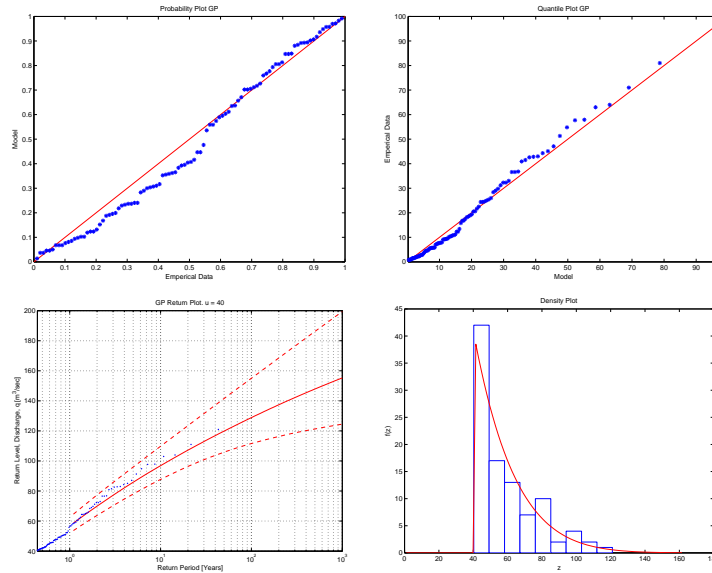
Figure C.45: (V026 TM DBM w/o DRC) CASE 3: Diagnostic plots for the threshold model
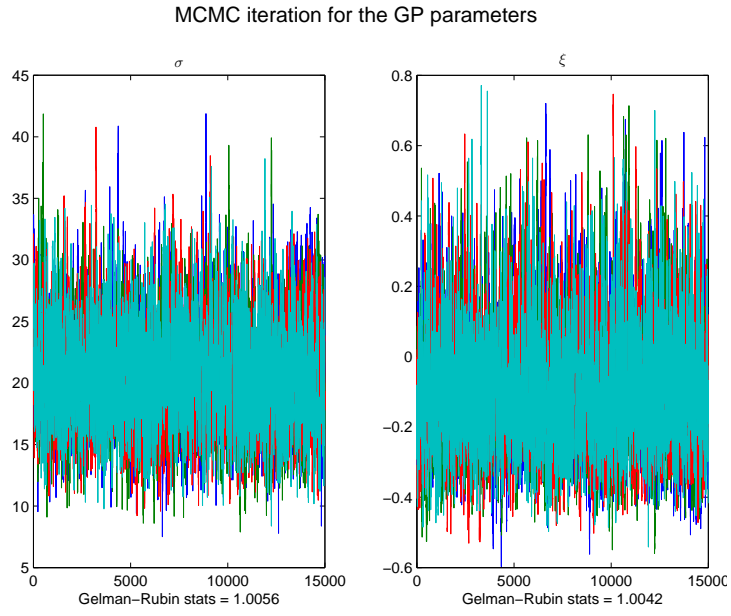
Figure C.46: (V026 TM FFM w/o DRC) Case 1: Markov chain Monte Carlo simulation for the parameters in the GP distribution

Figure C.47: (V026 TM FFM w/o DRC) CASE 1: Prior and posterior distributions for the GP parameters
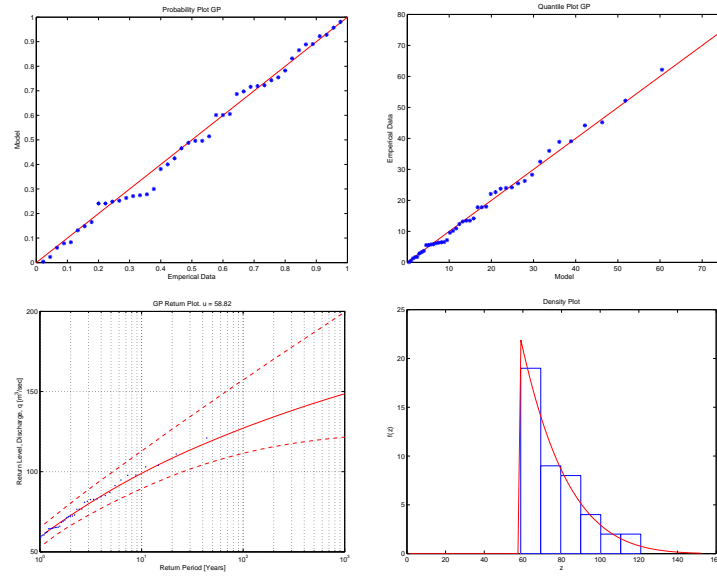
Figure C.48: (V026 TM FFM w/o DRC) CASE 1: Diagnostic plots for the threshold model
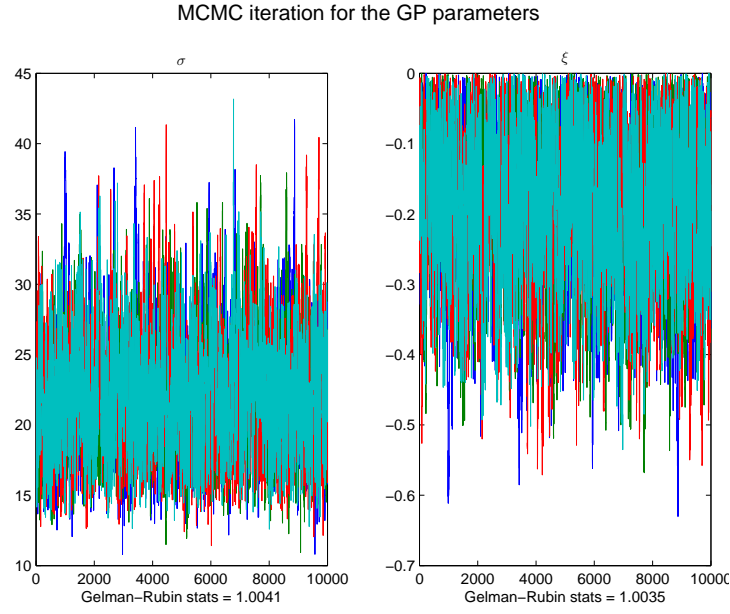

Figure C.49: (V026 TM FFM w/o DRC) Case 2: Markov chain Monte Carlo simulation for the parameters in the GP distribution

Figure C.50: (V026 TM FFM w/o DRC) CASE 2: Prior and posterior distributions for the GP parameters

Figure C.51: (V026 TM FFM w/o DRC) CASE 2: Diagnostic plots for the threshold model

Figure C.52: (V026 TM FFM w/o DRC) Case 3: Markov chain Monte Carlo simulation for the parameters in the GP distribution
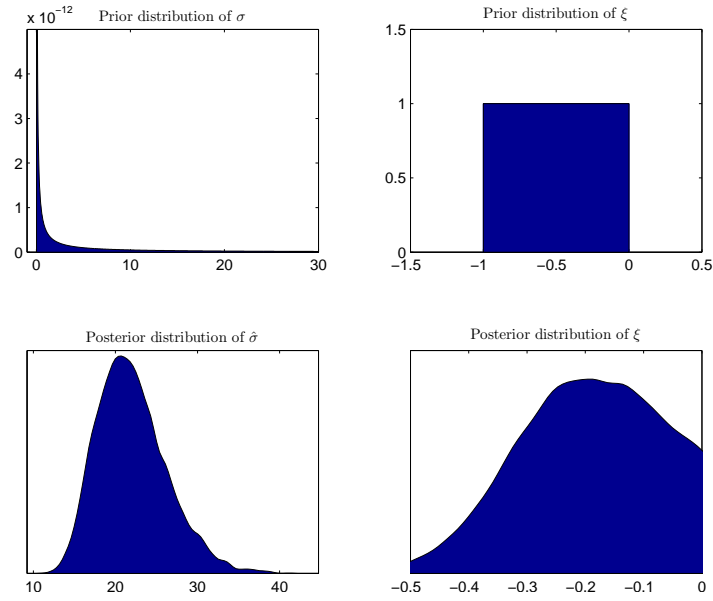

Figure C.53: (V026 TM FFM w/o DRC) CASE 3: Prior and posterior distributions for the GP parameters
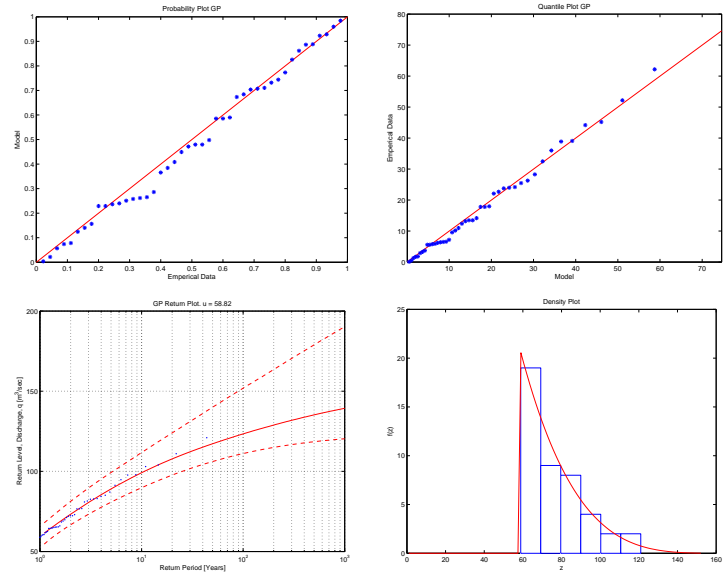
Figure C.54: (V026 TM FFM w/o DRC) CASE 3: Diagnostic plots for the threshold model

D. More details on the flood analysis for Svarta

In this appendix, figures and tables that are relevant to the research but were not displayed in the main text of the paper, are displayed. That includes probability plots, quantile plots and density plots for all cases of prior distributions. The prior and posterior densities of all the parameters in the GEV and GP distributions are also displayed for all cases. The appendix also includes the sampled Markov chain Monte Carlo (MCMC) chains, used to construct the posterior distributions for the parameters of both the generalized extreme value distribution (GEV) and the generalized Pareto (GP) distribution. The samples are displayed both in figures, and in tables as quantiles for all the models with and without the inclusion discharge rating curve uncertainty. The histogram of the prior and posterior distribution and the diagnostic plots for the models are shown for all models without the inclusion of discharge rating curve uncertainty.

Table D.1 shows a list of abbreviations regarding the following figures and tables. Every figure and table in the appendix is marked with some of these abbreviations and that explains which river the data belongs to and what kind of models were used to generate the results. For example, the text *(V010 BM w/DRC) Case 2* in the caption of a figure or a table, indicates that the data displayed comes from the river Svarta (V010), a block maxima model was used (BM) with a neg-gamma prior distribution for the shape parameter (Case 2), and the uncertainty in the discharge rating curve was taken into account in the calculations (w/DRC).

Table D.1: Abbreviations used to explain the origin of the data used to generate figures and tables

V010:	The river Svarta in Skagafjordur: 10 is the number of the gauging station measuring the data
Case 1:	The shape parameter, ξ, was sampled using a normal prior distribution
Case 2:	The shape parameter, ξ, was sampled using a neg-gamma prior distribution
Case 3:	The shape parameter, ξ, was sampled using a neg-beta prior distribution
BM:	A block maxima model
TM DBM:	A threshold model using the diagnostic based method for determining the threshold value
TM FFM:	A threshold model using the fixed frequency method for determining the threshold value
w/DRC:	A discharge rating curve uncertainty was taken into account in the calculations
w/o DRC:	A discharge rating curve uncertainty was not taken into account in the calculations

D.1. V010: With discharge rating curve uncertainty

D.1.1. Block maxima model

Block Maxima Model - Case 1: A normal prior distribution for the ξ parameter (BM w/DRC C1)

In Case 1, the prior distribution for ξ was chosen to be a normal distribution with a large variance, making it non-informative prior. The prior distribution for σ is a non-informative inv-χ^2 distribution and the prior distribution for μ is a normal distribution with large variance making it non-informative. So, in this case, the GEV parameters are not constricted in any way by their prior distributions. See further details on the prior distributions in Section 3.3.2. The construction of the posterior distribution of all the parameters is discussed in Section 3.3.3. The prior and posterior distributions for the GEV parameters are shown in Figure D.1

The simulated chains of posterior distributions for the GEV parameters are used to model the extreme behavior of the river. The simulated chains of the posterior
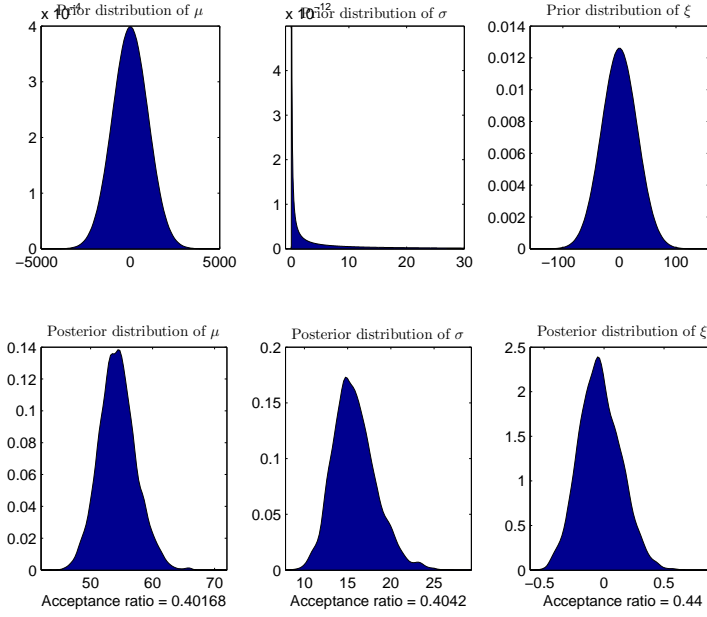
Figure D.1: (V010 BM w/DRC) CASE 1: Prior and posterior distributions for the GEV parameters

distributions of the parameters are shown in Figure D.7 and their quantiles are shown in Table D.2.

Figure D.2 shows the return period plot for Svarta as well as the quantile plot, the probability plot and the density plot. The Anderson-Darling p-value and the diagnostic plots in Figure D.2 are evaluated to check the validity of the model. The methods used for the model validation are discussed in Section 2.2.2.

The model seems to be a good fit for the data, having an Anderson-Darling p-value of $p_B = 0.46$. The diagnostic plots in Figure D.2 also indicate that the model fits the data reasonably well. The annual maximum value points on the probability plot all lie close to the unit diagonal and the points are close to linear on the quantile plot, which is both an indication to a good fit. Comparison between the probability density of the GEV distribution and the histogram of the POTs, indicates that the model is a good fit for the data. Plotting the annual maximum values on the return level plot also seem to indicate that the model fits the data well, since all the values are inside the 95% posterior interval of the return levels.
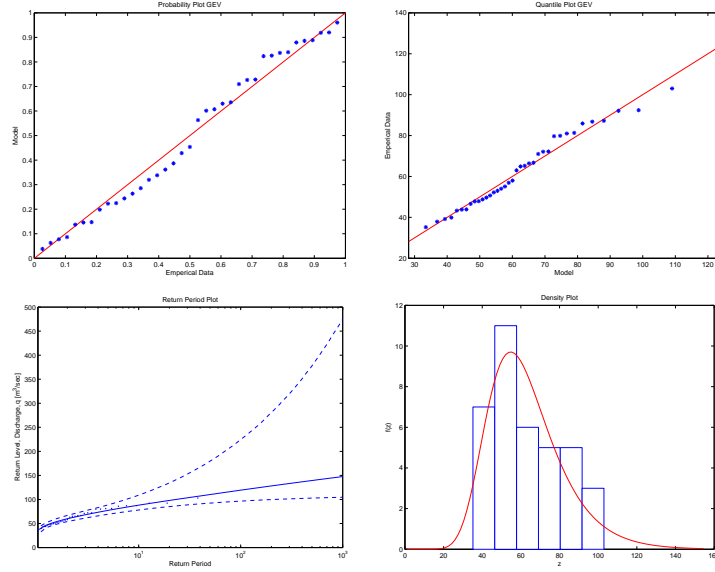
Figure D.2: (V010 BM w/DRC) CASE 1: Diagnostic plots for the block maxima model

Block Maxima Model - Case 2: A negative gamma prior distribution for the ξ parameter (BM w/DRC C2)

In Case 2, the prior distribution for ξ was chosen to be a negative gamma distribution. It contains only negative values having majority of the mass of the distribution is close to the y-axis. Therefore, in this case, the posterior density of the shape parameter of the GEV distribution is constricted to negative values only. The prior and posterior distributions for the GEV parameters are shown in Figure (D.3).

The simulated chains of the posterior distributions of the parameters are shown in Figure D.8 and their quantiles are shown in Table D.2.

Figure D.4 shows the return period plot for Svarta as well as the quantile plot, the probability plot and the density plot. The Anderson-Darling p-value of $p_B = 0.45$ indicates that the model is a good fit for the data. The probability plot in Figure D.4 also indicates that the model fits the data well. The annual maximum value points are close to linear on the quantile plot indicating a good fit to the model. Comparison between the probability density of the GP distribution and the histogram of the POTs indicates that the model could be a good fit for the data. Plotting the annual maximum values on the return level plot also seem to indicate that the model fits the data well.
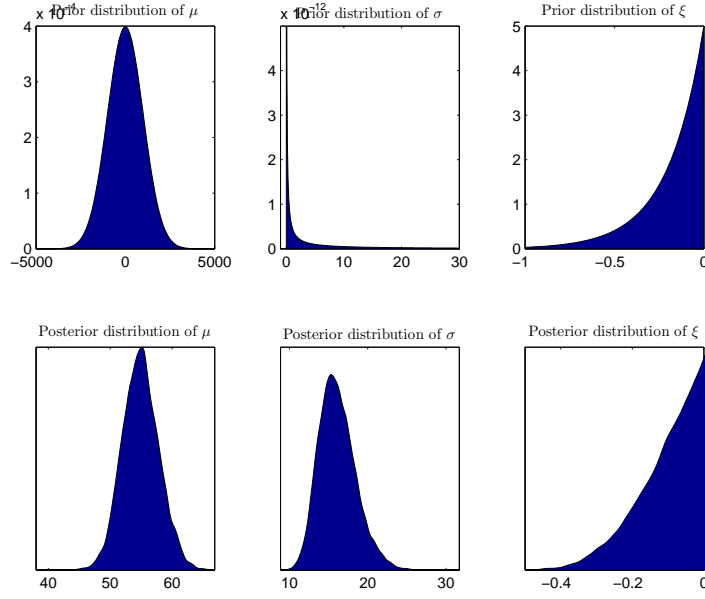
Figure D.3: (V010 BM w/DRC) CASE 2: Prior and posterior distributions for the GEV parameters

Block Maxima Model - Case 3: A negative beta prior distribution for the ξ parameter (BM w/DRC C3)

In Case 3, the prior distribution for ξ was chosen to be a negative beta distribution. It is a uniform distribution containing values on the interval $[-1;0]$ Therefore, in this case, the posterior density of the shape parameter of the GEV distribution is constricted to negative values only. The prior and posterior distributions for the GEV parameters are shown in Figure (D.5).

The simulated chains of the posterior distributions of the parameters are shown in Figure D.9 and their quantiles are shown in Table D.2.

Figure D.6 shows the return period plot for Svarta as well as the quantile plot, the probability plot and the density plot.

The Anderson-Darling p-value of $p_B = 0.43$ indicates that the model is a good fit for the data. The probability plot in Figure D.4 also indicates that the model fits the data well. The annual maximum value points are close to linear on the quantile plot indicating a good fit to the model. Comparison between the probability density of the GP distribution and the histogram of the POTs indicates that the model could be a good fit for the data. Plotting the annual maximum values on the return level plot also seem to indicate that the model fits the data well.
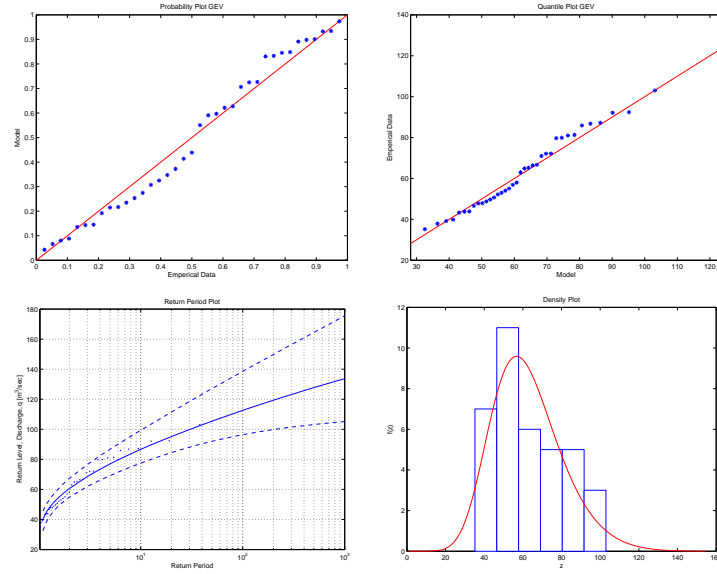
Figure D.4: (V010 BM w/DRC) CASE 2: Diagnostic plots for the block maxima model
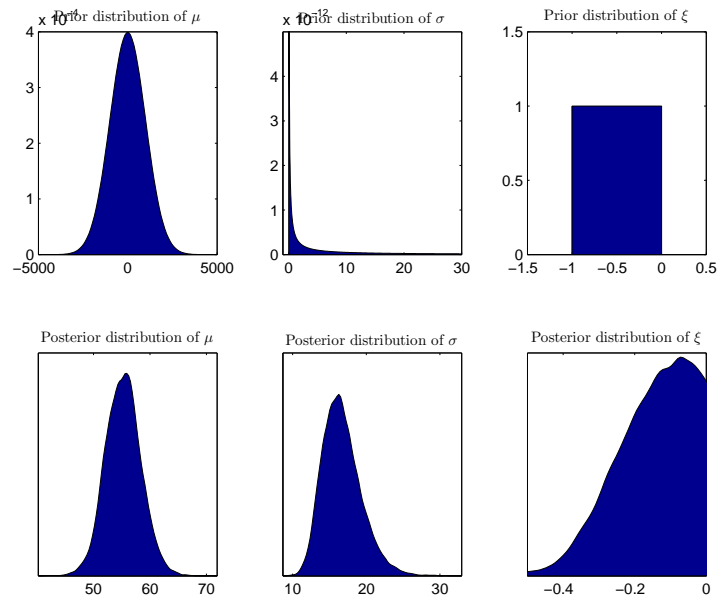

Figure D.5: (V010 BM w/DRC) CASE 3: Prior and posterior distributions for the GEV parameters

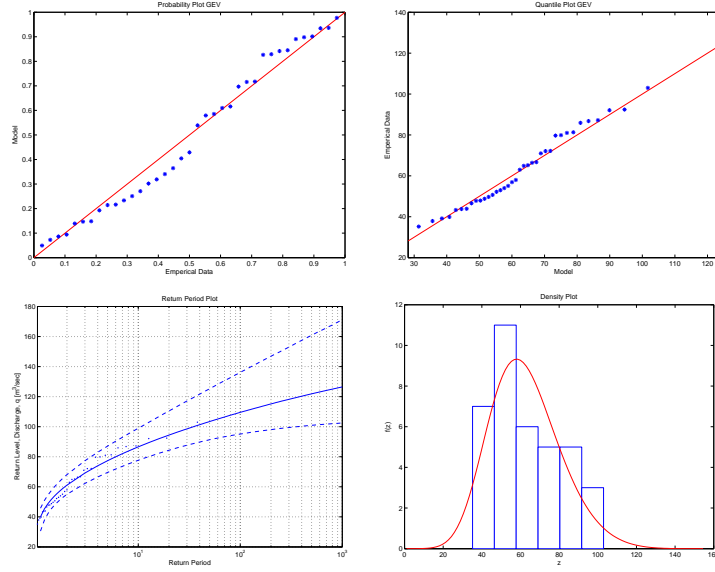## Block Maxima Model – Figures and tables displaying the posterior parameters of the GEV distribution

Figure D.6: (V010 BM w/DRC) CASE 3: Diagnostic plots for the block maxima model

Table D.2: (V010 BM w/DRC): Percentiles for the posterior distributions of the GEV parameters, sampled using a MCMC iteration scheme, for all three cases of prior distributions, calculated with DRC uncertainty

	Block Extrema with DRC								
	Percentiles for parameters in the GEV distribution								
	Normal			Neg-Gamma			Neg-Beta		
	μ	σ	ξ	μ	σ	ξ	μ	σ	ξ
2.5%	48.83	11.62	-0.34	49.34	12.16	-0.32	49.26	12.42	-0.38
25%	52.31	14.11	-0.15	52.91	14.46	-0.16	53.11	14.84	-0.22
50%	54.18	15.60	-0.04	54.86	15.91	-0.09	55.25	16.43	-0.14
75%	56.12	17.31	0.09	56.83	17.57	-0.04	57.28	18.24	-0.07
97.5%	60.37	21.51	0.34	60.86	21.40	-0.00	61.54	22.64	-0.01

MCMC iteration for the GEV parameters
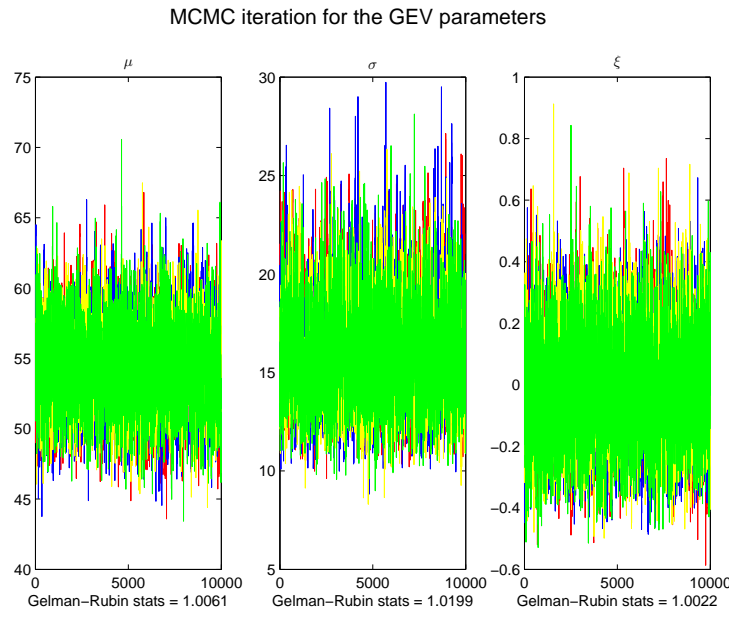
Figure D.7: (V010 BM w/DRC) Case 1: Markov chain Monte Carlo simulation for the parameters in the GEV distribution

MCMC iteration for the GEV parameters
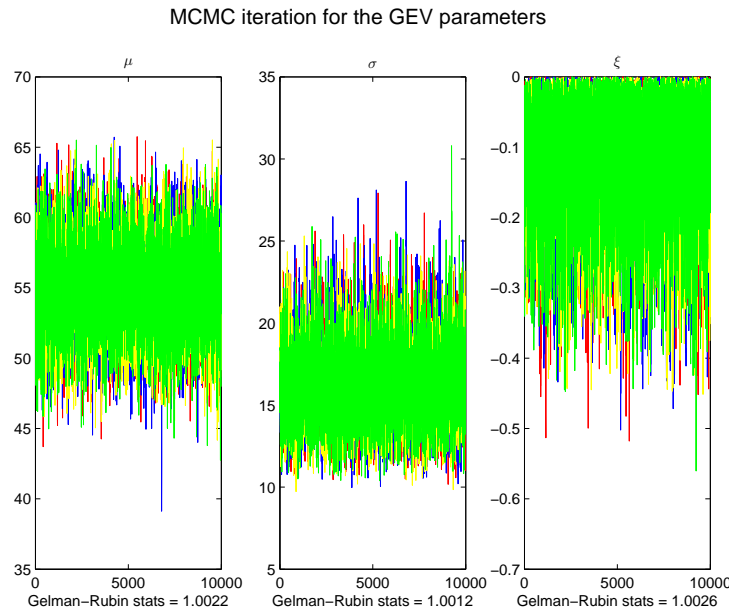
Figure D.8: (V010 BM w/DRC) Case 2: Markov chain Monte Carlo simulation for the parameters in the GEV distribution
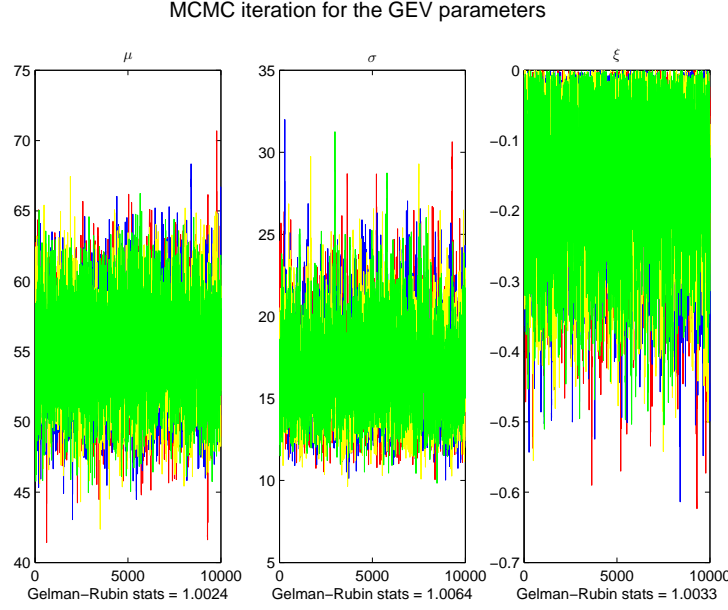
Figure D.9: (V010 BM w/DRC) Case 3: Markov chain Monte Carlo simulation for the parameters in the GEV distribution

D.1.2. Threshold model using the diagnostic based method (DBM) for determining the threshold value

Threshold model using diagnostic based methods for choosing a threshold–Case 1: A normal prior distribution for the ξ parameter (TM DBM w/DRC C1)

In Case 1, the prior distribution for ξ was chosen to be a normal distribution with a large variance, making it non-informative prior. The prior distribution for $\tilde{\sigma}$ is a non-informative inv-χ^2 distribution. So, in this case, the GP parameters are not constricted in any way by their prior distributions. The prior and posterior distributions for the GP parameters are shown in Figure D.10.

The model seems to be a good fit for the data, having an Anderson-Darling p-value of $p_B = 0.51$. The diagnostic plots in Figure D.11 also indicate that the model fits the data well. The annual maximum values on the probability plot all lie close to the unit diagonal and the points are close to linear on the quantile plot. Comparison between the probability density of the GP distribution and the histogram of the POTs indicates that the model is a good fit for the data. Plotting the annual maximum values on the return level plot also seem to indicate that the model fits the data well.
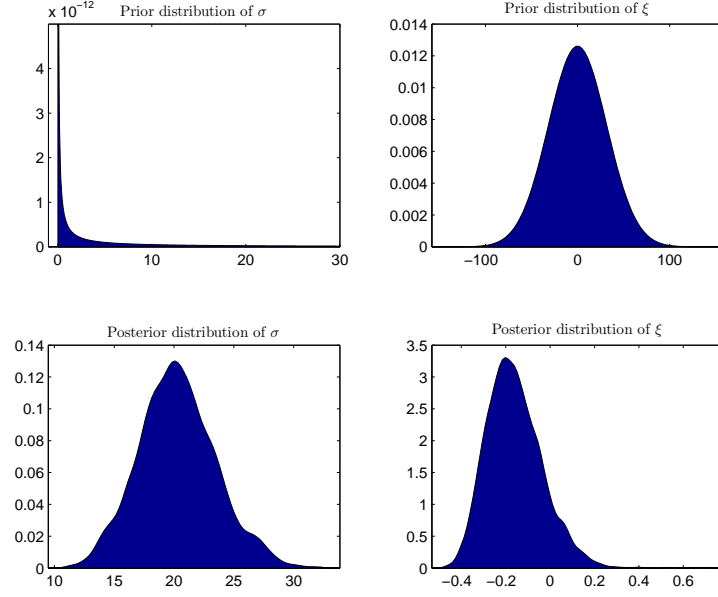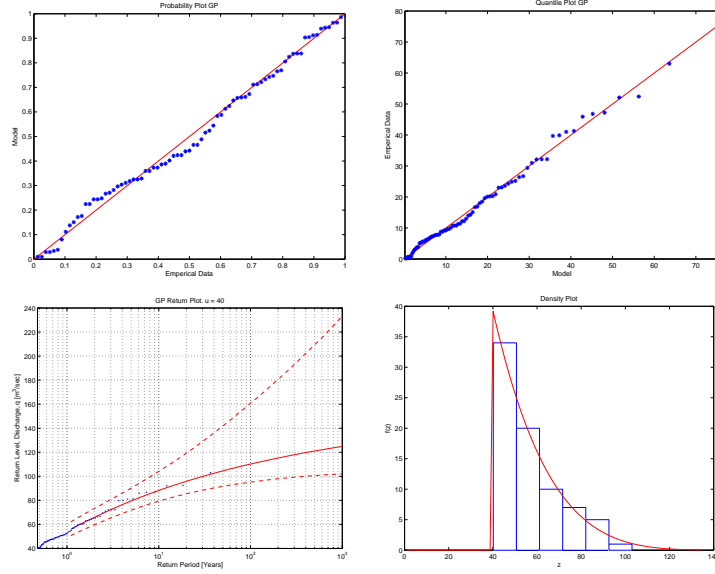
Figure D.10: (V010 TM DBM w/DRC) CASE 1: Prior and posterior distributions for the GP parameters
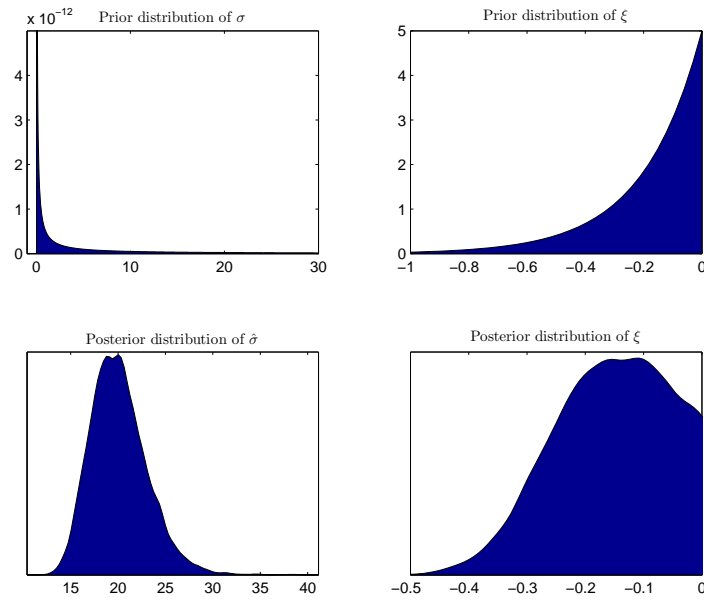
Threshold model using diagnostic based methods for choosing a threshold-Case 2: A negative gamma prior distribution for the ξ parameter (TM DBM w/DRC C2)

In Case 2, the prior distribution for ξ was chosen to be a negative gamma distribution. It contains only negative values having majority of the mass of the distribution is close to the y-axis. The prior distribution for $\tilde{\sigma}$ is a non-informative inv-χ^2 distribution. Therefore, in this case, the posterior density of the shape parameter of the GP distribution is constricted to negative values only. The prior and posterior distributions for the GP parameters are shown in Figure D.12.

The model seems to be a good fit for the data, having an Anderson-Darling p-value of $p_B = 0.55$. The diagnostic plots in Figure D.13 also indicate that the model fits the data well. The annual maximum values on the probability plot all lie close to the unit diagonal and the points are close to linear on the quantile plot. Comparison between the probability density of the GP distribution and the histogram of the POTs indicates that the model is a good fit for the data. Plotting the annual maximum values on the return level plot also seem to indicate that the model fits the data well.

Figure D.11: (V010 TM DBM w/DRC) CASE 1: Diagnostic plots for the Threshold Model

Figure D.12: (V010 TM DBM w/DRC) CASE 2: Prior and posterior distributions for the GP parameters
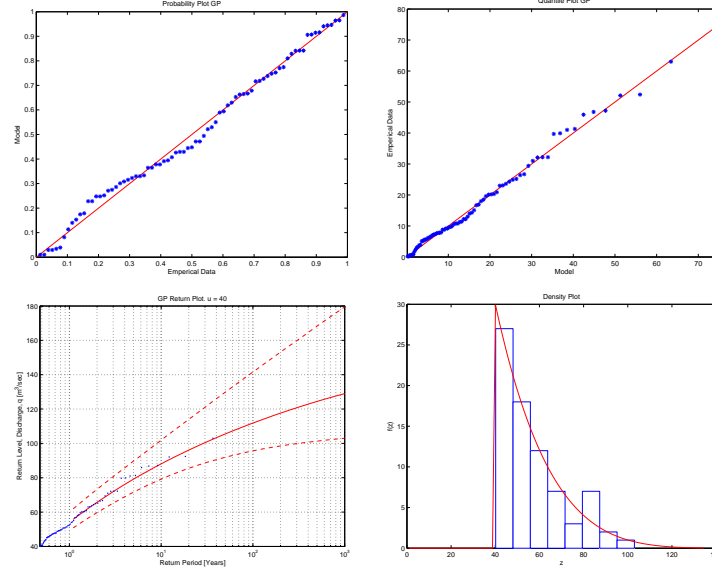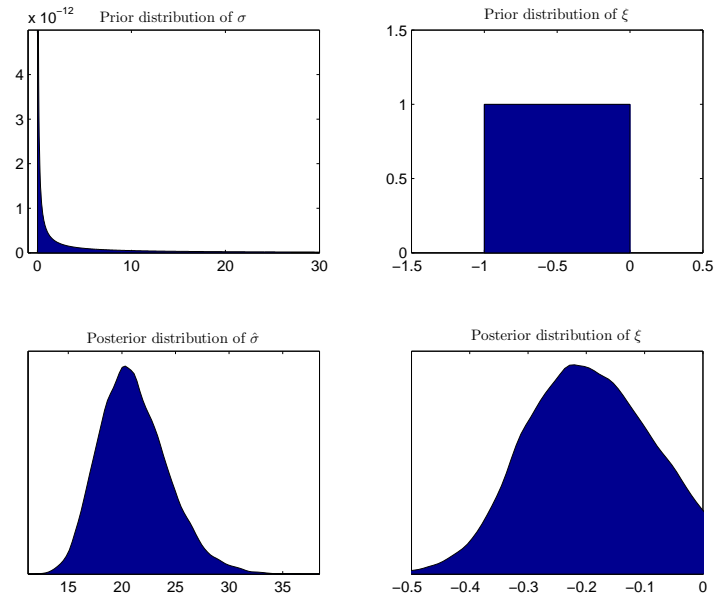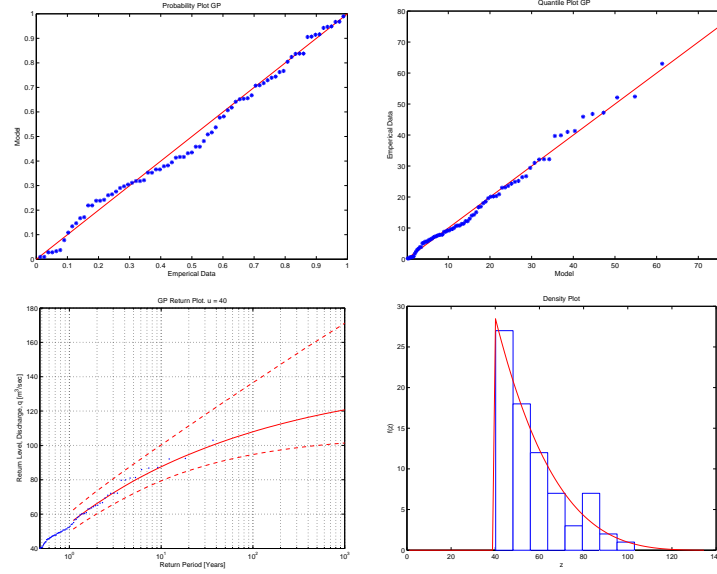
Figure D.13: (V010 TM DBM w/DRC) CASE 2: Diagnostic plots for the Threshold Model

Threshold model using diagnostic based methods for choosing a threshold- Case 3: A negative beta prior distribution for the ξ parameter (TM DBM w/DRC C3)

In Case 3, the prior distribution for ξ was chosen to be a negative beta distribution. It is a uniform distribution containing values on the interval $[-1; 0]$ The prior distribution for $\tilde{\sigma}$ is a non-informative inv-χ^2 distribution. Therefor, in this case, the posterior density of the shape parameter of the GEV distribution is constricted to negative values only. The prior and posterior distributions for the GP parameters are shown in Figure D.14.

The model seems to be a good fit for the data, having an Anderson-Darling p-value of $p_B = 0.53$. The diagnostic plots in Figure D.15 also indicate that the model fits the data well. The annual maximum values on the probability plot all lie close to the unit diagonal and the points are close to linear on the quantile plot. Comparison between the probability density of the GP distribution and the histogram of the POTs indicates that the model is a good fit for the data. Plotting the annual maximum values on the return level plot also seem to indicate that the model fits the data well.

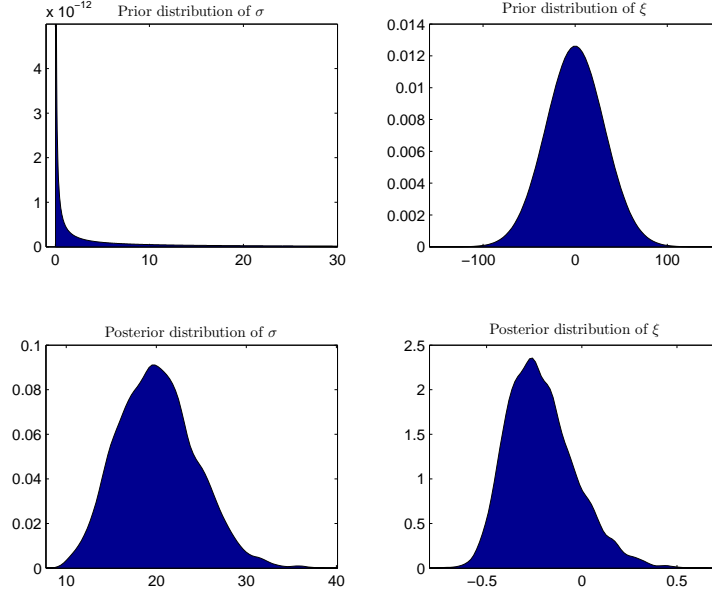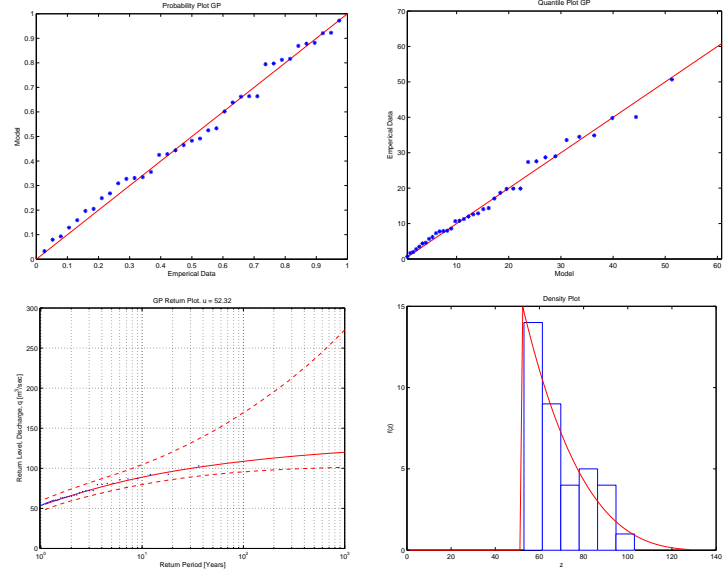*Figure D.14:* (V010 TM DBM w/DRC) CASE 3: Prior and posterior distributions for the GP parameters

Threshold model using the diagnostic based method (DBM) for determining the threshold value - Figures and tables displaying the posterior parameters of the GP distribution

Figure D.15: (V010 TM DBM w/DRC) CASE 3: Diagnostic plots for the threshold model

Table D.3: (V010 TM DBM w/DRC): Percentiles for the posterior distributions of the GP parameters, sampled using a MCMC iteration scheme, for all three cases of prior distributions, calculated with DRC uncertainty

	Normal		Neg-Gamma		Neg-Beta	
	σ	$\tilde{\xi}$	σ	$\tilde{\xi}$	σ	$\tilde{\xi}$
2.5%	14.50	-0.37	15.21	-0.35	15.75	-0.39
25%	18.20	-0.25	18.00	-0.22	18.87	-0.27
50%	20.31	-0.18	19.86	-0.15	20.87	-0.20
75%	22.65	-0.09	21.86	-0.08	23.13	-0.13
97.5%	27.41	0.11	26.76	-0.01	28.14	-0.02

Threshold model with DRC and u = 40
Percentiles for parameters in the GEV distribution
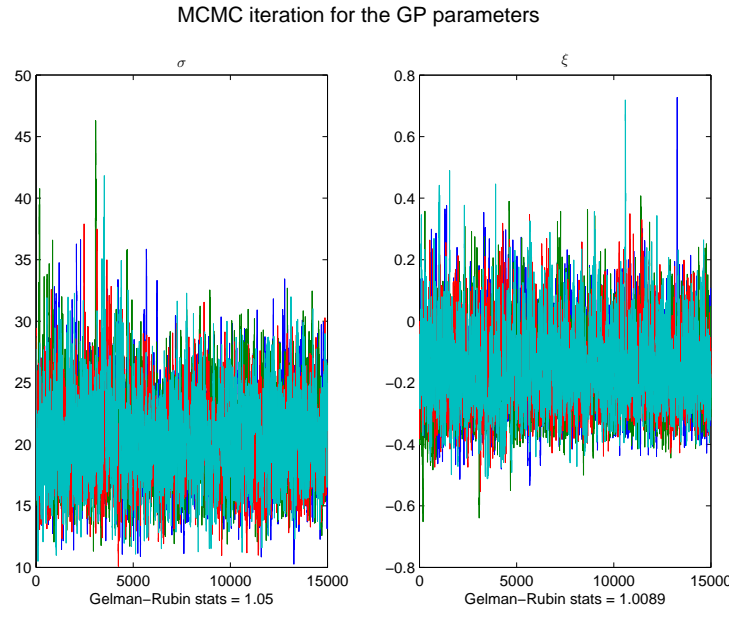
Figure D.16: (V010 TM DBM w/DRC) Case 1: Markov chain Monte Carlo simulation for the parameters in the GP distribution
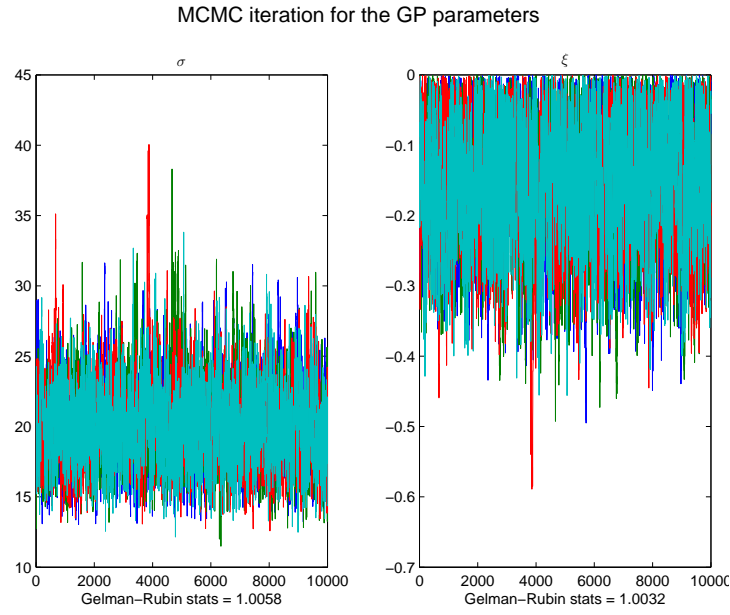
Figure D.17: (V010 TM DBM w/DRC) Case 2: Markov chain Monte Carlo simulation for the parameters in the GP distribution

MCMC iteration for the GP parameters
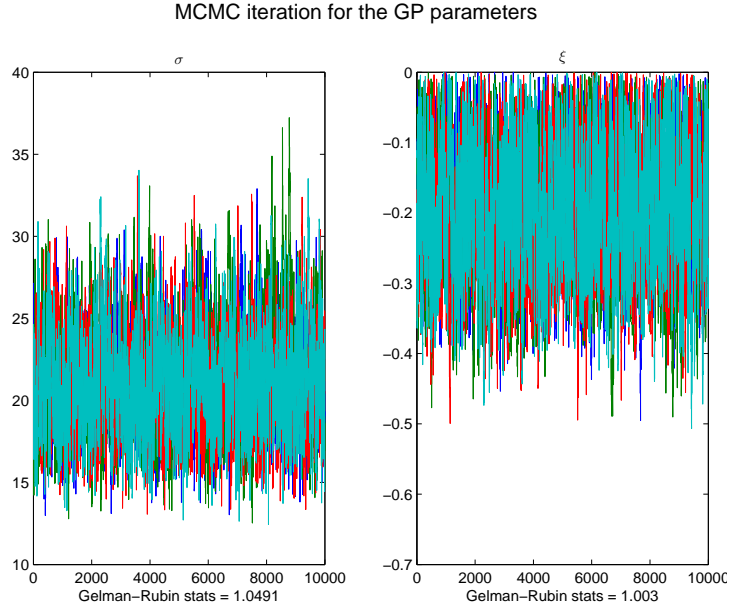
Figure D.18: (V010 TM DBM w/DRC) Case 3: Markov chain Monte Carlo simulation for the parameters in the GEV distribution

D.1.3. Threshold model using the fixed frequency method (FFM) for determining the threshold value

Threshold model using the fixed frequency method for choosing a threshold- Case 1: A normal prior distribution for the ξ parameter (TM FFM w/DRC C1)

In Case 1, the prior distribution for ξ was chosen to be a normal distribution with a large variance, making it non-informative prior. The prior distribution for $\tilde{\sigma}$ is a non-informative inv-χ^2 distribution. So, in this case, the GP parameters are not constricted in any way by their prior distributions. The prior and posterior distributions for the GP parameters are shown in Figure D.19.

The model seems to be a good fit for the data, having an Anderson-Darling p-value of $p_B = 0.59$. The diagnostic plots in Figure D.20 also indicate that the model fits the data well. The annual maximum values on the probability plot all lie close to the unit diagonal and the points are close to linear on the quantile plot. Comparison between the probability density of the GP distribution and the histogram of the POTs indicates that the model could be a good fit for the data. Plotting the annual maximum values on the return level plot also seem to indicate that the model fits the data well.

Figure D.19: (V010 TM FFM w/DRC) CASE 1: Prior and posterior distributions for the GP parameters

Threshold model using the fixed frequency method for choosing a threshold- Case 2: A negative gamma prior distribution for the ξ parameter (TM FFM w/DRC C2)

In Case 2, the prior distribution for ξ was chosen to be a negative gamma distribution. It contains only negative values having majority of the mass of the distribution is close to the y-axis. The prior distribution for $\tilde{\sigma}$ is a non-informative inv-χ^2 distribution. Therefore, in this case, the posterior density of the shape parameter of the GP distribution is constricted to negative values only. The prior and posterior distributions for the GP parameters are shown in Figure D.21.

The model seems to be a good fit for the data, having an Anderson-Darling p-value of $p_B = 0.59$. The diagnostic plots in Figure D.22 also indicate that the model fits the data well. The annual maximum values on the probability plot all lie close to the unit diagonal and the points are close to linear on the quantile plot. Comparison between the probability density of the GP distribution and the histogram of the POTs indicates that the model could be a good fit for the data. Plotting the annual maximum values on the return level plot also seem to indicate that the model fits the data well.
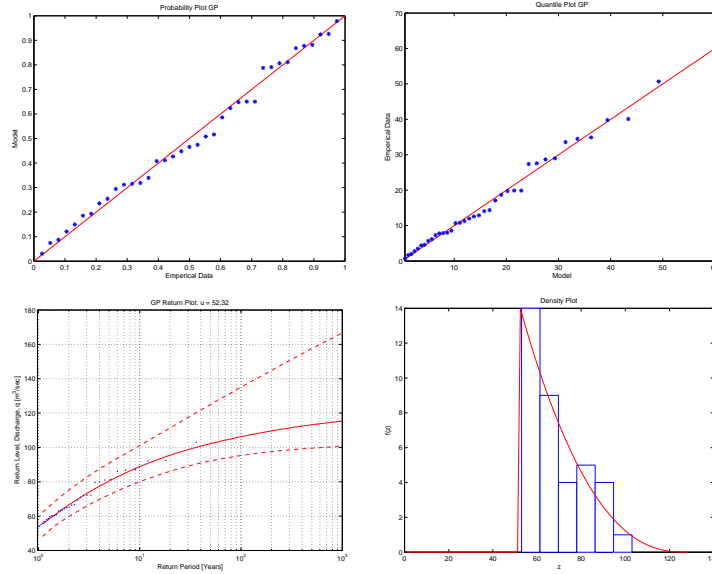
Figure D.20: (V010 TM FFM w/DRC) CASE 1: Diagnostic plots for the Threshold Model
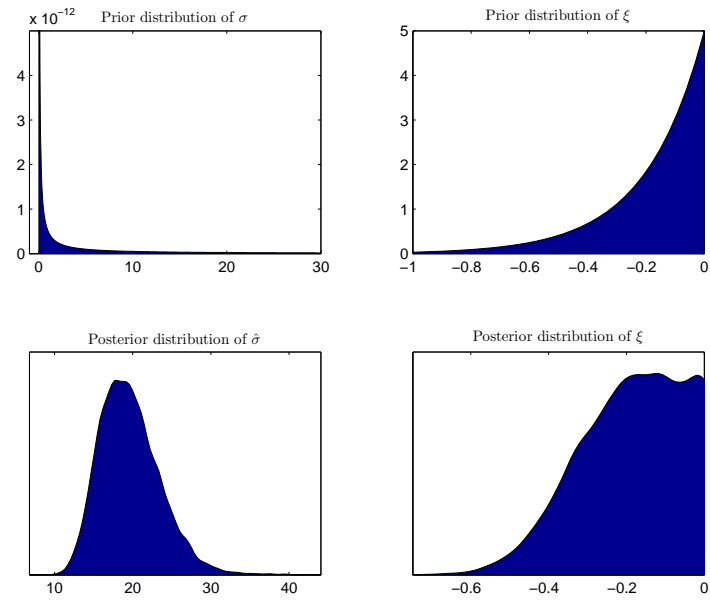
Figure D.21: (V010 TM FFM w/DRC) CASE 2: Prior and posterior distributions for the GP parameters
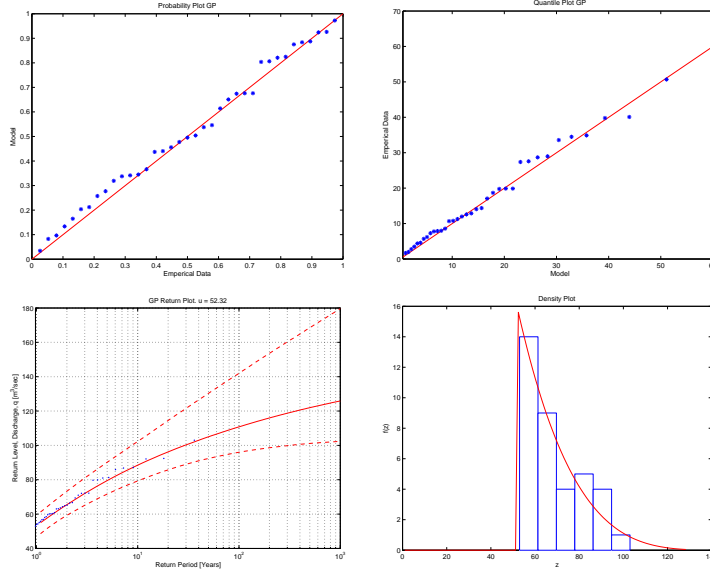
Figure D.22: (V010 TM FFM w/DRC) CASE 2: Diagnostic plots for the Threshold Model

Threshold model using the fixed frequency method for choosing a threshold- Case 3: A negative beta prior distribution for the ξ parameter (TM FFM w/DRC C3)

In Case 3, the prior distribution for ξ was chosen to be a negative beta distribution. It is a uniform distribution containing values on the interval $[-1; 0]$ The prior distribution for $\tilde{\sigma}$ is a non-informative inv-χ^2 distribution. Therefore, in this case, the posterior density of the shape parameter of the GEV distribution is constricted to negative values only. The prior and posterior distributions for the GP parameters are shown in Figure D.23.

The model seems to be a good fit for the data, having an Anderson-Darling p-value of $p_B = 0.61$. The diagnostic plots in Figure D.24 also indicate that the model fits the data well. The annual maximum values on the probability plot all lie close to the unit diagonal and the points are close to linear on the quantile plot. Comparison between the probability density of the GP distribution and the histogram of the POTs indicates that the model could be a good fit for the data. Plotting the annual maximum values on the return level plot also seem to indicate that the model fits the data well.
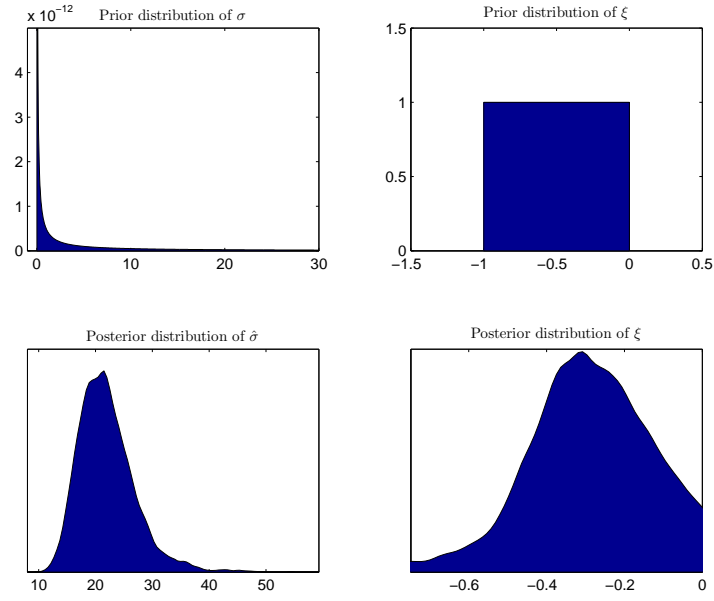
Figure D.23: (V010 TM FFM w/DRC) CASE 3: Prior and posterior distributions for the GP parameters

Threshold model using the fixed frequency method (FFM) for determining the threshold value – Figures and tables displaying the posterior parameters of the GP distribution

Figure D.24: (V010 TM FFM w/DRC) CASE 3: Diagnostic plots for the threshold model

Table D.4: (V010 TM FFM w/DRC): Percentiles for the posterior distributions of the GP parameters, sampled using a MCMC iteration scheme, for all three cases of prior distributions, calculated with DRC uncertainty

	Threshold model with DRC and u = 52					
	Percentiles for parameters in the GEV distribution					
	Normal		Neg-Gamma		Neg-Beta	
	σ	$\tilde{\xi}$	σ	$\tilde{\xi}$	σ	$\tilde{\xi}$
2.5%	12.73	-0.53	13.38	-0.47	14.35	-0.61
25%	17.26	-0.34	16.85	-0.28	18.51	-0.39
50%	20.00	-0.24	19.24	-0.18	21.37	-0.29
75%	23.21	-0.11	21.97	-0.09	24.60	-0.18
97.5%	31.19	0.18	28.20	-0.01	33.98	-0.03
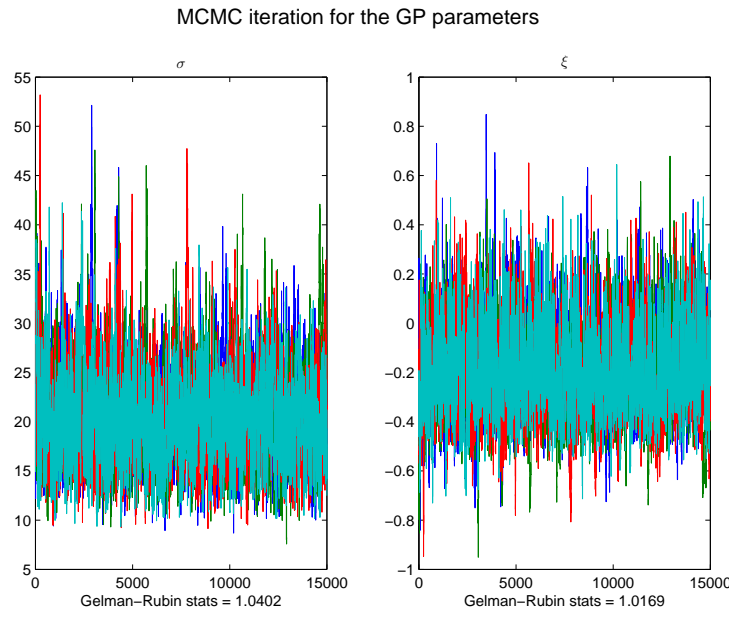
Figure D.25: (V010 TM FFM w/DRC) Case 1: Markov chain Monte Carlo simulation for the parameters in the GP distribution
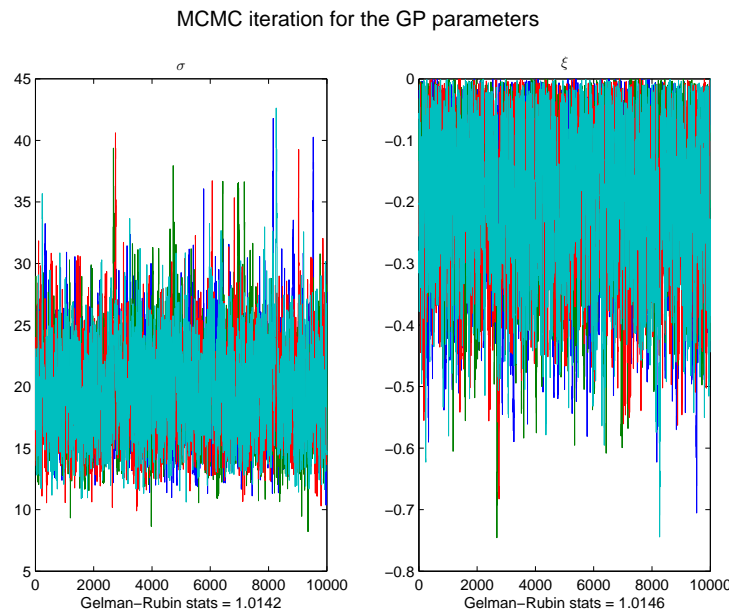
Figure D.26: (V010 TM FFM w/DRC) Case 2: Markov chain Monte Carlo simulation for the parameters in the GP distribution

MCMC iteration for the GP parameters
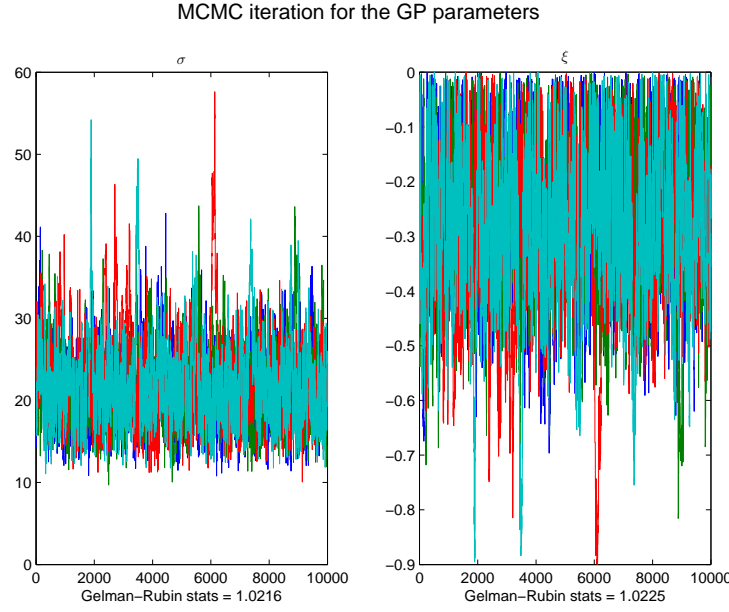
Figure D.27: (V010 TM FFM w/DRC) Case 3: Markov chain Monte Carlo simulation for the parameters in the GEV distribution

D.2. V010: Without discharge rating curve uncertainty

D.2.1. Block maxima model

Table D.5: (V010 BM w/o DRC): Percentiles for the posterior distributions of the GEV parameters, sampled using a MCMC iteration scheme, for all three cases of prior distributions, calculated without DRC uncertainty

|	Block Extrema without DRC								
	Percentiles for parameters in the GEV distribution								
	Normal			Neg-Gamma			Neg-Beta		
	μ	σ	ξ	μ	σ	ξ	μ	σ	ξ
2.5%	49.00	11.68	-0.33	49.25	12.31	-0.32	49.55	12.66	-0.38
25%	52.39	14.04	-0.14	52.95	14.51	-0.16	53.34	15.00	-0.23
50%	54.23	15.56	-0.03	54.80	15.93	-0.09	55.31	16.52	-0.14
75%	56.18	17.24	0.09	56.74	17.53	-0.04	57.30	18.18	-0.07
97.5%	59.99	21.23	0.34	60.73	21.44	-0.00	61.35	22.13	-0.01

MCMC iteration for the GEV parameters
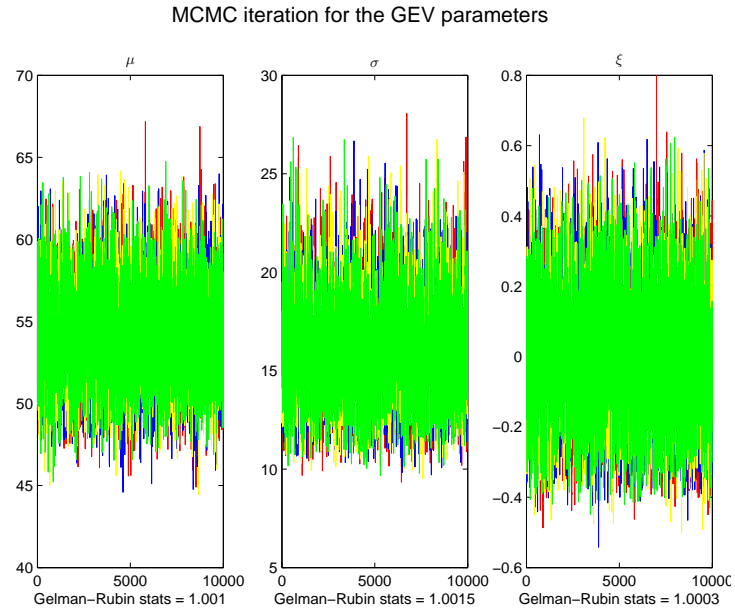
Figure D.28: (V010 BM w/o DRC) Case 1: Markov chain Monte Carlo simulation for the parameters in the GEV distribution
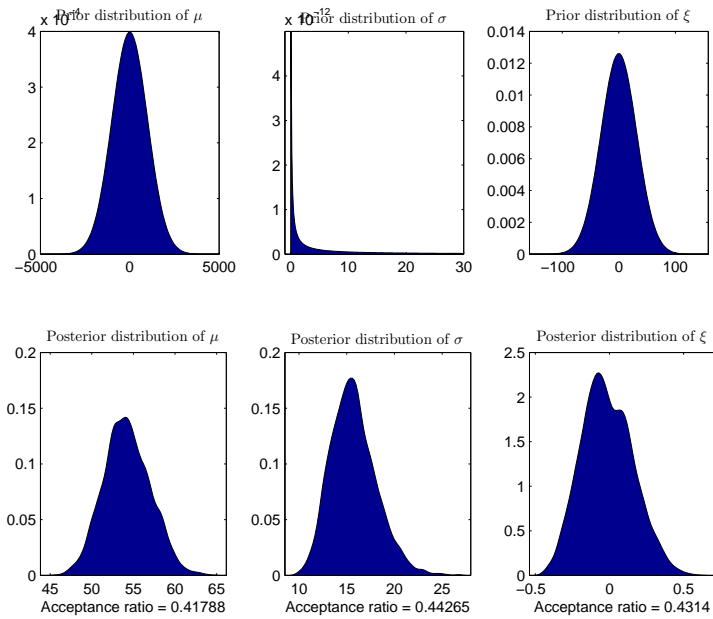
Figure D.29: (V010 BM w/o DRC) CASE 1: Prior and posterior distributions for the GEV parameters
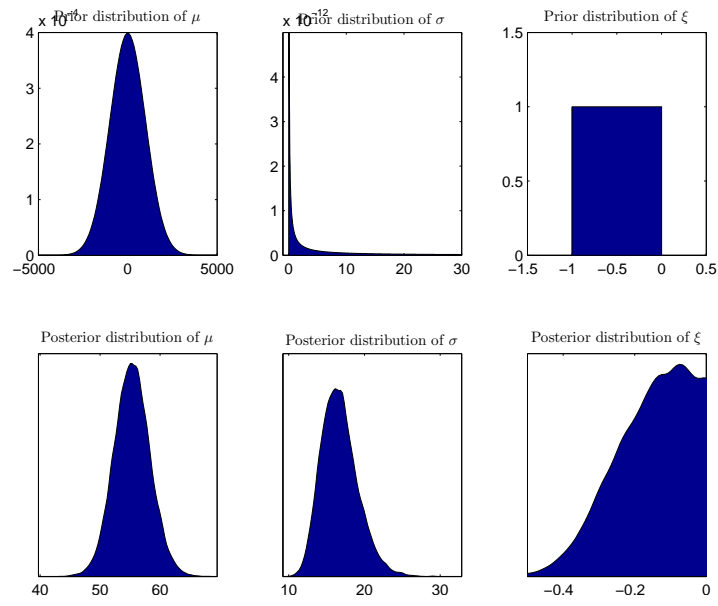
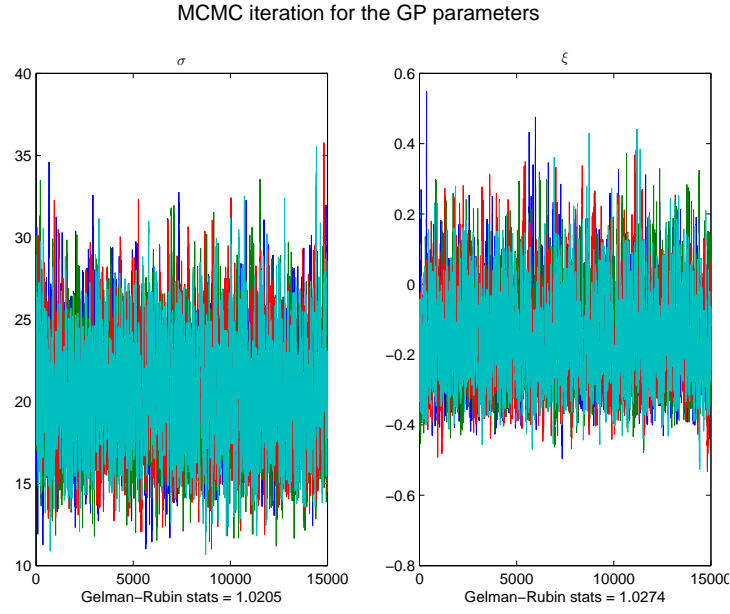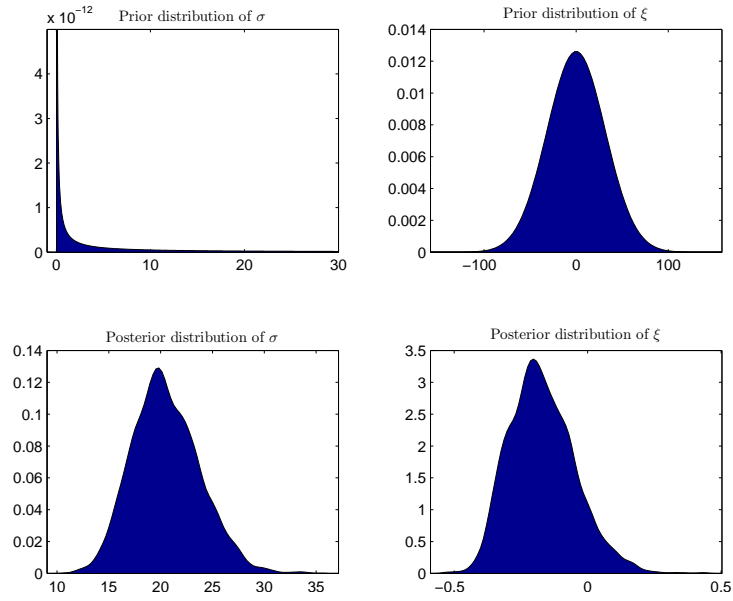*Figure D.30:* (V010 BM w/o DRC) CASE 1: Diagnostic plots for the block maxima model

D.2.2. Threshold model using the diagnostic based method (DBM) for determining the threshold value

Table D.6: (V010 TM DBM w/o DRC): Percentiles for the posterior distributions of the GP parameters, sampled using a MCMC iteration scheme, for all three cases of prior distributions, calculated without DRC uncertainty

	Threshold model with DRC and u = 40
	Percentiles for parameters in the GEV distribution
	Normal		Neg-Gamma		Neg-Beta	
	σ	$\tilde{\xi}$	σ	$\tilde{\xi}$	σ	$\tilde{\xi}$
2.5%	14.72	-0.37	15.24	-0.34	15.87	-0.38
25%	18.24	-0.25	17.98	-0.22	18.95	-0.27
50%	20.21	-0.18	19.71	-0.15	20.92	-0.21
75%	22.40	-0.09	21.68	-0.08	23.10	-0.13
97.5%	27.25	0.11	25.89	-0.01	27.82	-0.02
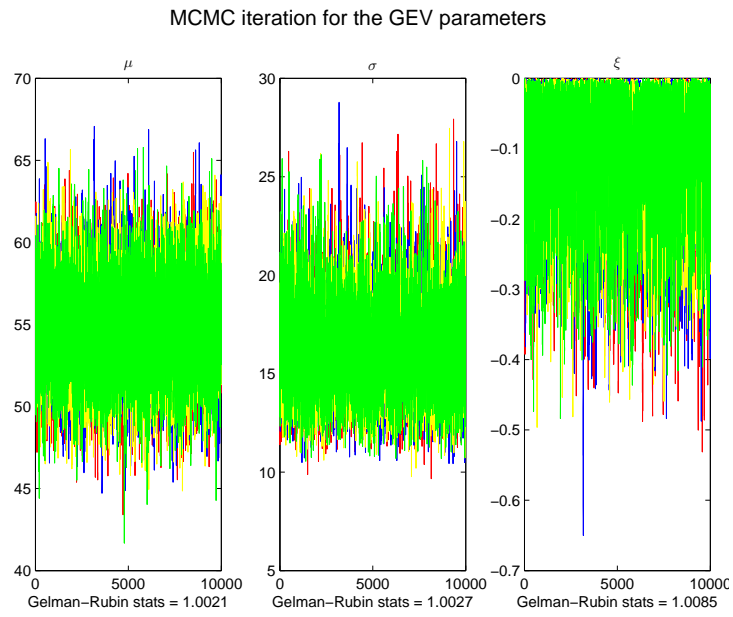
Figure D.31: (V010 BM w/o DRC) Case 2: Markov chain Monte Carlo simulation for the parameters in the GEV distribution
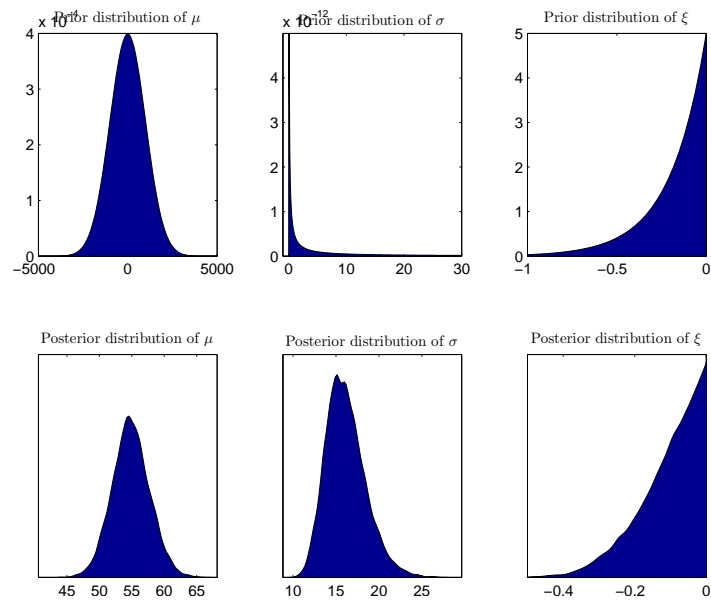
Figure D.32: (V010 BM w/o DRC) CASE 2: Prior and posterior distributions for the GEV parameters
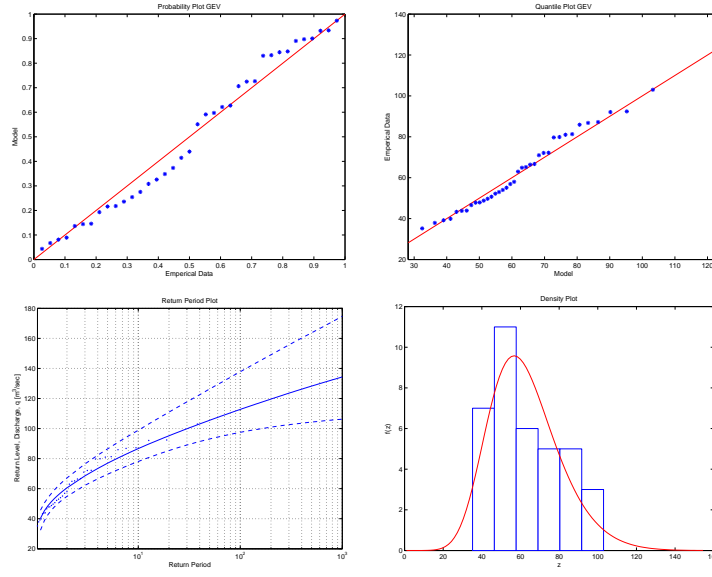
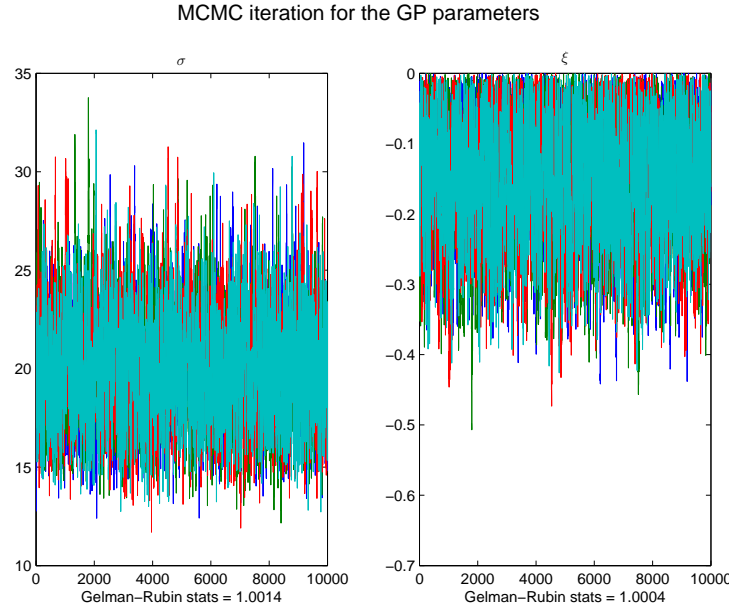*Figure D.33:* (V010 BM w/o DRC) CASE 2: Diagnostic plots for the block maxima model
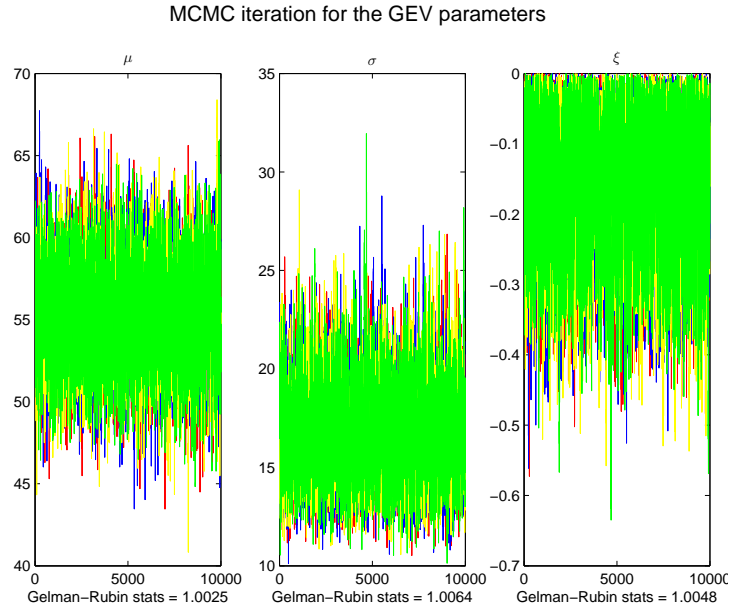
Figure D.34: (V010 BM w/o DRC) Case 3: Markov chain Monte Carlo simulation for the parameters in the GEV distribution

Figure D.35: (V010 BM w/o DRC) CASE 3: Prior and posterior distributions for the GEV parameters
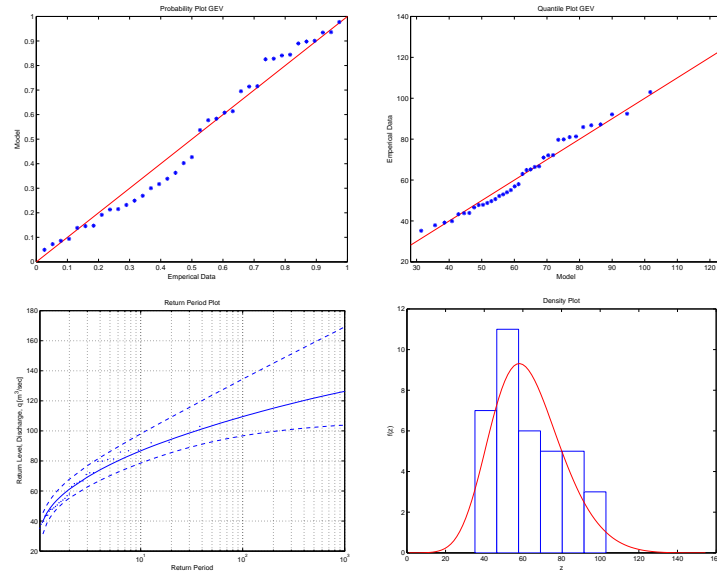
Figure D.36: (V010 BM w/o DRC) CASE 3: Diagnostic plots for the block maxima model

MCMC iteration for the GP parameters

Figure D.37: (V010 TM DBM w/o DRC) Case 1: Markov chain Monte Carlo simulation for the parameters in the GP distribution
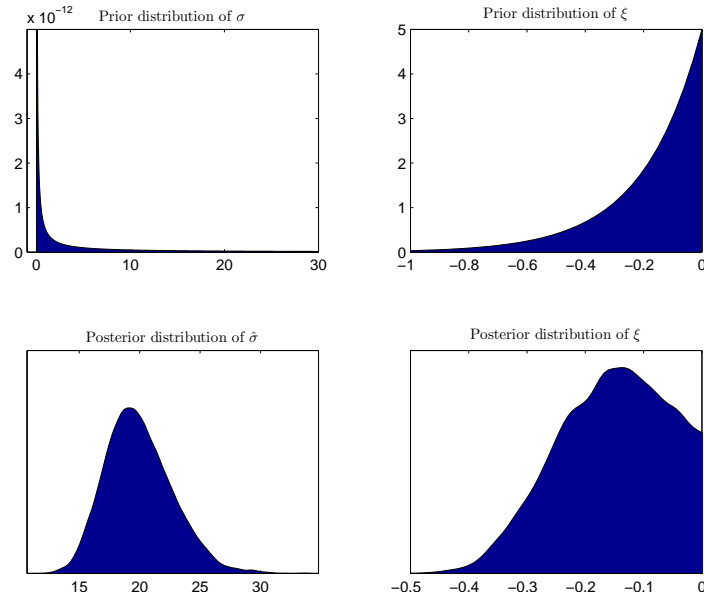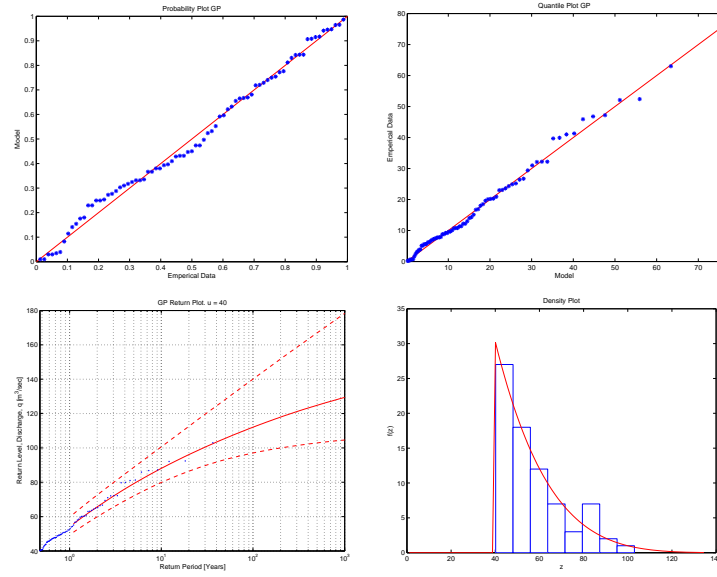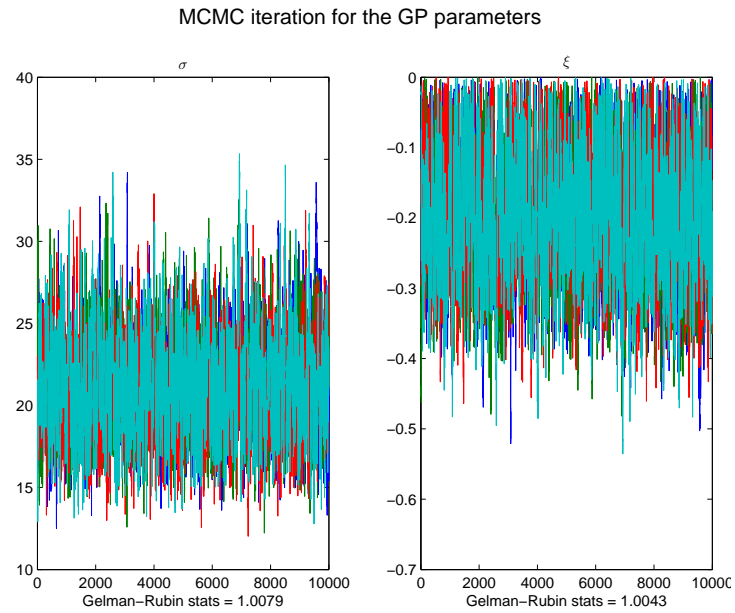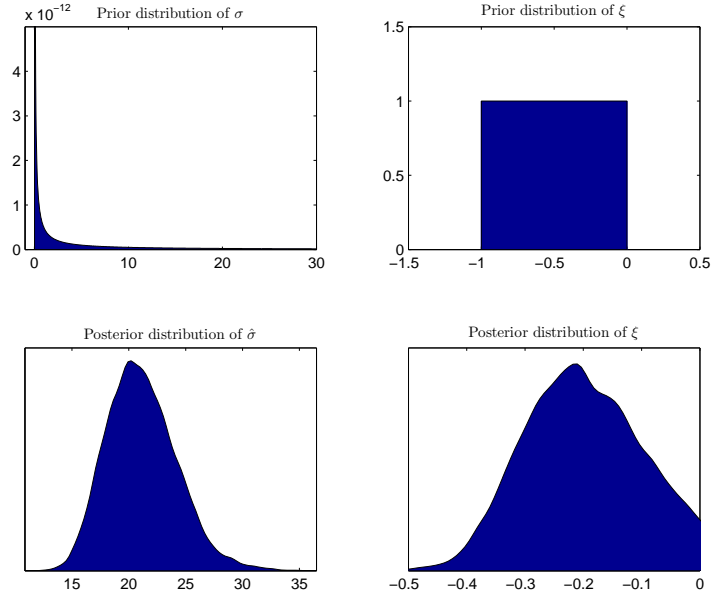

Figure D.38: (V010 TM DBM w/o DRC) CASE 1: Prior and posterior distributions for the GP parameters
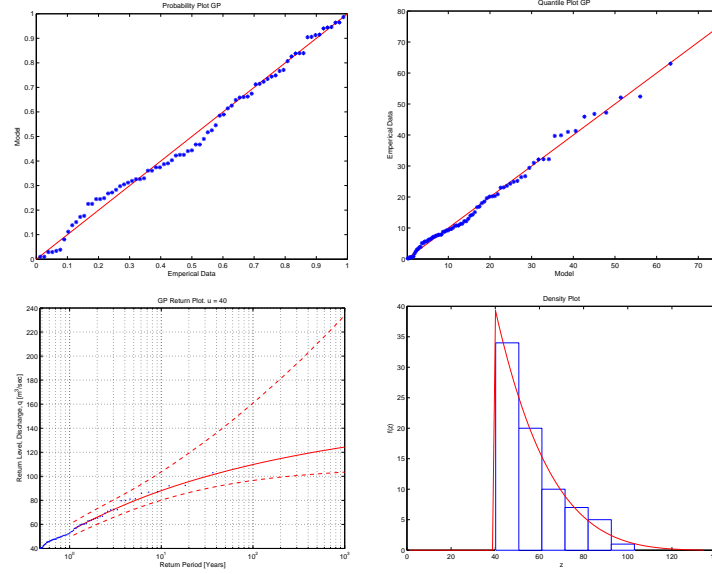
Figure D.39: (V010 TM DBM w/o DRC) CASE 1: Diagnostic plots for the threshold model

D.2.3. Threshold model using the fixed frequency method (FFM) for determining the threshold value

Table D.7: (V010 TM FFM w/o DRC): Percentiles for the posterior distributions of the GP parameters, sampled using a MCMC iteration scheme, for all three cases of prior distributions, calculated without DRC uncertainty

|	Threshold model without DRC and u = 52					
	Percentiles for parameters in the GP distribution					
	Normal		Neg-Gamma		Neg-Beta	
	σ	$\tilde{\xi}$	σ	$\tilde{\xi}$	σ	$\tilde{\xi}$
2.5%	13.65	-0.55	13.98	-0.49	14.86	-0.58
25%	18.20	-0.38	17.50	-0.30	19.00	-0.41
50%	21.10	-0.27	19.87	-0.20	21.81	-0.30
75%	24.42	-0.15	22.68	-0.10	25.22	-0.20
97.5%	31.72	0.14	29.25	-0.01	32.09	-0.03

Figure D.40: (V010 TM DBM w/o DRC) Case 2: Markov chain Monte Carlo simulation for the parameters in the GP distribution
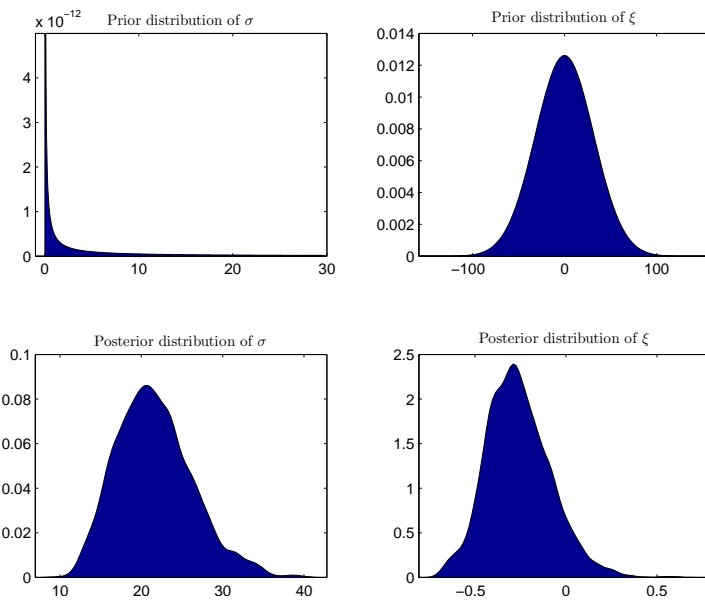

Figure D.41: (V010 TM DBM w/o DRC) CASE 2: Prior and posterior distributions for the GP parameters
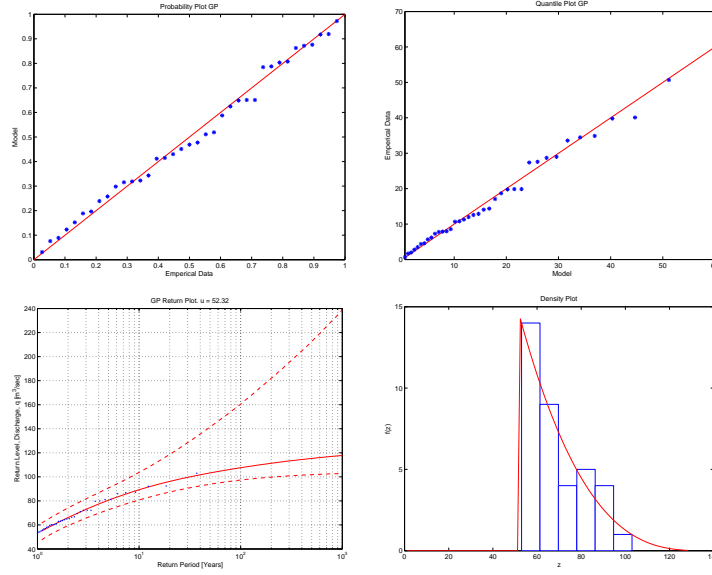
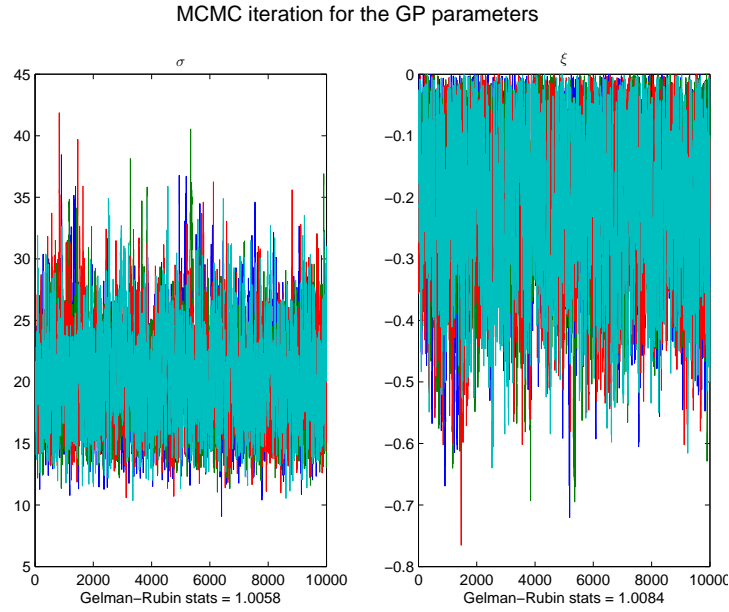*Figure D.42:* (V010 TM DBM w/o DRC) CASE 2: Diagnostic plots for the threshold model

Figure D.43: (V010 TM DBM w/o DRC) Case 3: Markov chain Monte Carlo simulation for the parameters in the GP distribution

Figure D.44: (V010 TM DBM w/o DRC) CASE 3: Prior and posterior distributions for the GP parameters
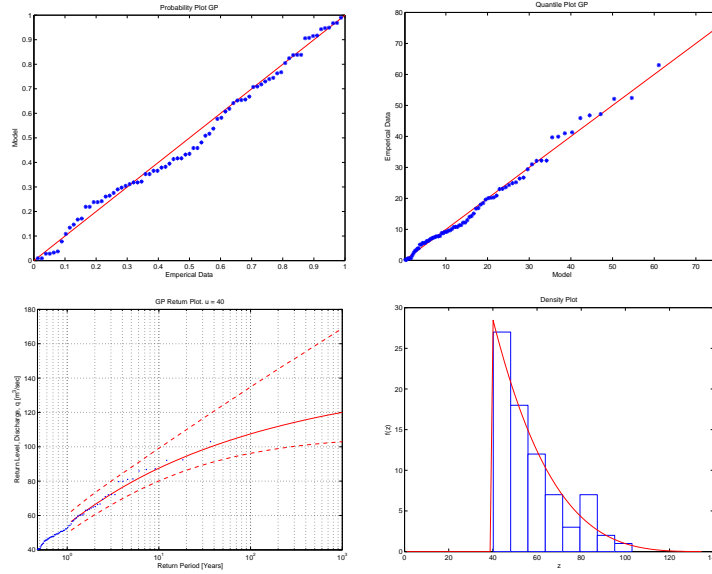
Figure D.45: (V010 TM DBM w/o DRC) CASE 3: Diagnostic plots for the threshold model
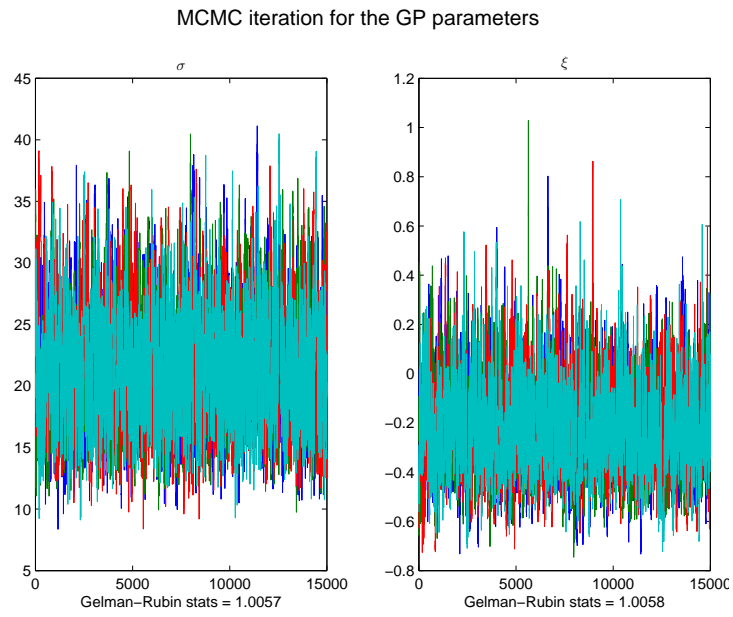
Figure D.46: (V010 TM FFM w/o DRC) Case 1: Markov chain Monte Carlo simulation for the parameters in the GP distribution
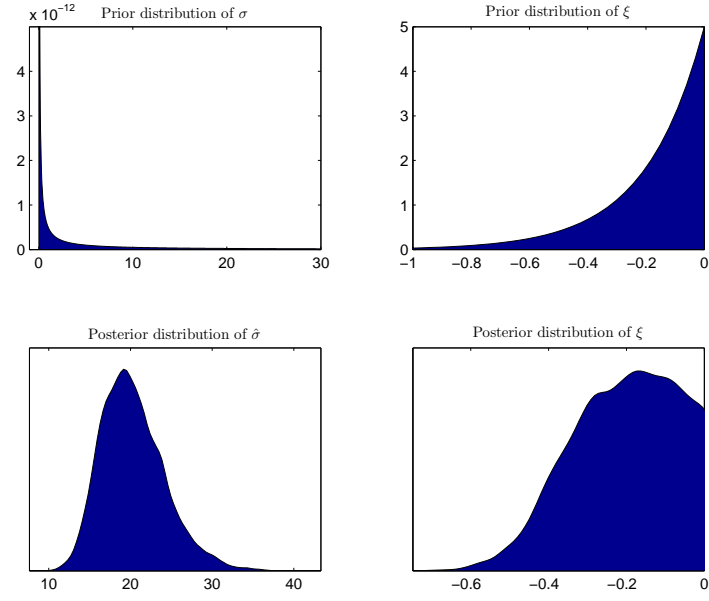

Figure D.47: (V010 TM FFM w/o DRC) CASE 1: Prior and posterior distributions for the GP parameters
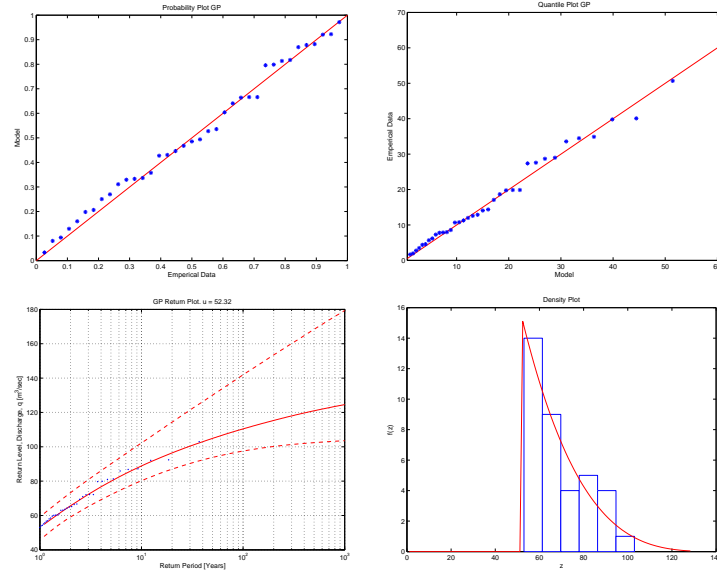
Figure D.48: (V010 TM FFM w/o DRC) CASE 1: Diagnostic plots for the threshold model

Figure D.49: (V010 TM FFM w/o DRC) Case 2: Markov chain Monte Carlo simulation for the parameters in the GP distribution

Figure D.50: (V010 TM FFM w/o DRC) CASE 2: Prior and posterior distributions for the GP parameters

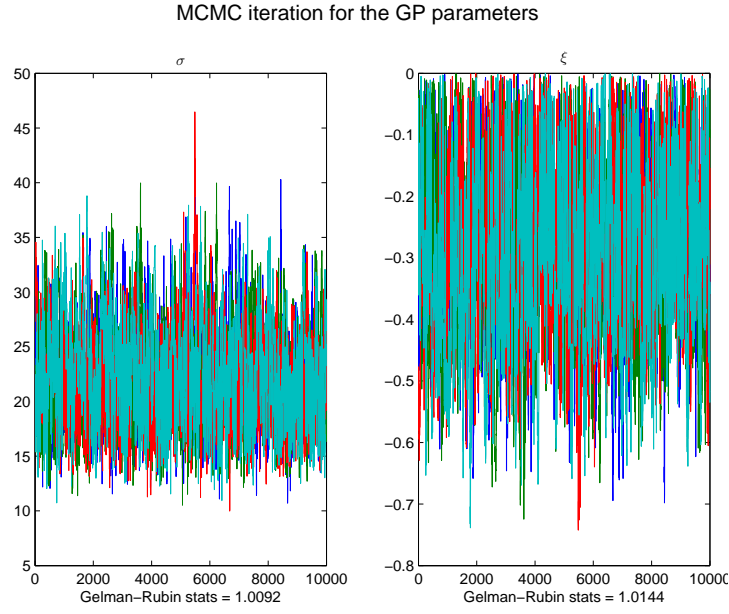*Figure D.51:* (V010 TM FFM w/o DRC) CASE 2: Diagnostic plots for the threshold model

Figure D.52: (V010 TM FFM w/o DRC) Case 3: Markov chain Monte Carlo simulation for the parameters in the GP distribution
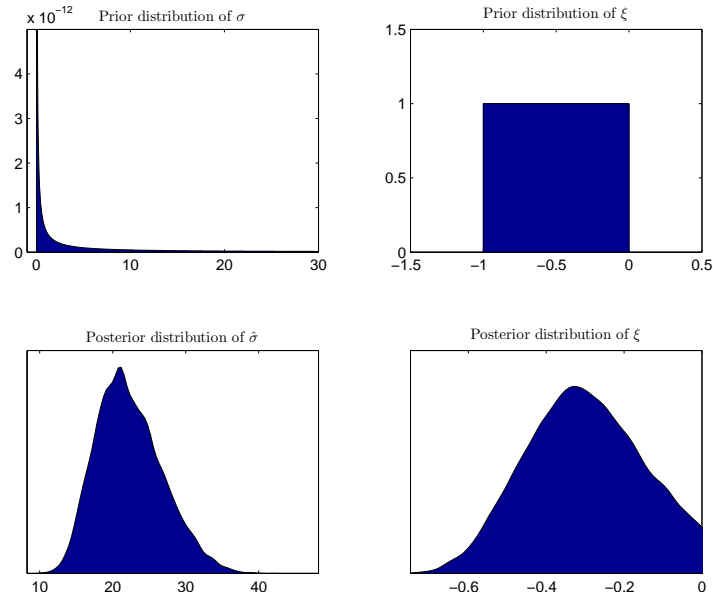

Figure D.53: (V010 TM FFM w/o DRC) CASE 3: Prior and posterior distributions for the GP parameters

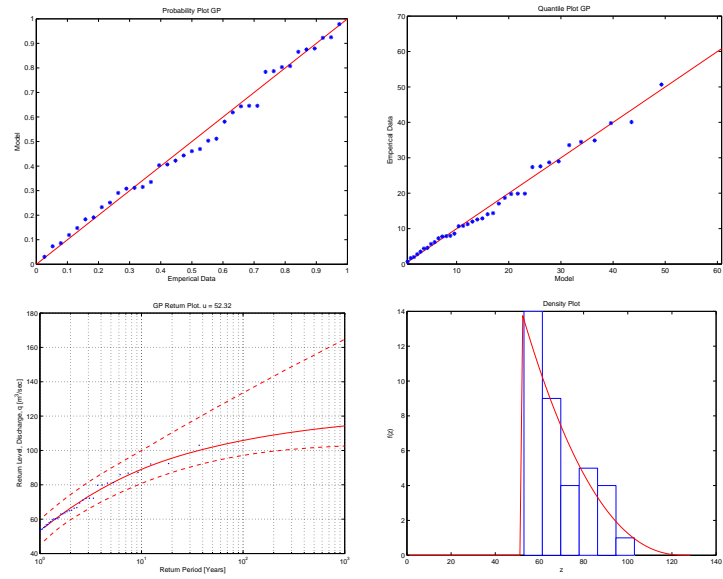*Figure D.54:* (V010 TM FFM w/o DRC) CASE 3: Diagnostic plots for the threshold model